THE UNIVERSITY OF QUEENSLAND

AUSTRALIA

Molecular Organisation, Physical and Digestion Properties of Less-Ordered Starch Matrices

Bin Zhang

(BSc, MSc in Food Science)

A thesis submitted for the degree of Doctor of Philosophy at

The University of Queensland in January 2015

Queensland Alliance for Agriculture and Food Innovation

Abstract

Starch, a major energy-providing carbohydrate for human beings, is synthesised in a condensed semi-crystalline granular form by ordered packing of two hydrophilic glucose polymers (amylose and amylopectin). It has a complex hierarchical structural structure, which can be described by at least four levels of organisation (i.e., molecular, lamellae, growth ring, and granular levels), ranging in length scale from nanometer to micrometer. From the point of view of food engineering, most starch based foods are processed before consuming, and become less ordered and more accessible to enzymes in most cases. So, the main focus of this thesis is on the molecular organisation, physical and digestion properties of less-ordered starch matrices induced by food processing, including swollen granule ghosts (chapters 4 and 5), starch extrudates (chapter 6) and freeze-dried B-type starch granules (chapter 7).

Before less-ordered starch matrices are investigated, chapter 3 of the thesis reports the influence of starch physical structure on the kinetics of degradation with either exo-acting or a mixture of endo- and exo-acting enzymes (α-amylase and amyloglucosidase respectively), using three physical forms of maize and potato starch as exemplars. For starch in granular form, all enzyme digestions followed first-order kinetics consistent with enzyme-substrate complex formation being rate-limiting, and there was marked synergism between the enzymes in the production of glucose. In contrast, although digestion of cooked starches was more rapid than for the granular form, there were antagonistic effects between endo- and exo-acting enzymes with evidence of first-order kinetics for only the mixed enzyme system. The rates of digestion of swollen granule ghosts cooked under low shear conditions were slower than for starches cooked under high shear conditions that prevent granule ghost formation.

Subsequently, the formation mechanism (chapter 4) and lubrication properties (chapter 5) of maize and potato starch ghosts (formed by cooking at 95 °C under dilute and low shear conditions) were studied. Amylase digestion of isolated starch ghosts with and without prior treatment with sodium dodecyl sulphate was used as a probe to study the mechanism of ghost formation, showing that neither integral nor surface proteins/lipids were crucial for control of either ghost digestion or integrity. From investigation of ghosts and ghost remnants after amylolysis for molecular components and glucan conformation, it was found that starch ghosts are enriched in amylopectin with less than 1% of

single/double helices within ghost remnants. Therefore, it is concluded that the ghost structure originates from physical entanglements of highly branched and large molecular size amylopectin molecules.

Lubrication has long been considered to play a critical role in oral perception of foods, and the importance of soft-tribology measurements has been realized by food scientists in the past few years. Starch granule ghosts are squeezed and sheared between oral surfaces and thereby contribute to the mouthfeel of some starch based foods and beverages. We evaluated the soft-tribological and rheological properties of aqueous ghost suspensions at different concentrations. The tribological profiles of both maize and potato starch ghosts with different concentrations are dominated by surface features such as size and integrity, which results in boundary and mixed lubrication. A markedly decreased friction coefficient (entrainment speed < 50 mm/s) with increasing concentration (up to 1% based on weight) of maize ghost suspension was observed, while the friction coefficient of potato ghosts did not change much with varying concentrations. We suggest that size and integrity of ghost particles (small and robust maize ghosts vs. large and fragile potato ghosts) affect soft-tribological properties, and could potentially contribute to the perception of starchy food in the mouth.

Chapter 6 of the thesis studied enzymic hydrolysis and structure of another less-ordered model food, starch extrudates. In this study, we processed starches with different amylose contents though extrusion using water as sole plasticizer to achieve less-ordered starch matrices, and found that extruded high-amylose starch has a lower digestion rate/extent compared with the same starch cooked in water and waxy/normal maize extrudates. The NMR and XRD data showed that about 80% of enzyme-resistant fractions in the digesta of high-amylose starch extrudates are amorphous, i.e. have no detectable molecular order. We suggest that the local molecular density of less-ordered starch matrices may control the digestibility, although the technical ability to measure submicron variability of local density is currently limited. The double helix content/crystallinity within the high-amylose maize starch digesta in cooked and extrudate forms are similar but the enzyme resistance is much lower for the extrudate form. We think this is strong evidence that dense molecular packing in amorphous material does play a role in restricting enzyme action.

In chapter 7, we report that oven- and ethanol- drying are mild dehydration methods which do not significantly affect the digestion, thermal or structural properties of starches.

However, freeze-drying can result in a remarkable increase in the digestion rate of B-type starches, but not A-type starches. Freeze-drying not only disrupts the surface morphology of potato starch granules, but also degrades both short- and long-range molecular order of the amylopectin, each of which can cause an increase in the digestion rate. We propose that the low temperatures involved in freeze drying compared with oven drying results in greater chain rigidity and lead to structural disorganization during water removal at both nanometer and micrometer length scales in B-type polymorphic starch granules, because of the different distribution of water within crystallites and the lack of pores and channels compared with A-type polymorphic starch granules.

Declaration by author

This thesis is composed of my original work, and contains no material previously published or written by another person except where due reference has been made in the text. I have clearly stated the contribution by others to jointly-authored works that I have included in my thesis.

I have clearly stated the contribution of others to my thesis as a whole, including statistical assistance, survey design, data analysis, significant technical procedures, professional editorial advice, and any other original research work used or reported in my thesis. The content of my thesis is the result of work I have carried out since the commencement of my research higher degree candidature and does not include a substantial part of work that has been submitted to qualify for the award of any other degree or diploma in any university or other tertiary institution. I have clearly stated which parts of my thesis, if any, have been submitted to qualify for another award.

I acknowledge that an electronic copy of my thesis must be lodged with the University Library and, subject to the policy and procedures of The University of Queensland, the thesis be made available for research and study in accordance with the Copyright Act 1968 unless a period of embargo has been approved by the Dean of the Graduate School.

I acknowledge that copyright of all material contained in my thesis resides with the copyright holder(s) of that material. Where appropriate I have obtained copyright permission from the copyright holder to reproduce material in this thesis.

Publications during candidature

Peer-Reviewed Papers

1. **Zhang, B.**; Dhital, S.; Gidley, M. J.* (2013). Synergistic and antagonistic effects of alpha-amylase and amyloglucosidase on starch digestion. *Biomacromolecules*, 14, 1945-1954.
2. **Zhang, B.**; Dhital, S.; Flanagan, B. M.; Gidley, M. J.* (2014). Mechanism for starch granule ghost formation deduced from structural and enzyme digestion properties. *Journal of Agricultural and Food Chemistry*, 62, 760-771.
3. **Zhang, B.**; Wang, K.; Hasjim, J.; Li, E.; Flanagan, B. M.; Gidley, M. J.; Dhital, S.* (2014). Freeze drying changes the structure and digestibility of B-polymorphic starches. *Journal of Agricultural and Food Chemistry*, 62, 1482-1491.
4. **Zhang, B.**; Dhital, S.; Gidley, M. J.* (2015). Densely packed matrices as rate determining features in starch hydrolysis. *Trends in Food Sci. Tech.,* 43, 18-31.
5. Dhital, S.; Warren, F. J.; **Zhang, B.**; Gidley, M. J.* (2014). Amylase binding to starch granules under hydrolysing and non-hydrolysing conditions. *Carbohydrate Polymers*, 113, 97-107.
6. Warren, F. J.; **Zhang, B.**, Waltzer, G.; Gidley, M. J.; Dhital, S.* (2015). The interplay of α-amylase and amyloglucosidase activities on the digestion of starch in *in vitro* enzymic systems. *Carbohydrate Polymers*, 117, 192-200.
7. Dhital, S.; Dabit, L.; **Zhang, B.**; Flanagan, B. M.; Shrestha, A. K.* (2015). Digestibility and supra-molecular structural properties of raw and cooked flours from commercially available milled rice. *Food Chemistry,* 172, 757-765.
8. Wang, K.; Wambugu, P. W.; **Zhang, B.**; Wu, A. C.; Henry, R. J.; Gilbert, R. G.* (2015). The biosynthesis, structure and gelatinization properties of starches from wild and cultivated African rice species *(Oryza barthii and Oryza glaberrima). Carbohydrate Polymers*, In press.

Conference Abstracts

1. **Zhang, B.**;* Dhital, S.; Flanagan, B. M.; Luckman, P.; Halley, P. J.; Gidley, M. J. Enzyme-resistant starch from amorphous matrices: Mechanisms and approaches. In *American Association of Cereal Chemist International (AACCI) Annual Meeting*, Providence, New Mexico, USA, October 2014. (Oral)
2. **Zhang, B.**;* Wang, K.; Hasjim, J.; Li, E.; Flanagan, B. M.; Gidley, M. J.; Dhital, S. Freeze drying changes the structure and digestibility of B-polymorphic starches. In

American Association of Cereal Chemist International (AACCI) Annual Meeting, Providence, New Mexico, USA, October 2014. (Poster)

3. **Zhang, B.**;* Dhital, S.; Flanagan, B. M.; Shelat, K. J.; Selway, N.; Stokes, J. R.; Gidley, M. J. Starch granule 'ghosts': From formation mechanism to lubrication properties. *64th Australian Cereal Chemistry Conference*, Brisbane, Australia, August 2014. (Oral)
4. **Zhang, B.**;* Dhital, S.; Gidley, M. J. Synergistic and antagonistic effects of alpha-amylase and amyloglucosidase on starch digestion. In *American Association of Cereal Chemist International (AACCI) Annual Meeting*, Albuquerque, New Mexico, USA, October 2013. (Oral)
5. **Zhang, B.**;* Dhital, S.; Gidley, M. J. Why are starch granule ghosts not hydrolysed completely? Molecular and microscopic insights into amylase digestion I. In *American Association of Cereal Chemist International (AACCI) Annual Meeting*, Albuquerque, New Mexico, USA, October 2013. (Poster talk)
6. **Zhang, B.**;* Dhital, S.; Gidley, M. J. Why are starch granule ghosts not hydrolysed completely? Molecular and microscopic insights into amylase digestion II. In *Starch Round Table*, Albuquerque, New Mexico, USA, October 2013. (Poster)
7. **Zhang, B.**;* Dhital, S.; Gidley, M. J. Effects of endo- and exo- acting enzymes on starch digestion *in vitro*. *46th Annual AIFST Convention,* Brisbane, Australia, May 2013. (Poster)
8. **Zhang, B.**;* Dhital, S.; Gidley, M. J. Structure-digestibility relationship of maize and potato granule ghosts. *2nd AIFST Food Science Summer School,* Melbourne, Australia, February 2012. (Poster)

Publications included in this thesis

1. **Zhang, B.**; Dhital, S.; Gidley, M. J.* (2015). Densely packed matrices as rate determining features in starch hydrolysis. *Trends in Food Sci. Tech.* 43, 18-31. Incorporated as Chapter 2.

Contributor	Statement of contribution
Zhang, B. (Candidate)	Wrote the paper (100%)
Dhital, S.	Edited paper (30%)
Gidley, M. J.	Edited paper (70%)

2. **Zhang, B.**; Dhital, S.; Gidley M. J.* (2013). Synergistic and antagonistic effects of alpha-amylase and amyloglucosidase on starch digestion. *Biomacromolecules*, 14, 1945-1954. Incorporated as Chapter 3.

Contributor	Statement of contribution
Zhang, B. (Candidate)	Designed and/or conducted experiments (70%) Analyzed and interpreted data (80%) Wrote the paper (100%)
Dhital, S.	Designed and/or conducted experiments (10%) Analyzed and interpreted data (20%) Edited paper (30%)
Gidley, M. J.	Designed and/or conducted experiments (20%) Edited paper (70%)

3. **Zhang, B.**; Dhital, S.; Flanagan, B. M.; Gidley, M. J.* (2014). Mechanism for starch granule ghost formation deduced from structural and enzyme digestion properties. *Journal of Agricultural and Food Chemistry*, 62, 760-771. Incorporated as Chapter 4.

Contributor	Statement of contribution
Zhang, B. (Candidate)	Designed and/or conducted experiments (70%) Analyzed and interpreted data (70%) Wrote the paper (100%)
Dhital, S.	Designed and/or conducted experiments (10%) Analyzed and interpreted data (20%) Edited paper (30%)

Flanagan, B. M.	Designed and/or conducted NMR experiments (10%) Analyzed and interpreted data (10%)
Gidley, M. J.	Designed and/or conducted experiments (10%) Edited paper (70%)

4. **Zhang, B.**; Wang, K.; Hasjim, J.; Li, E.; Flanagan, B. M.; Gidley, M. J.; Dhital, S.* (2014). Freeze drying changes the structure and digestibility of B-polymorphic starches. *Journal of Agricultural and Food Chemistry*, 62, 1482-1491. Incorporated as Chapter 7.

Contributor	Statement of contribution
Zhang, B. (Candidate)	Designed and/or conducted experiments (65%) Analyzed and interpreted data (70%) Wrote the paper (80%)
Wang, K.	Designed and/or conducted experiments (10%) Analyzed and interpreted data (20%) Wrote the paper (10%)
Hasjim, J.	Edited paper (10%)
Li, E.	Designed and/or conducted experiments (5%)
Flanagan, B. M.	Designed and/or conducted NMR experiments (10%) Analyzed and interpreted data (10%) Wrote the paper (10%)
Gidley, M. J.	Edited paper (20%)
Dhital, S.	Designed and/or conducted experiments (10%) Edited paper (70%)

5. Warren, F. J.; **Zhang, B.**; Waltzer, G.; Gidley, M. J.; Dhital, S.* (2015). The interplay of α-amylase and amyloglucosidase activities on the digestion of starch in *in vitro* enzymic systems. *Carbohydrate Polymers*, 117, 192 - 200. Incorporated as Appendix 4.

Contributor	Statement of contribution
Zhang, B. (Candidate)	Designed and/or conducted experiments (40%) Analyzed and interpreted data (20%) Edited paper (10%)
Warren, F. J.	Designed and/or conducted experiments (20%)

	Analyzed and interpreted data (30%) Wrote the paper (100%)
Waltzer, G	Designed and/or conducted experiments (40%)
Gidley, M. J.	Edited paper (40%)
Dhital, S.	Analyzed and interpreted data (50%) Edited paper (50%)

6. Dhital, S; Warren, F. J.; **Zhang, B.**; Gidley, M. J.* (2014). Amylase binding to starch granules under hydrolysing and non-hydrolysing conditions. *Carbohydrate Polymers*, 113, 97 - 107. Incorporated as Appendix 5.

Contributor	Statement of contribution
Zhang, B. (Candidate)	Designed and/or conducted experiments (20%) Analyzed and interpreted data (10%) Edited paper (10%)
Dhital, S.	Designed and/or conducted experiments (80%) Analyzed and interpreted data (70%) Wrote the paper (100%)
Gidley, M. J.	Edited paper (70%)
Warren, F. J.	Analyzed and interpreted data (20%) Edited paper (20%)

Contributions by others to the thesis

I acknowledge Dr Fred Warren for DSC analysis (Chapter 4) and fruitful discussions on digestion kinetics (Chapter 6), Dr Jovin Hasjim, Ms Kai Wang and Ms Sarah Chung for their technical assistance with SEC measurement (Chapters 4 and 6), Dr Heather Shewan and Dr Polly Burey for the HAAKE MAS 3 rheometer training and kind help (Chapter 5), and John Milne for the assistance of starch extrusion (Chapter 6). I also thank the facilities and scientific and technical assistance of Dr Kim Sewell and Dr Ying Yu of the Australian Microscopy and Microanalysis Research Facility at The University of Queensland.

Statement of parts of the thesis submitted to qualify for the award of another degree

None.

Acknowledgements

Foremost, I would like to express the sincere gratitude from the bottom of my heart to my principal supervisor, Prof Mike Gidley for his guidance and support during my PhD study. I can feel his patience, enthusiasm and immense knowledge pulling at me. I could not have imagined having a better teacher and mentor. My co-supervisor, Dr Sushil Dhital, has never failed to support me when times were tough, offer me invaluable advice.

Besides my supervisor, I would like to thank my thesis committee members: Prof Robert Gilbert and Prof Peter Halley for their encouragement, insightful comments, and professional suggestions.

My sincere thanks also go to A/Prof Jason Stokes for your excellent guidance on rheology and soft-tribology area; Dr Bernadine Flanagan for your NMR measurement and interpretation; Dr Kinnari Shelat for the assistance on rheometer training and fruitful discussions.

I thank the staffs and my fellow labmates at Centre for Nutrition and Food Sciences, Centre for High Performance Polymers, and Rheology and Biolubrication Laboratory: Dr Fred Warren, Dr Patricia Lopez-Sanchez, Dr Deirdre Mikkelsen, Dr Jovin Hasjim, Dr Paul Luckman, Dr Heather Shewan, Dr Polly Burey, Dr Gleb Yakubov, Sarah Chung, Cheng Li, Alex Wu, Enpeng Li, Ming Li, John Gorham, Nichola Selway, Prudence Powell for your kind help and support.

My greatest appreciation to the University of Queensland International Scholarship, Chinese Scholarship Council PhD Scholarship, and ARC Centre of Excellence in Plant Cell Walls for the financial support.

Last but not the least, I would like to thank my family: my wife Kai Wang and parents for endless love and support during my study in Australia.

Keywords

starch, *in vitro* enzymatic digestion, crystalline structure, lubrication, granule ‘ghosts’, extrusion, non-ordered structure, local density, enzyme-resistant fraction, kinetics

Australian and New Zealand Standard Research Classifications (ANZSRC)

ANZSRC code: 090801, Food Chemistry and Molecular Gastronomy (excl. Wine), 70%
ANZSRC code: 090408, Rheology, 20%
ANZSRC code: 090805, Food Processing 10%

Fields of Research (FoR) Classification

FoR code: 0908, Food Sciences, 80%
FoR code: 0904, Chemical Engineering, 20%

Table of Contents

List of Figures

List of Tables

List of Abbreviations

ΔH	enthalpy
μ	friction coefficient
AA	α-amylase
AMG	amyloglucosidase
ANOVA	analysis of variance
AUC	area under the curve
CLSM	confocal laser scanning microscopy/microscope
CP/MAS	cross polarised magic angle spinning
CT	cana tuber
Da	Dalton
DB	degree of branching
DMSO	dimethyl sulphoxide
DP	degree of polymerization
DSC	differential scanning calorimetry/calorimeter
ED	ethanol-drying / ethanol-dried
ERS	enzyme resistant starch
FT	frozen-thawed
FTIR	Fourier transform infrared
g	acceleration due to gravity
G50	Gelose 50
G80	Gelose 80
IM	immature maize
K	digestion rate coefficient
MG	maize ghosts or maize ghost suspension
MM	mature maize
MS	maize starch
NMR	nuclear magnetic resonance
NMS	normal maize starch
OD	oven-drying / oven-dried
PG	potato ghosts or potato ghost suspension
PS	potato starch
PT	potato tuber
R_h	hydrodynamic radius

RS	resistant starch
SBD	starch-binding domain
SDS	sodium dodecyl sulphate
SEC	size exclusion chromatography
SEM	scanning electron microscopy/microscope
t	digestion or incubation time
T_c	gelatinization conclusion temperature
T_m	melting temperature
T_o	gelatinization onset temperature
T_p	gelatinization peak temperature
U	entrainment speed
XRD	X-ray diffractometry/diffractometer
WMS	waxy maize starch

Chapter 1

Introduction

Starch is a major energy source in human diets, and is also an industrial commodity-product, extensively used in papermaking, minerals processing, personal care, renewable packaging, biofuels, and other non-food applications. Starch is biosynthesised in a condensed semi-crystalline granular form by the ordered packing of two hydrophilic glucose polymers (amylose and amylopectin) during photosynthesis. It has a complex hierarchical structure, which can be described by at least four levels of organization (i.e., molecular, lamellae, growth ring, and granular levels), ranging in length scale from nanometer to micrometer.

The rate, extent, and location of starch digestion in the small intestine are controlled by intrinsic host factors (e.g., passage rate and multiple enzyme interactions in small intestine, hormonal control, current health status) as well as starch or food structure factors. The undigested starch fraction which exits from the small intestine, is defined as resistant starch (RS), and passes to the large intestine where it functions as a prebiotic for bacterial fermentation.[1] The undigested starch entering the colon also lowers the calorific value of foods (the energy derived by the host from microbial fermentation being only about 30% of that from mammalian enzyme digestion),[2] as well as reducing the glycemic load and insulin responses, associated with reduced risk of developing type II diabetes, obesity, and cardiovascular disease.[3, 4] Fermentation of RS into short-chain fatty acids (acetate, propionate, and especially butyrate) in the colon is reported to protect colonic cells from DNA damage and reduce the risk of colon cancer.[5, 6] Study of starch digestion in human subjects is often expensive, ethically limited, resource intensive, and needs to take individual diversity into account. Therefore, resistant starch is most commonly measured by *in vitro* methods that simulate *in vivo* conditions of starch digestion and referred to as 'enzyme-resistant starch (ERS)'[7] to recognize that *in vitro* methods cannot predict the amount of starch that reaches the large intestine as there are variable host factors which determine this as well as properties of the starch/food.

Most starch-containing foods consumed by humans are processed or cooked by heating in the presence of water (partly) losing their enzyme resistant property. Although the digestion and functional properties of raw starches have been studied extensively, less

attention has been paid to thoroughly exploit the molecular organisation, digestion and physical properties of the non- or low-order starch matrices induced by cooking or processing. It has generally been accepted that crystallinity must play some role in determining enzyme digestion rate. However, recently it has been found that starch crystallinity alone does not always lead to an increase in enzyme resistance; for example, almost amorphous high-amylose starches can provide high yields of resistant fraction.[8] To gain a deeper understanding into the design of starch-containing foods with slow and/or incomplete digestion in the upper gastrointestinal tract, my PhD research mainly focuses on the development of a novel theory and methodology of enzyme-resistant starch with improved health benefits, formed from essentially amorphous (entangled) matrices. It is suggested that local starch molecular density has the major influence on amylase digestion kinetics, and that density sufficient to either limit enzyme binding and/or slow down catalysis can be achieved by either crystallization or dense amorphous packing.

Chapter 2

Literature Review

(Part of this chapter has been published in Trends in Food Sci. Tech. 43, 18-31*)*

*Bin Zhang, Sushil Dhital and Michael J. Gidley**

Centre for Nutrition and Food Sciences, ARC Centre of Excellence in Plant Cell Walls, Queensland Alliance for Agriculture and Food Innovation, The University of Queensland, St Lucia, Brisbane, QLD 4072, Australia

* Corresponding author.

Phone: +61 7 3365 2145; Fax: +61 7 3365 1177. Email address: m.gidley@uq.edu.au (M. Gidley)

2.1 Overview of starch structure at different length scales

Starch, a major digestible carbohydrate in human diets, is synthesised in a condensed semi-crystalline granular form by the ordered packing of two hydrophilic glucose polymers (amylose and amylopectin) during photosynthesis. It has a complex hierarchical structure, which can be described by at least four levels of organization (i.e., molecular, lamellae, growth ring, and granular levels), ranging in length scale from nanometer to micrometer.

2.1.1 Molecular level (Length scale: 0.1 ~ 100 nm)

Normal starch contains two types of polymers: amylose and amylopectin. Amylose comprises 15-35% of granules in most plants, is an essentially linear polymer of α-1,4-linked D-glucose units. The molecular weight (M_w) is between 10^4 and 10^6 g·mol^{-1}, and its average degree of polymerization (DP) is about 10^2 – 10^4.[9-11] Amylose contains up to 10 or more branch points (α-1,6-linkages) per molecule.[12, 13] Some mutants of starches, e.g. high-amylose maize starch, also consist of intermediate component molecules that have lightly branched structures with molecular size similar to amylose.[14, 15]

Amylopectin is a highly branched polymer of α-1,4, α-1,6-linked glucan with typically 5–6% α-1,6 linkages at their reducing end. The M_w of amylopectin ranges from 10^7 to 10^9 g·mol^{-1}, depending on the botanical origin, fractionation, and method used.[9-11] Branch chains of

amylopectin are designated as A-, B-, and C-chains (Fig. 2.1), which are arranged in clusters.[16] A-chains are defined as being unsubstituted by other chains and connected through α-(1→6)-linkage to the rest of the polymer. In contrast, B-chains are substituted by one or several other chains. In addition, each amylopectin polymer contains one single C-chain, carrying the sole reducing end.[16, 17] These chains are assembled as clusters, A- and B1-chains (short chains) form one cluster whereas B2-, B3- and B4-chanins extend though two, three and four clusters, respectively.[18]

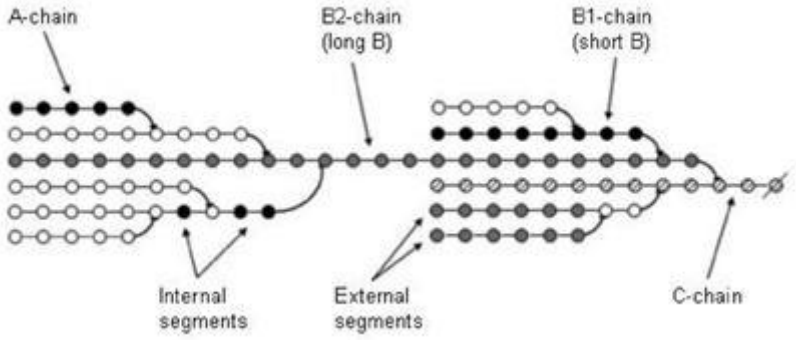

Figure 2.1. Schematic of chains in amylopectin.[17, 19]

2.1.2 Lamellae level (Length scale: ~ 9 nm)

Raw starch granules contain about 15% - 45% crystalline material.[20] The branch chains of amylopectin form double helices (length scale: 1~5 nm) and contribute to starch crystallinity, whereas amylose is considered to be in a largely amorphous state. Starch granules exhibit two main crystalline types identified by X-ray diffraction: A-type starch (mainly in cereals) has a larger population of short branch chains (A and B1 chains), whereas the B-type starch (mainly in tubers and amylose-rich type) has fewer short chains but more long chains (B2, B3 and longer chains).[18] The X-ray diffraction pattern of C-type starch (mainly in legumes) is a mixture of A- and B-type. The double helix packing arrangement and inter-crystalline water of different types of starches might also differ. The A-type crystal form of starches is monoclinic with 8 water molecules per unit cell, whereas the B-type is hexagonal with 36 water molecules per unit cell.[21, 22] The symmetry of double helices differs between A and B structures, maltotriose being the repeat unit in A-type and maltose in B-type structures.[23]

The thickness of a lamella is 9~10 nm as determined using small-angle X-ray scattering technique.[24] The clusters associated with lots of short chains and short repeating distance (9.0 nm for waxy maize starch) crystallize to A-type, whereas longer chains and distances (9.2 nm for potato starch) lead to B-type.[25]

The location of amylose molecules within starch granules is one challenging question remaining to be answered by starch chemists. At present, there are two hypotheses for explanation of the localization of amylose within amylopectin clusters: (a) accumulation of amylose chains within clusters in both amorphous and crystalline regions, in bundles between amylopectin clusters;[26] (b) co-crystallization of amylose molecules with amylopectin branch-chains within crystalline lamellae.[20, 27]

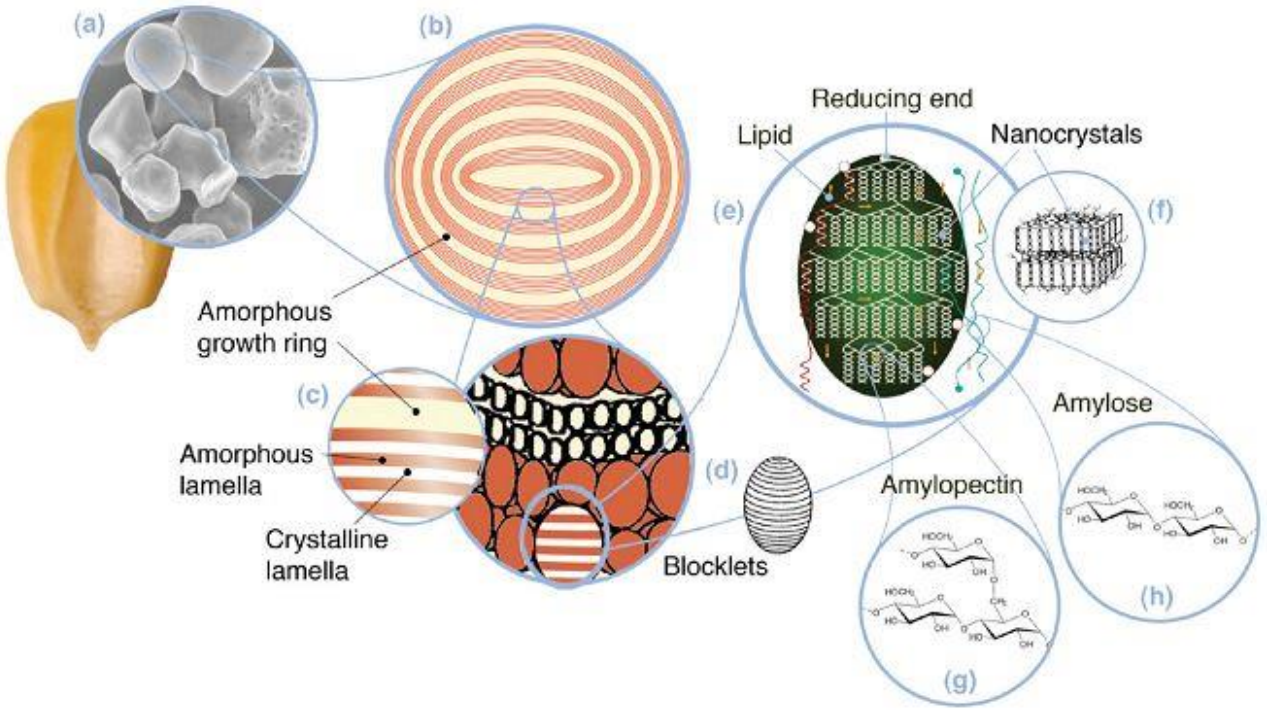

Figure 2.2. Multi-scale structure of starch granules.[19]

2.1.3 Growth ring level (Length scale: 120 ~ 500 nm)

The ‘growth rings’ represent alternating semi-crystalline and amorphous layers, which could be visualized by means of scanning electron microscopy using freeze cracked or partly hydrolyzed granules and light microscopy in hydrated granules. Growth rings grow from the hilum of the granule by apposition, about 120~500 nm thick. The number and thickness of growth rings are reported to be very dependent on botanical origins and amylose content.[26] Cameron and Donald (1992) suggested that the amorphous growth ring is as thick as the semi-crystalline one at least.[28] In contrast to amorphous growth rings containing starch polymers with non-ordered conformation, semi-crystalline layers are envisaged to contain alternating crystalline and amorphous lamellae.[29]

At present, it is suggested that 'growth rings' in either semi-crystalline or amorphous form consist of 'blocklets'.[30] However, the blocklet concept is not completely accepted. Generally, the 'blocklets' of B-type starches (e.g. potato starch, 200~500 nm in diameter) are larger than the A-type starches (e.g. wheat starch, 25~100 nm; maize starch, 20~120 nm in diameter).[30, 31] Consequently, it has been hypothesized by Gallant and co-workers that granule resistance is linked with the blocklet size (i.e. the degree of local crystallinity).[30]

2.1.4 Granular level (Length scale: 1 ~ 100 μm)

Starch granules from different botanical sources show characteristic particle shapes (spherical, polygonal, elongated, oval, etc.) and size (varying from submicron to 150 μm). Some starches (e.g. maize and potato) have a unimodal size distribution, whereas the *Triticeae* family starches (wheat, rye, and barley) have a bimodal size distribution consisting of A-type (larger, disk-like) and B-type (smaller, spherical) granules.[32] Starch granules show clear birefringence under a polarized light microscope: the observed 'Maltese' cross is characteristic of a radial orientation of crystallized polymers.[31]

The A-type starch granules have more pores on the surface than B-type starch granules. These pores go through the growth rings to the hilum of starch granules.[33] Wheat, potato, and oats granules are reported to have small protrusions on the surface. The size of these nano-sized particles suggests that they may correspond to either single or double helical amylopectin side chain clusters bundled into larger 'blocklets' packed in the lamellae within the starch granule.[34]

The amylose content increases with kernel maturity and granule size. Surface gelatinization has revealed that amylose content is slightly higher at the periphery than at the centre.[35, 36] This increase agrees with the report that granule-bound starch synthase I, the primary enzyme for amylose biosynthesis, increases and maximizes at late developmental stage of the storage organs.[37] The amylopectin molecules at the periphery also consist of a greater amount of shorter branch chains than those at the core of maize and potato granules.[35, 36] This could be attributed to the increase in expression of branching enzyme IIb, which is responsible for transferring short branch chains, during kernel development.[38]

2.2 Minor components in starch granules

Starch granules also contain other minor components in small quantities, such as lipids, proteins and minerals. Table 2.1 compares the chemical composition of some commercial starches. Lipids and proteins are present at both the periphery of the granule and inside the granule (e.g. trapped biosynthetic enzymes).

Table 2.1. Chemical composition of some commercial starches.[39-41]

Starch	Amylose (%)	Lipid (%)	Protein (%)	Phosphorus (%)	Ash (%)
Maize	27	0.7	0.35	0.02	0.1
Waxy maize	<1	0.15	0.25	0.01	0.1
Wheat	28	0.8	0.4	0.06	0.2
Tapioca	17	0.1	0.1	0.01	0.2
Potato	23	0.05	0.06	0.08	0.4
High-amylose maize	50~80	0.7	0.3	0.09	-

2.2.1 Lipids

The cereal starches contain a higher percentage of fatty substances (approximately 0.7~1.2%) compared to tuber and root starches (approximately 0.08~0.19%), which are predominantly lysophospholipids (wheat, rye and barley,) and free fatty acids (maize and other cereals).[42] Both surface and internal lipids may be present in a free state, in the form of amylose complexes or linked to starch polymers via ionic or hydrogen bonding.[41, 43]

The 'surface' material is defined as the extractable material under mild conditions.[44, 45] A large portion of the lipids is typically located at the periphery of the granule.[46] The surface lipids are mainly neutral lipids (e.g. triglycerides, free fatty acids, glycolipids, phospholipids etc.).[41, 47] Higher amounts of starch-lipid complexes have also been found at peripheral parts of kernels than inner parts.[48] Lipids inside starch granules are considered to be true starch lipids.[44] Isolation of the internal materials requires some disruptive methods like higher temperature extraction, chaotropic agents or degrading enzymes.[44] The internal lipids of cereal starches are mostly monoacyl lipids (e.g., lysophospholipids, free fatty acids),[49] and are thought to be membrane products.[45]

2.2.2 Proteins

The protein in starch granules generally consists of two distinct types: (a) storage proteins (e.g. gluten, gliadin proteins) from the endosperm; and (b) granule-associated proteins (GAPs), which are believed to be residual biosynthesis enzymes.[50] Surface proteins in starch granules are often dominated by storage proteins, and also contain some low molecular weight GAPs (M_ws of ~5, 8, 15, 19 and 30k Da); Higher molecular weight GAPs (M_ws of ~60, 77, 86, 95 and 149k Da) are located inside granules and termed 'internal proteins'.[51] However, some higher M_w GAPs (e.g. GBSS I, M_w ~60 k Da) are located at the granule surface, whereas certain of the lower M_w GAPs (e.g. the 30 k Da protein) can also be located at the core.[50, 52, 53] Association of surface proteins and lipids can act as a physical barrier to granule swelling and enzyme attack. The cross-linked surface proteins from mung bean starch decreased swelling power and enzyme susceptibility.[54] However, removal of surface proteins from rice starch by chymotrypsin treatment did not affect swelling.[55]

2.2.3 Phosphorus

Compared to other minerals, phosphorous is found in large quantities in starch granules. Phosphorus has three major forms in starches: phosphate monoesters, phospholipids and inorganic phosphorus. Most cereal starches contain phospholipids, whereas phosphorus in root and tuber starches is in the form of phosphate monoesters with some inorganic phosphorus.[56] Waxy starches contain mainly phosphorus in the form of phosphate monoester and small amounts of phospholipids.

Table 2.2. Phosphorus content in starches determined using ^{31}P nuclear magnetic resonance spectroscopy.[56]

Starch	Phosphate monoesters (%)	Phospholipids (%)	Inorganic phosphorus (%)
Maize	0.003	0.0097	0.0013
Waxy Maize	0.0012	ND	0.0005
Wheat	ND	0.058	Trace
Tapioca	0.0062	ND	Trace
Potato	0.086	ND	0.0048
High-Amylose Maize	0.005	0.015	0.0076

Phospholipids and phosphate monoesters have different impacts on paste properties of starch. Potato starch has a relatively large amount of negatively charged phosphate monoester (~0.086%) linked to the amylopectin, equivalent to one phosphate in 13 branch chains. The repulsion effect of negatively charged groups helps to untangle the crystalline polymers and extends the sphere of influence, resulting in increased paste viscosity and clarity and decreased gelatinization tempterature.[39] Cations of salts, such as Na^+ and Ca^{2+}, mask the negative charges of phosphate groups and reduce the repulsion force between negative charges on starch chains, thus lowering the viscosity of potato starch paste. Phospholipids, through starch-lipid complex formation, can decrease the paste clarity and viscosity.[57]

2.3 Starch swelling, gelatinization and retrogradation

Starch granules swell when heated in the presence of water, a process that requires the loss of ordered structures. Starch 'gelatinization' is an irreversible change from a semi-crystalline structure to an amorphous conformation, which is associated with granular swelling, water uptake, loss of double helice and birefringence, and starch solubilization. The changes from a gelatinized starch to a more ordered state during cooling and/or storage processes are referred to as 'retrogradation' (Fig. 2.3).

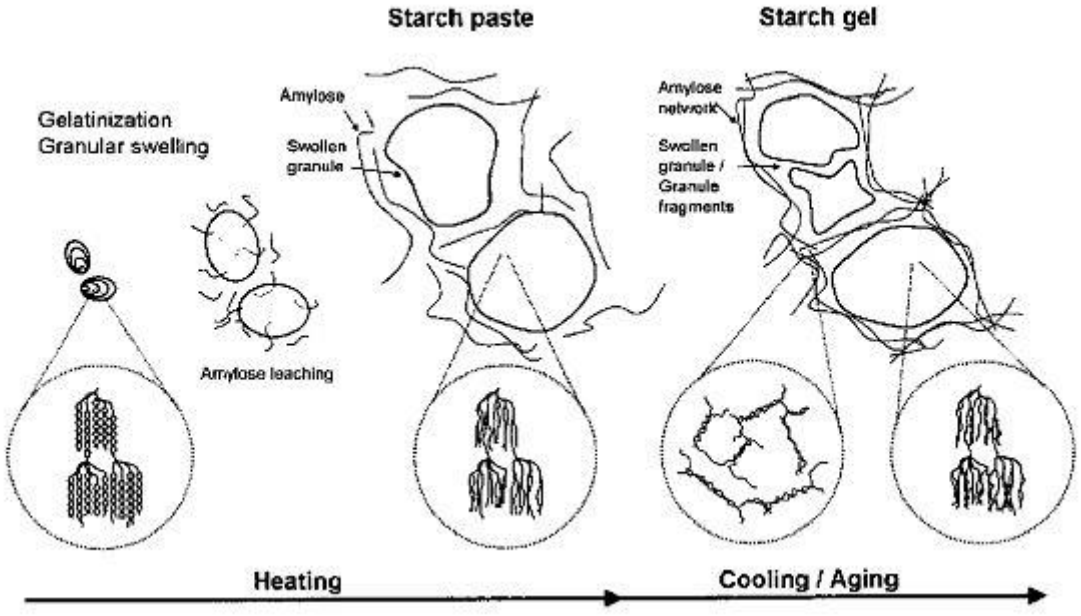

Figure 2.3. Schematic representation of starch swelling, gelatinization, and retrogradation processes.[58]

2.3.1 Swelling

Swelling is a characteristic behavior of starch, and is often regarded as the first stage of the gelatinization process. Amylose and low molecular weight amylopectin are the main materials leached out from granules, with the concentration of solubilized amylopectin increasing with temperature.[59] During granular swelling, the hydrogen bonds between starch chains are dissociated and replaced with hydrogen bonds with water molecules.[58] Swelling behaviour is primarily a property of amylopectin, while amylose acts both as a diluent and as an inhibitor of swelling, especially in the presence of lipids (which can form insoluble complexes).[60-64] Swelling processes can be monitored by different methods, such as light microscopy, viscosity and rheology.

Starch from different botanical sources has characteristic swelling behavior (rate and extent), resulting in various paste and rheological properties and application performance. Three classes of swelling behaviour of starch granule have been identified by Debet and Gidley[44]: (a) rapid swelling (e.g. waxy maize, potato, tapioca), (b) slow swelling that can be changed to rapid swelling by surface material extraction (e.g. wheat, maize), and (c) limited swelling (e.g. high amylose starches). The swelling behaviour of starch granules depends on polysaccharide composition (amylose and amylopectin) and minor components, mainly lipids and proteins. Rapidly swelling starches are more shear sensitive, and typically contain less proteins and lipids.[44] Lipids, proteins and amylose are all necessary to restrict swelling in wheat and maize starches.[44] However, swelling of the high-amylose starch is dominated by the starch polymer composition, and the lipids and proteins only have a secondary effect.[44]

2.3.2 Gelatinization

Starch gelatinization is an endothermic reaction, which corresponds to the dissociation of starch molecules from a semi-crystalline structure to an amorphous conformation. Water acts as a plasticizer in the gelatinization process, and the presence of water will decrease the glass transition (T_g) and the melting (T_m) temperatures. High water content (water/starch) > 2, is required to obtain the characteristic gelatinization temperature without limitation of water. Gelatinization is primarily a swelling driven process, and initial water absorption happens within amorphous growth rings as revealed by small angle X-ray/neutron scattering techniques.[65-67] Swelling within the amorphous regions imposes a stress upon the amylopectin crystalline structure, and ultimately this stress will cause double helix dissociation and breakdown of granule integrity.[68] Many techniques have

been employed to monitor this process, such as polarized light microscopy, (synchrotron) X-ray diffraction and scattering, nuclear magnetic resonance (NMR) and thermo-mechanical analysis. The gelatinization temperatures and enthalpy change are commonly measured by differential scanning calorimetry (DSC).

2.3.3 Retrogradation

Amorphous gelatinized starch is transformed to a more ordered state during the retrogradation process. The retrogradation process is a spontaneous one to lower free energy, which happens readily during cooling or storage. Starch precipitates, due to molecular interactions (mainly hydrogen bond between starch chains, e.g., formation of double helices), and forms during cooling and the aging process of starch dispersions.[69] Amylose retrogrades faster than amylopectin because of the linear structure and the higher mobility of the amylose molecules. Amylopectin retrogrades slowly over several days or weeks.[70, 71] Co-crystallization between amylose and amylopectin is likely enhanced, when amylose is present in a large concentration.[72] The presence of lipids forms complexes with amylose and can prevent amylose from retrograding. The common methods for measuring the retrogradation rate and extent are (synchrotron) X-ray diffraction, thermo-mechanical analysis and rheological techniques.

2.4 Classification and mechanisms of enzyme-resistant starch

Based on their origins, ERS have been classified into four categories: (1) physically inaccessible starch; (2) native granular (B- or C-type polymorph) starch; (3) retrograded starch; (4) chemically modified starch.[1] Recently, starch-lipid complex was proposed to be a new type of ERS.[73-75] This traditional classification implies that ERS is a thermodynamically defined physical entity. However considering the complexity of starch hydrolysis, recent evidence suggests that ERS can be better expressed as a kinetic phenomenon. In this way (physiological) resistant starch is understood as that fraction of starch which has not had sufficient time to be digested in the small intestine, rather than being completely resistant to amylolysis (with the possible exception of highly chemically-modified starches).

Understanding factors that influence the kinetics of starch hydrolysis requires identification of relevant rate limiting steps. It has recently been proposed that there are two types of rate-limiting steps, namely (i) barriers that slow down or prevent access/binding of enzyme to starch or (ii) structural features that slow down or prevent amylase action (after initial

binding) [76]: Intact plant tissues, whole grains and complex food products are perhaps the best representatives of an ERS material caused by barriers. In these cases, starch is encapsulated by dietary components such as proteins, lipids and plant cell walls, which restrict enzyme diffusion and hence access to starchy substrate. However, it is not only physical barriers which can limit binding, as the surface of certain granules (e.g. potato) show less binding of fluorescently-labelled amylase than maize starch granules [77] despite the surfaces of both being dominated by starch polysaccharides; indeed maize starch has more surface proteins and lipids than potato starch. This suggests that the supramolecular structure at exposed surfaces of B- or C- polymorphic starch granules is effectively a hard outer shell and acts as a barrier to limit rate-limiting binding of digestive enzymes, and account for its relatively resistant nature. Therefore, barriers which make binding rate-limiting and lead to ERS character are often found in unprocessed foods such as intact plant tissue, whole or partly milled grains and seeds, raw B-type starch etc.

Similarly, after initial binding, starch structural features such as chemical structure and local molecular density are likely to control the digestion kinetics of starch as these can hinder adoption of enzyme conformations that lead to productive hydrolysis. Examples of chemical structures leading to ERS character include α-limit dextrin (only resistant to α-amylase, not brush-border sucrose/isolmaltase or maltase/glucoamylase), pyrodextrin, chemical modified starches.[78-81] The currently accepted mechanism for the enzymatic resistance of this sub-category is that either the (introduced) branched glucan structures (e.g., α-limit dextrin, octenylsuccinate starch) or formation of atypical linkages (e.g., dextrinization) render the α-1,4 glucosidic linkages adjacent to the branch points inaccessible to amylase. A further category of the physical state of starch which can affect starch digestion rates is matrices/molecules with high local molecular density. Examples include some processed starches, including retrograded starch, starch-lipid complex, and some specific species/conditions (examples will be discussed later in this review). From the point view of food engineering, most starch-based foods are processed before consuming, and become less ordered and more accessible to enzyme in most cases after processing. However, the digestibility of processed starch is not always higher than that of (densely-packed) granular starch. Parchure and Kulkarni [82] reported that the ERS contents of rice and waxy amaranth starch subjected to pressure cooking were increased, compared to those of native starches.

Although much information is available on factors which impact on *in vitro* digestibility such

as starch characteristics, modification, encapsulation,[83-85] to the best of our knowledge, nothing similar has been summarized for ERS from densely packed food matrices (particularly for weakly- or non-crystalline forms). This review will focus on the role of local molecular density on starch digestion kinetics, with the principle being that density sufficient to either prevent/limit binding and/or slow down catalysis can be achieved by either re-crystallization or dense amorphous packing. We also briefly discuss enzyme interactions and data interpretation in commonly used *in vitro* starch digestion models, as this impacts on the characterization of the role of dense packing on starch amylolysis.

2.5 Starch digestion *in vitro*: Enzyme interaction and data interpretation

Resistant starch is defined as the sum of starch and products of starch degradation not absorbed in the small intestine of healthy individuals, and supposed to be predicted by physiological techniques.[86] Although several *in vivo* techniques such as ileostomy and intestine intubation have been accepted as a reliable and direct method and performed earlier for the study of carbohydrates and starch digestion,[86-88] *in vivo* models are expensive, ethically constrained, and specialized to nutritional or clinical study. *In vivo* trials typically use precisely controlled and repetitive meals, whereas humans are used to diverse diets so it is difficult to study a human diet in a well-controlled way to predict health outcomes.[89] The drawbacks also include that limited information is available for understanding the mechanism of food structural changes during the digestion time course. *In vitro* methods simulating various aspects of the complex human digestion environment are widely used to study the gastro-intestinal behaviour of food under relatively simple conditions and suitable for mechanistic studies and hypothesis building for food scientists.

2.5.1 Starch digestion *in vitro*: Enzyme interaction

As a biochemical mimic of *in vivo* conditions, *in vitro* study of starch digestion is normally carried out using two kinds of enzyme: porcine pancreatic or human salivary α-amylase, and fungal amyloglucosidase. The reason for the use of (excess) amyloglucosidase as a final step to convert all end products of α-amylase action to glucose is that mucosal α-glucosidases extracted from animal models are not yet available commercially, and fungal amyloglucosidase has similar functionality. The rate of enzymatic action is very dependent on conditions such as temperature and pH, although they occur generally at the optimal pH of ~5 and at temperatures around 37 °C. In this section, the structure of digestive enzymes and the nature of interaction between α-amylase and amyloglucosidase are briefly reviewed.

α-Amylases (α-1,4 glucan-4-glucanohydrolase, EC 3.2.1.1) comprise different kinds of enzymes from animals, plants, and microbes. In mammals, α-amylases are produced mostly by salivary glands and the pancreas. α-Amylases hydrolyze starch by an endo-action at inner α-1,4 linkages of starch molecules, and their products have α-configuration at the anomeric carbon of the newly produced reducing end. However, α-amylases from different sources have different product specificities, which are due to differences in the length, folding and amino acid sequences of the enzyme protein.[90] Human salivary and porcine pancreatic α-amylases, two commercial α-amylases commonly used for *in vitro* starch digestion, show similar 3D structures from X-ray crystallography.[91, 92] Either human salivary or porcine pancreatic α-amylase has three structural domains, about 5 nm in diameter. The domain A has a structure consisting of an eight-stranded alpha/beta barrel that contains the important active site residues.[93] Domain B, protruding between beta strand 3 and alpha helix 3, probably plays a role in maintaining protein conformation and Ca^{+} binding. The function of the C-domain is not known, but mutations in the C domain of the α-amylase from *Bacillus stearothermophilus* suggest that it is involved in enzyme activity.[94]

Human salivary and porcine pancreatic α-amylases also show similar actions on starch.[95] They hydrolyze starch to soluble oligosaccharides (G2 (maltose), G3 (maltotriose), G4 (maltotetraose)) and α-limit dextrins that have one or two α-1,6 linkages. Robyt and French [96] postulated that porcine pancreatic α-amylase has five D-glucose binding subsites and that the catalytic groups are located between the second and third subsites from the reducing-end subsite. This hypothesis has been confirmed by the 3D domain architecture deduced from X-ray crystallography.[93] However, human salivary α-amylase has six D-glucose binding subsites, with catalytic groups located between the second and third subsites.[97] Glucose is a very minor product of α-amylase digestion. Only G3 and G4 can be slowly hydrolyzed into maltose and glucose after prolonged incubation by a subsidiary site.[98] α-Amylases have a high degree of multiple-attack hydrolysis pattern, with an average of seven hydrolytic cleavages occurring per productive encounter for the porcine pancreatic α-amylase, and three for the human salivary α-amylase.[90, 99]

Another widely used starch degradation enzyme is amyloglucosidase (often called glucoamylase, EC 3.2.1.3, 8 – 10 nm in size), usually from *Aspergillus niger* (AMG-I). It can produce β-D-glucose from the non-reducing ends of starch chains by exo-hydrolysis of

both α-1,4 glycosidic linkages and, at a slower rate, α-1,6 glycosidic linkages.[100] The specific activity towards the α-1,6 linkage is only 0.2% of that for the α-1,4 linkage.[101] Only AMG-I contains an N-terminal starch-binding domain (which is essential for the enzyme to hydrolyze granular starches) that is distinct from the C-terminal catalytic domain (active site).[102] Recent studies indicate that the starch-binding domain not only binds onto starch, but also disrupts double helical structures and enhances the rate of hydrolysis.[103, 104] It was postulated that amyloglucosidase from *Aspergillus niger* has seven subsites for binding near the active site, and its catalytic site is located between subsites 1 and 2.[105] Moreover, the subsites possess variable affinities: the affinity of the first subsite is very low, whereas subsite 2 has the highest affinity and the affinity of the individual sites decreases from subsite 3 to 7.[106] Amyloglucosidase has a multi-chain hydrolysis mechanism, i.e., after the glycosidic bond is cleaved by amyloglucosidase, the remaining starch chain must dissociate and leave the active sites before glucose can leave.[107] The active sites of the amyloglucosidase are 'pocket like', which ensure that only a single, β-conformational glucose can be produced.

The conventional view of starch digestion is that α-amylase is the limiting digestive enzyme that determines overall digestion rate. This is indeed the case for granular starch digestion: α-amylase supplies new substrates for amyloglucosidase by endo-wise splitting of large molecules. However, it was recently found the mucosal α-glucosidases secreted in intestinal villus do not simply passively convert the end products of α-amylase digestion (i.e., malto-ologosaccharides) to absorbable glucose, but are capable of acting directly on polymeric starch.[108, 109] Therefore, the interdependence between human α-amylase (including salivary amylase and two forms of pancreatic amylase) and mucosal α-glucosidases need to be further investigated and taken into account when predicting the digestion rate/extent of starch with different physical structures.

2.5.2 Starch digestion *in vitro*: Kinetic data interpretation

Many starch digestion processes are heterogeneous reactions, involving an interaction between solid substrate (e.g., starch granules, food particles) and soluble enzymes. Although the starch can be gelatinized /processed, it seldom forms a true solution, and this structure is greatly influenced by the botanical source and previous processing history. Individual particles e.g. granular starches or processed starches vary in their response to enzymatic susceptibility,[110, 111] and what behaves as resistant starch in one person may not behave the same way in another,[112] presumably because of differences in enzyme

secretion levels, passage rates etc. For a given starch sample, only the mean value of digestion rate/extent for whole populations of particles can be measured under defined experimental conditions and enzyme concentration. Kinetic models and data interpretation for evaluating the rate of *in vitro* starch digestion are summarized below, including the classical Michaelis-Menten (M-M) kinetics more focusing on the initial rate and the first-order kinetics for prolonged hydrolysis.

2.5.2.1 Michaelis-Menten kinetics

The classical M-M kinetics is only appropriate for the initial stages of amylase digestion of starches (the part of a reaction in which <5% of the substrate has been consumed), as represented as following scheme:

$$E + S \underset{k_{-1}}{\overset{k_1}{\rightleftharpoons}} ES \overset{k_2}{\Rightarrow} E + P \qquad \text{(Eq. 2.1)}$$

The enzyme (E) and substrate (S) first combine to give an enzyme-substrate complex (ES). Then the chemical processes take place in a second step to break down ES and produce product (P) with a first-order catalytic constant k_{cat} (also called k_2 or the turnover number). It is found experimentally that the initial rate (v) of enzyme reaction on starch can be calculated by the M-M equation using three standard assumptions: (a) The enzyme concentration in the reactions is small relative to the substrate concentration; (b) Only initial rate conditions are considered. Thus, there is very little accumulation of P, and the formation of ES from E + P is negligible; (c) Steady-state assumption. The rate of breakdown of ES equals the rate of formation of ES.[113]

$$v = \frac{k_{cat} E_o S}{K_m + S} \qquad \text{(Eq. 2.2)}$$

where k_{cat} is catalytic constant, E_0 is the total enzyme concentration, K_m is the M-M constant which is equivalent to $(K_{-1}+K_2)/K_{+1}$, and S is the initial substrate concentration. The V_{max} is the maximum rate of the reaction, which equivalent to k_{cat} times E_0. The velocity of liberation of reducing sugars as a function of only initial (low) starch concentrations can be described through a simple M-M equation, because product inhibition and substrate exhaustion might cause the reaction velocity to decay with prolonged hydrolysis time.[114]

2.5.2.2 First-order kinetics

When starch or starch-containing foods are digested *in vitro* with amylase or in combination with amyloglucosidase, the rate of reaction decreases as the time is extended and plots of the concentration of product formed (or quantity of starch digested) against

time are logarithmic. The decrease of the digestion rate over time course is a natural feature of an exponential reaction.[115] This substrate decay process fits a single rate coefficient (i.e., first-order equation) as follows.[116]

$$C_t = C_\infty \left(1 - e^{-kt}\right) \quad \text{(Eq. 2.3)}$$

where t is the digestion time (min), C_t is digested starch at incubation time t, C_∞ is digestion at infinite time, and k is rate constant (min^{-1}). One obvious problem in using this simple equation comes from the need for an accurate estimate of C_∞.[115] Unless the enzyme-catalyzed digestion is allowed to run for a long time, digestibility curves cannot be guaranteed to have reached a true end point. In order to solve this problem, Butterworth, Warren, Grassby, Patel and Ellis [115] introduced a modified Guggenheim method to calculate the rate constant where C_∞ is unknown, and the equation is cast in the form:

$$\ln\left(\frac{dC}{dt}\right) = \ln(C_\infty k) - kt \quad \text{(Eq. 2.4)}$$

Thus, a plot of ln(dC/dt) against t is linear with a slope of $-k$, and the C_∞ can be calculated back from the intercept of the equation and slope k. The rate constant is a function of the fixed amylase and starch concentrations used in the digestion, and is therefore pseudo-first order.

Figure 2.4 shows amylase digestion data and fitting plots of raw and cooked wheat and pea starches.[115] For the cooked wheat and pea starches, the whole digestion process can be well fitted by first-order behavior with a single rate constant (k value) under a porcine pancreatic amylase concentration of 0.165 IU/mL (2.25 nM). In contrast, granular starch digestion shows a two-phase kinetic profile at a higher amylase concentration of 0.33 IU/mL (4.5 nM). This suggests that there is a rapid digestion process that takes place in the first 20 min, likely due to hydrolysis of more available polymers attached to the surface of starch granules. The subsequent first-order rate process is believed to be the main single rate process with lower k value of the pea starch for both processes at an amylase concentration of 0.33IU/mL (4.5nM) (Figure 1 C, D). Thus, the starch substrates do not seem to consist of distinct structural fractions such as rapidly digestible and slowly digestible starches that differ in digestion rate. Instead, the amount of starch digested fraction in a given sample is under kinetic more than thermodynamic control.[8] So starch fractions described as enzyme-resistant by remaining after digestion using a certain enzyme activity/time/temperature treatment can be further digested by e.g., application of more enzyme.[8] The first order model, however, cannot be directly applied in some *in vitro* cases, such as (i) those which use low catalytic dosages (giving a linear kinetic profile and resulting in zero-order kinetics,[117] (ii) when inhibitory products are allowed to build up,[118]

and (iii) where structural and molecular changes take place during the digestion process such as in high-amylose maize starch.[8, 119]

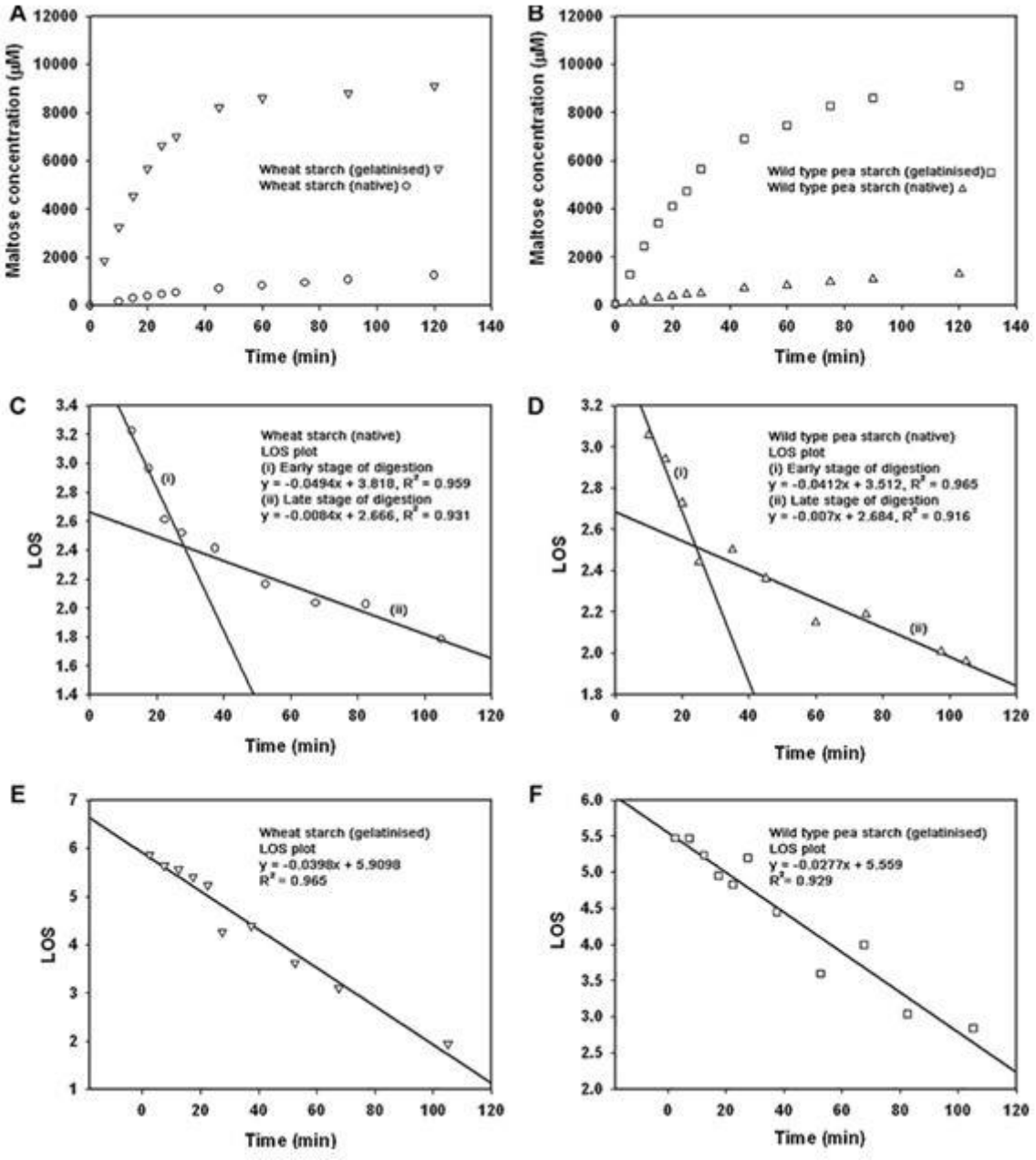

Figure 2.4. Digestion profiles and fitting plots of raw and cooked wheat and pea starches. Notes: Digestion profiles of raw and cooked wheat (A) and pea (B) starches; Fitting plots for raw wheat (C), raw pea (D), cooked wheat (E), and cooked pea (F) starches.[115]

2.6 ERS from densely packed matrices: mechanisms and categories

As illustrated above, if starch chains are arranged in an appropriate form with high local molecular density, lower digestion rate/extent can be achieved with potential for human health benefit. This can occur either through reductions in the ability of amylase to bind to the substrate and/or reduction in the rate of enzyme action once bound. Two potential

ways to produce densely packed ERS are (re-)crystallization and dense amorphous packing, which are reviewed below.

2.6.1 (Re-)crystallization

2.6.1.1 Retrogradation

Raw starches contain between 15% and 45% of crystalline material.[20] The branch chains of amylopectin form double helices and contribute to starch crystallinity, whereas amylose is considered to be in a largely amorphous state. The double helix packing arrangement and inter-crystalline water of different types of starches might also differ, which can be identified by X-ray diffraction or solid state ^{13}C NMR.[120] The dense A-type crystal form of starches is monoclinic with 8 water molecules per unit cell, whereas the B-type has a hexagonal unit cell with 36 water molecules per unit cell, and is more open compared to monoclinic unit cells.[21, 22] These crystalline unit cells are disrupted during cooking of starch in excess water, with a change from semi-crystalline starch structure to amorphous conformation. However, during cooling and/or storage, gelatinized starch is transformed from initially an amorphous state to a more ordered or crystalline state in a process termed retrogradation.

The typical conformational changes of amylose during retrogradation are shown in Figure 2.5. Amylose in aqueous solution exists as a random coil [121] that can re-crystallize into either A- or B-type double helices during cooling and the aging process of starch dispersions, as a spontaneous process resulting in a metastable state of lower free energy.[69] Infinite aggregation of double helices generates a three-dimentional network with different microstructure features such as cristallinity and porosity, which is based on interchain junction zones of double helices with DP 10 – 100.[122] Retrograded amylose is thermally very stable with a high melting temperature (120 - 170 ^{o}C), and amylose content and ERS yield are normally positively correlated.[123, 124] Amylose re-crystallizes much faster (completed within 24 h) than amylopectin (can continue for weeks) because of the linear glucan structure and higher mobility of amylose.[125, 126] The branched nature of amylopectin inhibits its recrystallization to some extent, and the partially crystallized amylopectin tends to form a network in excess water.[70, 71] A low melting temperature in the range of 40 - 60 ^{o}C can be obseved, due to the dimensions of the chains involved in the crystallisation process.[127] However, once debranched by isoamylase or pullulanase, the resulting short linear chains become mobile and can retrograde as linear amylose chains. These retrograded chains were shown to be effective in generating ERS.[128]

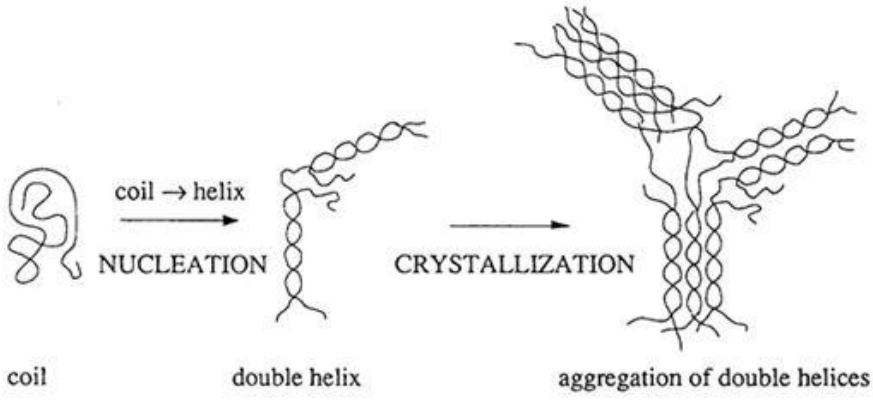

Figure 2.5 Conformational changes occurring during retrogradation.[129]

Storage time and temperature are critical factors in the formation of retrograded starch in an excess of water and hence, a determinant of the rate of starch digestion. Thus, manipulation of starch crystallization conditions is widely applied to control the digestibility of starch-based foods. Eerlingen, et al. [130] found that ERS yields of retrograded wheat starch strongly depend on the storage temperature and time, as shown in Figure 2.6. They found that initially (~15 min) formation of ERS is favored at 0 °C (yield about 4%), whereas the ERS content (~10%) after prolonged incubation was higher at 100 °C. The level of ERS at 68 °C had an intermediate formation rate at either initial or extended stages. The initial fast formation of ERS was explained by nucleation rate increases with decreasing temperature below the melting temperature (T_m, ~ 150 °C) and above the glass transition temperature (T_g, ~ -5 °C). However, over a longer time period, crystal growth was favored at 100 °C, closer to the T_m of the crystals. The theoretical maximum value of crystallization rate (both nucleation and growth) is expected at a temperature $T \approx 1/2 (T_g + T_m)$, which is close to 68 °C,[131] whereas the real aggregation rate is faster at lower temperatures due to decreased chain mobility.[132] A more effective way to increase crystallization is to temperature cycle between low nucleation temperatures and high crystal growth temperatures.[131] It should be noted that ERS content did not increase remarkably after reaching a plateau (Figure 2.3B), although the crystallinity increased with storage time at higher temperatures (68 and 100 °C). The storage temperature also influenced the type of crystal: a B-type crystal formed at 0 and 68 °C, whereas A-type polymorph structure formed at 100 °C. The A-type polymorph is suggested to be a thermodynamic product with dense crystals, whereas the B-type polymorph is the kinetic product requiring the least entropy change from solution.[133] The B-type crystallites may form temporarily, but this structure may rearrange to form the more stable A-type structure. A general rule is that A-

type crystallites are favored at high temperatures, short average chains, higher concentrations, and presence of salts, water-soluble alcohols, organic acids.[133, 134]

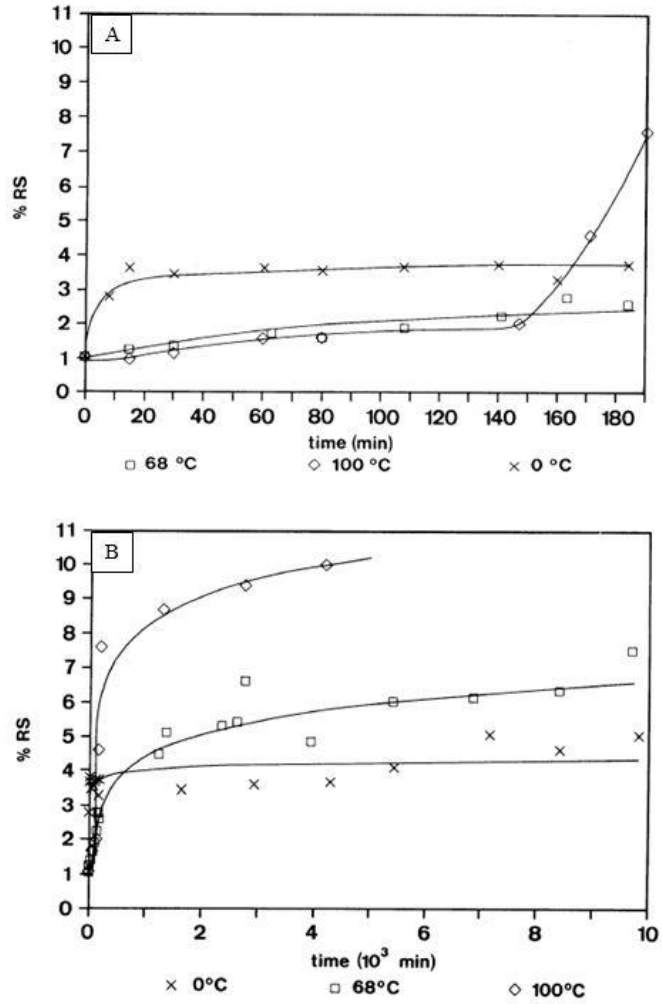

Figure 2.6. Kinetics of enzyme-resistant starch formation during wheat starch retrogradation at different temperatures (0, 68 and 100 °C) as a function of time (A, first 200 min; B, extended time period).[130]

Gidley and Bulpin [132] found that re-crystallization and gelation behavior of amylose in aqueous solution (0.2 – 5.0 %) show a dependence on chain length (synthesized *in vitro* using potato phosphorylase, degree of polymerization (DP) ranging from 40 to 2800). The maximum re-crystallization rate was found for chain lengths of ~ 100 residues in dilute (< 0.1 %) solution at initial stages of the process, corresponding to the so-called 'dissolving gap' for amylose in the DP range 35 - 900.[135] Short-chain amylose (DP < 110) can be re-crystallized at all concentration up to 5.0 % upon cooling hot aqueous solution (70 – 80 °C). More specifically, amylose with DP 40 and 65 results in fine and dense re-crystallized precipitates, whereas precipitates from DP 90 and 110 are less dense. For the amylose

with DP from 250 to 600, both re-crystallization and gelation occur for chain lengths of 250-660 residues, depending on the amylose concentration. For long-chain amylose (DP > 1100), gelation predominates over re-crystallization at all concentrations, due to the formation of a macromolecular network with extensive cross-linking (via hydrogen bonding and/or hydrophobic interactions). Eerlingen, Deceuninck and Delcour [126] found that the chain length (DP 19 - 26) and crystalline structure (type and crystallinity level) of the ERS obtained is independent to the amylose chain length (DP 40 - 610). A minimum DP of 10 and a maximum of 100 seems to be necessary to form the double helix.[122] However, according to Eerlingen, Deceuninck and Delcour [126], the yield of ERS increased with DP (~19 %, DP 40) to plateau values of 23 – 28 % (DP 100 - 610). It was postulated that short-chain amylose (DP 40 - 100) contains a relatively high concentration of chains that do not have dimensions critical for incorporation in the crystalline structure.

Although it is well understood that the molecular basis for amylose aggregation is the adoption of a left-handed, parallel-stranded double helical conformation followed by helix-helix aggregation,[69] mesoscopic information on retrograded starch is limited, particularly for the amorphous fraction. The amorphous fraction can be more easily degraded by acid than the crystalline fraction. It was proposed to consist of dangling chains (6 < DP < 30) and linked to double helices in the macroporous network, and proposed to be mainly responsible for the hydrodynamic behavior and the network porosity.[136] Cairns, et al. [137] prepared retrograded amylose gels and studied their ERS fraction after 24 h enzyme hydrolysis at 37 ^{o}C. The storage time (1 or 7 day) and enzyme hydrolysis did not affect the average molecular weight (DP 66) and size (8.3 nm) of retrograded crystallites, although the crystallinity of amylose gels with 7 days of storage was ca. 2 times higher than that of 1 day storage. They found that the ERS yield non-linearly increased with the level of crystallinity, due to a slow formation of perfect crystals from some internal defects. One model that was postulated is that the crystals (~10 nm long) may be discontinuous, with a substantial amorphous portion shielded from enzyme digestion by entrapment within the crystal structure.[137, 138] In principle, if starch polymers are arranged in a dense enough form (i.e., high local molecular density), they can decrease the digestion rate even if the food matrices are amorphous. Zhang, et al. [139] reported that the crystalline and amorphous contents of partially digested granular starches were unchanged from the native values. This could either mean that (as suggested by the authors) both crystalline and amorphous regions are digested side-by-side, suggesting that local density of non-order structures formed by plant biosynthesis is as high as that of crystalline regions, or that the rate-

limiting step for enzymic hydrolysis of granules occurs prior to active digestion i.e. binding is rate-limiting and any differences between the intrinsic rate of digestion of crystalline and amorphous fractions are small compared to a slower binding step.[76] In either case, non-crystalline material apparently contributes to the rate-limiting step, again illustrating the concept that it is not only crystalline material that can achieve sufficiently high molecular density to slow down amylase digestion.

It should be emphasised that the ERS is a measurement- and method-oriented concept, i.e., the enzyme resistance is explained by the limited time and concentration that the enzymes act on the starch substrate. Bird, et al. [140] suggested that the ERS yield of retrograded starch depends on the competition between the retrogradation kinetics (influencing local density of starch chains) and the kinetics of enzyme digestion. It seems likely that crystallization is only one route to achieving a dense packing of starch chains which hinders the enzyme accessibility or catalytic action, and dense packing of non-crystalline starch polymers may also be an effective mechanism for slowing digestion.

2.6.1.2 Amylose-lipid complex

Complexes between amylose and lipids, such as monoglycerides, fatty acids, lysophospholipids and surfactants, can significantly reduce the digestion rate and extent both *in vitro* and *in vivo*, representing another source of resistant starch.[73, 75] Amylopectin probably binds only one lipid per individual chain, and the complex formation retards the retrogradation process.[74, 141] Two distinct forms of amylose-lipid complexes have been defined based on the transition peak temperature: an amorphous form (Form I) that melts at a lower temperature (T_p < 100 ^oC) in differential scanning calorimetry thermograms, and a crystalline form (Form II) that has the V-type crystalline structure with a characteristic X-ray diffraction pattern with peaks around 7.5^o, 13^{o}and 20^o (2θ) and a higher melting temperature (T_p, 115 - 125 ^oC).[142, 143] Form I appears to have randomly oriented helices, whereas Form II has an ordered organization of amylose complexes. The amorphous form is less rigid and stable, and can be converted to the crystalline form through annealing at a temperature above the melting temperature of Form I but lower than that of Form II. Both the lipid/starch used and incubation conditions affect the complex formation: a general rule is that crystalline form are favored at higher temperatures, longer incubation time, longer amylose chain lengths, longer chain lengths of saturated lipids, lower unsaturation degree of lipids, lower number of *cis*- double bonds in the complexing lipid, as summarized by

Eliasson and Wahlgren [144]. Ionic head groups of lipids and chemically modified starch will not favor the formation of ordered type II structures.[145]

Godet, et al. [146] proposed a two-stage formation mechanism of the crystalline amylose-lipid complexes (Form II): (1) the formation of amylose-lipid complexes, in which each amylose chain is complexed with one or more lipid molecules and (2) the aggregation of complexes in a fringed micellar arrangement or a U-shaped folding. The crystalline complexes have helical chain segments ordered in structures with dimensions up to 14.5 nm.[147] The densely packed crystallized amylose-lipid complexes are supposed to be resistant to digestive enzymes. The enzymatic susceptibility of amylose has been ranked in the following way by Tufveson et al (2001): amorphous amylose > amylose-lipid complex > retrograded amylose.[148] Seneviratne and Biliaderis [149] found that the crystallinity level of the complex matrices was inversely related to the digestion rate and extent. However, this is not always the case as Tufvesson, Skrabanja, Björck, Elmståhl and Eliasson [148] reported that there was no difference in digestibility between amorphous Form I and crystalline Form II complex. It is therefore likely that it is the amylose-lipid complex that is important for enzyme digestion resistance rather than crystallization. The concept that single helices of complexed molecules are oriented perpendicular to the plane of the lamellae has been agreed.[138, 150] However, what the differences are between how the amorphous and crystalline forms are organized which further affects the local molecular density of the complex matrices, is not clear. We suggest that the nature of enzyme resistance of complex matrices has its origin in local chain density at the nanometer length scale which is relevant to binding/catalysis by amylase, rather than an average value of crystallinity.

2.6.1.3 Hydrothermal treatment

Annealing and heat-moisture treatment are two hydrothermal treatments that modify starch properties such as digestibility. Both processes involve incubation of starches in excess (> 60%) or intermediate (40 – 55%) water (annealing) or at low (< 35%) moisture levels (heat-moisture treatment) for a certain period of time, at a mobile rubbery state with a temperature above the glass transition temperature but below the gelatinization temperature.[151] Heat-moisture treatment is carried out at higher temperatures (90 - 120 ^{o}C), while annealing occurs below the gelatinization temperature of starches. Annealing does not change the overall repeat distance of crystalline and amorphous lamellae,[151, 152] but allows individual molecular reorganization and improves the crystalline

perfection between starch chains.[153] The crystallinity level (judged by X-ray diffraction) and interactions between starch chains in the amorphous and crystalline regions are increased after annealing treatment,[154] which may be expected to affect the digestion properties. A slight decrease in enzyme susceptibility after annealing was found for wheat, lentil, high-amylose maize and potato starches, presumably due to increased crystallite perfection and enhanced amylose–amylose and/or amylose–amylopectin interactions.[155, 156] We note that the enhanced ordering of double helices and improved alignments of starch chains is a route to achieve higher local density of helical structure through annealing. However, it was found that the impact of annealing on enzyme susceptibility can depend on starch botanical origin. Annealed barley, oat and sago starches are more easily hydrolyzed by α-amylases than native starches.[155, 157] Although the molecular reorganization of starch is slightly improved during annealing, the original starch architectures such as granule size, surface features may be more important with respect to digestion pattern/rate/extent in some cases.

Heat-moisture treatment under higher temperatures and low moisture promotes disruption of the crystalline structure and dissociation of the double helical structure in the amorphous region, followed by the rearrangement of the disrupted crystals.[158] The extent of these structural changes normally depends on botanical origin, accompanying changes to crystalline pattern (B to A + B) and level, physicochemical and digestion properties. Tuber or root starches are more sensitive to heat-moisture treatment than legume or cereal starches.[159] Normally, an increased digestibility of starch granules has been shown to occur following heat-moisture treatment, depending on treatment conditions and quantitatively varying among starch sources. In the case of potato and yam starches, crystalline disruption near the granule surface can degrade the outer physical barrier of these starch granules, decreasing the local molecular density of starch chains, consequently facilitating enzyme access and binding to starch granules.[158] Furthermore, the decreased digestibility also could result from the disruption of the double helices within the granules.

Although there are relationships between re-crystallization and densification of starch matrices, which would be expected to impact the enzymatic susceptibility,[76] it seems that crystallization is probably not only one route to achieving a dense packing of starch chains. This suggests that locally-dense non-crystalline structures could also decrease/prevent accessibility or action of enzymes. The factors affecting the formation of amorphous

matrices may also impact on re-crystallization processes, although this is less studied and understood up to now.

2.6.2 Non-crystalline dense packing

Although it is generally accepted that crystalline type and level of crystallinity must play some role in determining digestion rate and extent of starches, recent reports have shown that crystallinity may not be directly linked with the percentage of ERS obtained.[8, 160] Even for native starches, crystallinity alone also cannot explain the resistance to digestion. For example, the limited digestion rate of B-type polymorphic starches is controlled by surface barriers more than crystallinity.[110] On the other hand, some almost amorphous starch materials provide high levels of the resistant fraction.[7, 8] Thus, although crystallinity is one way to achieve local molecular density, it appears that non-crystalline chains can also pack in an enzyme-resistant form that is currently poorly understood and brings a new research challenge for food/polymer chemists.

Amorphous (also called 'non-crystalline') state is essentially a negative definition based on the absence of detectable molecular order, therefore making it difficult to quantify the molecular conformation of the matrices. From the evidence presented above, the measurement of local molecular density of starch matrices is the key to understanding the fundamental mechanism(s) of ERS from non-crystalline dense packing. However, the current technical ability to measure sub-micron variability of local density in starch/food matrices remains limited. From the current data available, non-crystalline starch with lower digestion rate and extent can be achieved by either (1) dense molecular structures at nanometer length scale or (2) densely packed matrices at (sub)micrometer length scale.

2.6.2.1 Dense molecular structures

Although the dense molecular structures leading to ERS character are often found in retrograded starch and starch-lipid complex as an aggregated/crystallized form, the double/single helices not involved in crystallites also can render the α-1,4 glucosidic linkages inaccessible to starch degrading enzymes. A- and B-type single crystals exhibit a 6-fold, left-handed double helical conformation with repeat distances of 2.13 and 2.08 nm respectively.[161-163] Aside from the differences in the amount of water discussed previously, the A- and B- type crystals differ only in that the former has a denser packed-structure, whereas the latter is more open. In aqueous solution at room temperature, starch chains with DP < 10 do not crystallize, while the A-type crystals resulted from starch chains with

DP from 10 to 12; chains longer than 12 crystallize as B-type.[164] The crystalline type can also be affected by crystallization at various water/alcohol concentrations, for example, A-, B- and V-type polymorph single crystals are precipitated at 15%, 0%, and 40% of ethanol concentration respectively.[150]

2.6.2.2 Densely packed matrices

Generally, starch supramolecular and granular structures are disrupted by thermal, moisture and energy inputs during extrusion cooking, which would be expected to increase the accessibility of starch-acting enzymes to starch polymers. However, among extrudates from different starch species, high-amylose maize starch after extrusion and storage shows a relatively high yield of ERS (>20%).[7] A number of extrusion parameters such as feed moisture, temperature, screw speed and storage conditions are known to affect the ERS content of extrudates. Extrusion of starch in the presence of sufficient water triggers a number of physicochemical and functionality changes in starch granules, such as the loss of granular structure associated with melting of crystallites and underlying helices, and generating an amorphous structure.[140, 165] This would be expected to increase the vulnerability of starch to amylase digestion. Upon cooling, hydrated amylose (and amylopectin) chains may undergo retrogradation by molecular re-association into double helices, and may consequently acquire resistance to enzyme digestion.[8] Therefore, extruded products may also lead to a higher RS content. Htoon, Shrestha, Flanagan, Lopez-Rubio, Bird, Gilbert and Gidley [8] reported that almost amorphous extrudate (~5% crystallinity) from high-amylose maize starch could deliver high ERS contents (~20%) *in vitro,* and that more generally there was no apparent correlation between ERS and crystallinity level from X-ray diffraction (Figure 2.7). The presence of amorphous material in the enzyme-resistant fractions is also consistent with resistance based on a kinetic mechanism rather than a specific crystalline structure that is completely undigested.[119] Shrestha, et al. [166] suggested that enzyme-resistance might be associated with a dense solid phase structure that is even non-/weakly-crystalline. X-ray scattering studies showed that the preferred characteristic dimension of the crystals formed was ~5 nm, suggesting that resistant crystals could be formed from chains with a maximum DP of ~13 and ~17 glucose units for double and single helices respectively with potential amorphous fringed ends.[119] We suggest that the local density of packing of starch chains controls its digestibility rather than just crystallinity, which represents just one mechanism of achieving high chain density. If these molecularly dense structures are aligned rigidly they could resist digestion and become ERS with health benefits.

Amorphous amylose-lipid complex (Form I) is another good example of non-crystalline ERS from densely packed matrices. Although the structure without obvious X-ray diffraction peaks is less rigid and thermo-stable, Tufvesson, Skrabanja, Björck, Elmståhl and Eliasson [148] found that there was no difference in digestibility between amorphous Form I and crystalline Form II complex under the preparation conditions used. That suggests that amorphous matrices can escape digestion under certain enzyme concentrations if the starch polymers are densely enough packed, which can be an effective mechanism for slow digestion rate/extent.

Other potential methods to achieve high ERS yields from largely amorphous granular starches include dense protein network formation et al. The dense protein network formed in pasta can also limit the access and binding of enzyme to embedded starch granules, and restrict the diffusion of water to the granules that reduces the starch gelatinisation to some extent.[167]

Apart from processed starchy food, non-crystalline dense packing also exists in nature. The amorphous growth rings within starch granules are perhaps the best representative. In contrast to semi-crystalline layers consisting of amylopectin clusters that in turn contain alternating crystalline and amorphous lamellae, amorphous growth rings are thought to contain amylose and amylopectin molecules in apparently unordered conformation. The number and thickness of amorphous layers depends on the botanical origin and amylose content.[26] According to Cameron and Donald (1992), the amorphous growth ring is at least as thick as the semi-crystalline one, which is thought to be 120~500 nm.[28] As discussed previously, Zhang, Ao and Hamaker [139] reported that the crystalline and amorphous growth rings of granular starches are apparently digested side-by-side, suggesting local density of amorphous growth rings is enough high to limit enzyme binding therefore achieve similar digestion rates as crystalline materials.

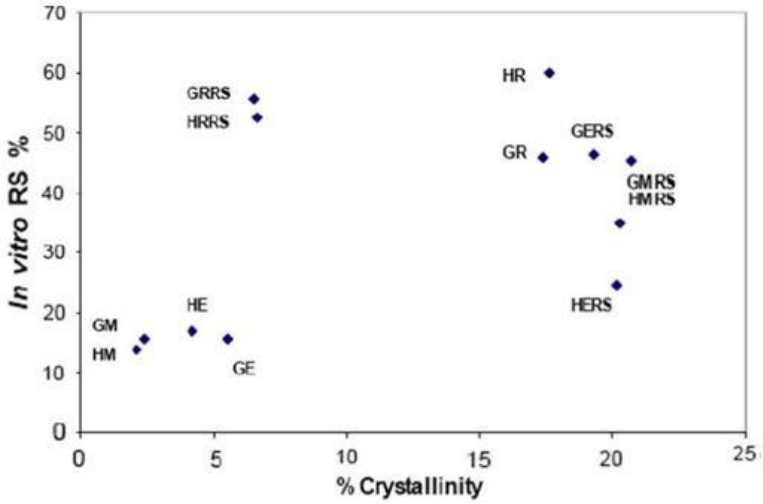

Figure 2.7. Enzyme-resistant starch levels compared with crystallinity from X-ray diffraction for arrange of high amylose maize samples.[8] (H, Hylon 7 starch; G, Gelose 80 starch; R, raw starch; M, mild processed; E, extreme processed; RS, isolated resistant starch fraction).

2.7 Objectives and hypotheses

The objective of the present work are to:

1. Elucidate the interplay of α-amylase and amyloglucosidase on starch substrates with different physical structures.
2. Investigate the molecular organisation and formation mechanism of starch granule ‘ghosts’.
3. Study the lubrication and rheology of isolated swollen starch granule suspensions over a wide range of concentrations, using maize and potato starches as exemplars.
4. Develop a novel theory and methodology of enzyme-resistant starch from essentially amorphous matrices through extrusion.
5. Study different dehydration effects including oven, ethanol or freeze drying on the digestion, thermal, or structural properties of starches.

The general hypotheses of this research work are that:

1. The digestion kinetic profiles and the interplay of α-amylase and amyloglucosidase are dependent on the physical structure of starches.
2. Three possible mechanisms underlying starch ghost formation can be proposed and tested: (i) the multi-micrometer skin structure of granule ghosts; (ii) double helices or dense entanglement of amylose and/or amylopectin; or (iii) proteins and lipids associated with the granule.

3. The size and integrity of starch ghost particles control the lubrication and rheological properties of starch pastes and gels.
4. Local molecular density of starch chains can control its digestibility rather than just crystallinity, which represents just one mechanism of achieving high local density of packing.
5. Harsh dehydration process can disrupt starch structures to some extent, and therefore alter the digestion and thermal properties.

2.8 Thesis structure

This thesis contains 8 chapters in total. Chapter 1 is the general introduction and motivation of the PhD projects, and chapter 2 details the literature review which outlines current understanding of starch structure and functional properties, enzyme interactions and data interpretation in commonly used in vitro starch digestion models, and the role of local molecular density on starch digestion kinetics. Chapter 3 is the first of five research chapters which studies the physical structures of starches in determining the digestion rate constant and interplay of acting enzymes. Chapter 4 investigates the formation mechanism of starch granule 'ghosts' with the probe of amylase digestion. Chapter 5 explores the soft-tribological and rheological properties of swollen starch granule suspensions over a range of concentrations, using maize and potato starches as exemplars. Chapter 6 prepares low-order starch matrices through extrusion and explores fundamental mechanism of ERS from essential amorphous matrices. Chapter 7 studies the dehydration effect on starch structure at different length scales and also functional properties such as in vitro digestion and gelatinisation, and lastly, chapter 8 outlines the general conclusions and offers potential further research direction.

Chapter 3

Synergistic and Antagonistic Effects of α-Amylase and Amyloglucosidase on Starch Digestion

(This chapter has been published in Biomacromolecules, 2013, 14, 1945-1954.)

*Bin Zhang, Sushil Dhital and Michael J. Gidley**

Centre for Nutrition and Food Sciences, ARC Centre of Excellence in Plant Cell Walls, Queensland Alliance for Agriculture and Food Innovation, The University of Queensland, St Lucia, Brisbane, QLD 4072, Australia

* Corresponding author.

Phone: +61 7 3365 2145; Fax: +61 7 3365 1177. Email address: m.gidley@uq.edu.au (M. Gidley)

3.1 Introduction

The enzymatic degradation of biomacromolecules often involves a combination of one or more endo-acting depolymerizing enzymes with one or more exo-acting enzymes that convert the products of endo-acting enzymes into monomer units or act directly, but usually inefficiently, on the intact biomacromolecule. These events are at the heart of biological and technological processes such as the conversion of starch or cellulose into glucose and the digestion of proteins into amino acids. While chemical structure determines the selectivity of enzymatic degradation, the physical nature of biomacromolecular substrates often controls the rate of enzymatic reactions. The interplay of endo- and exo-acting enzymes with the physical structure of their substrate is the subject of the present study, using starch as an example substrate and α-amylase and amyloglucosidase as example endo-acting and exo-acting enzymes, respectively.

Starch, an important energy reserve of plants, is a major energy-providing carbohydrate for both humans and animals. It is composed of two major α-glucans, amylose and amylopectin, representing almost 98 ~ 99% of starch dry weight. Amylose is a primarily

linear polymer of α-1,4-linked D-glucose units with few branches, whereas amylopectin is a related highly branched α-1,4, α-1,6-linked glucan with typically 5 ~ 6% α-1,6 linkages.[10] These polymers are biosynthesized as condensed granules with a semi-crystalline structure. In human diets, starch is generally consumed after cooking or subject to various processes during food production, whereas animal feeds or industrial conversion processes may utilize starch in granular forms. The release of glucose from starchy food and its association with many diet-related diseases including type II diabetes, obesity and cardiovascular disease has stimulated interest in both the quantity and quality of starch necessary to maintain the state of good health of an individual.[4, 168, 169] Native starch is digested slowly compared to processed starch as processing steps such as milling and cooking disrupt general granule integrity and reduce the amount of ordered structure, thereby increasing the accessibility of glucans to enzymes.[170] Study of starch digestion in human subjects is challenging, given the complexity of the human digestive process with multiple enzymes and hormonal control of these enzymes. As a biochemical mimic of *in vivo* conditions, *in vitro* study of starch digestion is normally carried out by two types of enzymes: (1) endo-acting enzyme (e.g., porcine pancreatic α-amylase), which cleaves α-1,4 linkages at random location, and (2) exo-acting enzyme, which hydrolyses the terminal or next-to-terminal linkage starting at the non-reducing end of the glucose polymer. Amyloglucosidase produces *β*-glucose in this way by hydrolyzing both α -1,4-linkages and α -1,6-linkages at a slower rate.[100] Although *in vitro* methods oversimplify the digestion mechanism in human and animal digestion tracts, such studies are still useful in investigations of rate and extent of starch digestion.[171]

Hydrolysis of granular starch is a heterogeneous reaction, involving a reaction between an enzyme in solution and a solid substrate represented by the granules.[172] This process includes the diffusion of enzymes to the granule surface, followed by adsorption and subsequent catalytic events.[129] The granular architecture and, more specifically, the surface organization of starch granules provide barriers to the diffusion and adsorption of the enzymes, which is proposed to be one of the main factors determining the kinetics and degree of hydrolysis.[140, 173] Once the outer shell barrier is damaged by mechanical force or enzyme reaction, the hydrolysis process occurs more rapidly.[173, 174] Granule surfaces are relatively impermeable to large molecules such as amylases, apparently due to tight packing of amylopectin and a higher concentration of amylose chains.[84] However, enzyme action is not exclusively an external surface phenomenon; as soon as the attack develops via weak areas, e.g., surface pores, hydrolysis proceeds very rapidly in a radial direction

with the formation of new channels. The hydrolysis is expected to be even faster for granules with existing channels as these structural features increase the effective surface area for enzyme reaction, and facilitate the rapid diffusion of amylases toward the granule interior, hydrolyzing in an 'inside-out' digestion pattern as observed in maize starch granules.[174, 175] Granular starch digestion occurs by a 'side-by-side' mechanism involving the simultaneous digestion of crystalline and amorphous regions,[139] although the non-ordered structure has been generally thought to be more easily digested.[31]

Standard enzyme kinetic models involve interactions between enzyme and substrate molecules in solution, for which hydrolysis rate is predominantly related to the inherent molecular structure.[176] Most studies of the *in vitro* digestion of gelatinized starch have been made by heating starch suspensions in a boiling water bath with various degrees of mechanical mixing.[80, 177, 178] Gelatinized starch prepared under low shear conditions contains granule residues (also termed 'granule ghosts'), even though almost all detectable ordered structure (crystallinity, helical order, and regularity of amylopectin clusters) is lost following completion of the gelatinization process.[71, 179] However, heating under shearing conditions leads to breakdown of granule ghosts resulting in a dispersion of smaller particles and dissolved polymer molecules. The change in physical properties of starch caused by previous processing history, such as the degree of gelatinization, gelling, or retrogradation, is known to have a marked influence on its enzymatic accessibility.[180, 181] Although enzymatic susceptibility of cooked starches have been studied,[80, 177] the susceptibility of starch ghosts to enzyme digestion has not been reported so far. This study aims to investigate the differences in enzymatic susceptibility of granular solid and swollen 'solution state' starch using α-amylase and amyloglucosidase, individually and in combination, in order to elucidate synergistic and antagonistic effects of these enzymes on these systems.

3.2 Experimental section

3.2.1 Materials

Maize starch (MS) was purchased from Penford Australia Ltd. (Lane Cove, NSW, Australia), and potato starch (PS) was from Sigma-Aldrich (St. Louis, MO, USA). The average apparent amylose contents of MS and PS were found to be 27.1% and 36.8%, respectively, using an iodine colorimetric method.[174] The relatively high value obtained for potato starch suggests that the method used also detected some long amylopectin branches. Maltose (M9171), maltotriose (M8378), and maltoheptaose (4-7872) were

purchased from Sigma-Aldrich. Amyloglucosidase from *Aspergillus niger* (EC 3.2.1.3, A7420, activity 31.2 unit/mg) and porcine pancreatic α-amylase (EC 3.2.1.1, A3176, activity 23 unit/mg) were obtained from Sigma-Aldrich.

3.2.2 Preparation of cooked starch and granule ghosts

Starch slurry (10 mL, 0.5% w/v) in a 50mL centrifuge tube (with a magnetic stirrer, 3 mm x 8 mm) was heated to 100 °C on a hot plate stirrer at a stirring rate of 1500 rpm for 30 min ('high shear cooking') and designated 'cooked starch'. Granule ghosts were isolated from maize and potato starches following an adaptation of a method reported previously.[59, 179] Starch (200 mg) was suspended in a small amount of cold water and then poured into hot water (95 °C, 40 mL). The dilute suspension (0.5% starch) was kept at 95 °C for 30 min at very low stir rate (250 rpm, 'low shear cooking') and then centrifuged (30 °C, 2000*g* for 15 min) to minimize the risk of retrogradation from leached amylose. The supernatant was removed, and the spun ghosts were washed twice by resuspending in hot water (90 °C) with gentle manual stirring followed by centrifugation. The washed ghosts were finally resuspended in excess water for *in vitro* digestion.

3.2.3 *In vitro* digestion of starch

Granular starches, cooked starches, and granule ghosts were digested with both α-amylase and amyloglucosidase, or with amyloglucosidase only. For the digestion with both enzymes, starch samples (50 mg, dry basis) were digested with 25 units α-amylase and 14 units amyloglucosidase in 30 mL of sodium acetate buffer (0.2 M, pH 6.0) in a shaking water bath at 37 °C. These enzyme activities were selected to allow monitoring of reaction progress for both slow (starch granules) and fast (cooked starch) digestion processes under identical conditions. Aliquots (0.5 mL) were removed at specific intervals during the digestion. Each aliquot was then mixed with absolute ethanol (1.0 mL) and centrifuged at 4000*g* for 10 min. The undigested granular starch left after centrifugation was freeze-dried for further microscopic analysis. The concentration of glucose in the supernatant was determined using a glucose oxidase / peroxidase enzymatic glucose reagent (TR 15104, Thermo Scientific, Noble Park, VIC, Australia) detected following reaction of the hydrogen peroxide produced from glucose with *p*-hydroxybenzoic acid and 4-aminoantipyrine to give a coloured quinoneimine, which was measured by absorbance at a wavelength of 505 nm. For the starch or oligosaccharide digestion with amyloglucosidase only, the same procedure was followed, only without α-amylase addition.

The glucose released (%) was calculated using the following equation (Eq. 3.1):

$$\text{Glucose released (\%)} = \frac{\text{total weight of glucose in supernatant} \times 0.9}{\text{dry weight of starch (oligosaccharide)}} \times 100\% \quad \text{(Eq. 3.1)}$$

where 0.9 is the molar mass conversion from glucose to anyhydroglucose (the starch monomer unit).

3.2.4 Scanning electron microscopy (SEM)

The freeze-dried starch sample was thinly spread onto circular metal stubs covered with double-sided adhesive carbon tape, and then platinum coated in a Sputter Coater (at 15 mA, 3 min for medium coating) in an argon gas environment, yielding approximately 10 nm coating thickness. Images of the starch granules were acquired with a Philips XL30 scanning electron microscope (Philips, Eindhoven, Netherlands) under an accelerating voltage of 5 kV. Multiple micrographs of each sample were examined at multiple magnifications and typical representative images selected.

3.2.5 First-order kinetics

When starch or starch-containing foods are digested *in vitro* with relatively high enzyme concentrations for long time periods, the rate of reaction decreases with time and plot of the concentration of product formed (or quantity of starch digested) against time is logarithmic.[115] This substrate decay process fits the standard first-order equation (Eq. 3.2) and has been used to investigate the kinetics of starch digestion.[116]

$$C = 1 - e^{-kt} \quad \text{(Eq. 3.2)}$$

where t is the digestion time (min), C is the fraction of digested starch at digestion time t, and k is the digestion rate constant (min^{-1}). The value of k can be obtained from the slope of a linear-least-squares fit of a plot of ln (1 – C) against t.

3.2.6 Statistical analysis

Results were expressed as means with standard deviations of at least duplicate measurements. Analysis of variance (ANOVA) was used to determine the least significance at $p < 0.05$ using Minitab 16 (Minitab Inc., State College, PA, USA), and correlation coefficients were determined by using Microsoft Office Excel 2011.

3.3 Results

3.3.1 Enzymatic hydrolysis of starch

The kinetic profile of starch digestion (Figure 3.1) was monitored by measuring the released glucose at specific intervals during digestion with both α-amylase and amyloglucosidase (AA/AMG), or with amyloglucosidase alone (AMG). While digestion with AMG alone will only release glucose, digestion with both enzymes could also release products of AA, which are subsequently converted to glucose by AMG. These intermediate products, e.g., malto-oligosaccharides may be present during the digestion, but the fact that there are examples of both granular (e.g., MS-N-AA/AMG, Figure 3.1 A) and cooked (Figure 3.1 C, D) starches which are fully converted to glucose under the experimental conditions used shows that any accumulated intermediate products do not prevent conversion to glucose. Irrespective of the enzymes used and the physical state of starch (granular, cooked, or granule ghosts), both maize and potato starches displayed monophasic digestion behavior, and maize starch was more rapidly digested compared to potato starch at each time point (Figure 3.1). The amyloglucosidase alone had only a low hydrolysis rate against native starch, but together with α-amylase the rate was much faster (Figure 3.1 A, B). After 24 h of digestion, almost all of the maize starch was hydrolyzed to glucose by both enzymes, whereas almost one-third of the potato starch was undigested. In agreement with previous reports,[182] maize starch showed a higher susceptibility toward glucoamylase compared to potato starch. The amounts of glucose released from maize starch granules (27.3%) after 24 h of amyloglucosidase digestion was higher than that of potato starch (23.2%).[182]

Gelatinization of starches disrupts structural features (e.g., semi-crystalline structure) that otherwise slow down enzyme action. For cooked starch and granule ghosts, the digestion behavior was not markedly different between maize and potato (Figure 3.1 C ~ F). The first 2 h of digestion was characterized by a steeply increasing concentration of released glucose, after which the release rate became slower. From 6 h of digestion onward, the amount of released glucose reached a plateau. When comparing digestion with different enzymes, it is clear that initial hydrolysis rate with amyloglucosidase only is higher than that with both α-amylase and amyloglucosidase (Figure 3.1 C ~ F).

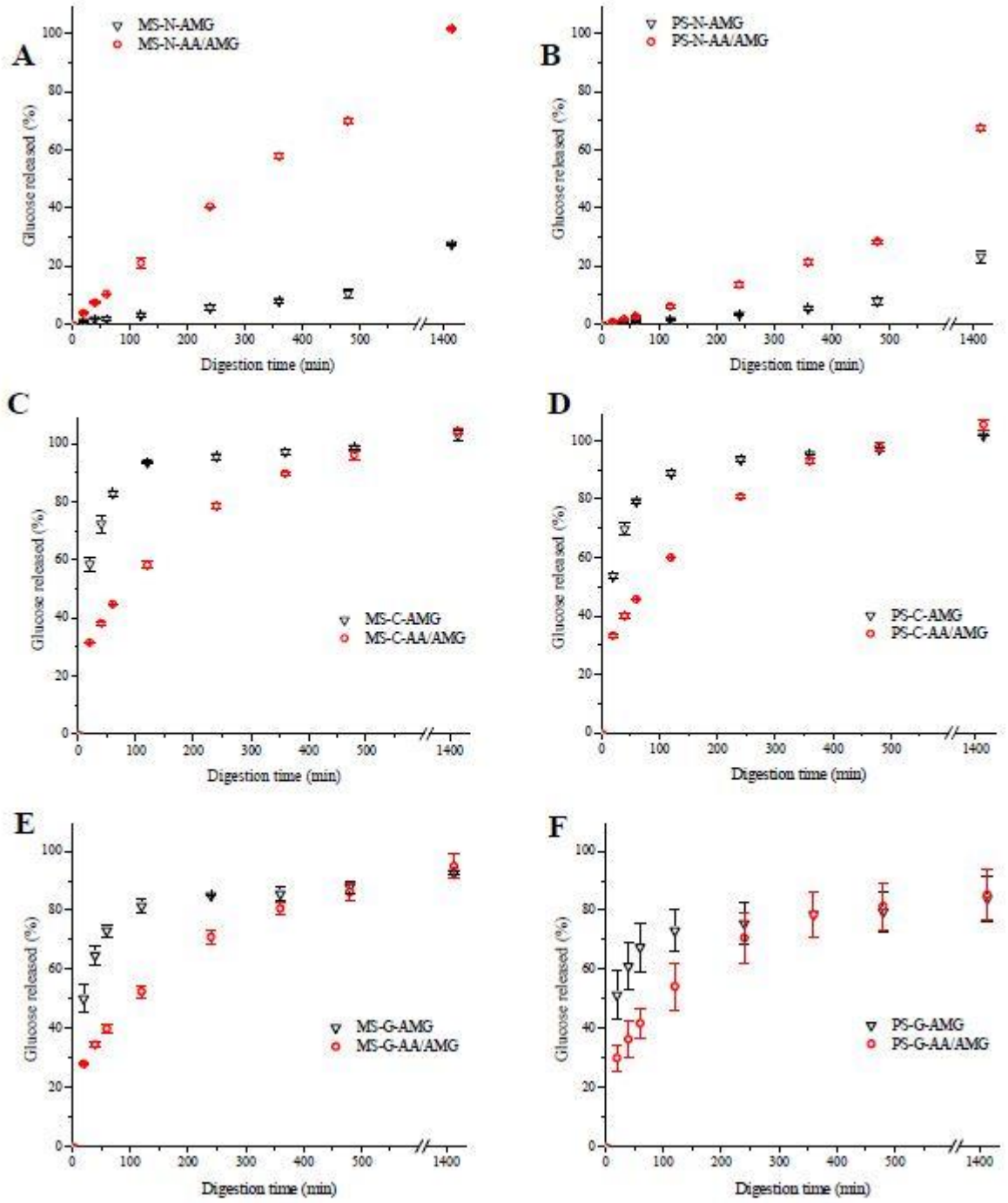

Figure 3.1. Kinetic profiles of native granular starch (A, B), cooked starches (C, D) and granule ghosts (E, F) digestion with both α-amylase and amyloglucosidase (AA/AMG), and with amyloglucosidase alone (AMG).

3.3.2 Oligosaccharide digestion with amyloglucosidase

Kinetic profiles of digestion with amyloglucosidase on linear oligosaccharides (maltose, maltotriose, and maltoheptaose) are shown in Figure 3.2 and compared with cooked maize starch. The initial rate of cleavage of α-1,4 glycosidic linkages of maltose was less than that in maltotriose at the same enzyme concentration. This trend continued for

digestion of the longer oligosaccharides and branched polymers (i.e., cooked maize starch) (Figure 3.2). These results are in close agreement with previous studies on the digestion of oligosaccharides with amyloglucosidase.[183, 184]

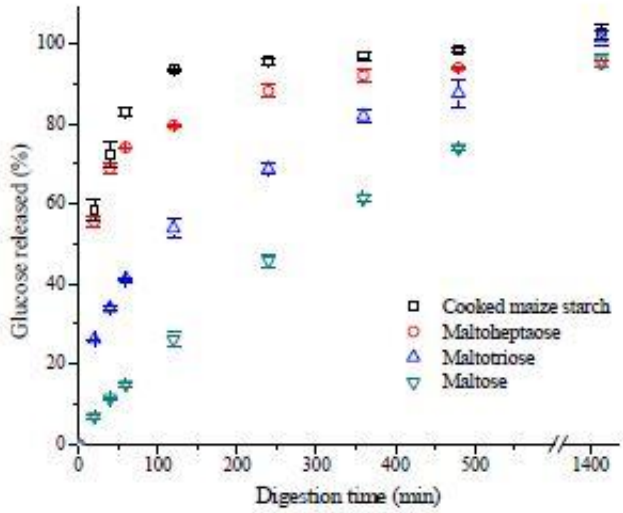

Figure 3.2. Kinetic profiles of linear oligosaccharide digestion with amyloglucosidase compared with cooked maize starch.

3.3.3 Morphology of native and partly digested starch granules

Electron micrographs of native maize and potato starch granules and the starch granules/fragments isolated from enzymatic hydrolysis are shown in Figures 3.3 and 3.4. Maize starch granules were 5 ~ 30 μm in size and round or irregular in shape with sharp edges and irregular surfaces with some small pores (Figure 3.3A). The digestion of maize starch with both α-amylase and amyloglucosidase was characterized by the formation of enlarged pores due to opening of channels within granules (Figure 3.3 B, D, F). Evidence of enzyme attack was clearly observed after 20 min hydrolysis with slightly roughened surfaces (Figure 3.3B). Moreover, after 2 h of digestion, more deep holes were observed possibly due to internal corrosion by starch-acting enzymes. On subsequent digestion, the surface pores and channels merged together resulting in an apparently hollow interior leading to the collapse of granule structure.[139, 185] After 8 h digestion, some granules had cracked open, and the layered structure of the growth rings in some granules was clearly visible (Figure 3.3F). It was not possible to isolate the digesta from 24 h of digestion, due to the complete hydrolysis of granules by both acting enzymes. The morphology of digested maize starch with amyloglucosidase alone (Figure 3.3 C, E, G, and H) was similar to that with both enzymes. Some fine pitting was noted on the surface after 24 h of

amyloglucosidase hydrolysis (Figure 3.3H), and granules had a roughened appearance comparable to the granules in the digestion with both enzymes.

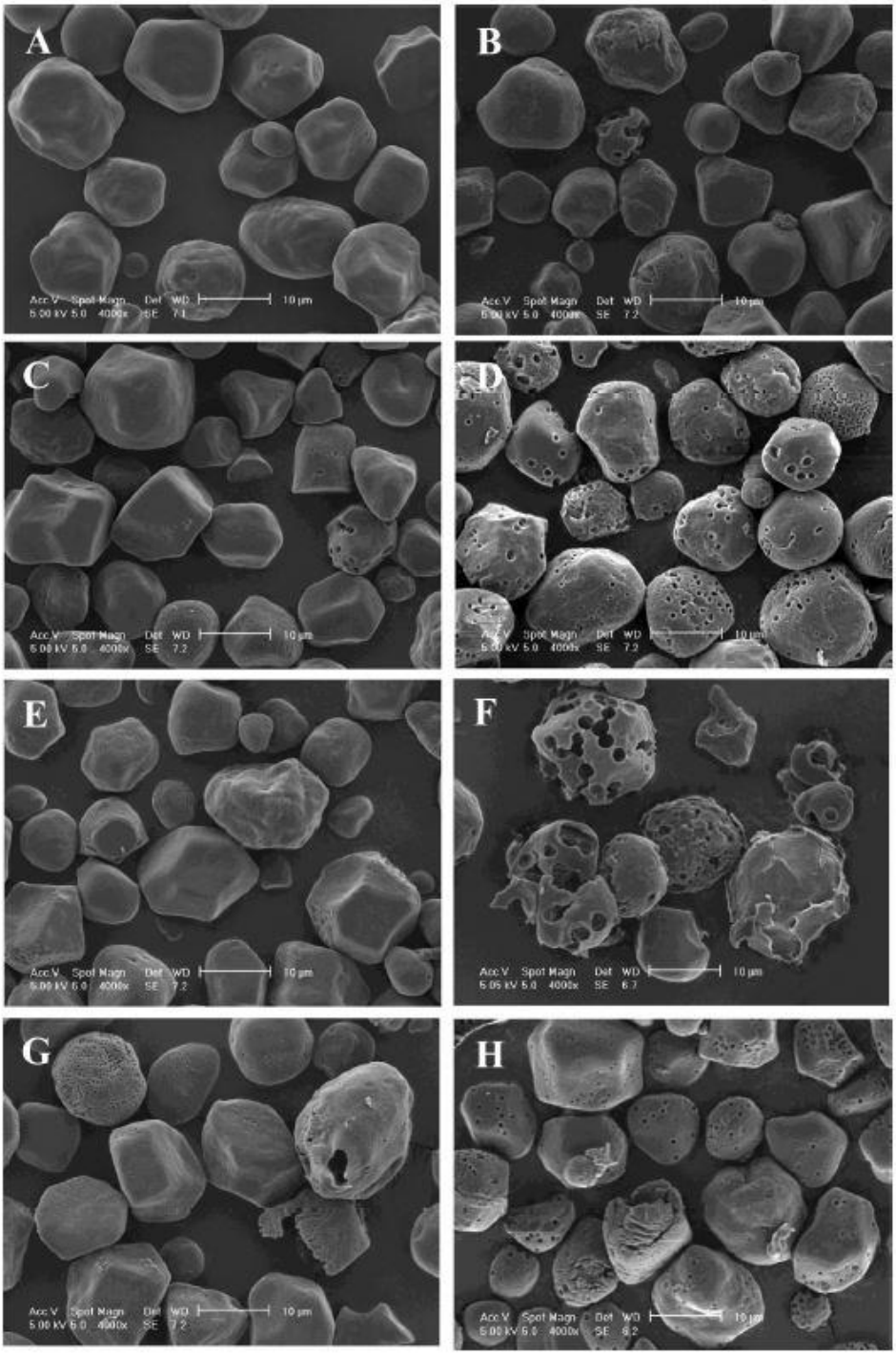

Figure 3.3. Morphology of maize starch granules/fragments isolated from *in vitro* digesta at different time intervals. Native maize starch (A); maize starch after 20 min, 2 h and 8 h digestion with α-amylase and amyloglucosidase (B, D, and F); maize starch after 20 min, 2 h, 8 h, and 24 h digestion with amyloglucosidase only (C, E, G, and H).

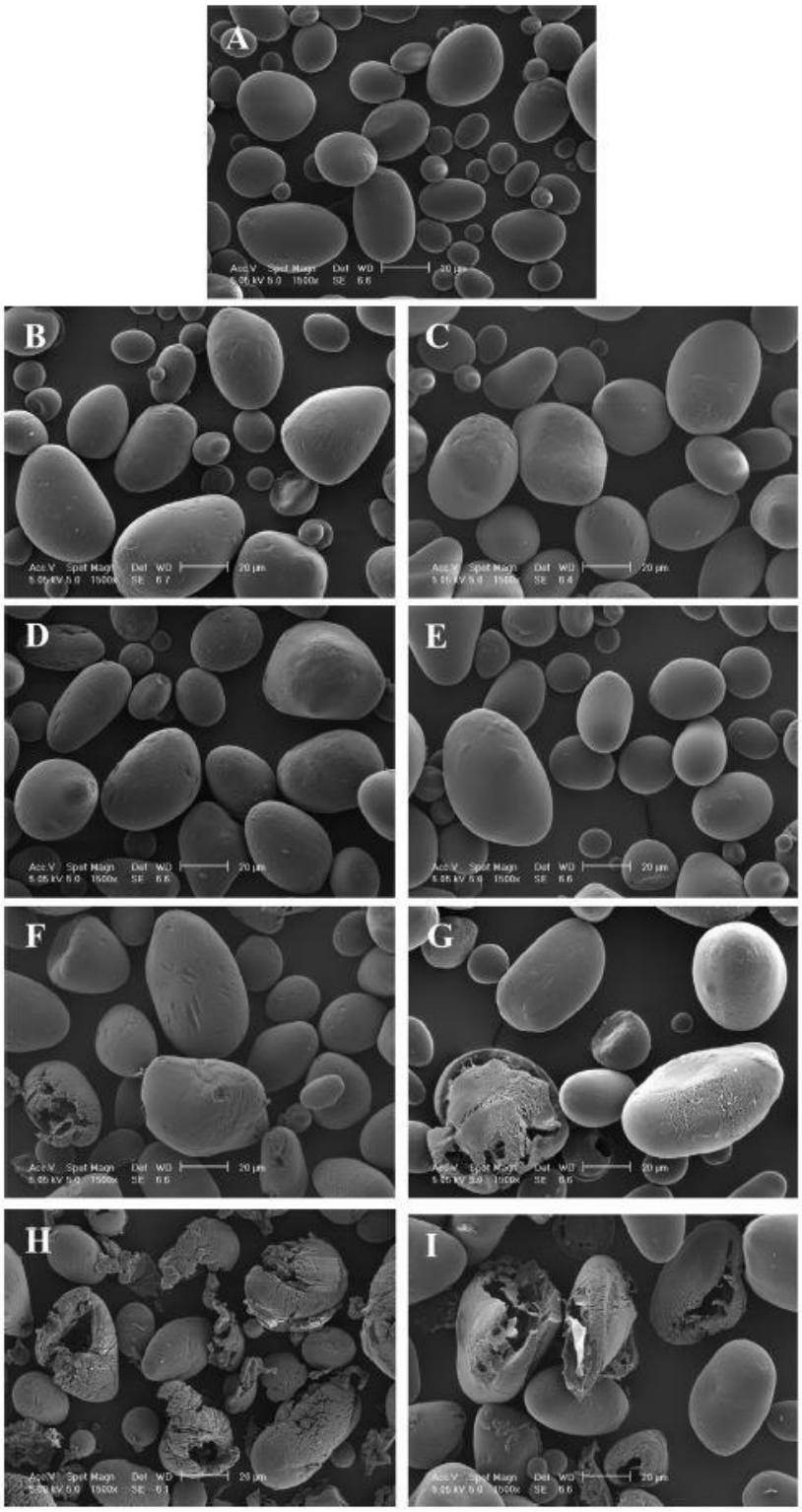

Figure 3.4. Morphology of potato starch granules/fragments isolated from *in vitro* digesta at different intervals. Native potato starch (A); potato starch after 20 min, 2 h, 8 h, and 24 h digestion with α-amylase and amyloglucosidase (B, D, F, and H); potato starch after 20 min, 2 h, 8 h and 24 h digestion with amyloglucosidase alone (C, E, G and I).

Potato starch showed a wide range of granule sizes (5 ~ 100 *μ*m) with ellipsoidal and round shapes but without visible pores (Figure 3.4A). At the early stage of digestion (within

2 h), granule surfaces were roughened with several apparent scratches on the surface ('exo-corrosion' digestion pattern) (Figure 3.4 B ~ E). On further hydrolysis for 8 and 24 h, increased surface roughness and formation of deep cracks were clearly visible for many granules (Figure 3.4 F ~ I). However, in contrast to maize starch there was less homogeneity in the digestion pattern on the potato starch granules: some granules became hollow with only more resistant external layers remaining, whereas other granules were only affected on the surface (Figure 3.4 F ~ I).

There were no major differences apparent between the morphology of digestion with amyloglucosidase alone and with a combination of α-amylase and amyloglucosidase (Figure 4.4).

3.4 Discussion

3.4.1 Synergism of endo- and exo- enzymes in granular starch digestion

Amyloglucosidase from *Aspergillus niger* (AMG-I) contain a starch-binding domain (SBD), and recent studies indicate that the SBD not only binds onto starch, but also disrupts double helical structures and enhances the rate of hydrolysis.[103, 104] For the exo-enzyme system alone, the digestion rate of native starch granules is slower as the available substrate concentration is restricted to the non-reducing end groups of the starch chain. The synergism of endo- and exo-enzymes is apparent in Figure 3.1 A and B, with the released glucose at different intervals in the mixed-enzyme system over twice as great as the corresponding value for the exo-enzyme system alone. When starch granules are used as a substrate, α-amylase supplies new substrate molecules for amyloglucosidase by endo-wise splitting of large molecules.[186] In addition, amyloglucosidase can peel starch molecules from the surface that is hypothesized to have protruding branches of amylopectin with non-reducing ends (known as the 'hairy billiard ball' model),[187] exposing new substrate to α-amylase.[188] α-Amylase is believed to normally be the rate-determining enzyme during native starch digestion but may be inhibited by oligosaccharide products, whereas amyloglucosidase converts potentially inhibitory oligosaccharides into non-inhibitory glucose. The inter-dependence of both enzymes needs to be taken into account when considering their use as an *in vitro* mimic or predictor of starch digestion rates and extents, at least for maize starches.[189]

When starch or starch-containing foods are digested *in vitro* with relatively high enzyme concentrations, the hydrolysis rate decreases as the time is extended and plots of the

concentration of product formed (or quantity of starch digested) against time are logarithmic.[116] Therefore, the kinetics can be described by a single rate coefficient (i.e., first-order kinetics). In Figure 3.5, it is clearly seen that all granular starch digestions follow first-order behavior, with all R^2 values above 0.99. The decrease in the observed rate of released product over the time course of the reaction is a natural feature of an exponential reaction.[115] Thus, the starch substrates do not seem to consist of distinct fractions that differ in digestion rate, i.e., there is no evidence for the presence of separate rapidly digestible and slowly digestible starch components as suggested by Englyst et al.[1] The amount of starch digested fraction in a given sample is under kinetic more than thermodynamic control, although certain fractions may be resistant to starch-acting enzymes.[8]

Table 3.1 summarizes digestion rate coefficients (*K*) obtained from the fit of first-order kinetics. The *K* value for both enzymes acting on maize starch is more than 3 times higher than that for potato starch, and for amyloglucosidase alone is ca. 5 times (potato) or 10 times (maize) less than corresponding values for both enzymes, clearly showing the synergistic action of the two enzymes at the concentrations used in this study. However, it should be noted that the digestion rate constant is a function of the fixed enzyme concentration used in the digestion and is therefore pseudo-first-order.[115] When starch granules are used as a substrate, the hydrolysis rate is expected to be limited by the rate at which the enzyme can diffuse into the substrate and form an enzyme-substrate complex (consistent with first-order kinetics) with the physical structure of starch also influencing the extent of hydrolysis.[110, 119] It has been suggested that during digestion, enzymes (size: ~ 5 nm for α-amylase; 8 ~10 nm for amyloglucosidase) tend to migrate inside the granule through susceptible sites, e.g., surface pores (0.1 ~ 0.3 μm), cavities and channels (0.07 ~ 0.1 μm), and return to the surface after all material is consumed.[190-192] Structural features like surface pores and channels are proposed to facilitate the adsorption and rapid diffusion of amylases toward granule interior in maize starch compared to potato starch apparently lacking such features. In general agreement with previously published observations,[139, 174] we confirmed that maize starch granules follow an 'inside-out' digestion pattern, in contrast to potato starch, that tends to be hydrolyzed from the surface by exo-corrosion mechanism.

3.4.2 Antagonism of endo- and exo- enzyme action on cooked starch and granule ghost digestion

In contrast to starch granules, when cooked starch and granule ghosts were used as a substrate, α-amylase did not lead to an increase in initial rate of digestion by mixed endo- and exo- enzymes compared with the exo-enzyme alone (Figure 3.1 C ~ F) under the concentration conditions used. At first sight, this seems to be counter to the generally accepted role of α-amylase in enhancing the action of amyloglucosidase by supplying new substrate molecules through endo-wise random splitting of large molecules.[186] However, the reaction rate of amyloglucosidase is very dependent on the polymerization degree of the substrate (Figure 3.2), which has been rationalized by the subsite binding affinities in the active site based on the results and model of Hiromi et al.[106, 193] Amyloglucosidase from *Aspergillus niger* is known to have seven subsites for binding near the active site, and its catalytic site is located between subsites 1 and 2.[105] Moreover, the subsites possess variable affinities: the affinity of the first subsite is very low, whereas subsite 2 has the highest affinity and the affinity of the individual sites decreases from subsite 3 to 7.[106] Although the position of the catalytic site between subsites 1 and 2 allows the hydrolysis of maltose, the binding affinity is low compared with longer oligosaccharides that can take advantage of the large number of subsites available.[105] This appears to be the reason why maltose (a main end product from porcine pancreatic α-amylase hydrolysis[96]) is slowly hydrolyzed by amyloglucosidase, and why longer oligosaccharides and soluble starch show such a big increase in catalytic efficiency.[184] The present results suggest that α-amylase hydrolysis, which carries out multiple attacks on linear portions of amylose and amylopectin with maltose and maltotriose as the main end products,[96] antagonistically hinders the more catalytically effective binding of amyloglucosidase to longer starch chains.

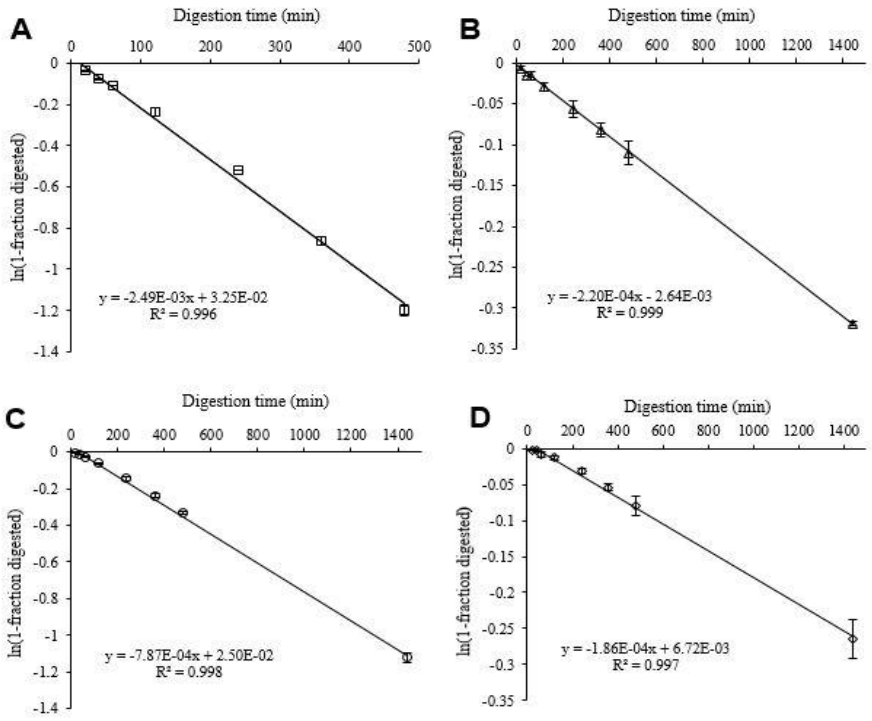

Figure 3.5. Fitting of first-order kinetics to native maize (MS) or potato (PS) starch digestion with both α-amylase and amyloglucosidase, and amyloglucosidase alone. (A, MS-N-AA/AMG; B, MS-N-AMG; C, PS-N-AA/AMG; D, PS-N-AMG)

Figures 3.6 and 3.7 show the results of fitting digestion data with first-order kinetics for cooked starch and granule ghosts, respectively. Each set of digestion data with both acting enzymes shows a good fit to first-order behavior, with R^2 values range between 0.94 and 0.99 (Figures 3.6 A, C and 3.7 A, C), but there is no first-order fit for digestion with amyloglucosidase alone for either cooked starch or granule ghosts (Figures 3.6 B, D and 3.7 B, D). As the first-order plots for ghost digestion do not go through the origin (Figure 3.7 A, C), this suggests that there is a rapid digestion process that takes place in the first 20 min that precedes a subsequent first-order rate process. This is likely to be due to hydrolysis of polymers that are loosely attached to the swollen ghost particles and which have similar enzyme susceptibilities to soluble starch. In support of this, the extent of hydrolysis after 20 min is very similar for cooked starch and granule ghost substrates (Figure 3.1 C ~ F).

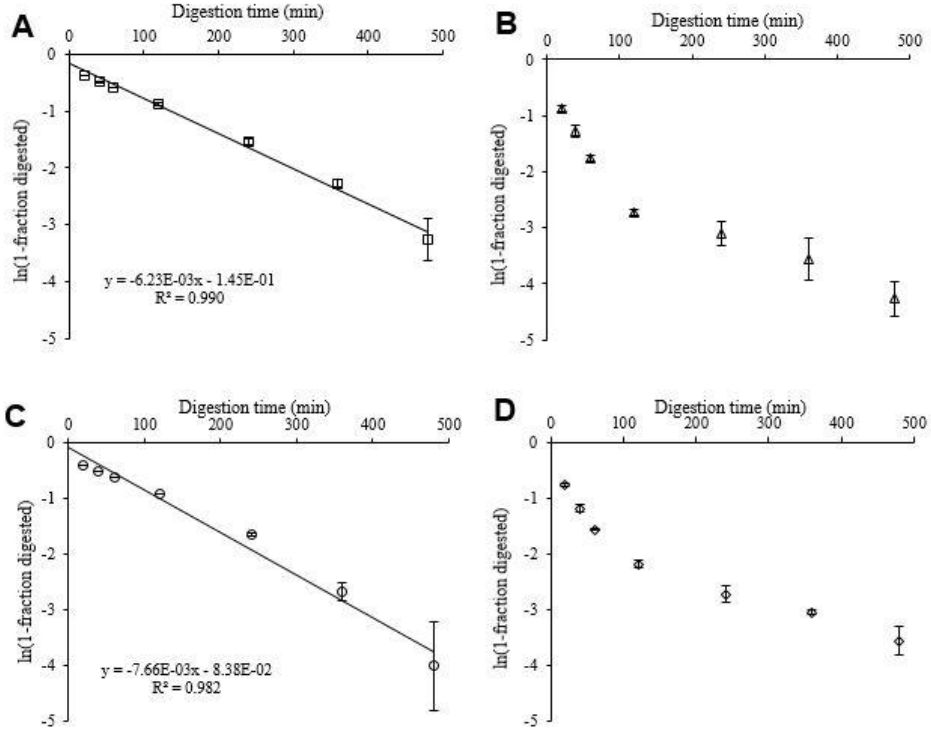

Figure 3.6. Fitting of first-order kinetics to the cooked starch digestion with α-amylase and amyloglucosidase. (A, MS-C-AA/AMG; B, MS-C-AMG; C, PS-C-AA/AMG; D, PS-C-AMG)

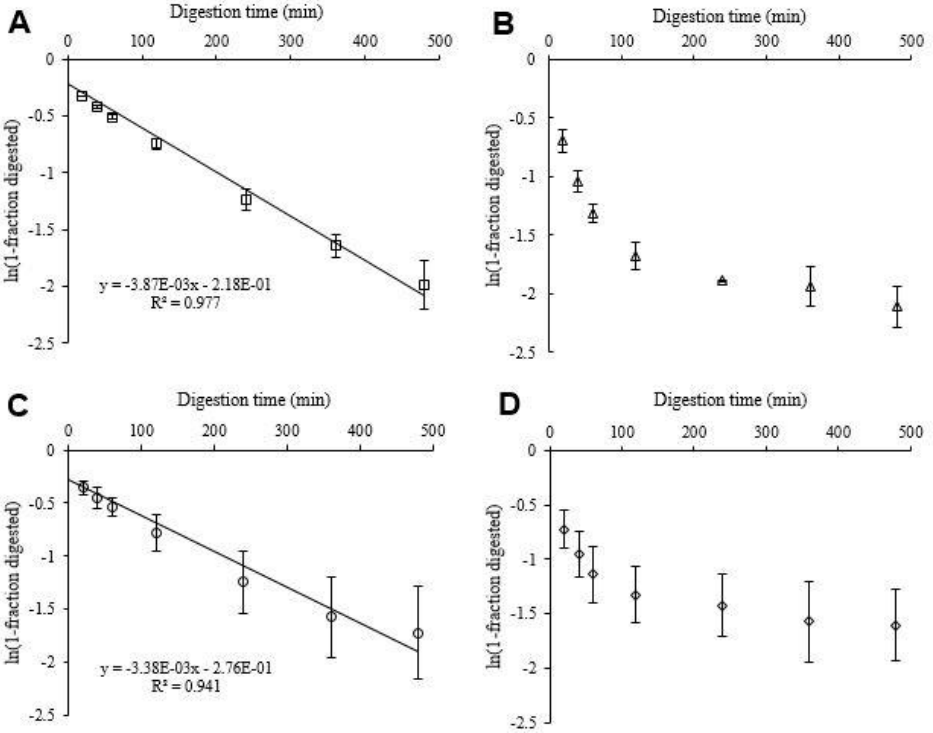

Figure 3.7. Fitting of first-order kinetics to the granule ghosts digestion with α-amylase and amyloglucosidase. (A, MS-G-AA/AMG; B, MS-G-AMG; C, PS-G-AA/AMG; D, PS-G-AMG)

3.4.3 Enzyme kinetics and rate-limiting steps

Across the range of samples studied, we hypothesize that first-order kinetics are due to formation of the enzyme-substrate complex being rate-limiting. In the case of granular starches, this applies to both mixed enzymes and amyloglucosidase alone, and we propose that this is primarily determined by the architecture of the granule impeding the formation of enzyme-substrate complexes. For cooked starch and granule ghosts, it is only the mixed enzyme system that shows evidence for first-order kinetics and we ascribe this to the rate-limiting (inefficient) binding of maltose and maltotriose, the primary products of α-amylase, to amyloglucosidase prior to conversion to glucose. In the absence of α-amylase, we propose that amyloglucosidase binds avidly with larger starch substrates so that enzyme-substrate complex formation is no longer rate-limiting and reaction rates are faster.

Table 3.1 summarizes digestion rate coefficients obtained from first-order kinetics fitting for both granular and hydrothermally processed (cooking with/without shearing) samples. For granules, rate coefficients are ca. 3 times less for potato vs maize starch for the mixed enzyme system, consistent with the presence of pores and channels in maize starch providing a greater effective surface area for productive enzyme-substrate complex formation.[110] Interestingly, for amyloglucosidase alone there is only a small difference in rate coefficients between the two granules, suggesting that surface reaction is more prevalent than for the mixed enzyme system. This is logical, as hydrolysis by α-amylase within pores and channels opens them up (Figure 3.3 B, D, F), whereas the same effect is less prominent for amyloglucosidase alone (Figure 3.3 C, E, G, H). Heat treatment above the gelatinization temperature increases *K* values markedly compared with native starch, and is consistent with enzyme accessibility to starch being greatly increased by the order-disorder transition induced by heating. Comparison of results for maize and potato indicate that the digestion processes (digestogram and *K* values) are indeed very similar for cooked starches. However, it was found that the digestion rate coefficient for granule ghosts is ca. 2 times lower than that for cooked starch. This shows that there is some restriction to ghost digestion ('low shear cooking') compared with cooked starch ('high shear cooking'). The formation of granule ghosts is thought to involve amylose molecules or possibly long branches of amylopectin and can be augmented by starch-based proteins and lipids, but there is no clear evidence for any structural organization of these components within ghosts.[59, 179] Whatever structural factors are responsible for ghost integrity may also be responsible for both the slower digestion rates compared with high shear cooking as well as the incomplete digestion after 24 h incubation (ca. 80% for

potato and ca. 90% for maize). Another possibility is that the intact multi-micron ghost structure may be responsible for their restricted digestion behavior. The size and robustness of granule ghosts are proposed to be determined by the relative rates of swelling and cross-linking, modulated by surface non-polysaccharide components.[179] In order to address this, the digestibility and structure of starch granule ghosts are under study and will be reported subsequently.

Table 3.1. Digestion rate coefficient (K, min^{-1}) of maize and potato starch samples [a].

MS	K_{MS}	PS	K_{PS}
MS-N-AA/AMG	$(2.49 \pm 0.05)\times10^{-3}$c	PS-N-AA/AMG	$(7.87 \pm 0.17)\times10^{-4}$d
MS-N-AMG	$(2.20 \pm 0.01)\times10^{-4}$d	PS-N-AMG	$(1.86 \pm 0.15)\times10^{-4}$d
MS-C-AA/AMG	$(6.23 \pm 0.57)\times10^{-3}$b	PS-C-AA/AMG	$(7.66 \pm 1.28)\times10^{-3}$a
MS-G-AA/AMG	$(3.87 \pm 0.39)\times10^{-3}$c	PS-G-AA/AMG	$(3.38 \pm 0.89)\times10^{-3}$c

[a] The data are averages of two measurements with standard deviation. Means in columns with different letters are significantly different ($p < 0.05$) by general linear model.

3.5 Conclusions

This study has shown that the physical structure of a biomacromolecular substrate can determine whether the actions of endo- and exo-hydrolyzing enzymes are synergistic or antagonistic. Furthermore, the kinetic profiles of hydrolysis are also found to be dependent on the physical structure with (under the conditions used) first-order kinetics found for condensed granular substrates where it is proposed that enzyme-substrate complex formation is rate-limiting. For cooked starch and granule ghosts, deviations from first-order kinetics indicate a fraction of more rapidly digested material (under combined exo- and endo-hydrolysis conditions) and a change in rate-limiting step under exo-hydrolysis conditions.

Chapter 4

Mechanism for Starch Granule Ghost Formation Deduced from Structural and Enzyme Digestion Properties

(This chapter has been published in J. Agric. Food Chem., *2014, 62,* 760-771*.)*

*Bin Zhang, Sushil Dhital, Bernadine M. Flanagan, and Michael J. Gidley**

Centre for Nutrition and Food Sciences, Queensland Alliance for Agriculture and Food Innovation, The University of Queensland, St. Lucia, Brisbane, QLD 4072, Australia

* Corresponding author.

Phone: +61 7 3365 2145; Fax: +61 7 3365 1177. Email address: m.gidley@uq.edu.au (M. J. Gidley)

4.1 Introduction

Many agriculture and food biopolymers are assembled in an ordered or crystalline form in nature to confer stability and minimize hydration-driven swelling in the native environment. However, once these molecules or assemblies are heated above the relevant melting temperature, most become soluble, at least initially. Examples include many proteins and polysaccharides. Starch, however, is an exception, as when native semi-crystalline granules are heated above their characteristic melting temperature under little or no shear, they swell and release some lower molecular weight components, but do not dissolve completely. Most applications of starch in food and industrial processes involve a heating step in the presence of water, which disrupts the ordered arrangement of polymers within granules (termed gelatinization). Gelatinized starches typically contain a mixture of solubilized polymers (mainly leached amylose and amylopectin molecules with low molecular weight) and residual granular structure (also termed (fragments of) granule 'ghosts').[59] The importance of starch granule ghosts in determining the properties of cooked starches is often underestimated in studies that treat gelatinized starch as a fully dissolved polymer solution, like other biopolymer solutions such as agar and gelatin.[179, 194] The presence of the large (10-200 μm) macromolecular architecture of granule ghosts

within an otherwise homogeneous polymer system can affect molecular processes, such as phase separation, and contribute to functional properties of starches that play important roles in texture and mouthfeel (e.g., viscosity, rheology, and tribology).[179]

Numerous studies of the structural changes associated with starch gelatinization have been reported,[65, 67, 195-197] but the factors that contribute to the stability of granule ghost structures are still not clear. Various approaches have been used to understand the robustness of granule ghosts, including selective extraction of surface non-polysaccharide components, treatment of ghosts with protein-degrading enzymes, and the study of waxy maize mutants with variable (low) amylose contents.[44, 179] On the basis of these studies, it has been hypothesized that ghost formation is due to the cross-linking of amylose chains and/or long amylopectin branches (previously presumed to be by double helices), modulated by surface non-polysaccharide components.[44, 179] However, direct experimental testing of this hypothesis has not been reported yet. Due to the lack of detectable ordered structure in granule ghosts[59] (e.g., crystallinity from X-ray diffraction, helical order, or regularity of amylopectin clusters from small-angle X-ray scattering), physical techniques used to study the intermolecular interaction of biopolymers, such as wide- and small-angle X-ray scattering, differential scanning calorimetry (DSC), ^{13}C nuclear magnetic resonance (NMR) and Fourier transform infrared (FTIR) spectrometry, may provide limited insight into the mechanism of ghost formation and stabilization. We have recently shown, however, that there is a fraction of granule ghosts that is relatively resistant to enzymatic digestion.[198] In this work we hypothesize that such enzyme-resistant fractions may be important in providing stabilizing structure to granule ghosts. We have therefore studied the susceptibility of granule ghosts toward enzymatic hydrolysis and investigated the macromolecular and ordered structures present in undigested residues as a probe of local structures that may be important in the formation and structure of ghosts.

Although there is some enzyme-resistant material present in granule ghosts formed under low shear cooking conditions from both maize and potato starches, high shear cooked starches are almost 100% digested, suggesting that granule ghosts are structurally different from high shear cooked starches.[198] In this study, amylase digestion is used as a probe to investigate the structure of granule ghosts isolated from maize and potato, two commonly used commercial starches with different ghost profiles (e.g., size and integrity), as exemplars. On the basis of concept that the enzyme resistant fraction is important for maintaining ghost integrity, at least three hypotheses for the underlying structural basis for

enzyme resistance can be proposed: (a) the multi-micrometer structure of granule ghosts acts as a barrier to limit enzyme access; (b) cross-linking or dense entanglement of amylose and/or amylopectin branches limits enzyme action; or (c) proteins and lipids associated with the granule may contribute to either barrier or local cross-linking mechanisms. To test these hypotheses, in this study morphological parameters of ghosts and digested remnants have been studied with different microscopic techniques, the molecular structure evolution during amylase digestion of granule ghosts has been monitored by ^{1}H NMR spectroscopy and size exclusion chromatography (SEC), and the conformation of polymers within ghosts and enzyme-resistant residues has been determined by ^{13}C CP/MAS NMR. On the basis of data obtained, mechanisms for starch granule ghost formation and stability are discussed.

4.2 Experimental procedures

4.2.1 Materials

Maize starch (MS) was purchased from Penford Australia Ltd. (Lane Cove, NSW, Australia), and potato starch (PS) was from Sigma-Aldrich. (St. Louis, MO, USA). Porcine pancreatic α-amylase (A3176, activity 23 unit/mg) and other chemicals were obtained from Sigma-Aldrich.

4.2.2 Depletion of proteins and lipids from granule surfaces

Treatment of starch granule slurries (20% w/v) with sodium dodecyl sulfate (SDS, 2% w/v) at 20 °C for 30 min was used to extract surface proteins and lipids[9]. Extracted granules were isolated by centrifugation and washed with > 10 volumes of cold deionized water until no foaming was observed in the washings. Despite the extensive washing, some SDS was retained by the granules as shown by the increase in sodium and sulfur contents after treatment (Appendix 1, Table A1-1).

4.2.3 Preparation of cooked starch and granule ghosts

Starch granule aqueous slurry (10 mL, 0.5% w/v) in a 50 mL centrifuge tube (with a magnetic stirrer, 3 mm x 8 mm) was heated to 100 °C on a hot plate stirrer at a stirring rate of 1500 rpm for 30 min (‘high shear cooking’) and designated ‘cooked starch’. Granule ghosts were isolated from maize and potato starches following an adaptation of a method reported previously.[59, 179] Starch (200 mg) was suspended in a small amount of cold water and then poured into hot water (95 °C, 40 mL). The dilute suspension (0.5% w/v starch) was kept at 95 °C for 30 min at a low stirring rate (250 rpm, ‘low shear cooking’) and then

centrifuged (30 °C, 2000 *g* for 15 min). The supernatant was removed, and the spun ghosts were washed twice by resuspension in hot water (90 °C) with gentle manual stirring followed by centrifugation. Ghost yield was defined as the weight ratio of freeze-dried pellet to initial starch. The washed ghosts were finally resuspended in excess water for microscopy and *in vitro* digestion. For SEC, NMR, and scanning electron microscopy (SEM) measurements, starch samples were precipitated by absolute ethanol, and dried under pressured nitrogen gas overnight.

4.2.4 Microscopy

Light microscopy was performed using a Zeiss Axio microscope (Oberkochen, Germany). One drop of fresh granule ghost suspension was placed on a glass slide and stained with 2% iodine solution, and the images were recorded by AxioCam ERc5s camera (Zeiss). For confocal microscopy, the staining procedure of fresh granule ghosts with Nile blue was adapted from the method described by Schirmer, et al. [199] Aqueous suspensions of granule ghosts (0.5 mL) and 40 *μ*L of aqueous Nile Blue solution (0.1 g/100 mL; N0766, Sigma-Aldrich) were transferred into 2 mL microcentrifuge tubes. After thorough mixing by repeated pipetting up and down, the stained solutions were incubated at 20 °C for 3 h. For confocal microscopic observation, the stained suspensions were dropped into the cavity of glass slides, sealed with a coverslip, and then observed using a LSM 700 confocal laser scanning microscope (CLSM, Zeiss). Excitation was at 639 nm with a diode laser operating at 2% of power capacity, and the emitted light was detected at an interval wavelength of 640 - 700 nm. Images of optical sections of granule ghosts were recorded with ZEN 2011 software (Zeiss, Oberkochen, Germany). For SEM, ethanol-dried samples were thinly spread onto circular metal stubs covered with double-sided adhesive carbon tape, and then platinum coated in a sputter coater. Images of the granule ghosts were acquired with a JEOL 6300 scanning electron microscope (JEOL Ltd., Tokyo, Japan) under an accelerating voltage of 5 kV.

4.2.5 Particle size distribution

Particle size analysis was carried out using a Malvern Mastersizer Hydro 2000MU (Malvern Instruments Ltd., Malvern, UK) following the method of Dhital, Shrestha and Gidley [110]. A refractive index of 1.34 was used for granule ghost size calculation. The starch samples were added to circulating water until an obscuration of >10% was recorded.

4.2.6 *In vitro* starch digestion

In vitro starch digestion was performed with porcine pancreatic α-amylase, from the method described by Zhang, Dhital and Gidley [198] with slight modifications. Starch samples (50 mg, dry basis) were digested with 2.5 units of α-amylase in 30 mL of sodium acetate buffer (0.2 M, pH 6.0) in a shaking water bath at 37 °C. Aliquots (0.2 mL) were removed at different intervals, mixed with 1.0 mL of 95 °C water, and then boiled for 10 min to inactivate enzymes. The reducing sugar value was measured by the Nelson-Somogyi method.[200] The maltose equivalent released (%) was calculated using the following equation (Eq. 4.1). Results were expressed as means with standard deviations of at least duplicate measurements.

$$\text{Maltose equivalent released (\%)} = \frac{\text{total weight of equivalent maltose in supernatant}}{\text{dry weight of starch}} \times 100 \qquad \text{(Eq. 4.1)}$$

4.2.7 Size exclusion chromatography

The fully branched and debranched size distribution of starch molecules during the course of *in vitro* digestion was obtained from an SEC system (Agilent 1100, Agilent Technologies, Waldbronn, Germany) equipped with a refractive index detector (RID-10A, Shimadzu, Kyoto, Japan) following the methods of Cave, et al. [201] and Hasjim, Lavau, Gidley and Gilbert [171] SEC samples were carefully prepared following the method described elsewhere,[171] and then injected into the following series of columns: precolumn, Gram30, Gram3000 (PSS, Mainz, Germany) for the fully branched distribution, and precolumn, Gram100, Gram 1000 for debranched distribution. The molecular size distribution data were plotted as SEC weight distribution, $w(\log V_h)$, against the hydrodynamic radius (R_h/nm). For linear polymers of uniform geometry, the size and molecular weight (or equivalently the degree of polymerization, DP) are uniquely related, and hence the size distribution can be processed to a molecular weight distribution using the Mark-Houwink equation.[201, 202] SEC calibration was performed using pullulan standards with molecular weights ranging from 342 to 1.66×10^6 Da (PSS, Mainz, Germany). The standards were dissolved in the SEC eluent and injected into the branched and debranched SEC setups to provide universal calibration curves to relate elution volume with R_h. Because of the calibration range, the R_h values above the upper limit of the standards available (~50 nm) are only semi-quantitative. The amylose content can also be calculated as the ratio of the area under the curve (AUC) of the debranched SEC distribution curves for the larger branches to the total AUC for all branches.[203] The

amylose contents of maize and potato starches determined in this way were 23.3±1.0 and 18.3±0.4% respectively.

4.2.8 ^{1}H Nuclear magnetic resonance spectroscopy

The degree of branching (DB) of starch molecules during the course of *in vitro* digestion was measured on a Bruker Avance NMR spectrometer (Bruker Biospin, Rheinstetten, Germany), operating at a Larmor frequency of 750 MHz for ^{1}H, equipped with a TXI5z probe following the method of Tizzotti, et al. [204] ^{1}H NMR spectra were recorded at 333 K with an 8 μs 90° pulse, a repetition time of 15.98 s (composed of an acquisition time of 3.98 s and a relaxation delay of 12 s) and 128 scans. The addition of a very low amount of TFA-d_1 to the medium causes the exchangeable protons of the starch hydroxyl groups and of the residual water to shift to higher frequency, leading to clear and well-defined ^{1}H NMR spectra. [204] DB is obtained using the following equation (eq. 4.2):

$$DB\ (\%) = \frac{I_{\alpha-(1,6)}}{I_{\alpha-(1,4)} + I_{\alpha-(1,6)}} \times 100 \qquad \text{(Eq. 4.2)}$$

where $I_{\alpha\text{-}(1,4)}$ and $I_{\alpha\text{-}(1,6)}$ are the ^{1}H NMR integrals of internal α-(1,4) and α-(1,6) linkages at ~5.12 and ~4.78 ppm, respectively.

4.2.9 ^{13}C CP/MAS Nuclear magnetic resonance spectroscopy

Starch samples were examined using a solid-state ^{13}C CP/MAS NMR spectrometer (Bruker MSL-300, Rheinstetten, Germany) at a ^{13}C frequency of 75.46 MHz. Approximately 200 mg of sample was packed in a 4-mm diameter, cylindrical, partially-stabilized zirconium oxide rotor with a KelF end-cap. The rotor was spun at 5 kHz at the magic angle (54.7º). The 90º pulse width was 5 μs and a contact time of 1 ms was used for all samples with a recycle delay of 3 s. The spectral width was 38 kHz; acquisition time 50 ms; time domain points 2 L; transform size 4 K; and line broadening 50 Hz. At least 2400 scans were accumulated for each spectrum. In the case of the 3 h digestion residues of maize and potato ghosts, it was necessary to collect 20000 scans, as only 50 mg was available. Spectra were referenced to external adamantine and were analyzed by resolving the spectra into ordered and amorphous subspectra and calculating the relative areas as described previously.[205] When percentage order is calculated, freeze-dried starches are compared with freeze-dried amorphous standards, and samples precipitated with ethanol are compared with ethanol-precipitated amorphous standards.

4.3 Results and discussion

4.3.1 Microscopic structure of granule ghosts

Fresh granule ghosts from maize and potato starches were isolated by centrifugation following the method reported by Debet and Gidley [179] This method ensures full gelatinization and maximum swelling (for most normal starches) when starch is heated at 95 °C for 30 min in excess water. The risks of retrogradation from leached amylose and shear degradation are minimized by the low starch concentration (< 1% w/v) and low stirring rate during ghost preparation respectively.[132] Light microscopy and particularly confocal microscopy suggest that ghost particles are essentially hollow with a surface 'skin' composed of apparently densely packed starch (Figure 4.1 A1 and B1). Granule ghosts have characteristic microscopic features depending on their botanical and genetic origins.[206] Fresh maize ghosts showed complex shapes and surface folds, but appeared overall fairly spherical, typically with a particle size between 15 and 35 μm (Figure 4.1 A1). In contrast, potato ghosts have a wide range of particle sizes (typically 50 – 150 μm) with more ellipsoidal shapes and significant amounts of granule fragments (Figure 1 B1). Expansion is so extensive that the resultant potato ghosts (ca. 4 times expansion in original diameter, i.e., ca. 64-fold increase in granular volume) are more fragile and sensitive to shear force, compared with maize ghosts (increasing only ca. 2 times in diameter) even under the low shear conditions used in ghost preparation. This is not surprising because potato starch contains an appreciable amount of phosphate monoester groups,[56] which are negatively charged and linked to potato amylopectin molecules. The resulting charge repulsion effect helps to untangle the individual branches and extends the degree of granule swelling.[39] Maize ghosts frequently appeared to have more localized regions of folds and wrinkles (Figure 4.1 A1, B1, insets), which may trap undispersed starch polymers.[194]

The morphology of granule ghosts was also investigated using CLSM after being stained by Nile blue, a water-soluble basic oxazine dye, which is one of the most suitable fluorescent staining agents for both granular and gelatinized starches in the absence of proteins.[199] CLSM micrographs of granule ghosts show isolated balloon-like structures, lacking their original contents (Figure 4.1 A1 and B1 insets). The skins of maize ghosts appear to be thicker and more substantial and do not show much deterioration or collapse, compared with potato ghosts (Figure 4.1 A1, B1 insets).

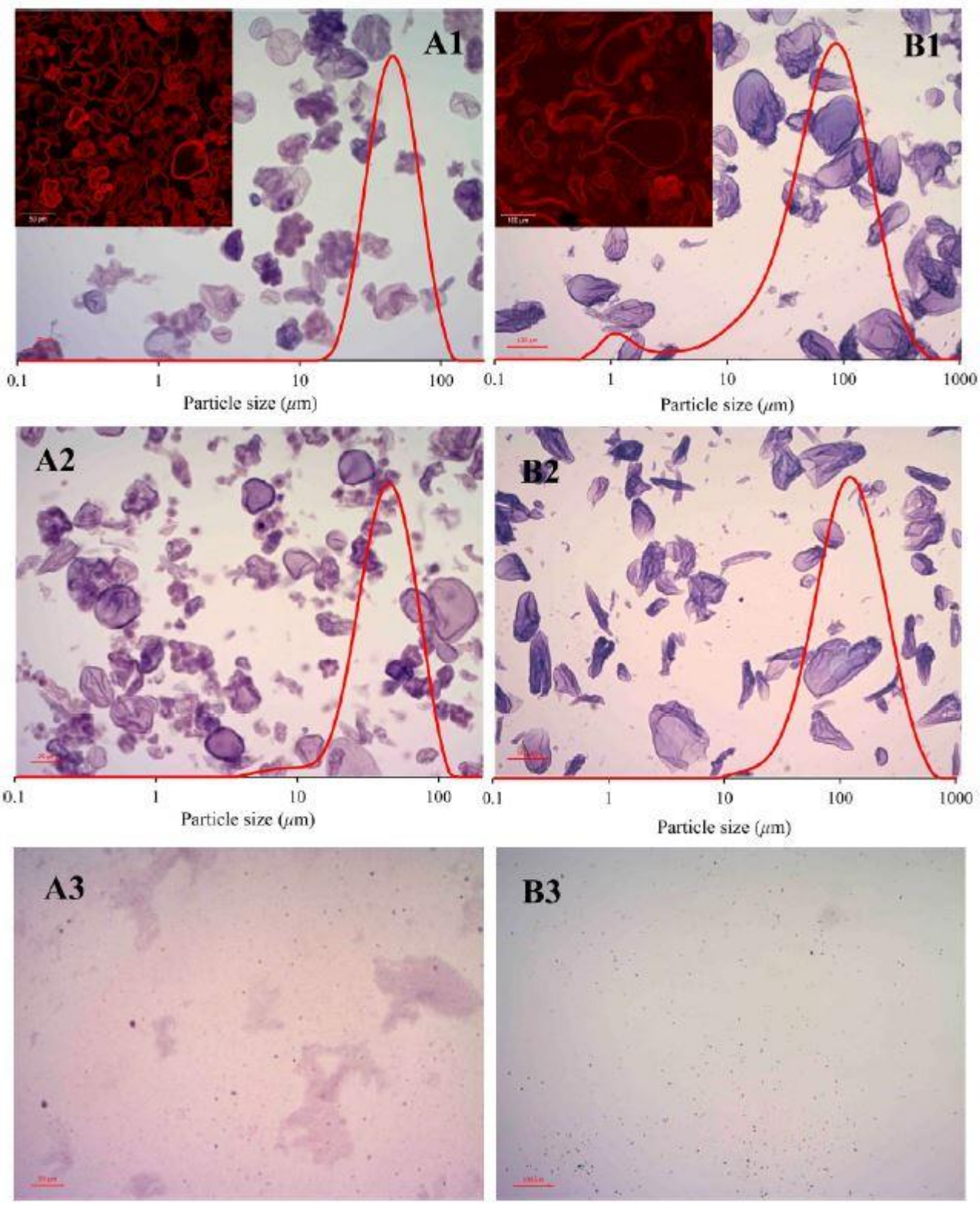

Figure 4.1. Light micrographs and particle size distribution of fresh granule ghosts (A, maize, scale bar = 20 μm; B, potato, scale bar = 100 μm) with/without SDS pre-treatment or high shear force (1, without any treatment; 2, with SDS pre-treatment; 3, with high shear force treatment after ghost formation). Insets in panels A1 and B1 are confocal microscopy images after staining with Nile Blue.

To visualize structure at higher resolution, fresh ghosts were precipitated with absolute ethanol, dried with N_2 gas, and examined by SEM. Although syneresis occurring during ethanol precipitation can reduce the roughness of surfaces,[207] the sizes of granule ghosts visualized by electron microscopy (Figure 4.2) are in agreement with the fresh ghosts (Figure 4.1) observed by light microscopy. Walls of the ghosts, especially those from maize, did not show much deterioration or collapse, which is consistent with CLSM images (Figure 4.1 A1). Surface pinholes were visible in some ethanol-precipitated ghost particles (Figure 4.2 C), and were of approximately the same size as before cooking (0.1 ~ 0.3 μm).[190] Potato ghosts (Figure 4.2 E, F) showed a spongier and more open structure and evidence for deterioration/fracture, probably due to the comparatively thinner walls of these more expanded hollow particles.

Starch granules, in addition to amylose and amylopectin, contain small quantities of minor components, such as lipids and proteins. The proportion of these components depends on the botanical origin and the degree of purification during extraction.[206] SDS can be used to solubilize at least some proteins and lipids from the surface of starch granules (see Appendix 1, Table A1-1).[44] The extraction of lipids/proteins from the granule interior is difficult, requiring more disruptive methods such as stringent extractions at higher temperatures, chaotropic agents or starch-degrading enzymes.[44] SDS washing of granules prior to ghost formation resulted in reduced ghost integrity (or robustness), especially for potato (Figure 4.1 A2, B2). As granule ghosts with SDS pre-treatment have more irregular shapes (some rod-like shapes for potato), it is not appropriate to assess the particle size by laser scatting techniques. These results are consistent with a previous report in which surface proteins and lipids were found to be a determinant of ghost robustness rather than ghost formation.[179] Shearing results in fragmentation of heated starch granules, and facilitates the development of a homogeneous matrix.[208] The multi-micrometer structure of ghosts can be efficiently disrupted by Ultraturrax homogenization (20000 rpm for 1 min), resulting in a dispersion of smaller particles and dissolved polymer molecules (Figure 4.1 A3, B3).

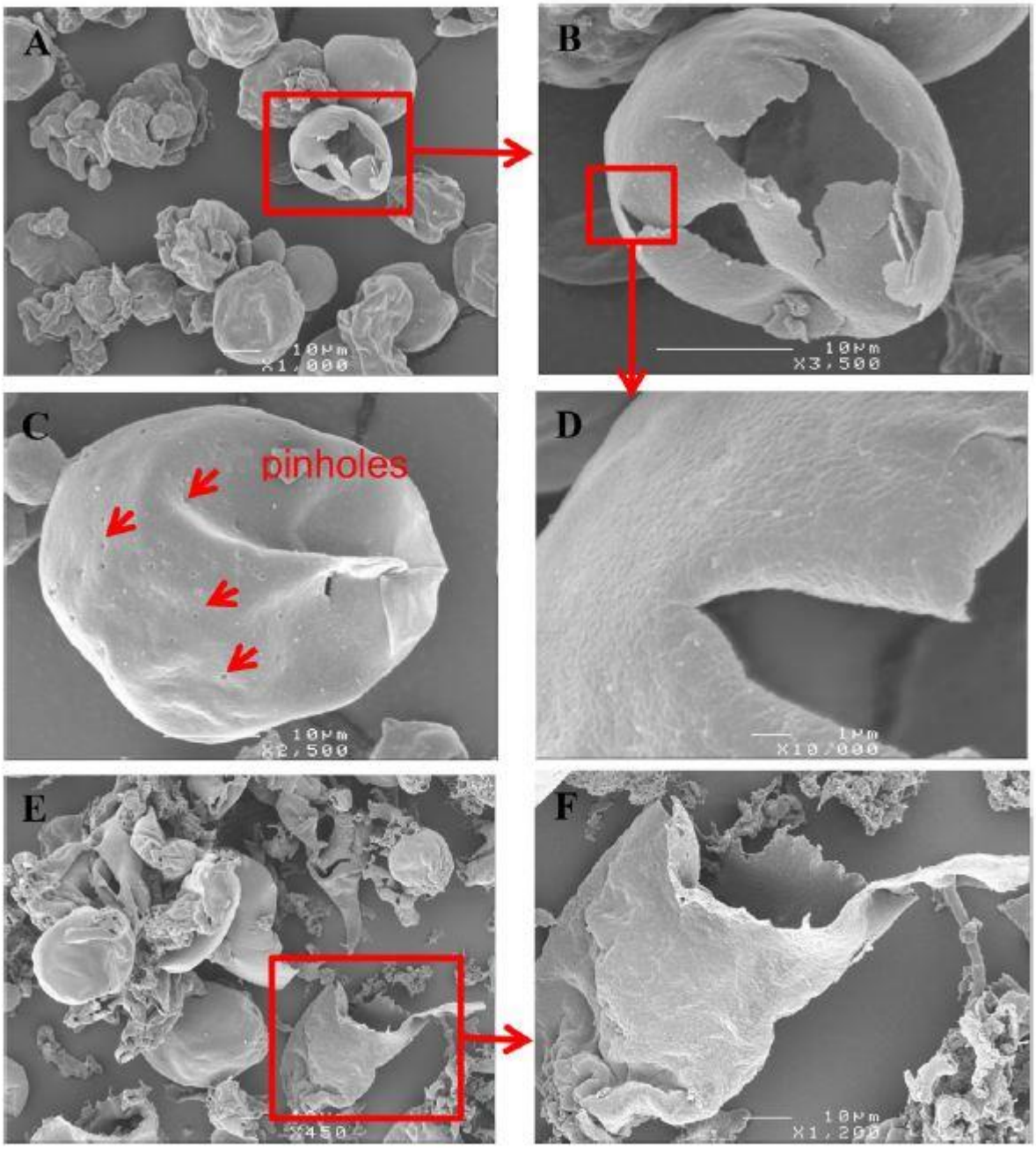

Figure 4.2. SEM micrographs of ethanol-precipitated granule ghosts (A-D, maize; E and F, potato).

4.3.2 α-Amylase digestion

For the range of starches examined here and previously, both surface non-polysaccharide material and polysaccharide chains themselves appear to be linked with ghost formation and/or resultant integrity.[44, 59, 179] The roles of the multi-micrometer structure (hypothesis a) and surface proteins/lipids (hypothesis c) during ghost formation were tested by breaking down the ghost particles by high-speed homogenization, or extracting surface components by SDS at room temperature respectively, with enzyme digestion being used as a structure/function probe. According to our previous findings, there is some enzyme-

resistant fraction present in granule ghosts after α-amylase and amyloglucosidase digestion, individually and in combination, compared with high-shear-cooked starch.[198] We suggest that the most enzyme-resistant fractions may play an important role in maintaining ghost integrity.

The kinetic profiles of granule ghost digestion were monitored by measuring the reducing sugar released at specific intervals during digestion with a low amount of α-amylase (Figure 4.3). In addition, the influence of maltose on the kinetics of α-amylase was also investigated (see Appendix 1, Figure A1-1), to confirm that the end products (i.e., malto-oligosaccharides) do not inhibit further α-amylase digestion under the conditions used.[209] For both maize and potato ghost samples, pre-treatment with SDS or post treatment by shearing did not change digestion behaviors markedly, but cooking with high shearing to prevent ghost formation resulted in a small increase in digestibility, particularly after 3 h of digestion (Figure 4.3 A and B). When the yield of enzyme-resistant fraction was quantified by weight, the high-shear-cooked starches were found to be almost completely digested after 3 h, particularly for potato (isolated yields of 2.1±0.3% for cooked maize, and 0.2±0.2% for cooked potato). Starch gelatinization disrupts structural features (e.g., semi-crystalline structure, original surface organization) that otherwise slow down enzyme action, and can cause surface rupture at stress points.[194] Digestion profiles suggest that SDS-extractable proteins/lipids are not crucial for control of either ghost digestion or ghost integrity. The skins of many ghosts appear incomplete, with cracks and openings on the micrometer scale and additional small (~20 nm) pores (particularly for maize starch) and fine particles (~400 nm, particularly for potato starch) [194, 210] Therefore, we propose that the formation of enzyme-substrate complexes, rather than the access of the enzyme to the granule ghost skin, primarily determines the rate-limiting step of enzyme digestion. Evidence that surface non-polysaccharide components alone are not sufficient to restrict swelling and affect resultant ghost formation also comes from a previous comparison of swelling profiles for a wide range of starches from different botanical origins.[44] This is logical, as starch polymers are the dominant components in ghosts.[179]

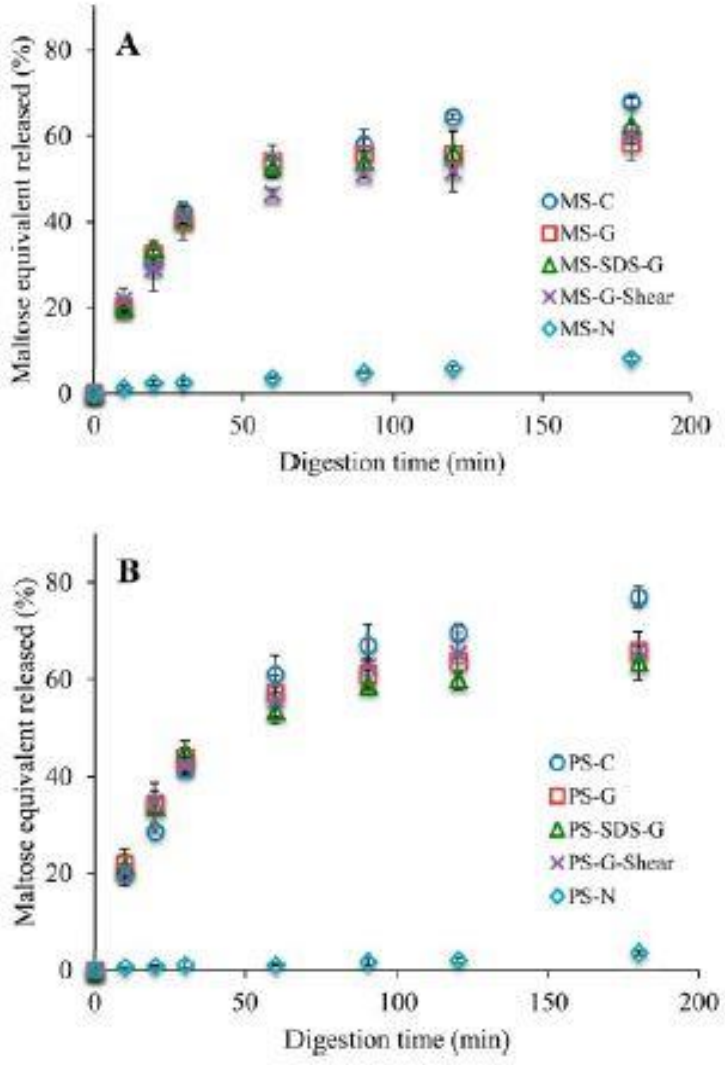

Figure 4.3. Amylase digestion profiles of granule ghosts (A, maize; B, potato). N, native starch; C, cooked starch prepared under high shear condition; G, granule ghosts; SDS-G, granule ghosts with SDS pre-treatment; Shear, with high shear treatment.

For maize and potato starches, temperatures of structural disorganization (as monitored by loss of birefringence or DSC) are relatively similar, yet swelling profiles show major differences.[211] However, once swollen, the digestibilities of potato and maize granule ghosts are comparable (Figure 4.3), but in both cases for starch cooked under shear, the maltose equivalents released are ca. 10% higher than for ghost samples after 3 h of hydrolysis, suggesting some structural differences between high-shear-cooked starch and granule ghosts. Up to now,[59] no direct evidence of any carbohydrate ordered structure has been found for ghosts by X-ray scattering / diffraction, ^{13}C NMR, or DSC (e.g., Appendix 1, Figure A1-2). For starch that has been solubilized and then become insoluble by retrogradation, the driving force is typically double-helix formation and subsequent crystallization, but there is currently no evidence that these structures exist in granule

ghosts, which have never been solubilized. The possible reasons could be that either the double-helical order is present within ghosts but lower than the detection limit of measurement techniques, or the polymer chains are just physically entangled without any fixed conformation in the skins of ghosts.

4.3.3 Molecular structures present in granule ghosts and their evolution during amylase digestion

Molecular size distribution of whole maize and potato starch molecules (Figures 4.4F and 4.5F, respectively) and chain length distributions of enzymatically debranched maize and potato starch samples (Figures 4.4A and 4.5A) were characterized using SEC. The fully branched SEC weight distribution of the whole molecules of the two starches showed an amylopectin peak (R_h between 40 and 300 nm, peak R_h = ~100 nm) and a shoulder for amylose molecules stretching from R_h of 1 to 40 nm. However, some hybrid components could also be present, such as molecules that are highly branched like amylopectin but with molecular size similar to that of amylose and also amylopectin molecules with extra-long branches.[212] The debranched SEC weight distribution can be empirically divided into two regions representing amylopectin branches (single-lamella branches, peak R_h ~1.5 nm or DP ~12; trans-lamella branches, peak R_h ~2.5 nm or DP ~50) and amylose branches (R_h ~3.5 – 80 nm, DP ~100 – 30000).[171, 213] Amylose molecules are typically smaller than amylopectin and tend to leach out from granules during swelling, as shown by amylose contents of maize (8.4 %) and potato (6.7 %) ghosts which are much lower than the starting starches (Figures 4.4B and 4.5B). Comparison of Figures 4.4F / 4.5F with Figures 4.4G / 4.5G shows that ghost formation is accompanied by loss of the lower molecular size molecules, again consistent with the amylose content results. During ghost formation, 15.1 and 38.8% of amylopectin (calculated from the amylose content of both granules and ghosts and the isolated yields of ghosts, see the Appendix 1) is leached out of maize and potato granules respectively, suggesting that either a proportion of ghosts do not survive the cooking process or that amylopectin molecules are leached alongside amylose. Despite differences in particle size and robustness, ghosts from maize and potato starch have similar fully branched and debranched molecular size distributions (Figures 4.4B, G and 4.5B, G).

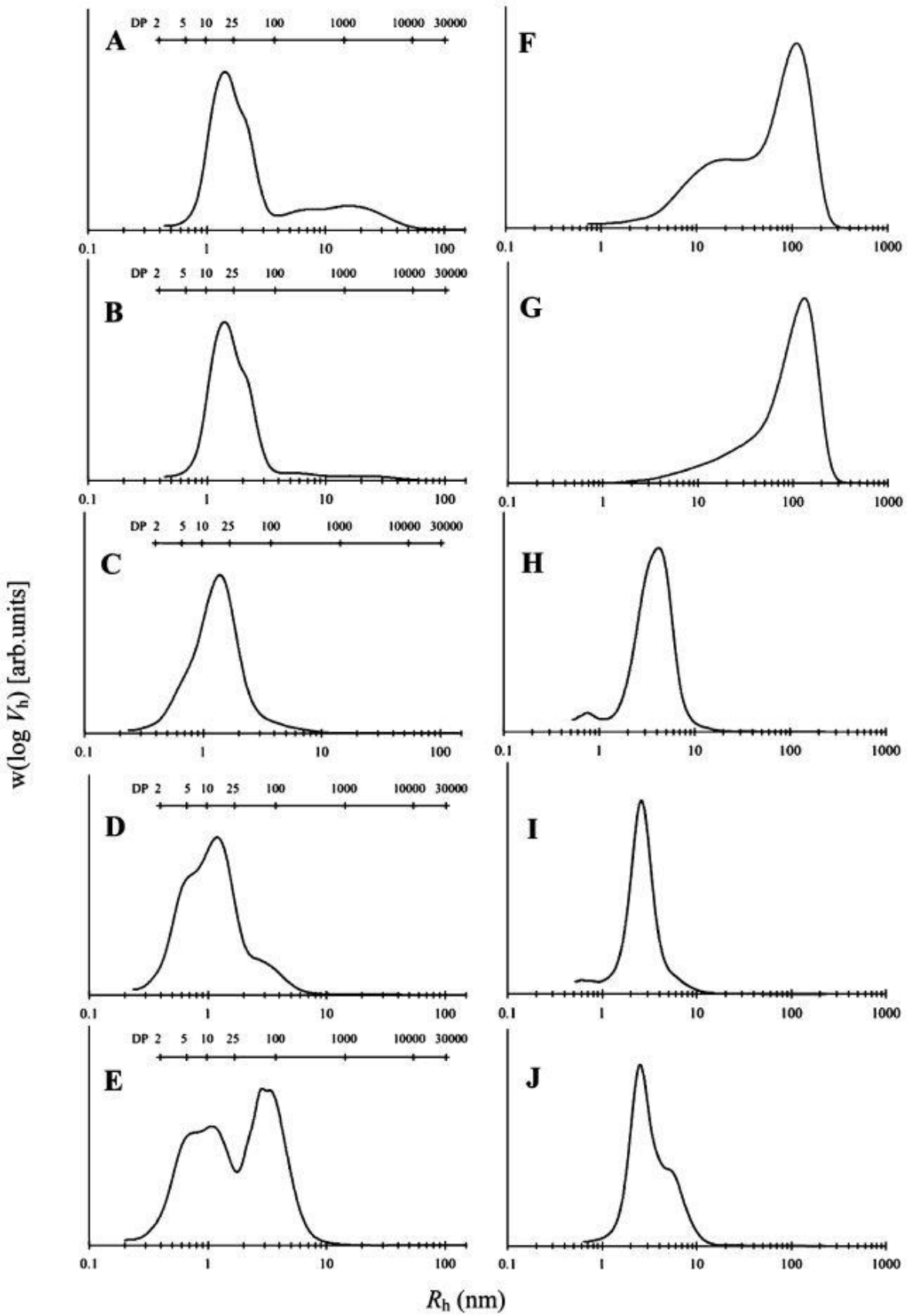

Figure 4.4. Size distributions of debranched (A-E) and whole (F-J) molecules from maize starch (A and F) and granule ghosts (B and G) after α-amylase hydrolysis for (C and H) 20, (D and I) 60, and (E and J) 180 min.

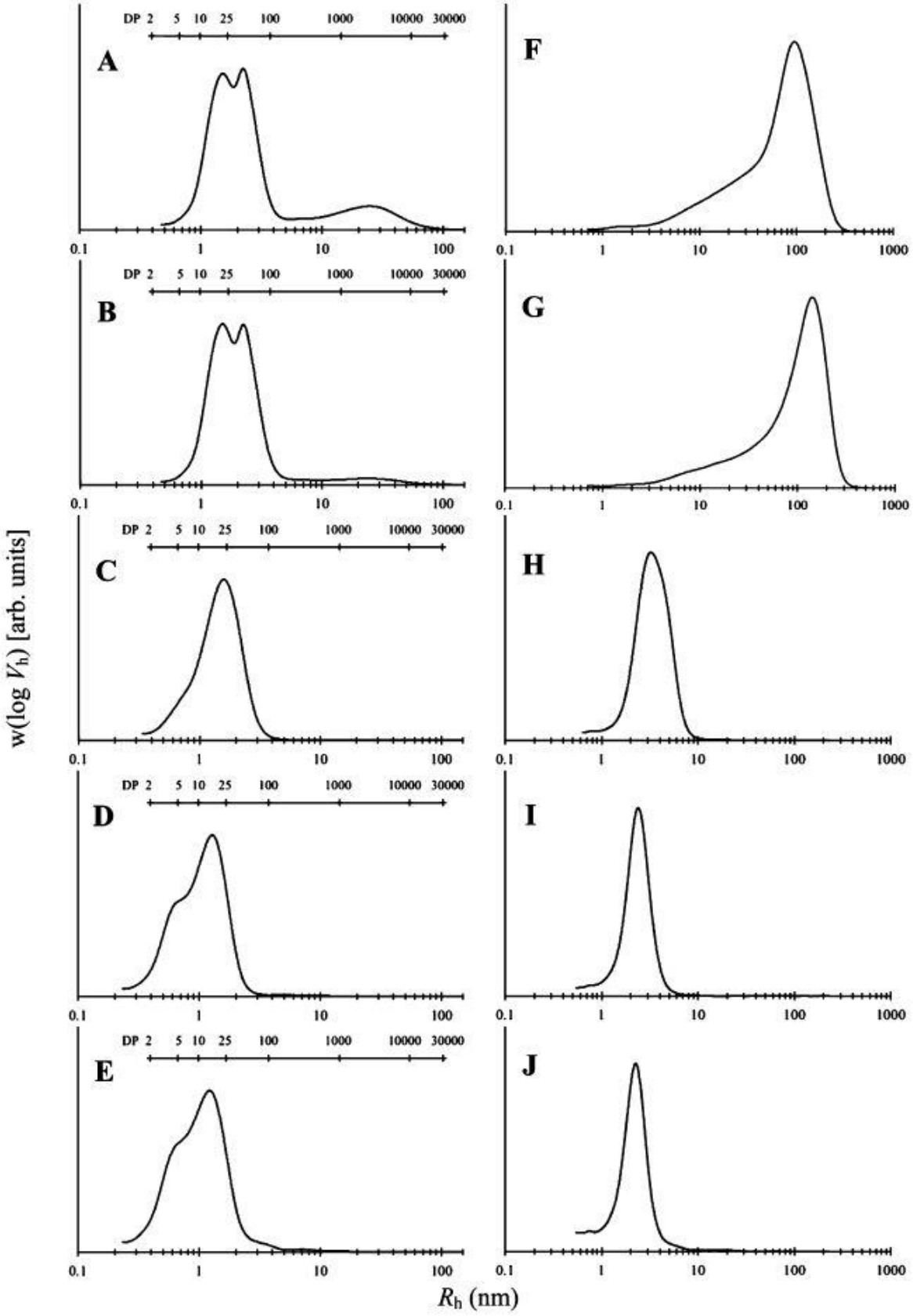

Figure 4.5. Size distributions of debranched (A-E) and whole (F-J) molecules from potato starch (A and F) and granule ghosts (B and G) after α-amylase hydrolysis for (C and H) 20, (D and I) 60, and (E and J) 180 min.

The debranched and fully branched SEC weight distributions of maize and potato ghosts and their evolution during amylase digestion are shown in Figures 4.4 and 4.5, and DB values calculated from ^{1}H NMR spectra are summarized in Table 4.1. DB values increase with digestion time, consistent with branched residues being less susceptible to digestion than non-branched residues, and potato DB values reach higher levels, suggesting a difference in the relative enzyme susceptibility of non-branched residues between maize and potato ghosts. The size distribution of whole starch molecules reveals that both amylose and amylopectin were quickly degraded to smaller molecules with a single R_h peak (~4 nm for maize; ~3 nm for potato) apparent within 20 min of digestion. The remnant small molecules were mainly degraded amylopectin and possibly contain some linear polymers, consistent with the fact that α-amylase is an endo-acting enzyme and likely to cleave α-1,4 linkages largely at random locations, and also in line with the increased DB values during digestion (Table 4.1). The corresponding chain-length distributions showed less changes of the degraded amylopectin together with a clear loss of longer amylose branches (R_h >10 nm, DP > 500) (Figures 4.4C and 4.5C), suggesting that α-amylase tends to cleave amylopectin molecules into clusters (which provide a barrier to enzyme access and hence prevent preferential digestion of inter-cluster amylopectin molecules[185]), and that digestion within clusters occurs at random. At the beginning of digestion (20 min), there was a gradual degradation of starch molecules as the peaks of both whole and debranched distributions were slightly shifted to lower R_h regions (Figures 4.4 and 4.5 D, F, I, J). In addition, it is noteworthy that the debranched chain distributions of 3-h-digested maize ghosts had bimodal peaks, whereas those from potato ghosts showed only one peak at R_h = ~1.5 nm with a shoulder that diminishes in size without changing shape (Figures 4.4E and 4.5E). The bimodal peaks of maize ghost residues are designated highly branched α-limit dextrin (peak observed at R_h ~1 nm) and longer chain polymers (R_h peak ~3.4 nm) respectively, which are consistent with their whole molecule distributions and DB values (Figures 4.4E, J; Table 4.1). Clusters of branching points within starch molecules will slow the amylase action because of steric hindrance. It is noteworthy that some long-chain polymers (DP > 100) survived, presumably from degraded amylose in original maize ghost particles. Cuevas, et al. [214] also found that the hot-water insoluble fractions in waxy rice starch contained DP ≥100 chains, which were absent in the hot-water soluble fractions. However, these long-chain components were not found for the potato ghosts with the same digestion time and similar digestion extents (Figure 4.3), in agreement with the higher DB values, compared with that of maize residues (Table 4.1). Furthermore, the α-limit dextrin peak indicates that whole amylopectin present in the

ghosts is reduced in size by α-amylase to ~2.5 nm remnant molecules, which is consistent with previous results.[171, 213]

Table 4.1. DB values (the number of branching points as a percentage of the total number of glucosidic linkages) of maize and potato ghosts and their evolution during amylase digestion.

sample [a]	DB (%)	sample [a]	DB (%)
MS	2.81	PS	2.11
MS-G	3.02	PS-G	2.17
MS-G-20	7.81	PS-G-20	4.82
MS-G-60	8.57	PS-G-60	12.75
MS-G-180	7.35	PS-G-180	11.95

[a] MS, maize starch; PS, potato starch; G, granule ghosts; 20, 60 and 180 represent hydrolysis for 20, 60 and 180 min, respectively.

4.3.4 Conformation of ghost residues after enzyme digestion

The macromolecular architecture of an apparently amorphous matrix such as granule ghosts is critical to their formation and stability. For starch granules, Biliaderis, et al. [215] proposed a three-phase model incorporating two distinct types of amorphous materials, that is, non-ordered inter-crystalline and bulk amorphous matrix, together with the crystalline domains of amylopectin clusters, accounting for order-disorder phase transitions of starch gelatinization. However, there is no reason to suppose that the same amorphous structures exist after gelatinization. As a probe of molecular conformation, molecular order (single helices, double helices) at short distance scale solid-state CP/MAS NMR spectra were recorded before and after enzyme digestion.

The ^{13}C CP/MAS NMR spectra of maize and potato ghosts prepared by freeze-drying or ethanol precipitation produce distinct NMR spectra (Figure 4.6A). Regardless of the botanical origin of starch, when the starches from the two drying methods are intensity matched at 84 ppm (Figure 4.6A), there is a difference in intensity between 92 and 100 ppm. By instead matching the intensity of a freeze-dried ghost spectrum, and an ethanol-precipitated ghost spectrum in the 92-100 ppm region and then subtracting the two spectra, a spectrum of V-type helices is revealed (Figure 4.6B). Spectra of all ethanol-precipitated ghosts clearly indicated the presence of V-type helices with peaks for C1 at

102.9 ppm and C4 at 81.5 ppm.[216] After 3 h of enzyme digestion, the resistant material was recovered by ethanol precipitation to separate it from the large amount of low molecular weight digestion products. NMR spectra (Figure 4.6C) therefore showed intensity consistent with V-type helices with peaks at 102.9 and 81.5 ppm. The ordered subspectra (Figure 4.6D) were obtained by matching the intensity at 84 ppm of the 3 h digestion residues and an ethanol-dried amorphous maize starch standard, and subtracting one from the other. Although there is no obvious order present when the total spectrum of 3-h-digested potato ghost is compared with the amorphous standard, upon subtraction of the two spectra it becomes apparent that a small amount of B-type double helices (13±2%) are found for the potato ghost digestion residue with peaks at 100.3 and 99.5 ppm. [216] [217-219] In contrast, the spectrum of the 3 h digestion residue from maize ghosts shows more V-type (19±2%) than the standard and the starting ghost material. As shown in Figure 4.6 A, B, ghosts (residues) isolated by ethanol precipitation have some V-type character. Consistent with this, digestion residues from both maize and potato starch ghosts have a signal for ethanol in the NMR spectrum (Figure 4.6C, 17 ppm). However, there are clearly also signals for lipids in the 3 h digestion residue from maize ghosts (Figure 4.6C, 33 and 23 ppm), and similar levels of ethanol peaks for both maize and potato 3 h digestion residues (Figure 4.6C, 17 ppm) can be detected.[220] We therefore propose that the enzyme-resistant V-type helices found in the digestion residue from maize ghosts are due to amylose-lipid complexes either present in the starting granule or formed during gelatinization and/or digestion processes.[74]

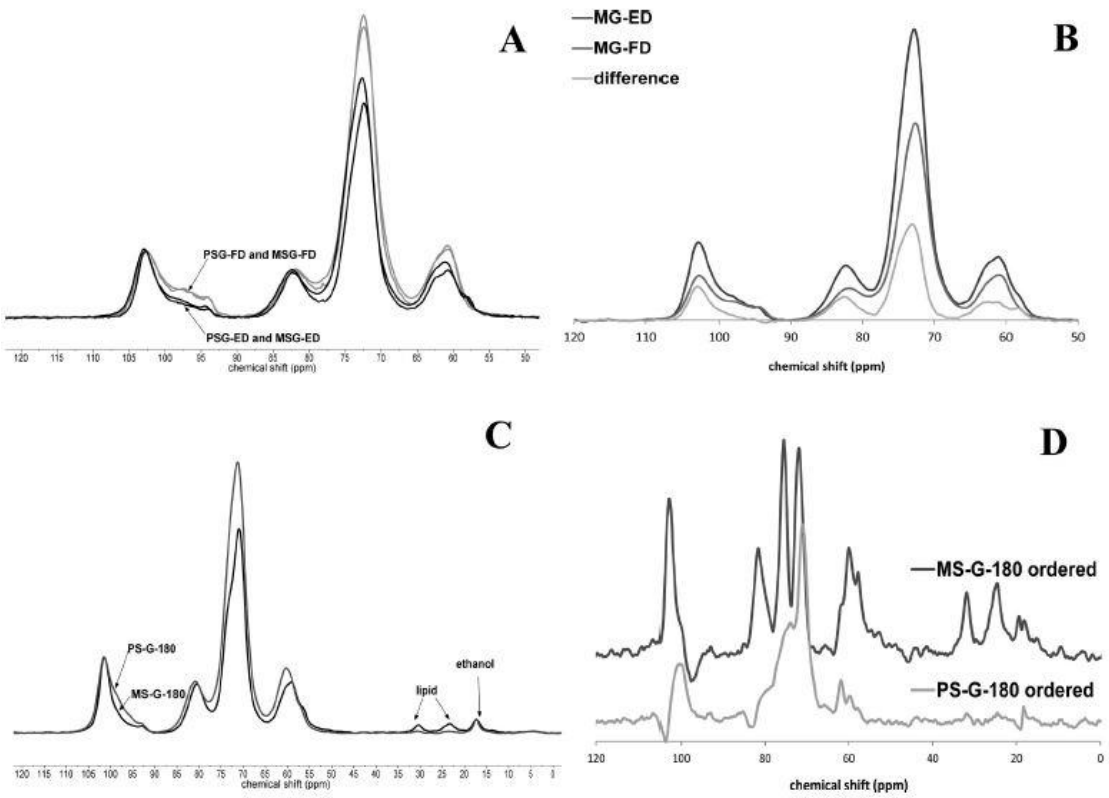

Figure 4.6. ^{13}C NMR spectra: (A) maize and potato ghosts with freeze-drying (FD) or ethanol-drying (ED); (B) maize ghosts with freeze- or ethanol- drying; (C) digestion residues from maize and potato ghosts. Separation of ^{13}C NMR spectra into ordered sub-spectra: (D) digestion residues from maize and potato ghosts. MS, maize starch; PS, potato starch; G-180, granule ghost hydrolysis for 180 min.

4.3.5 Proposed mechanism for granule ghost formation

At the early stage of heat/moisture-induced starch swelling, even at lower temperatures than those required for crystallite melting, amylose and a small amount of amylopectin molecules can leach out of granules.[30] Crystallite melting,[65] driven by double-helix dissociation,[195] causes granule swelling essentially by replacing hydrogen bonds between amylopectin chains with hydrogen bonds to water molecules,[58] thereby allowing swelling of high molecular weight amylopectin. Swelling behavior is primarily a property of amylopectin,[60] a main molecular component of ghosts, whereas amylose acts both as a diluent and as an inhibitor of swelling, especially in the presence of lipids/proteins, which can form insoluble complexes with amylose.[58, 63] An intact amylopectin surface is thought to form a continuous layer surrounding internal starch granule components.[194, 210] At certain critical stress points of granules, swelling eventually ruptures the envelope (e.g., Figure 4.2F), presumably by breakdown of the molecular interactions that holds the granule surface together. On the basis of the high level of enrichment of high molecular

size amylopectin, we suggest that molecular interaction between amylopectin units is responsible for the surface integrity of ghost particles. It has previously been shown by both small-angle and wide-angle X-ray scattering that there is no detectable crystalline or lamellar order in barley starch ghosts.[59] This lack of detectable organizational structure was further extended in this study through both DSC, which showed no detectable melting endotherms (Appendix 1, Figure A1-2) and solid state ^{13}C NMR which showed only amorphous features for both maize and potato freeze-dried ghost samples (Figure 4.6A). However, it is possible that a small amount of cross-linking through, for example, double helices could be present below detection levels of the X-ray, NMR and DSC techniques. The finding that there is a small amount of an enzyme-resistant fraction in maize (3.8±0.3%, calculated by weight of 3 h digestion residue) and potato (1.5±0.4%) starch ghosts suggests the possibility that this fraction provides a cross-linking or other stabilizing function in otherwise amorphous granule ghost structures.

From NMR (Figure 4.6) and SEC (Figures 4.4 and 4.5) results, the enzyme-resistant fraction of maize ghosts is enriched in amylose with 19% of the sample in a lipid-complexed single-helical form, and the enzyme-resistant portion of potato ghosts is enriched in amylopectin branches/clusters with 13% of the sample present as B-type double helices. In the case of maize, no evidence has been found for the presence of any potentially cross-linking double helices within ghosts, suggesting that double helices are not necessary to provide structure to ghost particles. Although the V-type helices from amylose-lipid complexes are not responsible for cross-linking starch chains as they involve only a single starch chain, they may help to rigidify segments of amylose within maize ghosts. Potato ghosts are more highly swollen and more sensitive to shear than maize ghosts, probably due to the repulsion effect from negatively charged phosphate groups during swelling. Despite similar amylose contents and enzyme digestibility to maize starch ghosts, the enzyme-resistant fraction from potato ghosts is qualitatively different, being based on amylopectin and containing at least some double helices. Normally, B-type double helices would be expected to be formed more readily from amylose and thereby potentially act to cross-link starch polymers. SEC data (Figure 4.5 E, J) for potato ghost enzyme-resistant residue, however, show that it contains predominantly amylopectin, consistent with largely intra-amylopectin double helices formed from adjacent branches, although cross-linking between amylopectin molecules cannot be ruled out. The presence of double helices in enzyme-resistant fractions of potato but not maize starch ghosts is consistent with the fact that the chain length distribution of amylopectin from potato is

longer than that of maize (Figures 4.4A and 4.5A), and the absence of V-type helices is consistent with the much lower lipid content of potato compared to maize starch.[41] However, it should be noted that the amount of double helices is low (~13% calculated for the 3 h digestion residue, corresponding to ~0.2% based on total starch ghost explaining why it cannot be detected in non-enzyme-treated ghosts) and, therefore, not likely to be a primary mechanism for ghost formation.

On the basis of the lack of detectable ordered structure in intact ghosts, and the low level of order within the small fraction of ghosts that are enzyme-resistant, it is apparent that the stable structure of ghosts is derived primarily from simple entanglement of non-ordered polymers, particularly amylopectin. The highly branched primary structure and very high molecular size of amylopectin (Figure 4.5) mean that each molecule can be involved in a large number of temporary entanglements, the sum of which can result in an effectively permanent multi-micrometer structure. Small amounts of amylose molecules may also be important to hold amylopectin molecules together by physical entanglements (e.g., maize and potato ghosts) and strengthen the cross-linking entanglements between amylopectin molecules. For example, starches from waxy maize lines with variable low levels of amylose formed granule ghosts with yield and integrity dependent on amylose content.[179] Surface proteins and lipids can also affect ghost properties. For those starches (e.g., wheat and maize) that have restricted swelling due to surface proteins/lipids,[44] ghosts prepared from SDS-treated granules show greater expansion due to the removal of constraining proteins and lipids, leading to a greater extent of swelling before sufficient cross-linking interactions occur to prevent dissolution.

4.4 Conclusions

In conclusion, the high molecular weight and highly branched primary structure of amylopectin will lead to many dynamic entanglements, which in combination seem to be sufficient to retain a stable ghost structure. The formation of ghosts as a consequence of extensive swelling of granules following gelatinization suggests that entanglements are formed during the swelling process, explaining why stable hydrated non-ordered starch structures starting from pre-isolated amylopectin have not been reported. The proposed mechanism for granule ghost formation not only confirms that double helices are not necessary to strengthen ghost structure, but also raises the question as to how enzyme-resistant fractions could be formed from an essentially amorphous (entangled) starch matrix. Crystallinity alone does not always lead to an increase in enzyme-resistance and

almost amorphous high-amylose starches can provide high yields of resistant fraction, although it has generally been accepted that crystallinity must play some role in determining enzyme resistance.[7, 8, 166]

Chapter 5

Lubrication and Rheology of Swollen Starch Granule Suspensions from Maize and Potato

Bin Zhang[a, b], *Nichola Selway*[c], *Kinnari J. Shelat*[a, b, c], *Sushil Dhital*[a, b], *Jason R. Stokes*[b, c], *and Michael J. Gidley*[a, b, *]

[a] Centre for Nutrition and Food Sciences, Queensland Alliance for Agriculture and Food Innovation, The University of Queensland, St. Lucia, Brisbane, QLD 4072, Australia

[b] ARC Centre of Excellence in Plant Cell Walls, The University of Queensland, St. Lucia, Brisbane, QLD 4072, Australiatable

[c] School of Chemical Engineering, The University of Queensland, St. Lucia, Brisbane, QLD 4072, Australia

* Corresponding author.

Phone: +61 7 3365 2145; Fax: +61 7 3365 1177. Email address: m.gidley@uq.edu.au (M. J. Gidley)

5.1 Introduction

Although most carbohydrate energy in higher plants is stored as semi-crystalline starch granules, the desirable physical properties of starch in food and industrial applications occur following a granule gelatinization process associated with loss of crystalline order. After heating in excess water with limited shear, starch granules swell to several times their initial size and release some low molecular weight polymers particularly amylose (an essentially linear glucose polymer), but do not dissolve completely and can persist as highly swollen forms (termed granule 'ghosts').[59] Ghosts can remain intact and keep their 'balloon'-like structure without internal contents to some degree that is dependent on the shear stress. Generally, these highly deformable ghost particles are thought to govern many of the characteristic physical properties of starch paste, solution, or gel networks such as viscosity, texture, and rheology.[221-223] For example, the presence of dilute or highly packed granule ghosts in some semi-solid starch-containing foods such as soups,

dressing, custards and sauces leads to ‘short’ texture, thick appearance and sometimes creamy mouthfeel.[224]

Granule ghosts isolated from normal starches such as maize and potato are enriched in amylopectin (a highly branched glucose polymer) with less than 10% of amylose.[79] Recently, we found that the ghost remnants after amylase digestion only contain less than 1% of single/double helices, and concluded that the ghost skin originates from physical entanglements of highly branched and large molecular size amylopectin molecules.[79] Fisher, et al. [225] reported that the potato ghost skin could support about 4000 mN/m tensile stress, approximately 1000 times higher than the yield stress of a red blood cell membrane. Starch components other than amylopectin (e.g., amylose, surface lipids and proteins, minerals et al.) also play a role in restriction of swelling extent,[44, 226] which can vary depending on the botanical origins of the starch.[206] Shear and heat stability of ghost particles can be modified though certain chemical/physical modification, e.g., chemical cross-linking (to strengthen the wall structure and achieve high shear resistance) and pre-gelatinization (to increase the heat sensitivity).

Starch paste/gel subjected to gelatinization and/or retrogradation exhibits a typical non-Newtonian and viscoelastic behavior, with a low yield stress and shear thinning behavior.[227] The size, integrity and concentration (phase volume) of ghost particles within the matrix are important parameters which determine the viscosity and viscoelastic properties. Desse, et al. [228] found strong deformation and solvent loss of individual swollen starch granules subjected to shear stress with the aid of a rheo-optical set-up. The morphological structure (e.g., size, shape and integrity) of ghost particles can be greatly influenced by their botanic origins, modification methods and processing conditions such as shear, cooking/storage temperature and time.[44, 227] The viscosity is governed by volume fraction of the ghost particles in the dilute regime, whereas the particle rigidity effect takes a decisive factor in the closely packed regime.[221] Steeneken [221] further suggested that both particle rigidity and volume fraction can be important between these two regimes. Ghost particles squeezed and sheared between e.g. oral surfaces as a lubricant, may be important in provoking swallowing and are expected to contribute to the mouthfeel of starch-based foods and beverages.[224]

While the rheological behavior of starch pastes/gels has been extensively investigated both experimentally and theoretically,[222, 223, 229] there are only a few studies that also

consider tribological properties or which directly focus on the dominant feature of gelatinized starch systems – granule ghosts. Using maize and potato starches as exemplars, the first objective of the present study is to probe the lubrication properties of starch ghost suspensions over a wide range of concentrations. Lubrication has long been considered to play a critical role in oral perception of liquid and semi-solid foods such as smoothness, creaminess. However, the accurate measurements of soft-tribology using smooth hydrophobic polydimethylsiloxane (PDMS) as rubbing material was only achieved in the past decade.[230] With these soft-tribological contacts, Selway and Stokes [231] found that semi-solid foods (yogurt and custard) with similar viscoelastic behavior can have different friction response, exhibiting different mouthfeel. The second objective of this study is to further understand the viscosity and viscoelastic properties of starch ghost suspensions in both dilute and concentrated regimes. We measured the small deformation oscillatory rheological behavior before and after repeated large deformation steady shear tests, combined with light microscopy of ghost particles before and after the test. The particle properties are discussed in terms of understanding the observed differences in soft-tribological response between maize and potato ghost suspensions.

5.2 Experimental

5.2.1 Materials

Maize starch was purchased from Penford Australia Ltd. (Lane Cove, NSW, Australia), and potato starch was from Sigma-Aldrich. (St. Louis, MO, USA). The apparent amylose contents of maize and potato starches were found to be 27.5% and 36.4% respectively, using an iodine colorimetric method.[232] Other chemicals used were obtained from Sigma-Aldrich.

5.2.2 Preparation of granule ghost

Granule ghosts were prepared by following a method reported previously.[79, 179] Starch (200 mg) was suspended in a small amount of cold water (~ 2 mL) and then poured into hot water (95 °C, 40 mL) with gentle mixing (250 rpm with magnetic stirrer bar). The dilute suspension (0.5% w/v starch) was cooked at 95 °C for 30 min and then centrifuged (30 °C, 2000 *g* for 15 min). The supernatant was removed, and the spun ghosts were washed twice by resuspension in hot water (90 °C) with gentle manual stirring followed by centrifugation. The fresh ghost particles were finally resuspended in water at a wide range of weight concentrations, i.e., (very) dilute system: 0.01% and 0.1%; concentrated system: 0.87% (fully packed) potato ghost suspension, 1%, 2%, 3% (fully packed) maize ghost

suspensions) for tribological and rheological measurements. The continuous phase of ghost suspensions was separated by centrifugation at 4000 g for 15 min.

5.2.3 Dry weight measurement

The solid content was determined in triplicate by drying the samples in a vacuum oven at 105 °C overnight. The solid content is calculated from the ratio of sample weight measured before and after drying.

5.2.4 Tribological / lubrication measurements

The friction measurements of all starch ghost suspensions and their continuous phases (20 mL) were performed at a controlled temperature of 35 °C on a Mini Traction Machine (MTM, PCS Instruments Ltd., UK), following the method of Bongaerts, et al. [233] and Selway and Stokes [231]. The tribometer was equipped with a PDMS smooth ball with a radius of 9.5 mm and a flat PDMS disc with a radius of 23 mm and a thickness of 4 mm (PCS Instruments Ltd., UK) as rubbing contact. The root-mean-square of asperities was about 8.6 nm for the smooth PDMS tribopairs, according to a previous report.[230] These specific materials were selected since they have been previously shown to provide data with correlations to sensory perception.[230, 231] Prior to the experiments the PDMS tribopairs were cleaned in an ultrasonic bath with 1% sodium dodecyl sulphate solution, followed by rinsing with de-ionized water. The friction force (F_f) was determined as a function of the applied entrainment speed (U) over a range between 1 and 1000 mm/s under the ball-on-disc configuration. The entrainment speed is defined as the average surface speed of ball and disc, i.e., $U = (U_{ball} - U_{disc})/2$, where U_{ball} and U_{disc} are the surface speeds of the ball and disc, respectively. The applied load (W) was set to 1 N for all tests, and the friction coefficient (μ) can be calculated as the friction force divided by applied load, i.e, $\mu = F_f / W$; the slide-to-roll ratio (SRR) was fixed at 50% to provide a mixed sliding and rolling motion. While friction coefficient (μ) was measured under both decreasing speed from 1000 to 1 mm/s and followed by increasing speed from 1 to 1000 mm/s, only data obtained from the decreasing speed step are discussed in the main text. Results were expressed as means with standard deviations of at least five times measurements.

5.2.5 Rheological measurements

The rheological measurements were carried out on an advanced controlled-stress rheometer (Haake Mars 3, Thermo Fisher Scientific, Karlsruhe, Germany) with a heat adjustable Peltier element and temperature controlled hood at a temperature of 35 °C. A

60 mm diameter parallel/plate geometry was used to measure steady state flow and viscoelastic properties of aqueous starch ghost suspensions. The gap was set at 200 μm for all experiments in order to avoid any slip or artefact due to the larger particulates, as the size of starch ghost particles as estimated from light micrographs were 15 – 35 μm for maize ghosts and 50 – 150 μm for potato ghosts.[79] The gap between parallel plates was always zeroed at a normal force of 4 N before each test, and gap error for this set of experiment was typically around 15 μm, calculated using a mathematical method of Davies and Stokes [234]. Prior to the tests, an oscillatory stress sweep test at a frequency of 1 rad/s was performed in order to determine the linear viscoelastic region of samples over a stress range from 0.001 to 100 Pa. To characterize the effect of shear force on the viscoelastic modulus of ghost suspensions at high-particle concentrations (0.87% PG, 1%, 2% and 3% w/w MG), an oscillatory frequency sweep test was performed to determine storage (G') and loss modulus (G") (step 1), followed by a steady shear viscosity measurement (step 2). The sample was then subjected to another oscillatory frequency sweep test (step 3) followed by a steady shear viscosity measurement (step 4), and a final oscillatory frequency sweep test (step 5). The oscillatory frequency sweep test was run at a stress within the linear viscoelastic region in the range of 0.01 to 10 rad/s, and the steady shear measurements were performed for shear rates ranging from 1 to 10,000 s^{-1}. Results were expressed as means with standard deviations of at least duplicate measurements. For the ghost suspensions at some dilute concentrations (0.01%, 0.1% w/w PG and MG), only steady shear measurements were performed for shear rates ranging from 1 to 10,000 s^{-1}.

5.2.6 Light microscopy

Light microscopy was performed using a Zeiss Axio microscope (Oberkochen, Germany). One drop of fresh ghost suspension was diluted and stained with 2% iodine solution, before being recorded by a Zeiss CCD camera (AxioCam ERc5s, Oberkochen, Germany).

5.2.7 Particle size distribution

Particle size analysis was performed on a Mastersizer Hydro 2000MU (Malvern Instruments Ltd., Malvern, UK) following the method of Zhang, Dhital, Flanagan and Gidley [79]. A refractive index of 1.34 was used for size calculation of ghost particles. The starch samples were added to circulating water until an obscuration of >10% was recorded. Each measurement was repeated three times with an accuracy of about 0.5%.

5.3 Results and Discussion

5.3.1 Tribological characterization of starch ghost suspensions

Lubrication behavior is inherently dependent on relative motion between the soft-contacts of the tribometer, which is classically presented as a Stribeck curve with three different regimes namely boundary, mixed and hydrodynamic lubrication. In the hydrodynamic regime, the high fluid (or hydrodynamic) pressure can fully support the applied load and separate the contact. This normally occurs at higher speeds with increased friction coefficients and shear force, although not all fluids have a hydrodynamic regime. Boundary lubrication normally occurs at lower speeds, higher load or with a poor lubrication system, as the fluid is excluded from the contact area, resulting in insufficient fluid pressure to support the applied load. In the mixed lubrication regime, the load can be partially supported by fluid pressure and partially by contacting asperities, i.e. intermediate between boundary and hydrodynamic lubrication. The friction coefficient under boundary and mixed regime conditions is more associated with surface characteristics, whereas the hydrodynamic regime is controlled by bulk rheological properties.[235]

The friction coefficient as a function of the entrainment speed for starch ghost suspensions as well as the continuous phase of the suspensions was investigated in a wide range of weight concentrations. For clarity, only data obtained from decreasing speed steps are plotted in Figure 5.1 (data for increasing speed steps are shown in Supporting Information Figure A2-1). The lubrication curves of all ghost suspensions (Figure 5.1 A, B) are within boundary and mixed regimes, with a thin film of lubricant and surface characteristics being dominant. Figure 5.1A shows that the lubrication properties of maize ghost suspensions are highly dependent on their particle concentration (phase volume) in the fluid. With decreasing values of entrainment speed at 1000 mm/s, all tribological profiles including water control show a gradually increased friction coefficient to a maximum point at a speed of 40 mm/s. It was observed that this maximum friction coefficient point decreased with an increased weight concentration (0.01%, 0.1% and 1% w/w) of maize ghost suspensions, indicating that ghost particles are entrained into the contact area as a lubricant. However, no further reduction in friction coefficient was observed for concentrated maize ghost systems (i.e., 1%, 2%, and 3% w/w). For the most dilute and concentrated (i.e., 0.01% and 3% w/w) maize ghost suspensions as well as water, there is a plateau in tribological profiles at low speeds between 1 and 40 mm/s. For other concentrations of maize ghost samples, a lower trend of friction coefficient was observed in this speed region (1 – 40 mm/s), possibly due to the deformation or breakdown of the elastomeric ghost particles in the direct contact.[231] Furthermore, a hysteresis was observed between the decreasing

speed steps and increasing speed steps, with the hysteresis extent being concentration dependent (Supporting Information Figure A2-1). This hysteresis phenomenon has been observed in other soft fluid gels such as agarose, without any mechanistic explanation.[236]

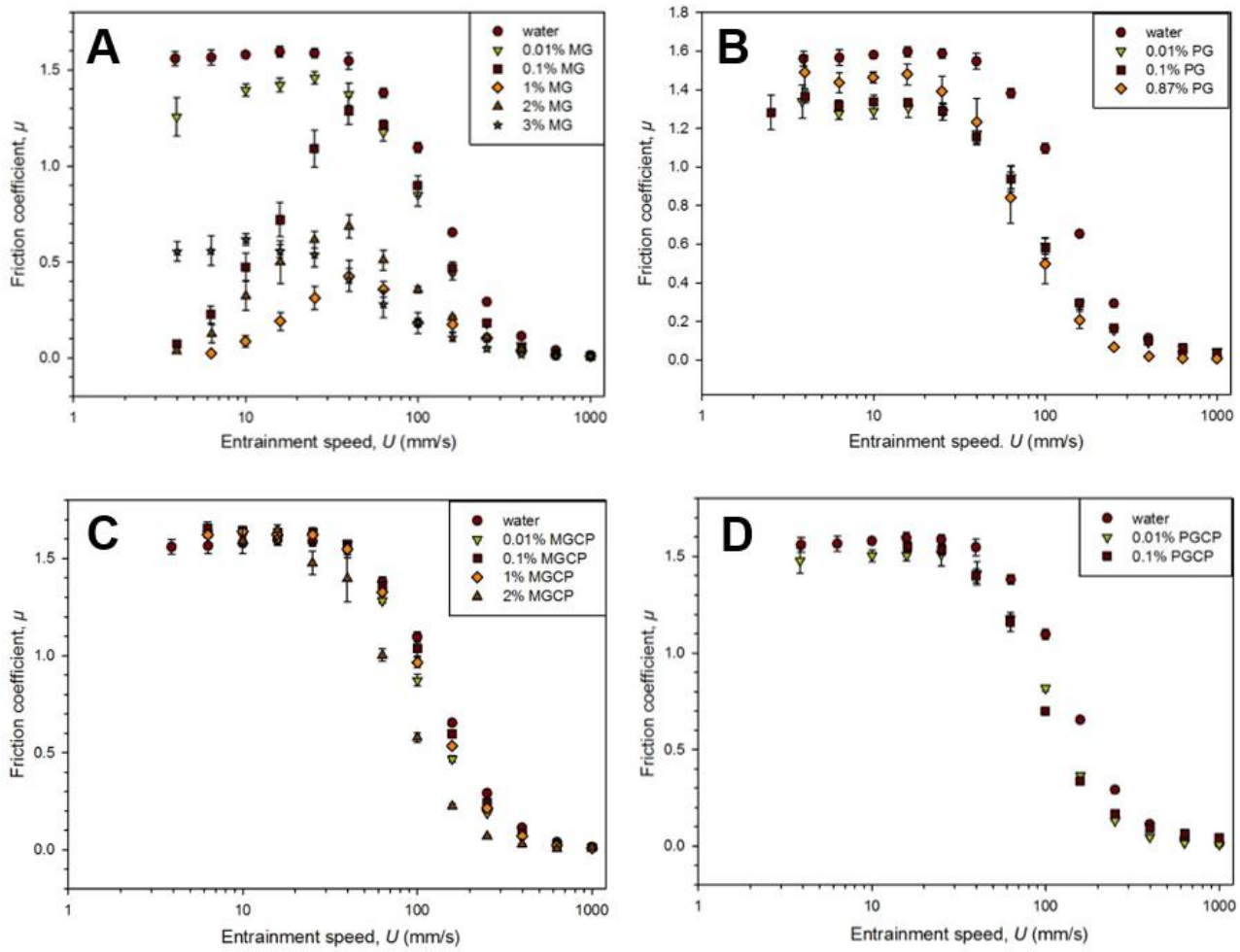

Figure 5.1. Friction coefficient as a function of entrainment speed for starch granule ghost suspensions (A, B) and their continuous phase (C, D) at different concentrations. (MG, maize starch ghost suspension; PG, potato starch ghost suspension; CP, continuous phase).

In the case of potato ghosts with various weight concentrations, all tribological profiles (Figure 5.1 B) starting from high speeds show a gradually increasing friction coefficient in the mixed regime and then a boundary plateau at lower speeds (< 30 mm/s). Compared with water control, only a slight reduction of friction coefficient is observed over the full range of entrainment speeds. It is noteworthy that the behavior of the potato ghost suspension is independent of weight concentration, indicating that the potato ghost particles are extruded or degraded by the soft-contacts. There is a negligible hysteresis

observed for potato ghost suspensions and all continuous phase (data not shown). The continuous phase of all ghost suspensions (Figure 5.1 C, D) shows similar tribological profiles with friction coefficient being close to water control, consistent with few starch polymers being present in the continuous phase.

Ghost particles have typical microscopic and elasticity features depending on botanical origins.[206, 237] Maize ghost particles have fairly spherical appearance with smaller size (around 15 - 35 μm), whereas ellipsoidal potato ghosts have a wide range of particle size (50 - 150 μm) with some apparent fragmentation during the isolation process (Figure 5.2, before test). In a previous study, we reported that potato ghosts can expand about ca. 16 fold in volume compared with the parent granule with skins being thinner, more fragile and sensitive to shear force, compared with maize ghosts (which increase ca. 4 times in volume cf. parent granules).[79] Maize ghosts subjected to the tribology test only resulted in slightly reduced integrity in morphology, whereas potato ghosts show significant amount of granule fragments (Figure 5.2).

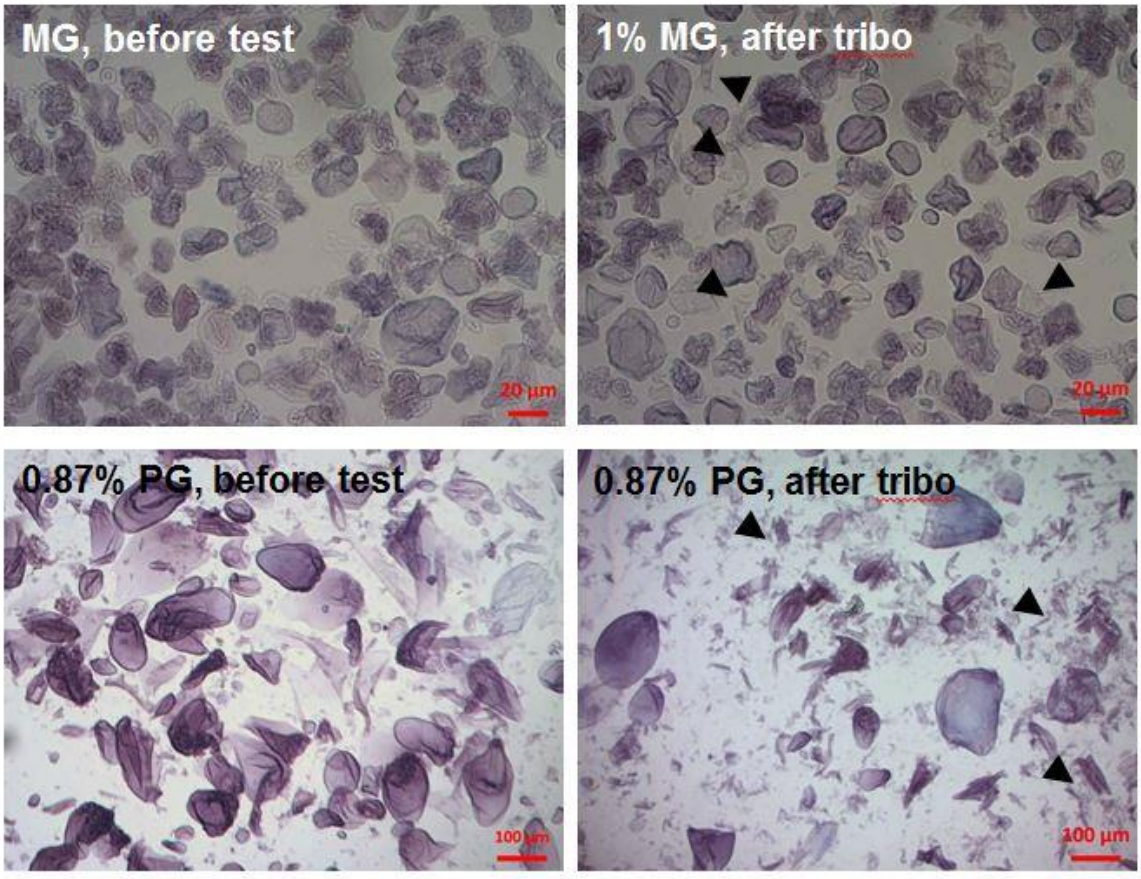

Figure 5.2. Light micrographs of starch granule ghost suspensions before and after being subjected to tribology test. (MG, maize starch ghost suspension; PG, potato starch ghost suspension; tribo, tribology test).

We also assessed the particle size of maize ghosts by laser light scattering, the results of which are presented in Figure 5.3 and Table 5.1. It not appropriate to assess particle size of potato ghosts by Mastersizer instrument, since microscopy analysis showed that shear degradation happened during measurement at the circulating fan speed of 2000 rpm (data not shown). Following tribology and rheology tests, the presence of an additional small particle component was seen by both light scattering (Figure 5.3) and microscopy (Figures 5.2 and 5.6). The laser scattering technique makes assumptions that granule ghosts are spherical and homogeneous in order to calculate particle sizes, resulting in an overestimate compared with apparent sizes from microscopy as shown in Table 5.1. Although laser scatting technique overestimates the actual size of maize ghosts, the presence of a small size fraction led to a slight reduction in calculated values of volume weight mean diameter ($d_{4,3}$) for maize ghosts after tribology and rheology tests with greater effects at higher ghost concentrations (Table 5.1) in agreement with light microscopic measurements.

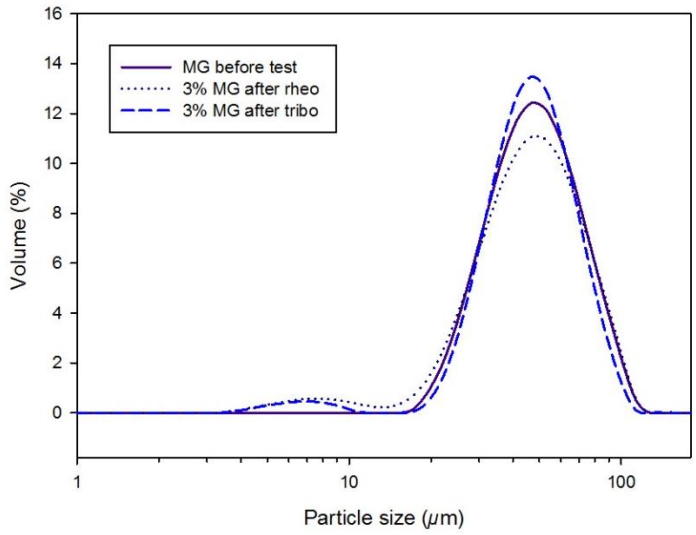

Figure 5.3. Particle size distributions of 3% maize ghost suspension before and after being subjected to tribology or rheology test. (MG, maize starch ghost suspension; tribo, tribology test; rheo, rheology test).

In order to understand the shear effect between soft-contacts in the tribometer on ghost particles in (very) dilute systems, parallel-plate rheometry at a gap of 200 μm was used to measure the steady state viscosity as a function of shear rate up to 10,000 s^{-1}, which is reported to be relevant to tribological measurements[231, 238], with results shown in Figure 5.3. All (very) dilute systems show a Newtonian plateau and similar viscosity at 35 °C

(Figure 5.3), except for 0.1% w/w potato ghost suspension with shear thinning behavior (data not shown). In such cases, we can deduce that there are only weak particle interactions in the (very) dilute ghost suspensions, which result in Newtonian liquid behavior rather than soft solid behavior. However, non-Newtonian behavior can be observed in dilute suspensions with higher ghost swelling capacity and phase volume (e.g., 0.1% w/w potato ghost suspension, comparing with the counterpart of maize), when starch ghost particle level exceeds a minimum concentration.[224] So, we it can be confirmed that the tribological changes of maize ghost suspensions in the (very) dilute regime (Fig 1A, 0.1% or less) are not only due to the viscosity as a function of shear rate, but more associated with the surface properties of the ghost particle such as affordable tension and modulus of the maize ghost particle under shear and/or pressure. In more concentrated conditions, maize ghost suspensions show a similar maximum friction coefficient (~0.5) at entrainment speed of around 40 mm/s, presenting a clear particulate lubrication behavior. In contrast, potato ghost suspensions show polymeric solution behavior with poor lubrication, which is independent of weight concentration or phase volume. We propose that this is due to the disintegration of those potato ghosts which are entrained within the tribometer gap, as suggested by the observation of numerous small particles after the tribology test, whereas maize ghosts were much less affected (Figure 5.2).

Table 5.1. Calculated values for volume weight mean diameter ($d_{4,3}$) in μm of starch granule ghost suspensions before and after being subjected to tribology and rheology tests. (MG, maize starch ghost suspension; PG, potato starch ghost suspension; tribo, tribology test; rheo, rheology test).

sample	$d_{4,3}$	sample	$d_{4,3}$
MG	47.60 ± 0.12		
1% MG after tribo	47.36 ± 0.14	1% MG after rheo	46.50 ± 0.53
2% MG after tribo	46.71 ± 0.20	2% MG after rheo	46.23 ± 0.85
3% MG after tribo	46.14 ± 0.09	3% MG after rheo	45.84 ± 0.05

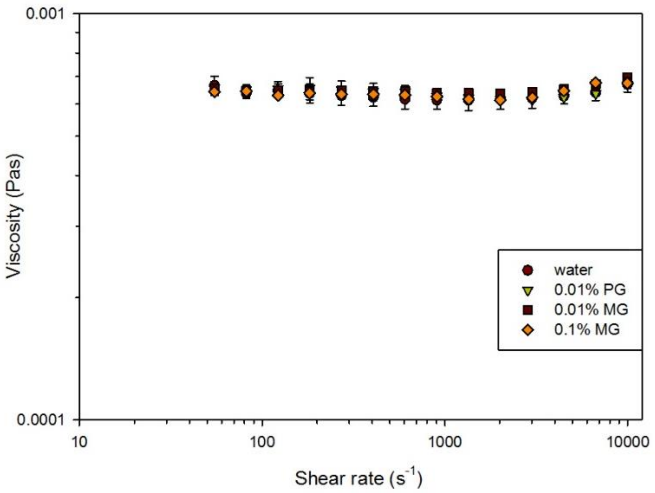

Figure 5.4. Steady state viscosity of dilute starch granule ghost suspensions. (MG, maize starch ghost suspension; PG, potato starch ghost suspension).

5.3.2 Rheological characterization of starch ghost suspensions after steady shear treatments

To gain further insight into the microstructure changes of ghost particles subjected to shear, a series of dynamic and steady state rheology experiments was carried out. As reported previously,[222] there is a threshold concentration for measuring elasticity, near the close-packing concentration. Therefore, we only investigated the viscoelastic modulus (G' and G") (step 1) and steady shear viscosity (step 2) of ghost suspensions at relatively high particle concentrations (i.e., 0.87% w/w potato ghost suspension, 1%, 2% and 3% w/w maize ghost suspensions), with results as presented in Figure 5.5 as average and standard deviation of duplicate measurements. For the first frequency sweep step, all concentrated ghost suspensions behave as a weak gel with the storage modulus exceeding the loss modulus but some dependence on the frequency (Figure 5.5, A, C, E, G). Increasing weight concentrations of maize ghost suspensions is expected to increase the particle phase volume, and consequently results in higher viscoelastic modulus and apparent viscosity values (Figure 5.5). For the close-packing concentrations (0.87% w/w potato ghost suspension cf. 3% w/w maize ghost suspension), lower swelling maize ghosts have higher storage modulus and viscosity values than higher swelling potato ghosts (Figure 5.5 E - H), consistent with a previous report.[221] Shear rates up to 10,000 s^{-1} in parallel-plate rheometry were used to understand potential shear effects on starch ghosts between soft-contacts in the tribometer. It was found that all ghost suspensions have typical non-Newtonian shear thinning flow behavior (i.e., viscosity decreases as a function of increasing shear rate) regardless of weight concentration, driven by the surface

approach though particle-particle interactions.[239, 240] The factors which influence the viscosity behavior of gelatinized starch suspension have been extensively studied for several decades.[221, 222, 229, 239] The viscosity is determined by the volume fraction of the ghost particles in dilute regimes, whereas the particle rigidity (size, shape and deformability) is the decisive factor controlling the strength of particle-particle interaction in the close-packing regime.[221, 239] Steeneken [221] further suggested that both particle volume fraction and rigidity might be important in a broad concentration range between two those limiting behaviors (e.g., 1% and 2% w/w maize ghost suspensions). Therefore, starches from different botanical origins have various pasting properties, and probably maize and potato are two typical representatives.[241]

The second and third small-amplitude oscillatory shear measurements (step 3 and 5) characterise mechanical properties after one or two shear treatments (steps 2 and 4), and can be interpreted in terms of ghost structure changes and particle-particle interaction after shear treatment.[242] After being sheared for one cycle, all ghost suspensions studied here display a marked decrease of storage and loss modulus, but still behaved as a weak gel with higher storage modulus than loss modulus over the frequency range (Figure 5.5 A, C, E, F). In addition, the differences between the storage modulus and the loss modulus after steady shear are smaller, especially for 1% w/w maize and 0.87% w/w potato ghost suspensions. After two cycles of steady state shear treatment, further decrease of viscoelastic modulus and apparent viscosity can be seen, but not as great as the differences caused by the first cycle (Figure 5.5 A, C, E). It has been proposed that the phase volume and rigidity of ghost particles are key variables for controlling the rheological behavior of gelatinized starch dispersions in concentrated regimes.[222] After the five-step rheological measurements, maize ghosts at concentrated regimes show reduced integrity in morphology (Figure 5.6 A - C), consistent with the corresponding particle size distribution (Figure 5.3) and volume weight mean diameter ($d_{4,3}$) data (Table 5.1). Ghost particles are elastic entities, and their inherent deformability and fragility in the concentrated systems, which are very dependent on the botanical origins and cooking conditions,[206] would dominate the system rheology. For example, low swelling starches such as maize have a much lower deformability and fragility, and produce greater thickening at high concentrations. Applied shear forces facilitate more particle-particle interaction (number of contact points) within concentrated ghost regimes, resulting in more granule damage during large deformation treatment of ghost granules as evidenced from light micrographs (Figure 5.6) and the reduction of $d_{4,3}$ values (Table 5.1). Almost all potato

ghost particles subjected to two-rounds of steady shear treatment show significant amounts of small rod-like fragments (Figure 5.6), due to the large deformation of particles under the high shear force.[228]. It is interesting that the fragments from potato ghosts after steady shear treatment are apparently different in morphology to potato ghosts after tribology test (Figure 5,2); we suggest that the more rounded fragments in the latter result from both rolling and shear effects between soft-contacts in the tribometer.

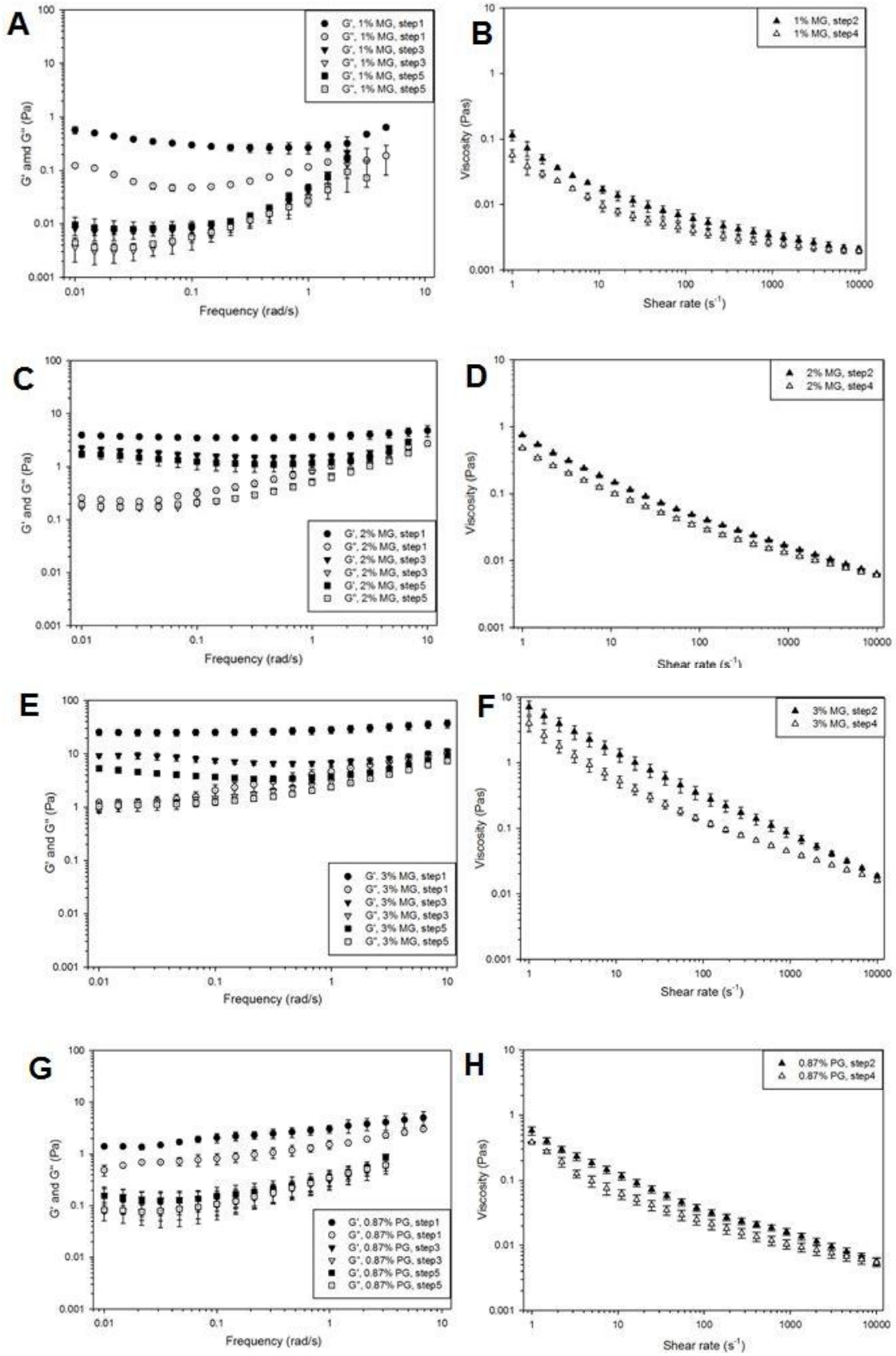

Figure 5.5. Five-step rheology for concentrated starch granule ghost suspensions: (A, C, E, G) storage modulus and loss modulus as a function of frequency (step1, 3 and 5); (B, D, F, H) steady state viscosity as a function of shear rate (step 2 and 4). (MG, maize starch ghost suspension; PG, potato starch ghost suspension).

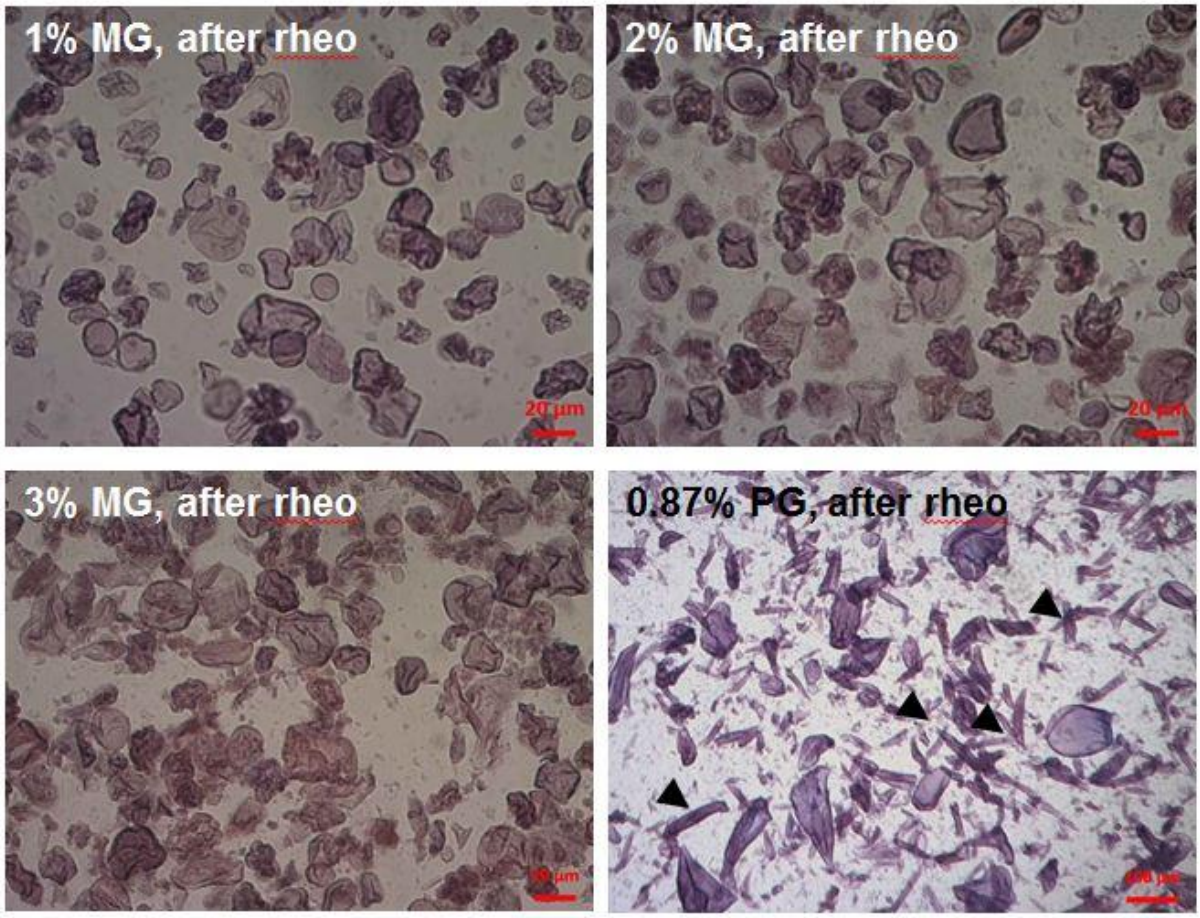

Figure 5.6. Light micrographs of starch granule ghost suspensions after being subjected to rheology test. (MG, maize starch ghost suspension; PG, potato starch ghost suspension; rheo, rheology test).

5.4 Conclusions

This paper has reported for the first time the lubrication and rheology of isolated swollen starch granule suspensions over a wide range of concentrations, using maize and potato starches as exemplars. Although all ghost suspensions show boundary and mixed lubrication, there are clear differences in tribology and rheology between maize and potato. Smaller size and more robust maize ghosts subjected to the tribology or rheology test only resulted in slightly reduced integrity in morphology, whereas large and fragile potato ghosts show significant amount of granule fragments after testing. A markedly decreased maximum friction coefficient point at an entrainment speed of 40 mm/s with increasing concentration (from 0.01% to 1% based on weight) of maize ghost suspensions was observed, while the apparent friction coefficient is concentration independent for potato ghosts although this is likely to be due to disintegration of fragile potato ghosts under tribological contact. We conclude that soft-tribological properties of starch ghost

suspensions can be due to either particulate (e.g. maize ghosts) or polymeric (particularly for potato ghosts) forms, the balance between which could potentially contribute to the perception of starch-containing food in the mouth.

Chapter 6

Extrusion Induced Low-Order Starch Matrices: Enzymic Hydrolysis and Structure

Bin Zhang[†], *Sushil Dhital*[†], *Bernadine M. Flanagan*[†], *Paul Luckman*[‡], *Peter J. Halley*[‡], *and Michael J. Gidley*[†,*]

[†] Centre for Nutrition and Food Sciences, Queensland Alliance for Agriculture and Food Innovation, The University of Queensland, St. Lucia, Brisbane, QLD 4072, Australia

[‡] School of Chemical Engineering, and Australian Institute for Bioengineering and Nanotechnology, The University of Queensland, St. Lucia, Brisbane, QLD 4072, Australia

* Corresponding author.

Phone: +61 7 3365 2145; Fax: +61 7 3365 1177. Email address: m.gidley@uq.edu.au (M. J. Gidley)

6.1 Introduction

As a major macronutrient to human health, dietary starch is converted to glucose by the mammalian enzyme system (i.e., α-amylases and mucosal α-glucosidases) and absorbed in the small intestine, and often provides more than 50% of total caloric intake.[243] Fast digestion of starch-containing foods may contribute to general chronic diseases in people such as type II diabetes, obesity, and cardiovascular disease. In contrast, starch with slow digestion rate has been proposed to control glycemic response and insulin secretion, and (partially) passes to the large intestine as resistant starch where it functions as a carbon source to stimulate bacterial fermentation, producing metabolites such as short-chain fatty acids.[88] In order to eliminate complex intrinsic host factors and individual diversity, resistant starch is most commonly measured by *in vitro* methods that simulate *in vivo* conditions of starch digestion and referred to as 'enzyme-resistant starch (ERS)' (to distinguish it from true RS which is defined as the amount of starch that escapes digestion in the small intestine and therefore passes to the large intestine),[7] particularly to elucidate the structure-digestibility relationships of starch-containing food.

While rapidly, slowly digestible and resistant starch fractions in the current classification suggested by Englyst and Cummings [88] have been widely used, recent evidence suggests that ERS can be better expressed as a kinetic phenomenon rather than a thermodynamically defined entity.[8, 115, 198] For example, potato starch granules (a type 2 'resistant' starch) are not completely resistant to hydrolysis when subjected to higher enzyme concentrations, although the digestion rate is slow.[244] The presence of amorphous material in enzyme-resistant fractions also confirms that the resistance is based on a kinetic mechanism rather than a specific crystalline structure that is completely undigested.[119] Kinetic analysis of starch digestion is a powerful tool to understand heterogeneous reactions between complex starch substrates and enzymes. There are two types of rate-limiting steps which determine enzymic digestion kinetics: (i) enzyme access/binding limited by physical barriers (e.g., intact plant tissues, whole grains and complex food products); (ii) enzyme catalysis limited by starch structural features, such as chemically modified starch, and crystalline/ordered forms such as retrograded starch and starch-lipid complex. The ERS classification based on mechanisms to achieve lower digestion rate/extent has been recently reviewed.[76, 245] Although it has been generally accepted that crystallinity plays a major role in determining ERS in the absence of non-starch physical barriers, recent evidence has shown that apparent crystallinity of native starches is not directly linked with the percentage of ERS obtained after extrusion.[7, 8, 166] Htoon, Shrestha, Flanagan, Lopez-Rubio, Bird, Gilbert and Gidley [8] reported that highly amorphous extruded high-amylose maize starches could deliver high ERS contents *in vitro*. Even for native starch granules, crystallinity alone cannot explain their relative resistance to digestion.[139] Therefore, there should be additional mechanisms involved in the formation of enzyme-resistant fractions apart from crystallinity. We hypothesise that the local molecular density of starch chains, in both native and processed starches, can control the digestion rate and extent. Although crystallinty is one way to achieve local molecular density, it appears that non-/weakly- crystalline chains can also pack in an equally enzyme-resistant form, the details of which are currently poorly understood.

Extrusion is a common commercial processing technique for starch-based foods such as pasta and breakfast cereals. The main advantages of extrusion processing include the ability to handle viscous polymers in the presence of plasticizer (normally water in food use). Similarly, the combination of a high temperature with a large amount of mechanical energy input during a short time period can be used to promote structural changes of

starch such as gelatinization, melting, degradation and fragmentation.[246] Generally, molecular, supramolecular and granular structures are disrupted by thermal (barrel temperature), humidity (plasticizer content) and energy input (e.g., screw speed, feeding rate, die size and screw configuration) during extrusion cooking, each of which could be expected to increase the accessibility of degrading enzymes to starch polymers in extruded products. The intense shear scission within the extruder can cleave α-(1→4), α-(1→6)-bonds as well as the ordered structure such as crystallites and double helical structure. Amylopectin (highly branched large molecule) is degraded to a larger extent than the essentially linear and lower molecular weight amylose, and the degradation of amylopectin mainly occurs in the outer branch chains.[247] The larger molecules of amylopectin together with high branching density and short branch length are associated with higher susceptibility to shear degradation.[247] Fragmentation of starch during extrusion depends on the operating conditions of the extruder such as screw speed, temperature, and moisture content as well as the type of starch used.

In the current paper, we aim to understand the structural origins of enzyme resistance especially from amorphous conformations using starch extrudate as a model system. For this purpose, three maize starches with different amylose contents were extruded with water as a sole plasticizer, and *in vitro* digestion kinetic and thermodynamic profiles of starch extrudates were examined. On the basis of the molecular and microscopic structures of initial extrudates and digestion remnants, mechanisms of enzyme resistance from starch matrices with non-/low-order conformation are discussed.

6.2 Experimental section

6.2.1 Materials

Three commercial starches, i.e., waxy (WMS), normal (NMS), and high-amylose (Gelose 50, G50) maize starches, were used in this study. NMS was from New Zealand Starch Ltd., (Auckland, New Zealand), and the other three starches were purchased from Ingredion Pty. Ltd., (Lane Cove, NSW, Australia). The apparent amylose contents of WMS, NMS, and G50 were found to be 0.1%, 27.5%, and 56.8%, respectively, using an iodine colorimetric method.[232] Porcine pancreatic α-amylase (A3176, activity 23 units/mg) and other chemicals were obtained from Sigma-Aldrich (St. Louis, MO, USA).

6.2.2 Extrusion processing

The extrusion processing was performed on a Haake Polylab co-rotating twin-screw

extruder (Thermo Fisher Scientific, Karlsruhe, Germany) equipped with a 3 mm diameter cylindrical die at a constant feed rate of 0.4 kg/h. The screw diameter was 16 mm, and the length/ diameter ratio was 42:1. The extruder configuration, temperature profile and interval assignment of the extruder barrel are shown in Figure 6.1. For WMS and NMS, the barrel temperature profile was set at 105, 115, 125, 130, 130, 130, 130, 125, 120 (last barrel), and 105 (die block) °C, and the screw speed was set at 60 rpm, and plasticizer (water) content was 35 wt%. In order to achieve higher gelatinization level of G50 starch, higher temperature profiles (105, 120, 135, 150, 150, 150, 150, 135, 120, and 105 °C), water content and screw speed were used (45 wt% and 80 rpm for batch 1; 50 wt% and 60 rpm for batch 2). All process parameters were automatically recorded by Haake Polysoft software (Thermo Fisher Scientific, Karlsruhe, Germany). Samples were collected when a steady motor torque was reached, then immediately frozen in a liquid nitrogen bath, freeze-dried to avoid any further retrogradation, and ground using a cryogenic mill (Freezer/Miller 6850, Metuchen, NJ, USA) for further digestion and structural analysis. In order to elucidate the particle size effect on digestion properties, the NMS and G50 extrudates were segregated by size using seven screen sieves (size: 20, 32, 53, 75, 90, 125 and 150 µm, Labtechnics, Kilkenny, Australia) under gravity with mechanical agitation using a sieve shaker (Labtechnics, Kilkenny, Australia).

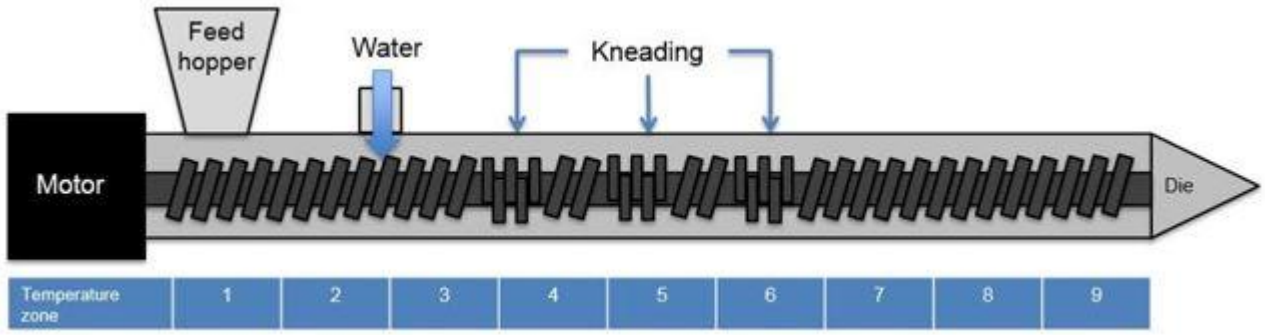

Figure 6.1. Scheme of the extrusion system in this study.

6.2.3 *In vitro* starch digestion and first-order kinetics

The *in vitro* starch digestion procedure was adapted from the method described by Butterworth, Warren, Grassby, Patel and Ellis [115] with slight modifications. Starch extrudate (~50 mg, dry basis) was incubated in 15 mL phosphate buffered saline (PBS) with 3.4 units α-amylase at 37 °C with constant mixing. For the control groups, starches were cooked at 100°C for 30 min in 15 mL PBS buffer with constant mixing, and cooled down to 37 °C before adding the enzyme solution. At timed intervals up to 120 min, 300 µL

of aliquot was mixed with 300 µL of ice-cold sodium carbonate solution (0.5 M) to stop the reaction, and centrifuged at 16,000 g for 5 min to remove undigested starch. The concentration of maltose equivalent (reducing sugar) in the supernatant was determined by the *para*-hydroxybenzoic acid hydrazide (PAHBAH) assay (H9882, Sigma),[248] and the maltose equivalent released (%) was calculated as follows.

$$\text{maltose equivalent released (\%)} = \frac{\text{total weight of equivalent maltose in supernatant}}{\text{dry weight of starch}} \times 100 \quad \text{(Eq. 6.1)}$$

The undigested starch residues collected as precipitate after centrifugation were washed twice with de-ionized water, then freeze-dried for further microscopic and structural analysis. The reducing sugar profile or digestogram was then fitted to first-order equation[115] (i.e., log of slope (LOS) plots) for the starch digestion kinetics as follows:

$$\ln\left(\frac{dC}{dt}\right) = \ln(C_\infty k) - kt \quad \text{(Eq. 6.2)}$$

where t is the digestion time (min), C is digested starch at incubation time t, C_∞ is digestion at infinite time, and k is rate constant (min^{-1}). The plot of $\ln(dC/dt)$ against digestion time t is linear with a slope of $-k$, and the C_∞ can be calculated from the intercept of the equation and slope k. The rate constant is a function of the fixed amylase and starch concentrations used in the digestion, and is therefore pseudo-first order. The physical structure of starches also plays an important role in determining the rate constant of starch digestion.[198]

6.2.4 Separation of soluble and insoluble fractions

In brief, starch sample (~50 mg, dry basis) was incubated in 15 mL water at 37 °C for 30 min with constant mixing. The suspension was then centrifuged at 4000 g for 10 min. The pellet (i.e., insoluble fraction) and the supernatant (i.e., soluble fraction) were frozen in a liquid nitrogen bath and dried using a freeze-dryer (VirTis Benchtop 4K, SP Industries, Inc., Warminster, PA),

6.2.5 Microscopy

Light microscopy was performed using an Olympus BX-61 light microscope (Tokyo, Japan) under bright or polarized field. The dried starch sample was suspended with glycerol and placed on the microscope slide before covering with a coverslip, and the images were recorded at 200X magnification. For the scanning electron microscopy (SEM), the starch sample was sprayed onto a circular metal stub covered with a double-sided adhesive carbon tape, then coated with platinum by a sputter coater (Eiko IB3, Mito, Japan) for 3 min at 15 mA. The images were acquired using a Philips XL30 scanning

electron microscope (Philips, Eindhoven, the Netherlands) under an accelerating voltage of 5 kV.

6.2.6 Differential scanning calorimetry

To characterize the extent of starch transformation after extrusion or digestion, extrudates/digesta were analyzed by a differential scanning calorimeter (DSC, DSC 1, Mettler Toledo, Schwerzenbach, Switzerland) following the method of Zhang, Huang, Luo and Fu [74] Starch samples (~5 mg) were mixed with de-ionized water to a moisture content of 70%, and hermetically sealed in a stainless steel pan. The scan was carried out from 20 to 180°C at a heating rate of 10 °C/min. The enthalpy change (ΔH) as well as the melting (T_m) temperature was determined from the thermograms by STARe software (Mettler Toledo, Schwerzenbach, Switzerland).

6.2.6 Wide angle X-ray diffractometry

X-ray diffraction measurements were performed with an X'Pert Pro X-ray diffractometer (XRD) (PANalytical, Almelo, the Netherlands) operating at 40 kV and 40 mA with Cu Kα radiation (λ) at 0.15405 nm. The scanning region was set from 3 to 40° of the diffraction angle 2θ with a step interval of 0.02° and a scan rate of 0.5°/min. The crystalline peak area and amorphous area were separated by PeakFit software (Version 4.12, Systat Software Inc., San Jose, CA, USA) following the method of Lopez-Rubio, et al. [249] Relative crystallinity was calculated as the ratio of the crystalline peak area to the total diffraction area.

6.2.7 ^{13}C CP/MAS nuclear magnetic resonance spectroscopy

Starch extrudates were analyzed by ^{13}C cross-polarized magic angle spinning (CP/MAS) nuclear magnetic resonance (NMR) spectroscopy before and after subsequent enzymic digestion, using a Bruker MSL-300 spectrometer (Bruker, Billerica, MA, USA) at a frequency of 75.46 MHz. Approximately 200 mg starch was packed in a 4-mm diameter, cylindrical, PSZ (partially stabilized zirconium oxide) rotor with a Kel-F end cap. The rotor was spun at 5 kHz at the magic angle (54.7°). The 90° pulse width at 5 μs and a contact time of 1 ms were used for all starches with a recycle delay of 3 s. The spectral width was 38 kHz, acquisition time 50 ms, time domain points 2 k, transform size 4 k, and line broadening 20 Hz. At least 1000 scans were accumulated for each spectrum. Spectral acquisition and interpretation methodology as described by Tan, Flanagan, Halley,

Whittaker and Gidley [205] were used to quantify the double helices, single helices, and amorphous conformational features.

6.2.8 Size exclusion chromatography

The whole (fully branched) and debranched size distribution of starch molecules were analyzed by a size exclusion chromatography (SEC) system (Agilent 1100, Agilent Technologies, Waldbronn, Germany) equipped with a refractive index detector (RID-10A, Shimadzu, Kyoto, Japan) following the method of Cave, Seabrook, Gidley and Gilbert [201] and Zhang, Dhital, Flanagan and Gidley [79] with minor modification. For fully branched size distribution, starch (2 mg) was dissolved in 1 mL DMSO solution containing 0.5% (w/w) LiBr (DMSO/LiBr) at 80 °C in a thermomixer (Eppendorf, Hamburg, Germany) for 24 h. Samples were mixed well and centrifuged at 4000 g for 10 min. Supernatant was transferred into a SEC vial then injected into the following series of columns: precolumn, Gram30, and Gram3000 (PSS, Mainz, Germany). The injection volume was 100 μL, the flow rate was 0.3 mL/min, and the temperature was 80 °C. For debranched size distribution, starch (~ 4 mg) was dissolved in 1.5 mL DMSO/LiBr in the same way as that of the fully branched samples. The dissolved starch was then precipitated using 6 mL absolute ethanol. The recovered starch pellet was dissolved in 0.9 mL of warm deionized water in a boiling water bath for 15 min. After being cooled to room temperature, the starch dispersion was mixed with 5 μL sodium azide solution (40 mg/mL), 0.1 mL acetate buffer (0.1M, pH 3.5), and 2.5 μL isoamylase (1000U/mL, Megazyme, Co. Wicklow, Ireland), in sequence, and the debranching reaction was carried out at 37 °C for 3 h. The debranched starch dispersion was neutralized to pH ~7 dropwise with 0.1 M NaOH solution, then heated in 80 °C water bath for 2 h to inactivate enzyme. Debranched samples were freeze-dried and comprised ~6 mg/mL starch in DMSO/LiBr, then injected into PSS Gram100 and 1000 columns following a pre-column. The injection volume was 100 μL, the flow rate was 0.6 mL/min, and the temperature was 80 °C.

The molecular size distribution data were plotted as SEC weight distribution, $w(\log V_h)$ as a function of the hydrodynamic radius (R_h/nm). For branched starch molecules, there is no unique correspondence between size and molecule weight.[250] For linear polymers of uniform geometry, the size and molecular weight (or equivalently the degree of polymerization, DP) are uniquely related, and hence the size distribution can be converted to a molecular weight distribution using the Mark-Houwink equation.[201, 202] The Mark-

Houwink parameters *K* and *α* for linear starch polymers in DMSO/LiBr at 80 °C are 0.0150 mL/g and 0.743, respectively.[247]

6.2.9 Statistical analysis

Results were expressed as means of duplicate measurements unless otherwise specified. Analysis of variance (ANOVA) was used to determine significance at $p < 0.05$ using Minitab 16 (Minitab Inc., State College, PA, USA), and correlation coefficients were determined using Microsoft Office Excel 2013.

6.3 Results

6.3.1 *In vitro* starch digestion

In vitro digestion kinetic profiles of control (i.e., cooked starches) and experimental (i.e., starch extrudates) groups were monitored by reducing sugar assay with a fixed α-amylase activity, with results shown in Figure 6.2A. The digestion rate and extent of starch or starch-containing food are very dependent on the enzyme type(s) and the concentration conditions used.[244] For example, α-amylase and amyloglucosidase act synergistically in the production of glucose from granular starch digestion, whereas there is an antagonistic effect for cooked starches.[198] Therefore, this kinetic study used α-amylase alone to investigate digestion rate/extent of starches in cooked or extrudate forms. In order to obtain a logarithmic digestion curve and fit first-order kinetics, a selected α-amylase activity condition (3.4 unit per 50 mg starch) was used to convert sufficient starch substrate to oligosaccharide products over the time course, showing logarithmic curves for all starch samples.[115, 244] It should be noted that the selected amylase activity is dependent on the physical nature of a starch subtract; for example, a relatively higher amylase concentration is needed for native starches compared to cooked forms, and also depends on the botanic origins.[115, 198]

LOS fitting analysis (shown in Appendix 3, Figure A3-S1) was applied to the starch digestion kinetic profiles to obtain first-order coefficients (*k*), showing that all digestion profiles can be described by a single-phase pseudo-first order process ($R^2 > 0.90$). Single rate coefficients of starches in cooked and extrudate forms and digestion extents after 2 h of digestion are summarized in Table 6.1. Comparison of the digestion rate and extent of WMS and NMS in cooked and extrudate forms indicated that the digestion processes (digestogram and *k* values, Figure 6.2A and Table 6.1) are indeed very similar. Compared to other cooked starches, cooked G50 starch shows slightly lower digestion rate and

extent (0.0400 min^{-1}, 56.5%, respectively). However, it was found that the digestion rate coefficient for two G50 extrudate batches (batch one, 0.0238 min^{-1}; batch two, 0.0244 min^{-1}) is ca. 2 times lower than that of WMS and NMS extrudates. In addition, among extrudates from different initial amylose contents, high-amylose starch shows relatively higher enzyme resistance towards amylase (yield of ERS at 2 h of digestion > 40%), consistent with previous reports.[7, 8]

In order to elucidate the effect of particle size on enzymic susceptibility, NMS and G50 extrudates were fractionated into various sizes by sieving, and analyzed for amylase digestion kinetics with results presented in panels B and C of Figure 6.2. Small and medium size fractions (32 – 125 μm) did not affect the digestion kinetic profiles much (digestogram and *k* values). As shown in Appendix 3, Table A3-S1, the majority (relative yields > ca. 85%) of extrudates were in the small and medium size fractions, in agreement with their overall digestion kinetics. As the particle size increased, a marked reduction in starch digestibility for the larger size particles (>125 μm) of both NMS and G50 extrudates was observed.

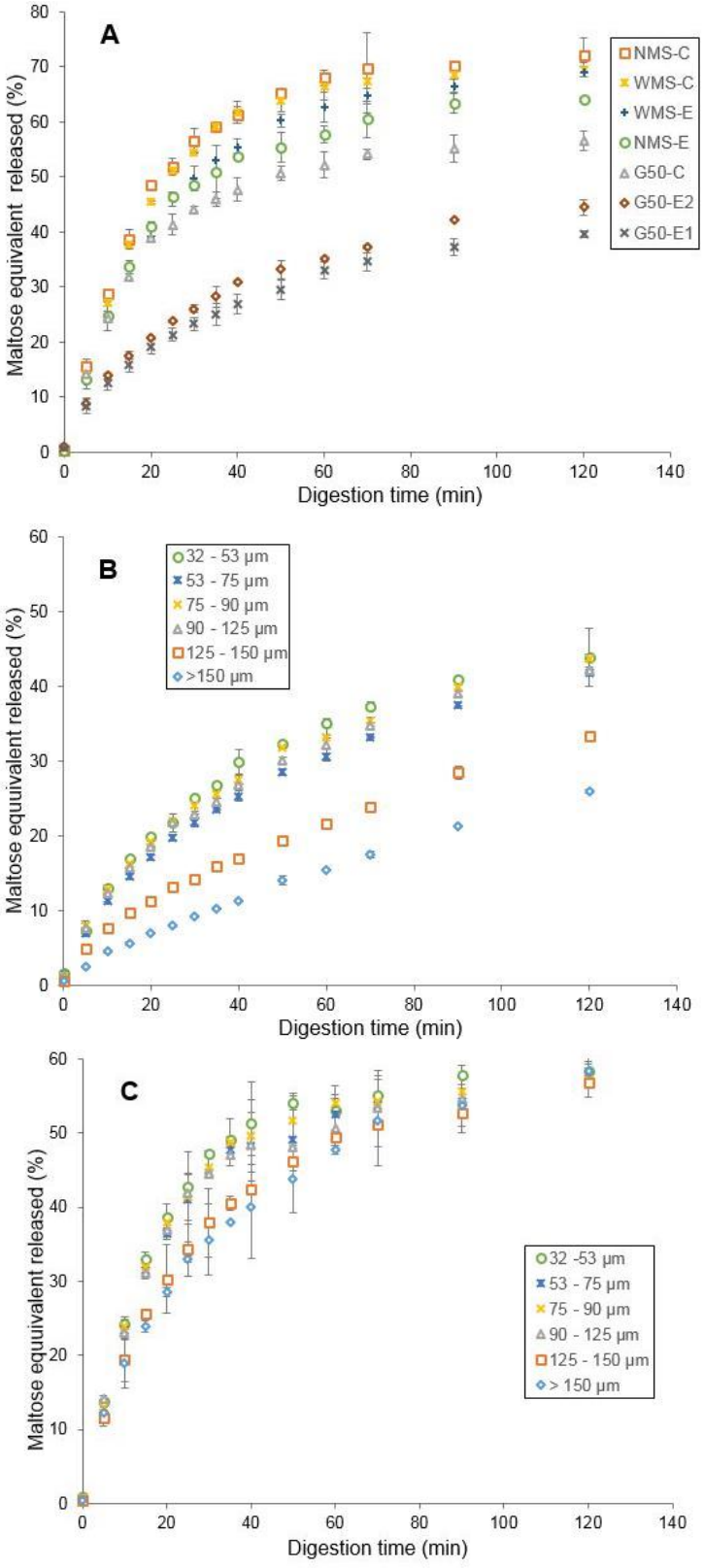

Figure 6.2. (A) Digestion kinetic profiles of waxy, normal and high-amylose maize starches subjected to cooking or extrusion process. Digestion kinetic profiles of size fractionated extruded high-amylose (B) and normal (C) maize starches. (WMS, waxy maize starch; NMS, normal maize starch; G50, high-amylose maize starch; E, extrudate; N, native; C, cooked).

Table 6.1. Digestion rate coefficient (k, min^{-1}) and reducing sugar released extent after 2 h digestion of starches in cooked and extrudate forms.[A] (WMS, waxy maize starch; NMS, normal maize starch; G50, high-amylose maize starch; E, extrudate; N, native; C, cooked; D, 2 h digestion residue)

sample	k (min^{-1})	Reducing sugar released (%)	extrudate	K (min^{-1})	Reducing sugar released (%)
WMS-C	0.0481	72.2(3.2) a	WMS-E	0.0403	69.1(1.0) a
NMS-C	0.0447	69.6(1.2) a	NMS-E	0.0408	64.1(0.3) b
G50-C	0.0400	56.5(1.8) c	G50-E1	0.0238	42.7(0.5) d
			G50-E2	0.0244	44.5(1.4) d

[A] Means ± standard deviations from at least two measurements. Values in the column with different letters are significantly different at $p < 0.05$.

6.3.2 Microscopic structure of extruded starches and their digestion residues

Electron and light micrographs of extruded starches and their 2 h of digestion residues/fragments are shown in Figure 6.3. The G50 starch granules before extrusion (Figure 6.3 C1 and C2) show spherical or elongated rod shapes with apparently unimodal particle size distribution varied from 5 to 20 µm as reported previously.[251] Under polarized light, native G50 starch granules show characteristic birefringence with clear Maltese crosses centered at the hilum (Figure 6.3 C1). From SEM and light microscopy (Figure 6.3 A2 – A4, B2 – B4), extrusion and cryo-milling resulted in both fragmentation and aggregation with a wide size distribution ranging from 10 to 200 µm. Although the WMS and NMS extrudates show condensed and irregularly-shaped surface structures under SEM, they could be partly dissolved in water or PBS buffer quickly (from experimental observations). For the starch that has been solubilized, the driving force of hydration/swelling is higher than the rate of retrogradation, otherwise insoluble recrystallized double helices would be formed.[79] No birefringence can be detected from WMS and NMS extrudates (Figure 6.3 C2 – C3), suggesting that complete gelatinization is induced by extrusion. In contrast, extruded G50 starches still show a low level of birefringence and distorted Maltese crosses (Figure 6.3 C4), indicating that the current extrusion conditions did not fully melt the ordered structure. A number of different extrusion conditions (e.g. maximum temperatures from 130 °C to 150 °C) and water contents (from

35 % to 50 %) were evaluated, but none were able to produce G50 extrudates lacking any birefringence. Complete melting of high-amylose starches by extrusion in the presence of non-aqueous plasticizers or solvents is possible,[252] but for this study we limited ourselves to water as the only plasticiser for relevance to food processing. The densely packed surface structure of G50 extrudates (Figure 6.3 A4) is similar to the counterpart of WMS and NMS extrudates (Figure 6.3 A2-3), but was constrained from swelling extensively in water or buffer (as shown in Figure 6.3 4A) unlike WMS or NMS extrudates. By the end of the 2h digestion process, a marked reduction in particle size was observed compared to the initial G50 starches in cooked or extrudate form, as shown in panels A5 – A6 and B5 – B6 of Figure 6.3. Most digestion residues were present as smaller particles with a similar size of around 10 µm, along with a few large aggregates. Under polarized light, relatively lower levels of birefringence and some clear Maltese crosses can be identified from digesta of cooked or extruded G50 starches (Figure 6.3 C5 – C6), indicating that the digestion remnants were composed of G50 granules tightly embedded in a starch matrix (extrudate) or residual granules with incomplete melting of double helices during extrusion or cooking.

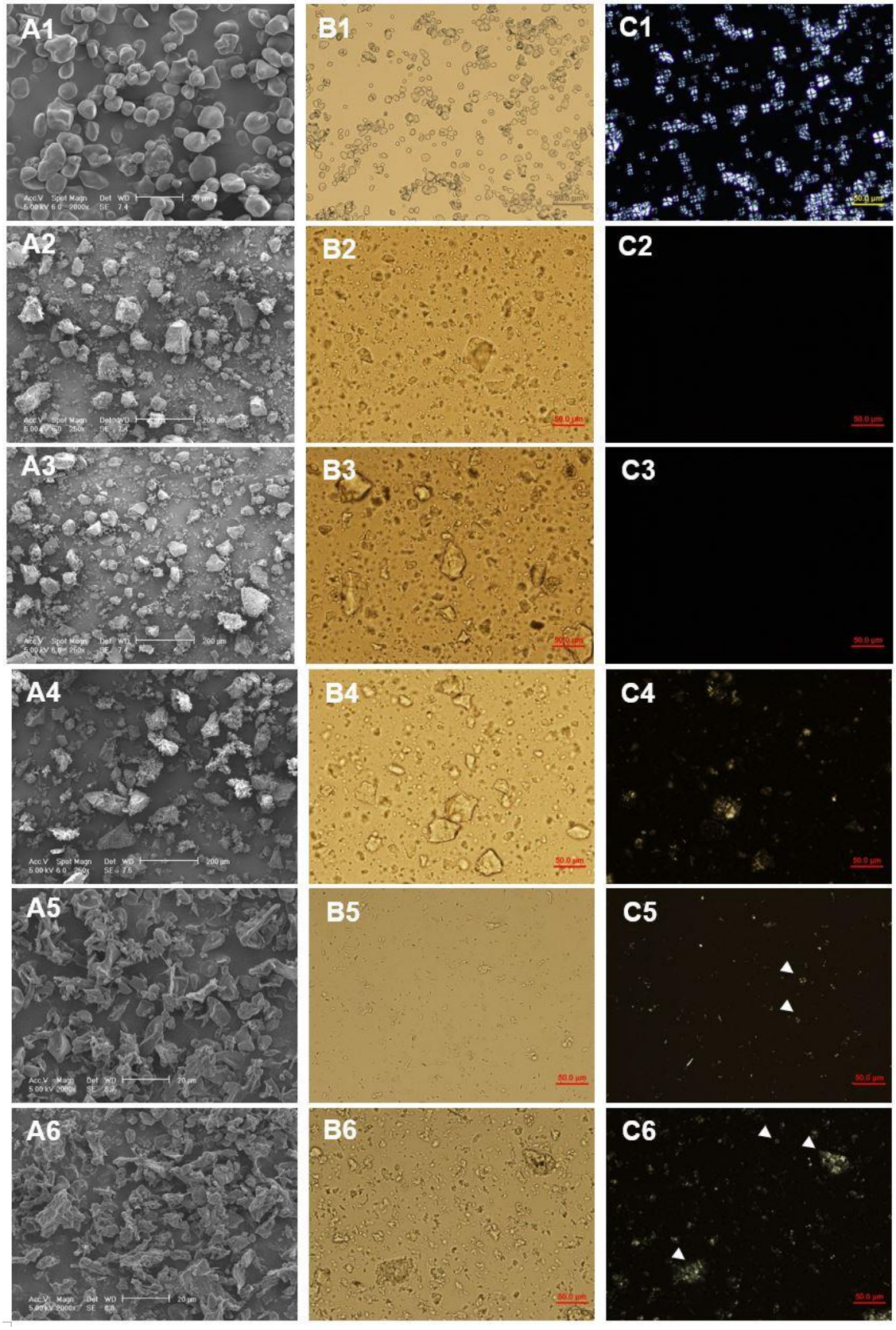

Figure 6.3. Micrographs (A, scanning electron micrographs; B and C, light micrographs under bright field or polarized light respectively) of extruded starches (1: native G50 starch; 2, 3, 4: extruded waxy, normal, and high-amylose maize starches respectively) and their 2 h digestion residues from cooked G50 (5) and extruded G50 (6) starches. (Arrows are some representative Maltese crosses of starch granules).

6.3.3 Molecular order and crystallinity before and after digestion

The molecular order (i.e., helical content) and crystallinity level of starch extrudates before and after enzymic hydrolysis were quantified by solid-state NMR spectroscopy and XRD respectively, as shown in Figure 6.4 and Table 6.2. The melting (peak) temperature and enthalpy determined by DSC for different starch samples after extrusion and after 2 h of digestion, are summarized in Table 6.2 as well. Extrusion processing under the selected condition leads to the almost fully gelatinization of waxy and normal maize starches, as shown by <5% A-type double helices and <1% crystallinity (Table 6.2) as well as DSC thermograms without any endothermic peak up to 180 ^{o}C (data not shown) consistent with the absence of birefringence in Figure 6.3 A2-3. As observed in Figure 6.4, native high-amylose G50 starch displays a typical B-type diffraction pattern with major peaks at ~5, 14, 17, 22 and 24^{o} 2θ, and a clear peak at ~20^{o} 2θ is ascribed to V-type single helices.[120] However, V-type polymorph does not always imply a fatty acid complexed with amylose molecules,[253] and this formation is favored under high-shear extrusion conditions as reported elsewhere.[160] After processing, the G50 extrudates shows mostly B-type polymorph with some clear evidence for V-type peaks (e.g., at ~8, 13, 20^{o} 2θ, see Figure 6.4) and about 50% reduction of B-type double helix and crystallinity levels (Table 6.2), compared to the original native form. The DSC thermograms for extruded G50 starches had a board endothermic peak ranging from 113 to 130 ^{o}C and peaking at around 120 ^{o}C. In addition, the enthalpy of this peak was very low and not significantly different from batch one to batch two (between 1.5 and 1.9 J/g), which could be attributed to the melting of retrograded amylose formed either during or immediately after extrusion.

The digestion residues of G50 starches in cooked and extrudate forms also show a mixture of B- and V- type polymorphs from X-ray diffractograms (Figure 6.4). Similar to the corresponding extrudate samples, only B-type double helices were detected from NMR spectroscopy, presumably because of some randon coil-like amylose molecules without any inclusion formed during extrusion as described previously.[253] The levels of molecular and crystalline order were slightly higher for the ERS residues (~17% double helix and ~17% crystallinity) than for the starting extruded G50 starches (9-12% double helix and 11-17% crystallinity). As would be expected, the enzyme resistant ordered helical structure B-type could be from either accumulated or newly formed double helices during time course of digestion.[137] Lopez-Rubio, Flanagan, Shrestha, Gidley and Gilbert [119] suggested that partly degraded shorter amylose chains show high mobility, and can self-assemble into more enzyme resistant double helices during digestion. However, it is noteworthy that

the molecular order and crystallinity levels of the digesta were close to the corresponding native G50 starch as shown in Table 6.2, showing that still more than 80% of the 2h digestion residue fraction is amorphous. The melting temperature and enthalpy of the digestion residues were slightly lower compared to starting G50 extrudates, probably due to partial degradation of double helices by α-amylase.

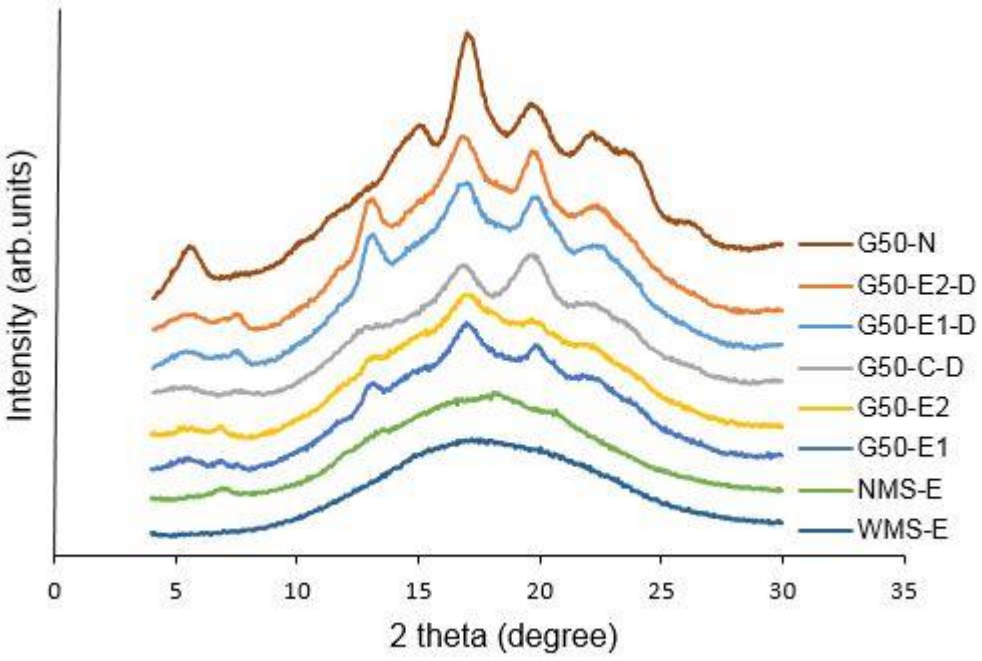

Figure 6.4. X-ray diffractograms of extruded starches and their 2 h digestion residues (WMS, waxy maize starch; NMS, normal maize starch; G50, high-amylose maize starch; E, extrudate; N, native; C, cooked; D, 2 h digestion residue).

Table 6.2. Molecular order, crystallinity and thermo property of extruded starches and 2 h digestion residues.[A] (WMS, waxy maize starch; NMS, normal maize starch; G50, high-amylose maize starch; E, extrudate; N, native; C, cooked; D, 2 h digestion residue)

sample	^{13}C NMR		XRD		DSC	
	double helix (%)	single helix (%)	A-or B-type	V-type	T_m (°C)	ΔH (J/g)
WMS-E	4	0	<1	0	-	-
NMS-E	5	1	<1	3	-	-
G50-E1	12	0	17	2	118.8(0.7) b	1.9(0.1) bc
G50-E2	9	0	11	1	122.3(0.9) a	1.5(0.2) c
G50-N	22	5	26	3	79.8(0.3) e	9.8(0.4) a
G50-C	ND [B]	ND [B]	9	3	ND [B]	ND [B]
G50-C-D	21	0	16	1	102.5(0.3) d	2.7(0.2) b
G50-E1-D	17	0	15	4	115.1(0.7) c	1.3(0.1) c
G50-E2-D	16	0	17	5	115.6(0.6) c	1.2(0.1) c

[A] XRD and NMR calculations are within SD of 2%. Means ± standard deviations from at least two measurements. Values in the same column with different letters are significantly different at $p < 0.05$. T_m and ΔH are melting temperature and enthalpy change, respectively.

[B] Not determined.

6.3.4 Molecular size distributions

The molecular size distributions of enzymatically debranched and fully branched starch polymers were characterized using SEC. All SEC weight distributions were normalized to yield the same height of the highest peak to bring out detailed features and to facilitate qualitative comparison and interpretation, and are presented in Figures 6.5 and 6.6. Typical chain length distributions of debranched starch molecules (e.g., native G50 starch, Figure 6.6 A) shows bimodal peaks representing amylopectin branches (single-lamella, peak R_h ~1.5 nm or DP ~ 16; trans-lamella, R_h peak ~2.5 nm, DP ~50) and amylose branches (R_h ~5 – 80 nm, DP ~100 – 10000).[79, 254] The branched SEC weight distribution of native G50 starch (see Figure 6.6 E) exhibits two distinct peaks for amylose and amylopectin molecules separated at R_h ~200 nm. It is noteworthy that shear degradation of dissolved starch molecules in DMSO/LiBr happens during SEC separation, especially for amylopectin which is sufficiently degraded to a smaller size to result in overestimation of the amylose peak.[9] The fully branched SEC distribution of extruded G50 starch (Figure

6.6 F) shows a unimodal peak with a large reduction in amylopectin size. Degradation during extrusion preferentially operates on the large molecular size and highly branched primary structure of amylopectin, whereas whole amylose molecules could be largely retained. [247] The mechanical/shear force induced by extrusion processing is believed to randomly cleave glycosidic bonds in branches of amylopectin, but with more pronounced action adjacent to rigid crystallites in granular starches.[255] This is consistent with the lack of qualitative difference in the debranched chain length distributions between native and extruded G50 starches, as shown in panels A and B of Figure 6.6.

The branched SEC weight distributions for soluble starch fractions show a single peak with a smaller molecular size (R_h peak ~10 nm, Figure 6.5 E, G) compared to the bimodal peaks for the insoluble fractions of cooked and extruded G50 starches (Figure 6.5 E - H), indicating that these lower molecular size molecules could be dissolved in water or PBS buffer before enzyme reaction happened. The branched SEC data of all extruded G50 samples in either soluble or insoluble form show slightly lower R_h peaks than corresponding cooked starches (Figure 6.5 E, G cf. F, H), consistent with the shear degradation mechanism discussed above. In addition, comparison of the debranched SEC data (Figure 6.5 A - D) also shows that incubation of both cooked and extruded starches in the PBS buffer at 37 ^oC is accompanied by the partial dissolution of both amylose and amylopectin with low molecular size: less release with degraded polymers for the extrudate form and more for cooked G50 starch. Starch samples after 2h of amylase digestion were greatly degraded in whole molecular size (Figure 6.6 G, H), and contained a mixture of amylopectin (R_h peak ~2 nm, DP ~25) and long chain polymers (R_h >~5 nm, DP >~100) interpreted from Figure 6.6 C, D. There were more long chain polymers with R_h ~ 10 nm in the digestion residues from G50 extrudates (Figure 6.6 C cf. D) as well as larger polymers (R_h > 10 nm; Figure 6 G cf. H), which might play important roles in restricting enzyme action.

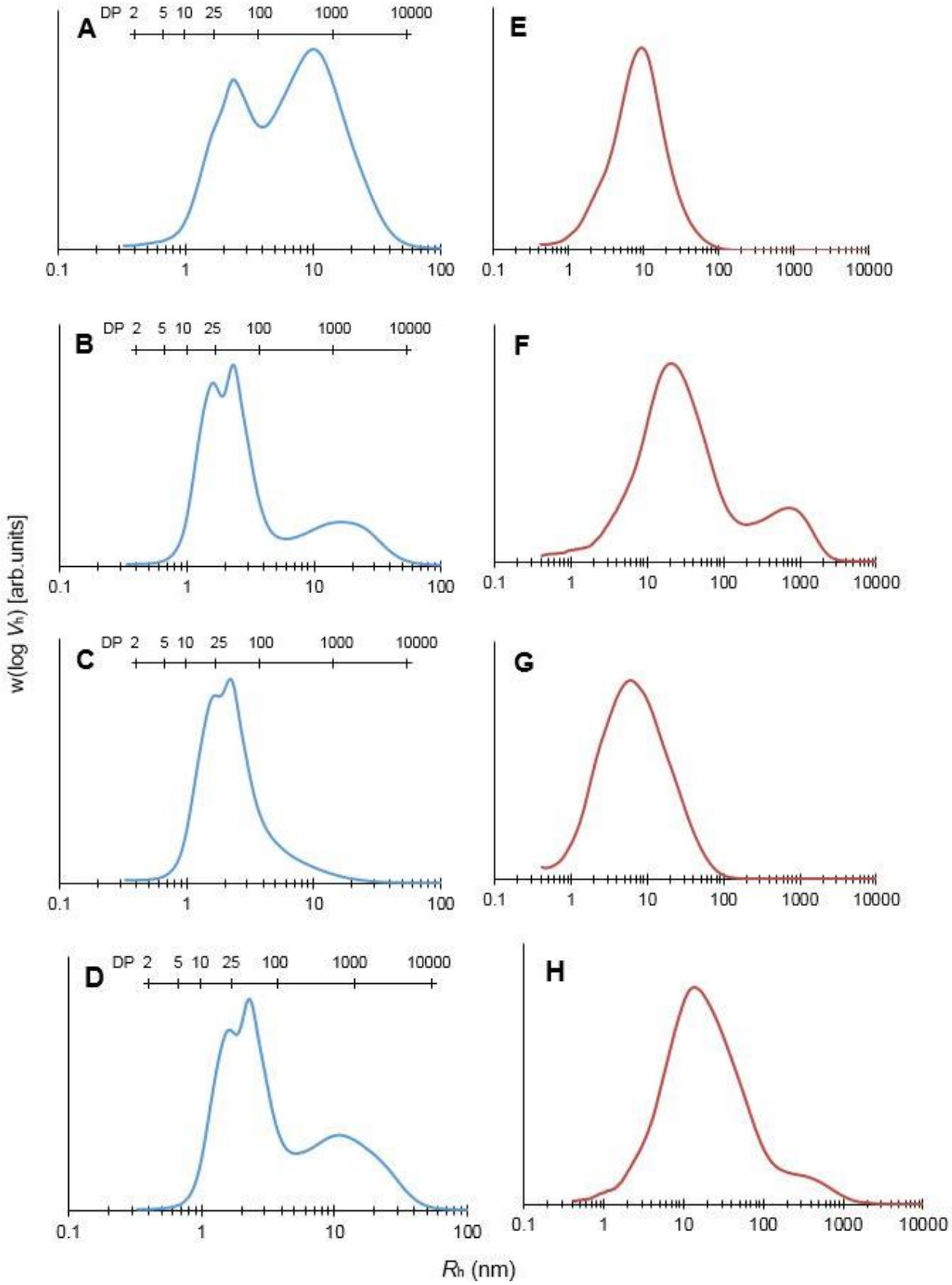

Figure 6.5. Size distributions of debranched (A - D) and whole (E - H) molecules from the soluble fraction of cooked (A, E) and extruded (C, G) G50 starches, and the insoluble fraction of cooked (B, F) and extruded (D, H) G50 starches.

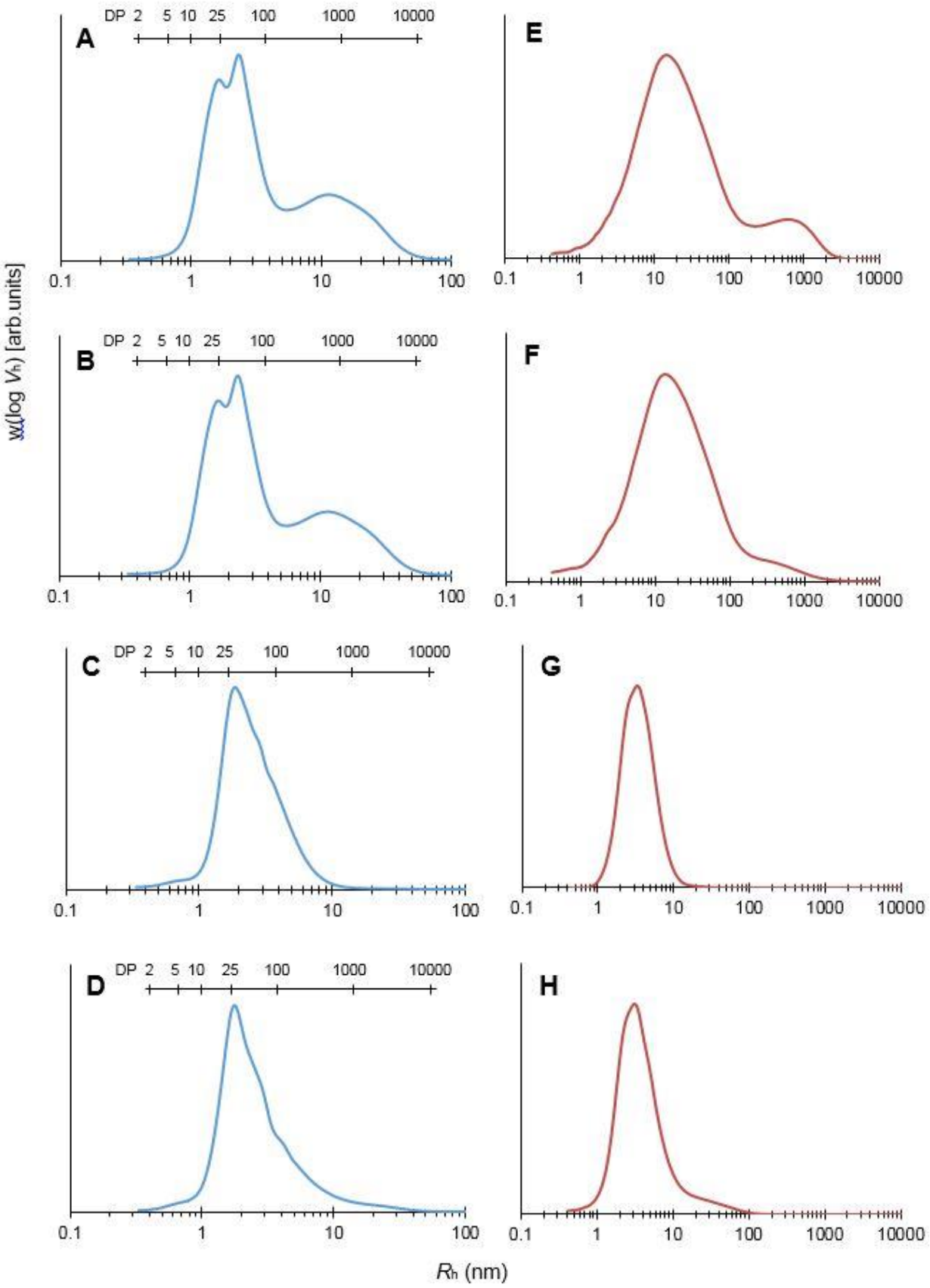

Figure 6.6. Size distributions of debranched (A - D) and whole (E - H) molecules from native (A, E) and extruded (B, F) G50 starches and 2 h digestion residues of cooked (C, G) and extruded (D, H) G50 starches.

6.4 Discussion

Generally, molecular, crystalline, and granular structure of starches from nanometer to micrometer length scales are disrupted by the intense thermo-mechnical energy input of an extruder, which would be expected to generate an amorphous structure and increase the accessibility of starch molecules for enzymic hydrolysis. [140, 165] Although the WMS and NMS extrudates have a densely-packed surface structure in the dried state (Figure 6.3 A2 - 3), the local molecular density of starch matrices is temporary and is lost when subject to hydration, leading to higher digestion rate and extent compared to G50 extrudate. Therefore, there was no major difference in digestion rate coefficients between WMS and NMS extrudates in cooked and extrudate forms, as shown in Table 6.1. Insufficient gelatinization of G50 starch which results in survival of some double helices and micron-scale structures (detected by DSC, SEC) leads to a higher yield of ERS fraction compared with cooked NMS and WMS. Among three maize starch extrudates with different initial amylose contents, only high-amylose G50 starch shows relatively lower digestion rate and extent, compared with almost fully digested WMS and NMS extrudates (Figure 6.2 A). From the electron micrographs of G50 extrudates before and after digestion presented in Figure 6.3 and previous reports,[166, 256] it was found that all the granules were grossly disrupted and deformed within the extruder by mechanical force and heat/moisture induced swelling. Therefore, there was more homogeneity in the digestion pattern in contrast to native starch. Recently, Shrestha, Blazek, Flanagan, Dhital, Larroque, Morell, Gilbert and Gidley [256] suggested that the digestion-limiting features in extruded starches are molecular and/or mesoscopic factors rather than the granular level, although the physical architecture of extrudates also can act as a barrier to prevent enzyme access to some extent. Size fraction did not markedly influence the digestion kinetic profiles (Figure 6.2 B, C), indicating that enzymic hydrolysis of fine and medium size fractions for NMS and G50 extrudates was hydrolysis-limited rather than access/binding-limited. However, a small amount of coarse aggregates from both extrudates (yield < ca. 15%) shows much lower digestibility, possibly due to the effect of diffusion barriers to enzyme access.

We also investigated the changes in starch molecular composition and organization that occurred after extrusion and digestion, including molecular size distributions, double/single helical and crystallinity levels, and thermal properties. It is highly likely that the ordered features play some role in restricting enzymic hydrolysis, as indicated by a small increase in double helical and crystallinity levels for enzyme-resistant fractions of G50 extrudates after 2 h digestion (Table 6.2). Lopez-Rubio, Flanagan, Shrestha, Gidley and Gilbert [119]

suggested that the characteristic dimension of the resistant crystals formed was ~5 nm with a maximum DP of ~13 and ~17 glucose units for double and single helices respectively. These ordered structures were later suggested to be associated with some highly branched amorphous fringed ends coating on the surface of double helices, providing a physical barrier to enzyme access/binding which slows the digestion rate.[256] However, almost amorphous starch matrices were achieved by extruding G50 starch under the conditions used here, with ca. 90% fractions being amorphous (judged by NMR and XRD). These non-crystalline chains from high-amylose starches can pack in an enzyme-resistant form following extrusion processing and deliver slow digestion rate, consistent with previous findings.[7, 8] This suggests that the local molecular density (packing) of starch chains can control the digestion rate/extent within low-order starch materials, and crystallinity alone may not be sufficient to explain enzyme resistance,[8] and that tightly packed non-crystalline regions can also be enzyme resistant, provided they are constrained from swelling extensively in water. Comparison of G50 starches in cooked and extrudate forms, showed some differences in both fully branched and debranched SEC weight distributions of residues recovered after 2 h digestion. The debranched SEC weight distributions of these two digestion residues cover a broad range of chain lengths (Figure 6.6 C, D). It is noteworthy that more long chain polymers (R_h > 10 nm, DP > 500) survived, in agreement with the fully branched size distributions (Figure 6.6 G, H). The SEC results suggest that the residues with longer chain polymers (presumably from native or degraded amylose molecules) conferred relatively higher local molecular density in the original G50 extrudates.

The non-crystalline or amorphous state is based on the absence of detectable molecular order, but entanglements of amorphous glucan chains can give rise to tightly packed non-ordered matrices increasing localized molecular density. Another example of such locally-dense non-ordered starch structures is in the surface envelope of granule ‘ghosts’: the residual undissolved fraction of starch granules cooked in excess water with limited shear.[79] However, the technical measurement of local molecular density to quantify sub-micron variability of starch matrices is challenging, and would be the key to studying the structural origins of enzyme resistance from amorphous conformation. Some attempts have been made to measure the free-volume radius distribution of polymeric materials ranging from nanometer to sub-micrometer length scale by positron annihilation lifetime spectroscopy, which is a potential technique to quantify the local molecular density.[257] Comparing molecular order (judged by NMR, XRD and DSC, Table 6.2) and relative

enzyme digestion rates (Table 6.1) in cooked vs extruded, it was found that double helix/crystallinity contents and melting temperatures were similar but enzyme resistance was much greater for extruded forms. We suggest that this is strong evidence that tightly packed amorphous material at (sub)micrometer length scale has a role to play in restricting enzyme action.

Resistant starch in a physiological context is a kinetic concept, i.e., the resistant fraction has not had sufficient time to be hydrolyzed in the small intestine, rather than being absolutely resistant to enzyme. Given enough time and enzyme activity at optimized *in vitro* working conditions, all starch substrates can be fully degraded into oligosaccharides or glucose, depending on the interplay of acting enzymes used. To aid in the design of processed starch-containing food with slow digestion, the starch polymers of the matrices are only required to be packed densely enough at (sub)micrometer length scale to escape enzymic hydrolysis in the small intestine. The best example of dense molecular packing in nature is perhaps the amorphous growth rings within granular starch, which are digested apparently side-by-side with crystalline growth rings.[139] The apparent side-by-side enzymic degradation may be due to slow and rate-limiting step of enzyme binding to granules, i.e., once bound, a (portion of a) granule is digested relatively rapidly irrespective of any intrinsic difference in digestion of amorphous and crystalline features. However, understanding of the biosynthesis pathway and molecular organization of amorphous growth rings is a future challenge for developing a novel methodology of enzyme-resistant starch with improved health benefits, from essentially amorphous matrices other than (re)crystallization.

The individual variations in humans such as glycemic and insulin responses are significant when all food associated factors including ingested particle size are controlled.[258] Ranawana, Clegg, Shafat and Henry [258] further suggested that the influence of gastric emptying is relatively small and independent of particle size. Thus, we can propose that the digestive aspects subsequent to the gastric phase such as secretion of digestive enzymes and passage rate in the small intestine may be contributing significantly to individual variations of digestion rate and resultant glycemic response, without considering any food structuring factor. Therefore, the physiological status of an individual needs to be distinguished for personalized nutrition, as *in vitro* experiments cannot predict the heterogeneous and complex human digestive condition.

6.5 Conclusions

In summary, three maize starches with different amylose contents were processed though extrusion with water as the sole plasticizer to achieve low-order starch matrices, with only extruded high-amylose starch exhibiting lower subsequent digestion rate/extent. On the basis of NMR and XRD data, the double helix/crystallinity contents and melting temperatures of high-amylose starches in cooked and extruded forms were similar (ca. 80% amorphous fraction), but enzyme resistance was much greater for extruded forms. We suggest that the local density of packing of starch chains can control its digestibility rather than just crystallinity, which represents just one mechanism of achieving high local density of packing. If these molecularly dense structures are on about a (sub)micron length scale or longer, they could restrict enzyme action with potential health benefits.

Chapter 7

Freeze-Drying Changes the Structure and Digestibility of B-Polymorphic Starches

(This chapter has been published in J. Agric. Food Chem., *2014, 62, 1482-1491.)*

*Bin Zhang, Kai Wang, Jovin Hasjim, Enpeng Li, Bernadine M. Flanagan, Michael J. Gidley, and Sushil Dhital**

Centre for Nutrition and Food Sciences, Queensland Alliance for Agriculture and Food Innovation, The University of Queensland, Brisbane, Queensland 4072, Australia

* Corresponding author.

Phone: +61 7 3346 7373; Fax: +61 7 3365 1177. Email address: s.dhital@uq.edu.au (S. Dhital)

7.1 Introduction

Starch is the main energy reserve in many plants, comprising mainly two types of glucose polymers, namely, amylose and amylopectin, in the form of semi-crystalline granules. Amylose is a primarily linear polymer consisting of α-1,4-linked D-glucose units with few long branches, whereas amylopectin is a highly branched polymer made up of mainly α-1,4 linkages and ~5% α-1,6-linkages forming a large number of short branches. In starch granules, the branches of amylopectin are often in a double-helical conformation and contribute to the crystallinity of granules (normally between 15% and 45%), whereas amylose is considered to be largely in an amorphous conformation with some single helical V-type crystalinity.[20] Starch granules isolated from various botanical origins show different shapes (spherical, oval, disk-shaped, etc.) and sizes (submicrometer to larger than 100 μm) as well as surface morphologies, such as the presence of pinholes that connect the hilum to the surface through interior channels. Furthermore, the amylose content, the branch-chain length, and the molecular weight of starch molecules vary among starches from various botanical origins. These structural differences can influence the digestibility and other functional properties of starch.

Starch granules are commercially available in dry form for extended shelf life and for potential savings on transport and storage costs, and thus a drying process is essential after starch granules have been isolated from plants, such as from grains, legumes, and tubers. Common food laboratory and industry practices for drying isolated starch granules include oven (heat) drying, freeze-drying, and ethanol (solvent exchange) drying. Drying conditions have been reported to damage the surface and alter the interior structure of starch granules, eventually affecting their properties, such as chemical reactivity, gelatinization, retrogradation, and pasting properties.[259-263] In a previous study, Apinan, et al. [264] found that freeze-dried potato starch granules displayed higher enzymatic susceptibility than heat-dried potato starch granules, which was explained to be caused by the alteration of the surface structure during the drying process. However, the effects of freeze-drying on molecular structure and packing are less understood and have not yet been reported. Because of the inherent structural and morphological differences between the A- and B-type polymorphic starches, conclusions drawn from B-type polymorphic starches, such as potato starch, might not represent the mechanism for A-type polymorphic starches, such as maize and wheat starches. Thus, the objective of the present study was to understand the changes in molecular, crystalline, and granular structure (including surface morphology) of starch granules caused by drying processes (oven, freeze, and ethanol drying) and how they affect the digestibility of starch granules. Starch granules were isolated from mature and immature maize kernels and mature potato tubers before being subjected to different drying methods. The use of both mature and immature maize kernels was to identify the effects of kernel drying in the field.

7.2 Experimental section

7.2.1 Materials

Maize cobs from different maturity stages of plants were selected from a local farm (Warwick, QLD, Australia) by visual observation (late R4 and early R6 plants, as described by WeedSOFT decision support system) and designated as immature maize (IM) and mature maize (MM), respectively. The kernels were manually scraped from the cobs using a knife for determination of moisture content and isolation of starch granules. The moisture contents of IM and MM kernels averaged from six cobs were 66.8 and 37.6%, respectively, with standard deviations of 4.1 and 2.5% respectively. Potato tubers (PTs) (of similar sizes 70 ± 6 g) were also collected from a local farm (Killarney, QLD, Australia). Canna tubers (CTs) were collected from a local garden in St. Lucia, QLD, Australia. Gelose 50 (G50)

and Gelose 80 (G80) starches were obtained from Penford Australia Ltd. (now Ingredion Pty. Ltd., Lane Cove, NSW, Australia), and both are high-amylose maize starches.

Porcine pancreatin and fluorescein isothiocyanate conjugate tagged dextran (FITC-dextran, molar mass 20 kDa) were obtained from Sigma-Aldrich Pty. Ltd. (Castle Hill, NSW, Australia), and amyloglucosidase from *Aspergillus niger* (EC 3.2.1.3, 3260 U/mL) was from Megazyme International Ltd. (Bray, Co. Wicklow, Ireland). The pancreatin had 4 times the activity specified by United States Pharmacopeia (USP), i.e., at least 100 USP units of amylase and protease and at least 8 USP units of lipase per mg of product.

7.2.2 Starch isolation and drying processes

Brushed and washed PTs were peeled manually, diced, and stored in 0.1 M NaCl solution before starch isolation. Similarly, maize kernels were stored in 0.1 M NaCl solution. Starch granules were isolated from the maize kernels and PTs using the method of Whistler, et al. [265] and the purified starch granules were kept in 0.025% sodium azide solution until being used for further analyses or subjected to various drying methods. The apparent amylose contents of IM, MM, and PT starches, determined by an iodine colorimetric method,[203] were 20.2%, 25.3% and 30.3%, respectively. The purified starches from IM, MM, and PT were dehydrated using three methods: oven, freeze, and ethanol drying. For oven drying (OD), wet starch granules were dried in an oven at 40°C for 48 h, manually ground, and passed through a sieve with openings of 125 μm. For freeze-drying (FD), wet starch granules were frozen in a liquid nitrogen bath (from -210 to -196 °C) and dried using a freeze-dryer (VirTis Benchtop 4K, SP Industries, Inc., Warminster, PA, USA), ground, and sieved in the same way as the OD starch samples. For ethanol drying (ED), wet starch granules were washed using absolute ethanol, centrifuged, and dried in a fume hood at ambient temperature under a flow of N_2. To separate the effects of freezing and drying steps during FD, starch granules were also frozen in a liquid nitrogen bath and then thawed at room temperature (frozen-thawed, FT). The wet (W) controls were starch granules that had never been dried.

CT starch granules were isolated in a same way as the PT starch granules and subjected to ED and FD processes. The G50 and G80 starch granules were dried commercially by the manufacturer and were dispersed in water before being subjected to ED and FD processes.

7.2.3 *In vitro* starch digestion

Starch was digested following the method of Dhital, Shrestha and Gidley [110] with slight modifications. Starch granules (~50 mg, dry basis) were suspended in 15 mL of sodium acetate buffer (0.2 M, pH 6.0). Freshly prepared enzyme solution (500 μL) containing pancreatin (2 mg/mL) and amyloglucosidase (28 U/mL) was added to the starch suspension, and the mixture was incubated in a water bath at 37°C with shaking. Aliquots (0.3 mL) were removed at specific time intervals, mixed with absolute ethanol (0.9 mL), and centrifuged at 4000 *g* for 10 min. The undigested starch residues collected as precipitates after centrifugation were freeze-dried for further microscopic analysis. The concentration of glucose in the supernatant was determined using an enzymatic glucose reagent (TR 15104, Thermo Scientific, Noble Park, VIC, Australia), and the absorbance was measured at 505 nm. The glucose release (%) was calculated as follows:

$$\text{Glucose release (\%)} = \frac{\text{total weight of glucose in supernatant} \times 0.9}{\text{dry weight of starch}} \times 100 \qquad \text{(Eq. 7.1)}$$

where 0.9 is the molar mass conversion from glucose to anyhydroglucose (the starch monomer unit). The glucose profile or digestogram was then fitted to a first-order equation[116] for the kinetics of starch digestion as follows:

$$C = 1 - e^{-kt} \qquad \text{(Eq. 7.2)}$$

where t is the digestion time (min), C is the fraction of digested starch at digestion time t, and k is the digestion rate constant (min^{-1}). The value of k can be obtained from the slope of a linear-least-squares fit of a plot of ln (1 – C) against t.

7.2.4 Scanning electron microscopy

Starch granules were thinly spread onto a circular metal stub covered with a double-sided adhesive carbon tape. The starch granules were then coated with platinum to approximately 10-nm thickness using a sputter coater (Eiko IB3, Mito, Japan) for 3 min at 15 mA in an argon-gas environment. Images of the starch granules were acquired using a Philips XL30 scanning electron microscope (SEM, Philips, Eindhoven, The Netherlands) under an accelerating voltage of 5 kV and at several magnifications; 4000 and 1500 × magnifications were used to obtain representative images for maize (IM and MM) and PT starches, respectively.

7.2.5 Confocal laser scanning microscopy

Starch granules (~1 mg) were dispersed in 500 μL of FITC-dextran solution (2 mg/mL) in a microcentrifuge tube and mixed at 300 rpm overnight at room temperature in a

thermomixer (Eppendorf, Hamburg, Germany).[266] The mixture was spread onto a glass slide and covered with a glass slip and observed using an LSM 700 confocal laser scanning microscope (CLSM, Zeiss, Oberkochen, Germany). The excitation wavelength of the argon ion laser was set at 488 nm and was operating at 2% of capacity power, and the emission light was detected at 492 – 600 nm. The images of optical sections of granules were recorded with ZEN 2011 software (Zeiss, Oberkochen, Germany).

7.2.6 Differential scanning calorimetry

A differential scanning calorimeter (DSC, DSC 1, Mettler Toledo, Schwerzenbach, Switzerland) with an intra cooler was used to analyze the gelatinization properties of starch, following the method of Zhang, Huang, Luo and Fu [74] Starch granules (~5 mg) were mixed with deionized water (~12 mL) by a needle and hermetically sealed in an aluminum pan. The pan was held at 10°C for 1 min and then heated to 95°C at 10 °C/min. The enthalpy change (ΔH) and the onset (T_o), peak (T_p), and conclusion (T_c) temperature of starch gelatinization were calculated from the DSC endotherm using STARe software (Mettler Toledo, Schwerzenbach, Switzerland).

7.2.7 Wide angle X-ray diffractometry

Starch granules were equilibrated in a chamber with 44% relative humidity at 20 °C for 48 h, to give a moisture content of ~11% w/w. X-ray diffraction analysis was performed with an X'Pert Pro powder X-ray diffractometer (PANalytical, Almelo, The Netherlands) operating at 40 kV and 30 mA with Cu Kα radiation (λ) at 0.15405 nm. The scanning region was set from 3° to 40° of the diffraction angle 2θ, which covers all of the significant diffraction peaks of starch crystallites. A step interval of 0.02° and a scan rate of 0.5°/min were employed for all samples. The percentages of crystalline and amorphous starch from the total scattering and the relative degree of crystallinity were determined following the fitting method of Dhital, et al. [267]

7.2.8 Fourier transform infrared spectroscopy

Fourier transform infrared (FTIR) spectra of starch granules were obtained using a Spectrum 100 FTIR spectrometer (Perkin-Elmer, Norwalk, CT, USA) with an attenuated-total-reflectance (ATR) single-reflectance cell with a diamond crystal. For each spectrum, 32 scans were recorded over the range of 1200–800 cm^{-1} at a resolution of 4 cm^{-1}. A single-beam spectrum of the clean crystal was obtained as the background. The ratio of absorbance at 1045 cm^{-1} to that at 1022 cm^{-1} was calculated to represent the short-range

ordered structure of starch.[268]

7.2.9 Solid-state nuclear magnetic resonance spectroscopy

Starch samples were analyzed by solid-state ^{13}C cross-polarized magic-angle-spinning (CP/MAS) nuclear magnetic resonance (NMR) spectroscopy using a Bruker MSL-300 spectrometer (Bruker, Billerica, MA, USA) at a frequency of 75.46 MHz. Approximately 200 mg of starch was packed in a 4-mm diameter, cylindrical, PSZ (partially stabilized zirconium oxide) rotor with a Kel-F end cap. The rotor was spun at 5 kHz at the magic angle (54.7°). The 90° pulse width at 5 μs and a contact time of 1 ms were used for all starches with a recycle delay of 3 s. The spectral width was 38 kHz, the acquisition time was 50 ms, the number of time domain points was 2 k, the transform size was 4 k, and the line broadening was 20 Hz. At least 1000 scans were accumulated for each spectrum. The spectral acquisition and interpretation methodologies as described by Tan, Flanagan, Halley, Whittaker and Gidley [205] were used to quantify the double helices, single helices, and amorphous conformational features.

7.2.10 Statistical analysis

Results are expressed as means with standard deviations of at least duplicate measurements. In the case of XRD and NMR spectroscopy, only one measurement was performed. The standard deviations of XRD and NMR measurements are typically within 2%.[249] Analysis of variance (ANOVA) was used to determine the least significance at $p < 0.05$ using Minitab 16 (Minitab Inc., State College, PA, USA), and correlation coefficients were determined using Microsoft Office Excel 2011.

7.3 Results and discussion

7.3.1 Dehydration effects on starch digestion kinetics

Although *in vitro* methods oversimplify the digestion mechanisms in human and animal digestive tracts, such studies are still useful for comparing the digestion rates/extents among starches with different structures. Granular starches follow a 'side-by-side' digestion process involving the apparently simultaneous digestion of crystalline and amorphous regions. As model studies consistently report that amorphous starch is digested more rapidly than crystalline starch, this suggests that the digestions of the molecular and crystalline structures are not the rate-limiting steps for either *in vitro* or *in vivo* digestion.[139, 171, 185] The digestograms of PT, MM, and IM starch granules subjected to different drying methods are shown in Figure 7.1. All samples show increasing trends of

glucose release within 6 h digestion time without reaching a plateau. All digestograms follow first-order behavior with R^2 values above 0.99, and the digestion rate coefficients (*k*) are summarized in Table 7.1. The *k* values of MM and IM starches were ca. 2 times higher than those of PT starch, which agrees with the results reported by others.[110, 198]

There are no significant differences among the *k* values of OD, ED, and W samples of each type of starch (PT, MM, and IM) (Table 7.1), and they show similar digestograms (Figure 1). Therefore, the OD and ED methods do not seem to influence the digestion properties of PT, MM, and IM starches.

The PT-FD starch, on the other hand, shows greater glucose release under the same *in vitro* digestion method with a significantly higher *k* value than the other PT samples (Figure 7.1A and Table 7.1). The FD (or lyophilization) process consists of two steps: the formation of ice (freezing) and the sublimation of the ice as water molecules under vacuum (drying). To identify which step, freezing or sublimation step is critical for the increased starch digestion rate, the digestion kinetics of PT-FT, i.e., PT sample with freezing step only, was determined. There are no significant differences between the *k* values of PT-FT and PT-W samples (Table 7.1), suggesting that the rapid formation of ice crystals in liquid nitrogen bath does not alter the digestion properties of PT starch granules. This is consistent with the observation of Waigh, et al. [269] that some structural disorder of starch granules occurring at sub-zero temperatures is reversible. Therefore, the differences between the *k* values of PT-FD and PT-W samples are likely caused by the sublimation step, including the external mass transfer of water vapor near the surface and the internal mass transfer from the inside of the PT starch granules.[270] This phenomenon, however, was not observed with MM and IM starches, where FD treatment does not significantly increase the *k* values of the starch granules compared with the W control counterparts and those from other drying methods (OD and ED). Thus, at least two hypotheses can be raised for the increased digestion rate of PT-FD starch: (1) FD breaks the smooth surface organization of potato starch granules that otherwise act as a barrier preventing the diffusion of enzymes into the inside or hilum of the granules; and/or (2) starch molecular features, namely, starch crystallinity and molecular order, are disrupted during FD, leading to higher accessibility of enzymes to bind with starch molecules.

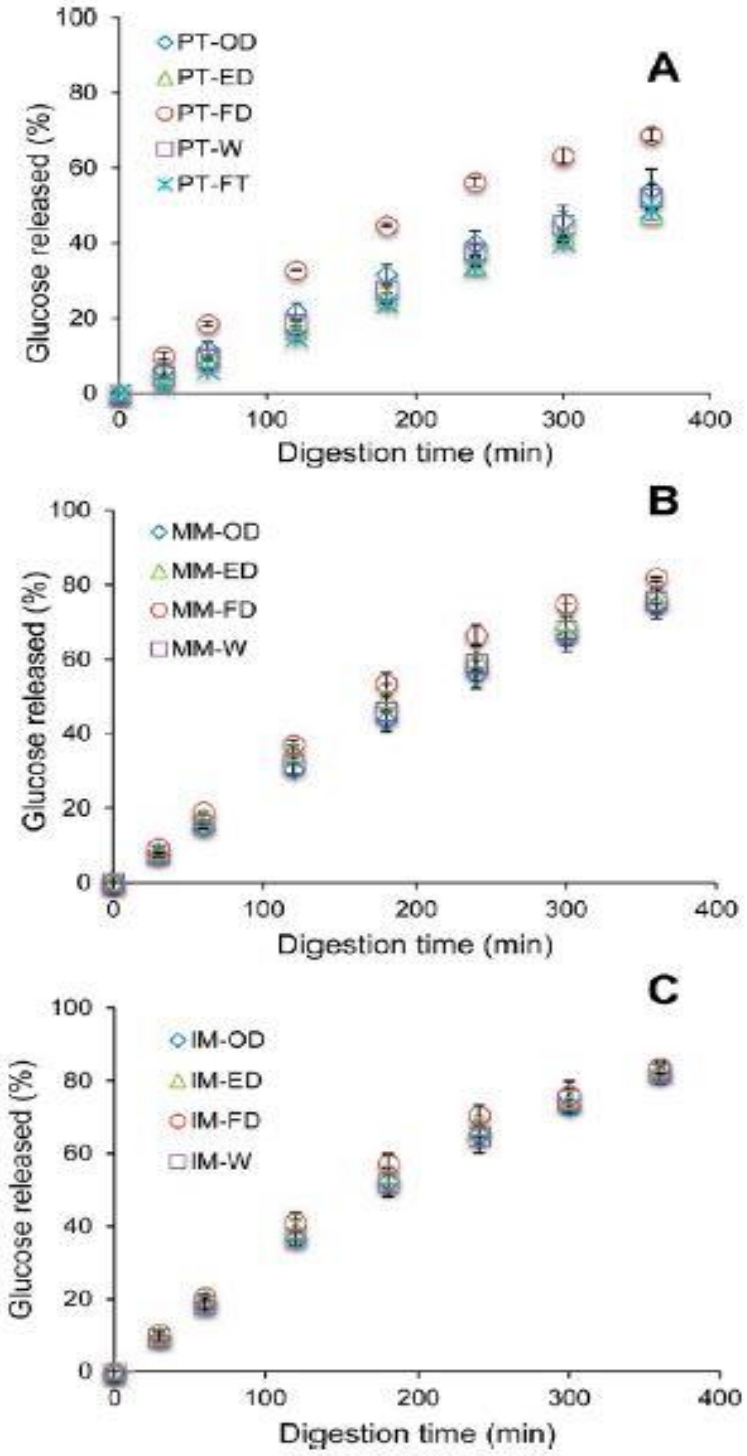

Figure 7.1. Digestion kinetic profiles of potato tuber (PT), mature maize (MM), and immature maize (IM) starch granules subjected to oven drying (OD), ethanol drying (ED), and freeze-drying (FD) as well as PT starch granules after freezing and immediate thawing (FT), compared with wet/never dried controls (W).

Table 7.1. Digestion rate coefficient (k, min^{-1}) of starch samples. [A]

Treatment [B]	PT	MM	IM	CT	G50
OD	(2.15 ± 0.27)×10^{-3} b	(3.81 ± 0.43)×10^{-3} c	(4.69 ± 0.33)×10^{-3} c	ND	ND
ED	(1.83 ± 0.02)×10^{-3} b	(4.21 ± 0.45)×10^{-3} c	(4.94 ± 0.29)×10^{-3} c	(5.50± 0.01)×10^{-4} d	(6.16 ± 0.63)×10^{-4} d
FD	(3.29 ± 0.19)×10^{-3} a	(4.81 ± 0.19)×10^{-3} c	(5.11 ± 0.39)×10^{-3} c	(7.68 ± 0.89)×10^{-4} d	(7.30 ± 0.22)×10^{-4} d
W	(2.06 ± 0.20)×10^{-3} b	(3.97 ± 0.44)×10^{-3} c	(4.81 ± 0.50)×10^{-3} c	ND	ND
FT	(1.89 ± 0.00)×10^{-3} b	ND	ND	ND	ND

[A] Means ± standard deviations from two measurements. Values in the same column with different letters are significantly different at $p < 0.05$.

[B] PT, potato tuber; MM, mature maize; IM, immature maize; CT, canna tuber; G50, Gelose 50; OD, oven-dried; ED, ethanol-dried; FD, freeze-dried; W, wet/not dried FT, frozen-thawed; ND, not determined.

7.3.2 Surface architecture of granular and partly digested starches

Electron micrographs of PT, MM, and IM starch granules subjected to various drying methods are shown in Figure 7.2. MM and IM starch granules have either round or irregular shapes with diameters of 5 - 30 μm, whereas PT starch granules have either ellipsoidal or round shapes with a wide range of granule sizes (5 - 100 μm). The variations in granule shape and size within each starch sample are likely due to the termination of starch granule synthesis at different growth stages and/or the synthesis of starch granules at different grain developmental stages. In general, maize starch granules show the presence of pores on the granule surface, whereas potato starch granules have smooth surfaces lacking pores.[271] The high k values of MM and IM starch granules compared with those of PT starch granules can be related to the surface pores linking the hilum and surface through interior channels, facilitating the 'inside-out' digestion from the hilum to the surface of the granules.[33, 174] On the other hand, the smooth surface structure of PT starch granules limits the enzyme diffusion, and hence, the digestion takes place from the surface (exo-corrosion).

PT-FD starch granules exhibit relatively more wrinkles or scratches on their surface than PT-OD and PT-ED starch granules, which show similar smooth surface structures (Figure 7.2). The scratches and roughness are likely caused by the forced distortion of starch granules due to local explosive release of water vapour from the built-up pressure inside the rigid granules, as the water molecules try to escape through the solid internal structure and smooth surface structure under the vacuum conditions. The presence of pores and channels on the surface and inside the MM and IM starch granules, respectively, facilitates the escape of water molecules during FD, resulting in no apparent changes to the granular structure when compared with the W controls and those after OD and ED processes.

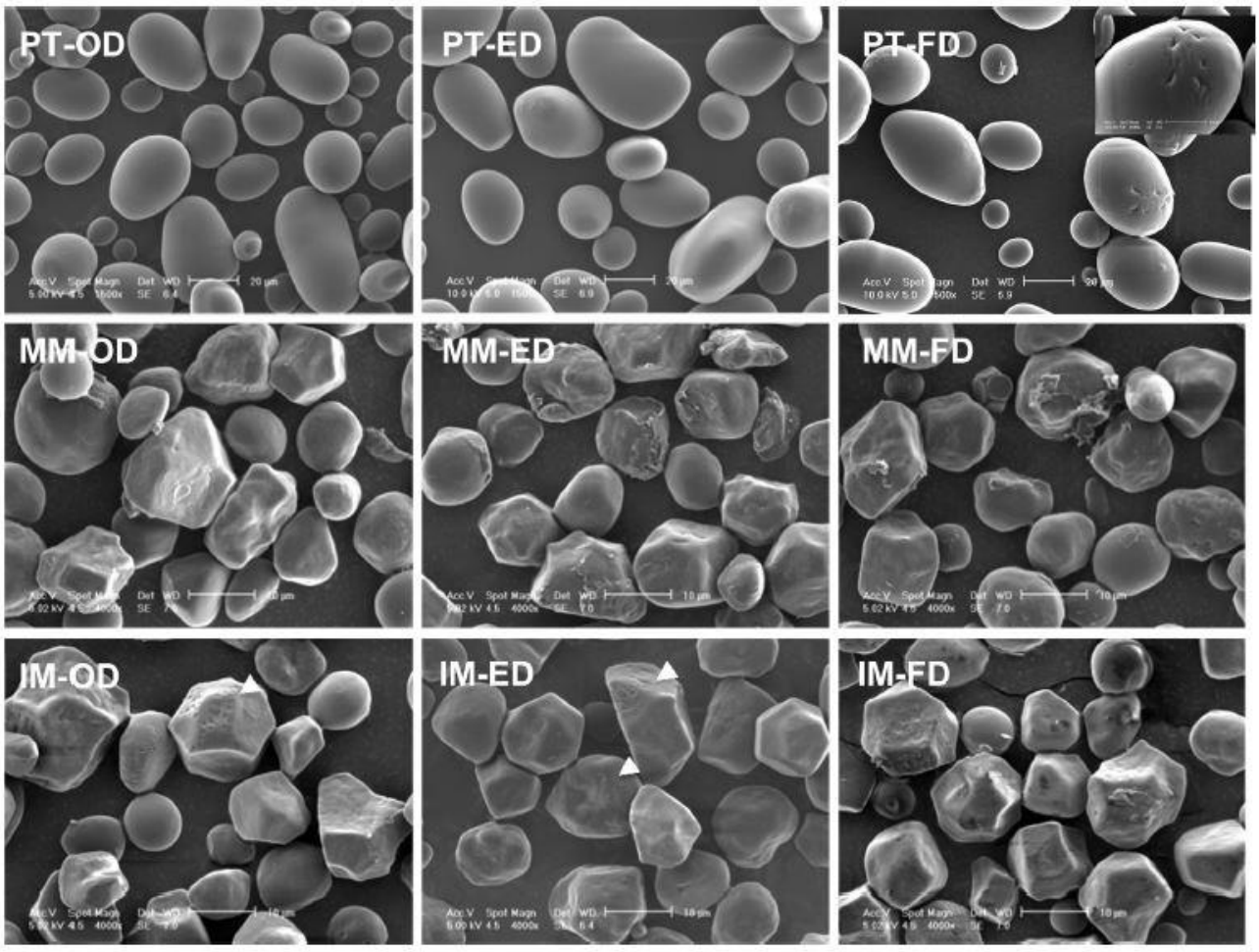

Figure 7.2. Morphologies of potato tuber (PT), mature maize (MM), and immature maize (IM) starch granules subjected to oven drying (OD), ethanol drying (ED), and freeze-drying (FD), compared with wet/never dried controls (W).

Some micro-pores might be generated during FD, but would not easily be observed by SEM, because the pores could be covered by the platinum sputter coating (at least 10-nm thickness) used in the sample preparation. To assess the possible generation of micro-

pores, a fluorescent FITC dextran probe (molar mass 20 kDa, R_h ~3.3 nm) was used, and its diffusion into starch granules was observed using CLSM.[266] The size of the FITC dextran probe is similar to that of α-amylase, the rate-determining enzyme during granular starch digestion;[198] therefore, the diffusion of this probe can be used to identify the ability of *α*-amylase to diffuse into starch granules. CLSM micrographs of PT, MM, and IM starch granules in the FITC dextran solution are presented in Figure 7.3. No qualitative differences are observed in the internal structures of MM-ED, MM-FD, IM-ED, and IM-FD starch granules, which show the characteristic central cavity and extended channels of various sizes. There are, however, apparent differences between the internal structures of PT-ED and PT-FD starch granules. No detectable internal fluorescence can be detected within PT-ED starch granules, especially at the hilum, after they had been exposed to the FITC dextran probe, suggesting that the surface of PT starch granules was not greatly damaged by the ED process, and that it was impermeable to the enzyme-sized FITC dextran because of the effective barrier of tightly packed starch molecules.[84] The FITC dextran probe, on the other hand, can diffuse into the hilum of the PT-FD starch granules under the same diffusion conditions as for the PT-ED starch granules. This clear distinction suggests that the surface of the PT-FD starch granules is more porous than those of the PT-OD and PT-ED starch granules.

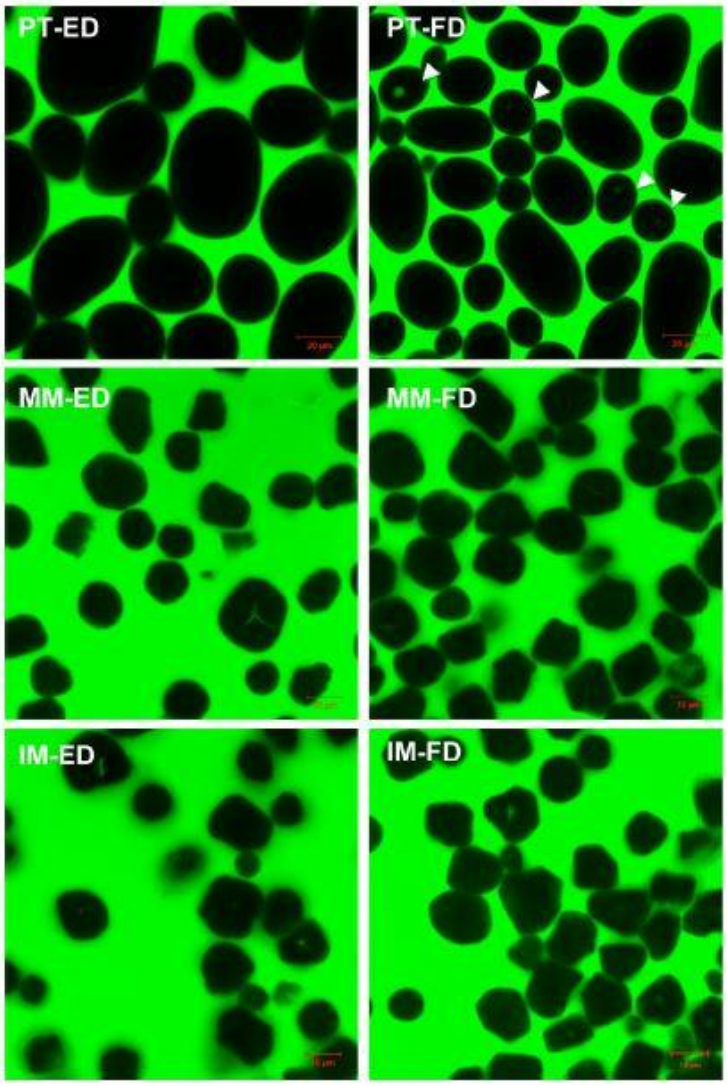

Figure 7.3. CLSM micrographs of ethanol- and freeze-dried starch granules suspended overnight in FITC dextran solution (PT, potato tuber; MM, mature maize; IM, immature maize; ED, ethanol-dried; FD, freeze-dried).

After 1 h *in vitro* digestion, the surface pores of maize starch granules (MM-ED, MM-FD, IM-ED, and IM-FD) became larger (Figure 7.4). The maize starch granules were broken into smaller fragments and debris, sometimes with visible growth rings after 5 h *in vitro* digestion. The hydrolytic pattern of the amylolytic enzymes on starch granules is not random, with the surface pores and internal channels being rapidly attacked in the beginning of the digestion. The apparent diameter of these internal channels ranges from 0.007 to 0.1 *μ*m, whereas that of the surface pores is larger, varying between 0.1 and 0.3 *μ*m.[190, 271, 272] The presence of surface pores and internal channels in maize starch granules enables the diffusion of enzymes, i.e., α-amylase (diameter, 3−4 nm) and amyloglucosidase (diameter, 8−10 nm), into the hilum of starch granules during digestion,[33, 190, 273] allowing the internal corrosion or 'inside-out' digestion pattern.[139] After

prolonged digestion, the internal structure of starch granules becomes hollow, which can then be easily broken into smaller fragments or debris. There are no qualitative differences among MM-ED, MM-FD, IM-ED, and IM-FD starch granules, consistent with their insignificantly different *k* values.

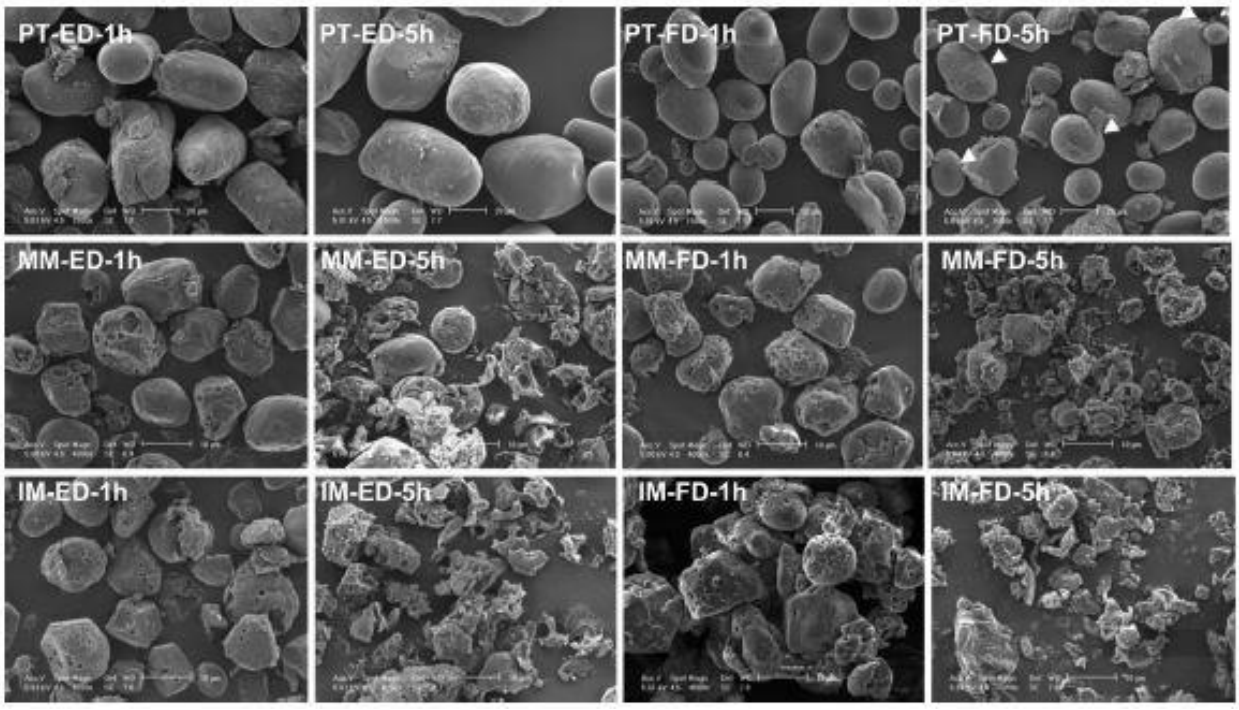

Figure 7.4. Morphologies of ethanol- and freeze-dried starch granules/fragments after 1 and 5 h *in vitro* digestion (PT, potato tuber; MM, mature maize; IM, immature maize; ED, ethanol-dried; FD, freeze-dried).

On the other hand, the granule surfaces of PT-ED and PT-FD starch granules were roughened, sometimes with visible scratches, after 1 h of *in vitro* digestion (Figure 7.4). A further increase in surface roughness, sometimes with deep cracks, is observed on some granules after 5 h *in vitro* digestion. Potato starch granules lack surface pores and internal channels, and thus, they are slowly digested because the enzymes have to break through the dense molecular packing at the surface of starch granules to diffuse into the hilum ('exo-corrosion' digestion pattern).[110] Furthermore, some pinholes can be observed on the surface of the PT-FD starch granules, but not the PT-ED starch granules, after 5 h *in vitro* digestion. The SEM images of digested PT-FD starch granules are consistent with the higher porosity of undigested PT-FD starch granules deduced from CLSM micrographs (Figure 7.3). However, the drying process does not change the overall starch digestion pattern: 'inside-out' pattern for maize starch granules and 'exo-corrosion' pattern for potato starch granules.

7.3.3 Gelatinization properties

Starch gelatinization is an endothermic transition corresponding to the dissociation of amylopectin double helices from a semi-crystalline structure to an amorphous conformation.[195] The gelatinization properties of starch granules dried using different methods are summarized in Table 7.2. The gelatinization temperatures of maize and potato starch granules, except PT-FD starch granules, range from 64 to 78 °C, which are within the range reported by others.[211] The gelatinization temperatures and ΔH values of MM starch granules are slightly higher than those of IM starch granules, which is likely due to the annealing of starch granules during field drying of MM.[274] All dehydrated starch granule samples show lower gelatinization temperatures and ΔH values than their W control counterparts. The FD process significantly decreases ($p < 0.05$) both the gelatinization temperatures and ΔH values of all starch granule samples, especially the PT starch granules. Other drying methods (OD and ED), in comparison, result in only slightly lower gelatinization temperatures and ΔH values, suggesting that OD and ED induce fewer structural changes than FD and/or the W controls were annealed during storage in the solution. The gelatinization temperature reflects the heat stability of the crystallites, whereas the ΔH value is associated with the amount of molecular order and crystallinity.[195] Therefore, the disruption of the crystalline arrangement (long-range ordered structures) and/or the reduction in the amount of double helices (short-range ordered structures) might have occurred during the FD process. To further understand the differences in the starch gelatinization properties after drying processes, the crystallinity and molecular conformation of starch after drying were analyzed and compared.

Table 7.2. Gelatinization properties (measured by DSC) of potato and maize starches under different drying conditions. [A]

Starch sample [B]	T_o (°C)	T_p (°C)	T_c (°C)	ΔH (J/g)
PT-OD	63.3 ± 0.5cd	66.2 ± 0.6ef	71.5 ± 0.7fg	19.7 ± 0.8ab
PT-ED	63.6 ± 0.3ef	66.4 ± 0.4g	71.7 ± 0.5g	19.3 ± 0.3b
PT-FD	49.7 ± 0.2h	56.0 ± 0.4h	63.7 ± 1.2h	11.8 ± 0.3gh
PT-W	63.9 ± 0.1de	66.7 ± 0.1fg	72.0 ± 0.4fg	20.1 ± 0.1a
MM-OD	65.3 ± 0.1b	70.2 ± 0.0b	75.5 ± 0.0b	13.1 ± 0.1de
MM-ED	64.5 ± 0.0cd	69.4 ± 0.1c	75.1 ± 0.1b	12.5 ± 0.2efg
MM-FD	63.3 ± 0.1f	68.2 ± 0.1d	74.0 ± 0.1cd	12.1 ± 0.1fgh
MM-W	67.9 ± 0.3a	72.7 ± 0.1a	78.1 ± 0.1a	14.5 ± 0.4c
IM-OD	64.7 ± 0.2c	68.7 ±0.1d	73.6 ± 0.5de	12.7 ± 0.5def
IM-ED	63.3 ± 0.5f	68.2 ± 0.1d	74.0 ± 0.2cd	13.3 ± 0.1d
IM-FD	62.7 ± 0.2g	67.4 ± 0.2e	73.6 ± 0.2ef	11.4 ± 0.4h
IM-W	64.8 ± 0.1bc	69.5 ± 0.0c	74.6 ± 0.0bc	13.5 ± 0.1d

[A] Means ± standard deviations from two measurements. Values in the same column with different letters are significantly different at $p < 0.05$. T_o, T_p, T_c, and ΔH are onset temperature, peak temperature, conclusion temperature, and enthalpy change, respectively.

[B] PT, potato tuber; MM, mature maize; IM, immature maize; OD, oven-dried; ED, ethanol-dried; FD, freeze-dried; W, wet/not dried.

7.3.4 Starch crystallinity and molecular order

XRD is used to study the type and level of starch crystallinity or long-range order. X-ray diffractograms of PT, MM, and IM starch granule samples are shown in Figure 7.5A. Maize starch granules, irrespective of the drying method or stage of maturity, exhibit the A-type polymorph (major peaks at ~15 °, 17 °, 18 ° and 23° 2θ) with similar peak heights and widths. The percentages of crystallinity, calculated from the ratio of the total peak area to the total diffraction area, are similar for all maize starch granules (Table 7.3). On the other hand, PT starch granules show the B-type pattern (major peaks at ~5 °, 17 °, 22 ° and 24° 2θ) with marked differences observed in the type and level of crystallinity between the PT-OD/ED and PT-FD starch granules, where the peaks in the diffractogram of the PT-FD starch granules are lower and broader (less sharp) than those in the diffractogram of their OD/ED counterparts. Furthermore, the percentage crystallinity of the PT-FD starch granules is about 50% of that for the PT-OD and PT-ED starch granules. The results

indicate that FD significantly alters the crystalline structure of the PT starch granules.

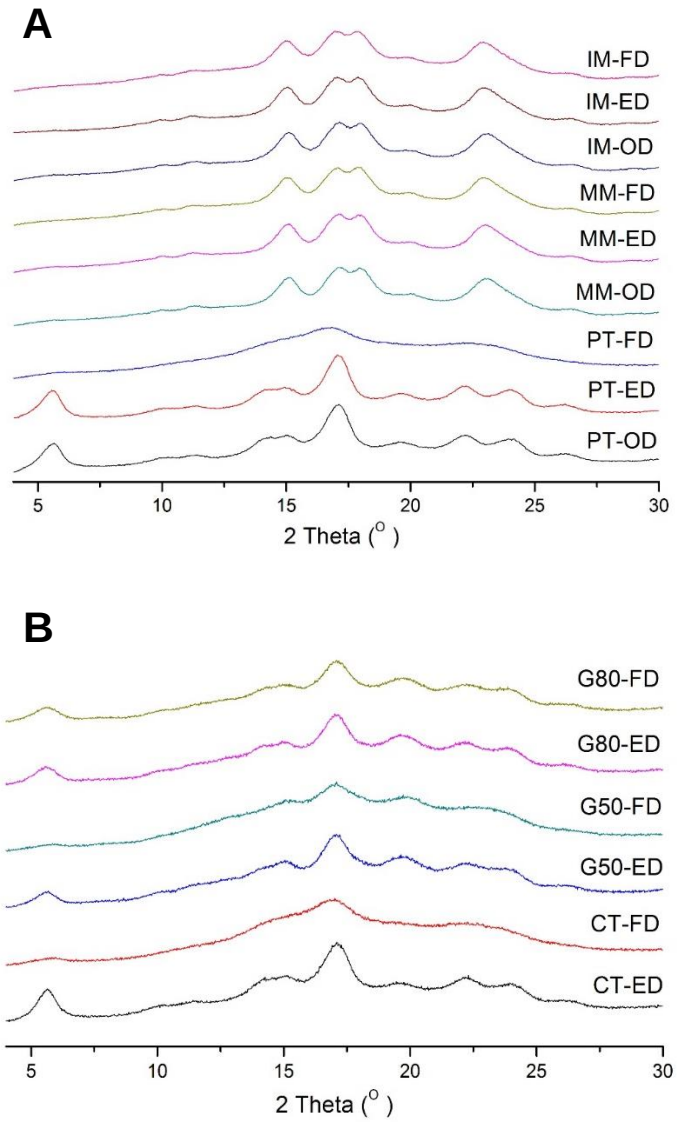

Figure 7.5. X-ray diffractograms of oven-, ethanol- and freeze-dried starch granules (PT, potato tuber; MM, mature maize; IM, immature maize; CT, canna tuber; G50, Gelose 50; G80, Gelose 80; OD, oven-dried; ED, ethanol-dried; FD, freeze-dried).

Solid-state NMR spectroscopy was used to determine whether the changes observed in long-range crystalline order are consistent with the changes in short-range molecular order; NMR spectra are shown in Figure 7.6. All maize starch granules, irrespective of drying method and stage of maturity, display similar spectra with a triplet in the C1 region at 101.6, 100.4, and 99.3 ppm, typical of the A-type double helical conformation.[216] The PT-OD and PT-ED starch granule samples display a doublet in the C1 region with distinctive signals at 110.79 and 99.72 ppm, expected for the B-type polymorphic starch.[217, 218, 275] However, the intensity of this doublet is greatly reduced in PT-FD starch granules, where it is no longer visible in the NMR spectrum. To calculate the degree of

molecular order in the starch granule samples, gelatinized maize starch is used as an amorphous standard and its intensity at 84 ppm is matched to those in the NMR spectra of the starch granule samples.[205] Subtraction of the sample NMR spectrum from the amorphous standard spectrum reveals a doublet or a triplet in the C1 region for the double helix and a smaller peak around 103 ppm for the V-type single-helix.[217] Calculating the areas of these peaks gives the percentages of double-helical, single-helical, and amorphous starch shown in Table 7.3. The results of molecular order from NMR analysis are similar for all maize starch granule samples, in good agreement with the degree of crystallinity from XRD, indicating that both the long-range crystallinity and the short-range molecular order are conserved under the three drying methods. A similar phenomenon was observed for the PT-OD and PT-ED starch granule samples; however, a notable difference of a ~40% reduction in double-helical order was observed for the PT-FD starch granule sample, which is slightly lower than the loss of crystalline order (~50%) analyzed by XRD. It was reported in a previous study,[195] that the amount of double helices is higher than the degree of crystallinity and, thus, not all double helices participate in the crystalline structure in native starch granules. The results suggest that FD causes slightly greater disruption to the long-range crystalline packing of PT starch granules than the short-range molecular order, that is, the misalignment or disruption of crystallites with less unwinding of the double helices.

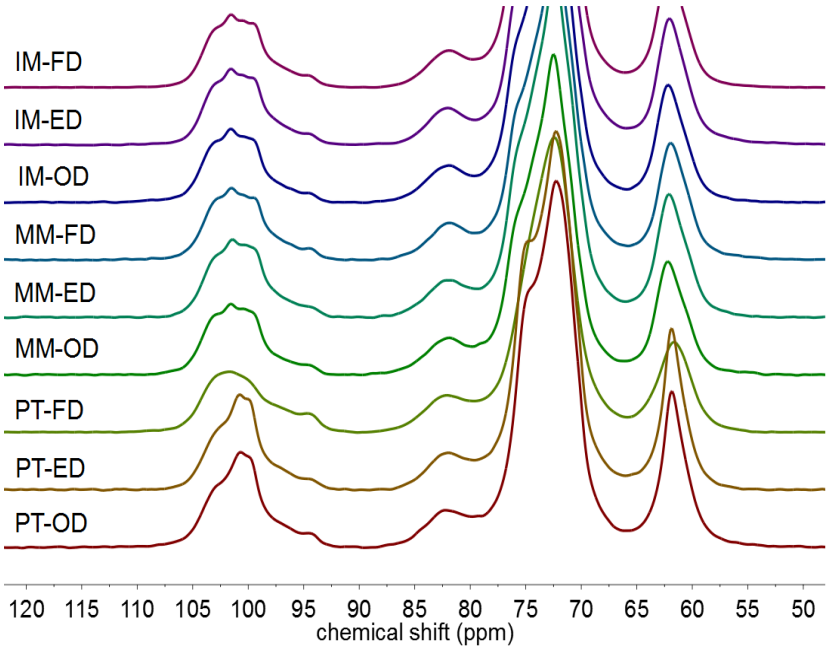

Figure 7.6. ^{13}C CP/MAS NMR spectra of oven-, ethanol-, and freeze-dried starch granules (PT, potato tuber; MM, mature maize; IM, immature maize; OD, oven-dried; ED, ethanol-dried; FD, freeze-dried).

The ratios of absorbance at 1045 and 1022 cm^{-1} from the FTIR spectra have been associated with ordered (organized) and amorphous (less organized) structures of starch, and their absorbance ratio can be used as an index to characterize the short-range alignment of double helices.[268] The absorbance ratios for all maize starch granule samples are similar (Table 7.3), irrespective of their drying method and stage of maturity, whereas that of the PT-FD starch granule sample is significantly lower than those of the PT-OD and PT-ED starch granule samples. The FTIR results are in good agreement with the XRD and NMR results, indicating that a decrease in the molecular order of PT starch granules by FD, which is likely to be associated with the disruption of double helices. As observed from the gelatinization properties of PT starch granule samples (Table 7.2), the PT-FD starch granules have considerably lower T_o and ΔH values, whereas these values are almost conserved for other drying methods compared with the PT-W control. The current results corroborate previous reports, that showed a reduction in the enthalpy change and gelatinization temperatures of potato starch granules but not wheat starch granules after FD.[276-278]

From previous reports and the current findings, it is evident that freeze-drying has less of an effect on the structure and molecular packing of A-type polymorphic cereal starches (wheat and maize) than those of potato starch granules. This raises an interesting question as to the effects of drying methods on other B-type polymorphic starches from both cereals and tubers, which have not yet been reported but which would be useful for understanding the mechanism behind the alteration of molecular packing of freeze-dried starches. In a recent report, Zhang, et al. [279] reported an increase in the crystallinity of starch granules isolated from freeze-dried Chinese yam; however, this does not represent the freeze-dried isolated starch granules.

Table 7.3. Crystallinity (quantified by XRD) and molecular order (measured by ^{13}C CP/MAS NMR) of potato and maize starches under different drying conditions. [A]

Starch sample[B]	XRD	FTIR	^{13}C CP/MAS NMR		
	Crystallinity (%)	1045/1022 ratio[C]	Double helix (%)	Single helix (%)	Amorphous (%)
PT-OD	36.1	0.705 ± 0.002 a	44	2	54
PT-ED	37.1	0.703 ± 0.002 a	44	5	51
PT-FD	18.8	0.653 ± 0.005 b	30	0	70
MM-OD	31.9	0.659 ± 0.008 b	36	3	61
MM-ED	32.0	0.655 ± 0.003 b	41	4	55
MM-FD	29.9	0.641 ± 0.002 b	43	4	53
IM-OD	31.6	0.654 ± 0.003 b	35	3	62
IM-ED	32.1	0.650 ± 0.005 b	41	4	55
IM-FD	29.5	0.651 ± 0.003 b	39	4	57

[A] XRD and NMR calculations are within SD of 2%. Means ± standard deviations from two FTIR measurements.

[B] PT, potato tuber; MM, mature maize; IM, immature maize; OD, oven-dried; ED, ethanol-dried; FD, freeze-dried.

[C] Means ± standard deviations from two measurements. Values in the same column with different letters are significantly different at $p < 0.05$.

The X-ray diffractograms of additional B-type polymorphic starches (CT, G50, and G80) after being subjected to ED and FD processes are presented in Figure 7.5B. Similarly to the PT starch granules, the diffraction peaks of CT and G50 starch granules are shorter and broader after the FD process than after the ED process, confirming the ability of FD to alter the molecular packing of B-type polymorphic starches. The decrease in crystallinity or increase in amorphous character results in an increase in the enzymatic hydrolysis rate of B-type canna and Gelose starches (Table 7.1). However, the effects of FD are less apparent for G80 starch granules, probably because of the high amylose content and/or very small granular size of G80, which needs further investigation.

Apart from changes in surface morphology, the increased digestion rate of FD starches could be due to differences of molecular order in starch granules, related to the starch polymorphism rather than the botanical sources, e.g., cereal grains versus tubers. At least two molecular-level hypotheses can be proposed to explain the alteration of short- and long- range molecular order after freeze-drying (but not freeze-thaw treatment) in B-polymorphic starches. First, the higher amount of intra-crystalline water in B-type polymorphic starch might distort the helical organization of amylopectin molecules by sublimation. However, this hypothesis should also apply to oven-dried samples, which do not show the effect. Alternatively, B-type starches with more stable intermolecular structures compared to A-polymorphic starches, due to more longer branch chains, might hinder the passage of subliming water, ultimately increasing internal pressure and destabilizing the helical structure and molecular order under high vacuum. In contrast, because of the lower and more scattered inter-crystalline water and loosely packed internal structure caused by a larger population of short amylopectin branches, the subliming water molecules can escape A-type granules more easily exerting lesser internal pressure. A key difference between the oven drying and freeze-drying methods is the effect of temperature on starch chain mobility. The greater rigidity of starch chains during freeze-drying compared with oven-drying means that, although both processes involve removal of vapor-phase water, the lower temperature involved in freeze-drying is more likely to result in local fracture and structure disorganization events as a result of water removal. We therefore propose that the effect of freeze-drying on B-type polymorphic starches is

due to a combination of local (crystalline packing, long branches) and larger-scale (lack of pores and channels) effects, resulting in structural disorganization from nanometer to micronmeter length scales.

7.4 Conclusions

In summary, oven and ethanol drying are mild dehydration methods that do not significantly affect the digestion, thermal, or structural properties of starches compared with their counterparts that have never been dried. However, freeze-drying can result in a marked increase in the digestion rate of B-type polymorphic starches, but not that of A-type polymorphic starches. Freeze-drying not only generates some micro-pores on the surface of potato starch granules, but also disrupts both crystallinity and molecular order, each of which can cause an increase in the digestion rate.

Chapter 8

General Conclusions and Future Direction

8.1 Summary of thesis research

This thesis has investigated in detail the molecular organization, physical and digestion properties of non- or low-order starch matrices induced by processing including cooking, extrusion and freeze-drying. Before food processing effects were investigated, the influence of starch physical structure on the digestion kinetics (amyloglucosidase and α-amylase alone and combination) was studied using three physical forms of maize and potato starch as exemplars. In granular form, there was synergism between the enzymes in the production of glucose. In contrast, α-amylase and amyloglucosidase showed antagonistic effects in digestion of cooked starches. Antagonism was ascribed to the rapid production of low molecular weight oligomers by α-amylase, which are less efficiently digested by amyloglucosidase than polymeric substrates. This has been detailed in chapter 3.

After heating in excess water under little or no shear, starch granules do not dissolve completely but persist as highly swollen fragile forms, commonly termed granule ‘ghosts’. In chapter 4, amylase digestion of isolated granule ghosts from maize and potato starches is used as a probe to study the mechanism of ghost formation, through microstructural, mesoscopic, and molecular scale analyses of structure before and after digestion. Digestion profiles showed that neither integral nor surface proteins/lipids were crucial for control of either ghost digestion or integrity. On the basis of the molecular composition and conformation of enzyme-resistant fractions, it was concluded that the condensed polymeric surface structure of ghost particles is mainly composed of non-ordered but entangled amylopectin (and some amylose) molecules, with only limited reinforcement through partially ordered enzyme-resistant structures based on amylose (for maize starch; V-type order) or amylopectin (for potato starch; B-type order). The high level of branching and large molecular size of amylopectin is proposed to be the origin for the unusual stability of a solid structure based primarily on temporary entanglements.

Chapter 5 reported for the first time the tribological and rheological properties of isolated starch ghost suspensions from maize and potato over a range of concentrations. Smaller size and more robust maize ghosts subjected to the tribology or rheology test only resulted in slightly reduced integrity in morphology, whereas large and fragile potato ghosts show significant amounts of granule fragments after testing. A markedly decreased maximum friction coefficient point at an entrainment speed of 40 mm/s with increasing concentration (from 0.01% to 1% w/w) of maize ghost suspensions was observed, while the apparent friction coefficient is concentration independent for potato ghosts although this is likely to be due to disintegration of fragile potato ghosts under tribological contact. We conclude that soft-tribological properties of starch ghost suspensions can be due to either particulate (e.g. maize ghosts) or polymeric (particularly for potato ghosts) forms, the balance between which could potentially contribute to the perception of starch-containing food in the mouth.

In chapter 6, waxy, normal and high-amylose maize starches were extruded with water as sole plasticizer to achieve low-order starch matrices. Of the three starches, we found that only high-amylose extrudate showed lower digestion rate/extent than starches cooked in excess water. The ordered structure of high-amylose starches in cooked and extruded forms was similar, as judged by NMR, XRD and DSC techniques, but enzyme resistance was much greater for extruded forms. We suggest that the local molecular density of packing of starch chains can control the digestion kinetics rather than just crystallinity, with the emphasis being that density sufficient to either prevent/limit binding and/or slow down catalysis can be achieved by dense amorphous packing.

Starch granules isolated from maize (A-type polymorph) and potato (B-type polymorph) were subjected to different dehydration methods including oven (heat), freeze, and ethanol (solvent exchange) drying, and subsequent structure and digestibility changes were further investigated. Oven and ethanol drying do not significantly affect the digestion properties of starches compared with their counterparts that have never been dried. However, freeze drying results in a significant increase in the digestion rate of potato starch, but not that of maize starch. The structural and conformational changes of starch granules after drying were

investigated at various length scales using scanning electron microscopy, confocal laser scanning microscopy, X-ray diffraction, FTIR, and NMR spectroscopy. Freeze drying not only disrupts the surface morphology of potato starch granules (B-type polymorph), but also degrades both short- and long-range molecular order of the amylopectin, each of which can cause an increase in the digestion rate. In contrast to A-polymorphic starches, a range of B-polymorphic starches are more disrupted on freeze drying with reduction of both short and long range molecular order. We propose that the low temperatures involved in freeze drying compared with oven drying results in greater chain rigidity, and leads to structural disorganization during water removal at both nm and μm length scales in B-type granules, due to the different distribution of water within crystallites and the lack of pores and channels compared with A-type granules.

8.2 Recommendation for future research

Understanding molecular organization, physical and digestion properties of low-order starch matrices is useful for designing the next-generation of starch-containing foods with improved nutrition and sensory properties to be more available to consumers. Whilst considerable progress has been made, further studies will need to be conducted, including

1. Direct evidence of physical entanglements of starch polymers within granule ghosts is needed. Some high-resolution microscopic techniques such as atomic force microscopy, transmission electron microscopy could be used to investigate the molecular organization of ghost particles in hydrated form.
2. How to link the tribology and rheology data of ghost suspensions as a starchy model food with the perception of starchy food in the mouth? This is a future research direction for the food oral processing area.
3. An amorphous state is essentially a negative definition based on the absence of detectable molecular order. Further work is required to better understand the nature of non-crystalline matrices that results in slow digestion rate/extent, such as the local density and entanglement of starch chains through application of material and polymer science principles.
4. Methods such as positron annihilation lifetime spectroscopy may provide improved methods for determining local molecular densities of starch matrices in a non-

destructive manner.[257, 280] This will be a key future challenge in fundamental starch research.

5. Methods to increase the molecular densities of starch matrices independent of crystallinity should be developed. This will provide practical outcomes including better methods for increasing RS in processed starches. It will also be a significant advance in starch theory, and the understanding of non-crystalline dense packing.

6. Determining what aspects of high-amylose starches contribute to their relative enzyme resistance following dense packing by extrusion. Is it because the longer amylopectin branches and greater amount of amylose are more able to pack in a dense fashion, or is it because once densified under limited water conditions such as in extrusion, these molecular features restrict swelling during subsequent hydration? This will advance our theoretical understanding of the physical packing of amylose in amorphous matrices, with implications for greater understanding of the organisation of amylose within starch granules.

Bibliography

1. Englyst, H. N.; Kingman, S. M.; Cummings, J. H., Classification and measurement of nutritionally important starch fractions. *Eur J Clin Nutr* **1992**, *46*, S33-S50.

2. Englyst, H. N.; Macfarlane, G. T., Breakdown of resistant and readily digestible starch by human gut bacteria. *Journal of the Science of Food and Agriculture* **1986**, *37*, 699-706.

3. Behall, K. M.; Hallfrisch, J., Plasma glucose and insulin reduction after consumption of breads varying in amylose content. *Eur J Clin Nutr* **2002**, *56*, 913-920.

4. Brand-Miller, J. C.; Holt, S. H. A.; Pawlak, D. B.; McMillan, J., Glycemic index and obesity. *Am J Clin Nutr* **2002**, *76*, 281S-285S.

5. Van Munster, I. P.; Tangerman, A.; Nagengast, F. M., Effect of resistant starch on colonic fermentation, bile-acid metabolism, and mucosal proliferation. *Digest Dis Sci* **1994**, *39*, 834-842.

6. Topping, D. L.; Bajka, B. H.; Bird, A. R.; Clarke, J. M.; Cobiac, L.; Conlon, M. A.; Morell, M. K.; Toden, S., Resistant starches as a vehicle for delivering health benefits to the human large bowel. *Microb Ecol Health Dis* **2008**, *20*, 103-108.

7. Chanvrier, H.; Uthayakumaran, S.; Appelqvist, I. A. M.; Gidley, M. J.; Gilbert, E. P.; Lopez-Rubio, A., Influence of storage conditions on the structure, thermal behavior, and formation of enzyme-resistant starch in extruded starches. *J Agric Food Chem* **2007**, *55*, 9883-9890.

8. Htoon, A.; Shrestha, A. K.; Flanagan, B. M.; Lopez-Rubio, A.; Bird, A. R.; Gilbert, E. P.; Gidley, M. J., Effects of processing high amylose maize starches under controlled conditions on structural organisation and amylase digestibility. *Carbohydr Polym* **2009**, *75*, 236-245.

9. Gidley, M. J.; Hanashiro, I.; Hani, N. M.; Hill, S. E.; Huber, A.; Jane, J. L.; Liu, Q.; Morris, G. A.; Rolland-Sabate, A.; Striegel, A. M.; Gilbert, R. G., Reliable measurements of the size distributions of starch molecules in solution: Current dilemmas and recommendations. *Carbohydr Polym* **2010**, *79*, 255-261.

10. Buleon, A.; Colonna, P.; Planchot, V.; Ball, S., Starch granules: structure and biosynthesis. *Int J Biol Macromol* **1998**, *23*, 85-112.

11. Gilbert, R. G., Size-separation characterization of starch and glycogen for biosynthesis-structure-property relationships. *Anal Bioanal Chem* **2011**, *399*, 1425-1438.

12. Hizukuri, S.; Takeda, Y.; Yasuda, M.; Suzuki, A., Multi-branched nature of amylose and the action of debranching enzymes. *Carbohydr Res* **1981**, *94*, 205-213.

13. Takeda, Y.; Maruta, N.; Hizukuri, S., Examination of the structure of amylose by tritium labeling of the reducing terminal. *Carbohydr Res* **1992**, *227*, 113-120.

14. Li, L.; Jiang, H.; Campbell, M.; Blanco, M.; Jane, J.-L., Characterization of maize amylose-extender (ae) mutant starches. Part I: Relationship between resistant starch contents and molecular structures. *Carbohydr Polym* **2008**, *74*, 396-404.

15. Baba, T.; Arai, Y., Structural features of amylomaize starch .3. Structural characterization of amylopectin and intermediate material in amylomaize atarch granules. *Agr Biol Chem Tokyo* **1984**, *48*, 1763-1775.

16. Peat, S.; Whelan, W. J.; Thomas, G. J., Evidence of multiple branching in waxy maize starch. *J Chem Soc* **1952**, 4546-4548.

17. Perez, S.; Bertoft, E., The molecular structures of starch components and their contribution to the architecture of starch granules: A comprehensive review. *Starch/Starke* **2010**, *62*, 389-420.

18. Hizukuri, S., Polymodal distribution of the chain lengths of amylopectins, and its significance. *Carbohydr Res* **1986**, *147*, 342-347.

19. Le Corre, D.; Bras, J.; Dufresne, A., Starch nanoparticles: A review. *Biomacromolecules* **2010**, *11*, 1139-1153.

20. Zobel, H. F., Molecules to granules: A comprehensive starch review. *Starch/Starke* **1988**, *40*, 44-50.

21. Zobel, H. F., Starch crystal transformations and their industrial importance. *Starch/Starke* **1988**, *40*, 1-7.

22. Imberty, A.; Buleon, A.; Tran, V.; Perez, S., Recent advances in knowledge of starch structure. *Starch/Starke* **1991**, *43*, 375-384.

23. Gidley, M. J.; Bulpin, P. V., Crystallization of maltooligosaccharides as models of thecrystalline forms of starch: Minimum chain-length requirement for the formation of double helices. *Carbohydr Res* **1987**, *161*, 291-300.

24. Jenkins, P. J.; Cameron, R. E.; Donald, A. M., A universal feature in the structure of starch granules from different botanical sources. *Starch/Starke* **1993**, *45*, 417-420.

25. Jane, J. L.; Wong, K. S.; McPherson, A. E., Branch-structure difference in starches of A- and B-type X-ray patterns revealed by their Naegeli dextrins. *Carbohydr Res* **1997**, *300*, 219-227.

26. Yuryev, V. P.; Krivandin, A. V.; Kiseleva, V. I.; Wasserman, L. A.; Genkina, N. K.; Fornal, J.; Blaszczak, W.; Schiraldi, A., Structural parameters of amylopectin clusters and semi-crystalline growth rings in wheat starches with different amylose content. *Carbohydr Res* **2004**, *339*, 2683-2691.

27. Jenkins, P. J.; Donald, A. M., The influence of amylose on starch granule structure. *Int J Biol Macromol* **1995**, *17*, 315-321.

28. Cameron, R. E.; Donald, A. M., A small-angle X-ray scattering study of the annealing and gelatinization of starch. *Polymer* **1992**, *33*, 2628-2636.

29. Yuryev, V. P.; Kozlov, S. S.; Noda, T.; Bertoft, E.; Blennow, A., Influence of different GBSS I and GWD combinations on the amylose localization within wheat and potato starch granules. *Starch: Achievements in Understanding of Structure and Functionality* **2007**, 1-47.

30. Gallant, D. J.; Bouchet, B.; Baldwin, P. M., Microscopy of starch: Evidence of a new level of granule organization. *Carbohydr Polym* **1997**, *32*, 177-191.

31. Gallant, D. J.; Bouchet, B.; Buleon, A.; Perez, S., Physical characteristics of starch granules and susceptibility to enzymatic degradation. *Eur J Clin Nutr* **1992**, *46*, S3-S16.

32. Ao, Z.; Jane, J.-l., Characterization and modeling of the A- and B-granule starches of wheat, triticale, and barley. *Carbohydr Polym* **2007**, *67*, 46-55.

33. Fannon, J. E.; Gray, J. A.; Gunawan, N.; Huber, K. C.; BeMiller, J. N., The channels of starch granules. *Food Sci Biotechnol* **2003**, *12*, 700-704.

34. Szymonska, J.; Krok, F., Potato starch granule nanostructure studied by high resolution non-contact AFM. *Int J Biol Macromol* **2003**, *33*, 1-7.

35. Pan, D. D.; Jane, J. L., Internal structure of normal maize starch granules revealed by chemical surface gelatinization. *Biomacromolecules* **2000**, *1*, 126-132.

36. Jane, J. L.; Shen, J. J., Internal structure of potato starch granule revealed by chemical gelatinization. *Carbohydr Res* **1993**, *247*, 279-290.

37. Dry, I.; Smith, A.; Edwards, A.; Bhattacharyya, M.; Dunn, P.; Martin, C., Characterization of cDNAs encoding two isoforms of granule-bound starch synthase which show differential expression in developing storage organs of pea and potato. *Plant Journal* **1992**, *2*, 193-202.

38. Gao, M.; Fisher, D. K.; Kim, K. N.; Shannon, J. C.; Guiltinan, M. J., Evolutionary conservation and expression patterns of maize starch branching enzyme I and IIb genes suggests isoform specialization. *Plant Mol Biol* **1996**, *30*, 1223-1232.

39. Swinkels, J. J. M., Composition and properties of commercial native starches. *Starch/Starke* **1985**, *37*, 1-5.

40. Gracza, R., Minor constituents of starch. *Starch: Chemistry and technology* **1965**, *1*, 105-132.

41. Vasanthan, T.; Hoover, R., A comparative-study of the composition of lipids associated with starch granules from various botanical sources. *Food Chem* **1992**, *43*, 19-27.

42. Appelqvist, I. A. M.; Debet, M. R., Starch-biopolymer interactions - A review. *Food Rev Int* **1997**, *13*, 163-224.

43. Morrison, W. R., Starch lipids and how they relate to starch granule structure and functionality. *Cereal Food World* **1995**, *40*, 437-&.

44. Debet, M. R.; Gidley, M. J., Three classes of starch granule swelling: Influence of surface proteins and lipids. *Carbohydr Polym* **2006**, *64*, 452-465.

45. Morrison, W. R., Lipids in cereal starches: A review. *J Cereal Sci* **1988**, *8*, 1-15.

46. Baldwin, P. M.; Melia, C. D.; Davies, M. C., The surface chemistry of starch granules studied by time-of-flight secondary ion mass spectrometry. *J Cereal Sci* **1997**, *26*, 329-346.

47. Morrison, W. R., Starch lipids: A reappraisal. *Starch/Starke* **1981**, *33*, 408-410.

48. Andersson, L.; Fredriksson, H.; Bergh, M. O.; Andersson, R.; Aman, P., Characterisation of starch from inner and peripheral parts of normal and waxy barley kernels. *J Cereal Sci* **1999**, *30*, 165-171.

49. Vasanthan, T.; Hoover, R., Effect of defatting on starch structure and physicochemical properties. *Food Chem* **1992**, *45*, 337-347.

50. Baldwin, P. M., Starch granule-associated proteins and polypeptides: A review. *Starch/Starke* **2001**, *53*, 475-503.

51. Greenwell, P.; Schofield, J. D., Wheat-starch granule proteins and their technological importance. *Cereal Food World* **1987**, *32*, 680-680.

52. Rayasduarte, P.; Robinson, S. F.; Freeman, T. P., In-situ location of a starch granule protein in durum-wheat endosperm by immunocytochemistry. *Cereal Chem* **1995**, *72*, 269-274.

53. Han, X. Z.; Hamaker, B. R., Location of starch granule-associated proteins revealed by confocal laser scanning microscopy. *J Cereal Sci* **2002**, *35*, 109-116.

54. Oates, C. G., Studies on mung bean starch: Granule stability. *Food Hydrocolloids* **1991**, *4*, 365-377.

55. Hamaker, B. R.; Griffin, V. K., Change the viscoelastic properties of cooked rice though protein disruption. *Cereal Chem* **1990**, *67*, 261-264.

56. Kasemsuwan, T.; Jane, J. L., Quantitative method for the survey of starch phosphate derivatives and starch phospholipids by P-31 nuclear magnetic resonance spectroscopy. *Cereal Chem* **1996**, *73*, 702-707.

57. Medcalf, D. G.; Youngs, V. L.; Gilles, K. A., Wheat starches .2. Effect of polar and nonpolar lipid fractions on pasting characteristics. *Cereal Chem* **1968**, *45*, 88-&.

58. Srichuwong, S.; Jane, J.-l., Physicochemical properties of starch affected by molecular composition and structures: A review. *Food Sci Biotechnol* **2007**, *16*, 663-674.

59. Prentice, R. D. M.; Stark, J. R.; Gidley, M. J., Granule residues and ghosts remaining after heating A-type barley-starch granules in water. *Carbohydr Res* **1992**, *227*, 121-130.

60. Tester, R. F.; Morrison, W. R., Swelling and gelatinization of cereal starches .1. Effects of amylopectin, amylose, and lipids. *Cereal Chem* **1990**, *67*, 551-557.

61. Tester, R. F.; Morrison, W. R., Swelling and gelatinization of cereal starches .2. Waxy rice starches. *Cereal Chem* **1990**, *67*, 558-563.

62. Tester, R. F.; Morrison, W. R., Swelling and gelatinization of cereal starches .3. Some properties of waxy and normal nonwaxy barley starches. *Cereal Chem* **1992**, *69*, 654-658.

63. Morrison, W. R.; Tester, R. F.; Snape, C. E.; Law, R.; Gidley, M. J., Swelling and gelatinization of cereal starches .4. Some effects of lipid-complexed amylose and free amylose in waxy and normal barley starches. *Cereal Chem* **1993**, *70*, 385-391.

64. Blazek, J.; Gilbert, E. P.; Copeland, L., Effects of monoglycerides on pasting properties of wheat starch after repeated heating and cooling. *J Cereal Sci* **2011**, *54*, 151-159.

65. Donovan, J. W., Phase transitions of the starch-water system. *Biopolymers* **1979**, *18*, 263-275.

66. Cameron, R. E.; Donald, A. M., A small-angle X-ray scattering study of the absorption of water into the starch granule. *Carbohydr Res* **1993**, *244*, 225-236.

67. Jenkins, P. J.; Donald, A. M., Gelatinisation of starch: A combined SAXS/WAXS/DSC and SANS study. *Carbohydr Res* **1998**, *308*, 133-147.

68. Donald, A., Understanding starch structure and functionality. *Eliassion AC Starch in food: structure, function and applications* **2004**, 156-184.

69. Gidley, M. J., Molecular mechanisms underlying amylose aggregation and gelation. *Macromolecules* **1989**, *22*, 351-358.

70. Fredriksson, H.; Silverio, J.; Andersson, R.; Eliasson, A. C.; Aman, P., The influence of amylose and amylopectin characteristics on gelatinization and retrogradation properties of different starches. *Carbohydr Polym* **1998**, *35*, 119-134.

71. Miles, M. J.; Morris, V. J.; Orford, P. D.; Ring, S. G., The roles of amylose and amylopectin in the gelation and retrogradation of starch. *Carbohydr Res* **1985**, *135*, 271-281.

72. Russell, P. L., The aging of gels from starches of different amylose amylopectin content studied by differential scanning calorimetry. *J Cereal Sci* **1987**, *6*, 147-158.

73. Ai, Y. F.; Hasjim, J.; Jane, J. L., Effects of lipids on enzymatic hydrolysis and physical properties of starch. *Carbohydr Polym* **2013**, *92*, 120-127.

74. Zhang, B.; Huang, Q.; Luo, F. X.; Fu, X., Structural characterizations and digestibility of debranched high-amylose maize starch complexed with lauric acid. *Food Hydrocolloids* **2012**, *28*, 174-181.

75. Hasjim, J.; Lee, S.-O.; Hendrich, S.; Setiawan, S.; Ai, Y.; Jane, J.-l., Characterization of a novel resistant-starch and its effects on postprandial plasma-glucose and insulin responses. *Cereal Chem* **2010**, *87*, 257-262.

76. Dhital, S.; Warren, F. J.; Butterworth, P. J.; Ellis, P. R.; Gidley, M. J., Mechanisms of starch digestion by alpha-amylase: Structural basis for kinetic properties. *Critical Reviews in Food Science and Nutrition* **2014**, Accepted for publication

77. Dhital, S.; Warren, F. J.; Zhang, B.; Gidley, M. J., Amylase binding to starch granules under hydrolysing and non-hydrolysing conditions. *Carbohydr Polym* **2014**, *113*, 97-107.
78. Bai, Y. J.; Cai, L. M.; Doutch, J.; Gilbert, E. P.; Shi, Y. C., Structural changes from native waxy maize starch granules to cold-water-soluble pyrodextrin during thermal treatment. *J Agric Food Chem* **2014**, *62*, 4186-4194.
79. Zhang, B.; Dhital, S.; Flanagan, B. M.; Gidley, M. J., Mechanism for starch granule ghost formation deduced from structural and enzyme digestion properties. *J Agric Food Chem* **2014**, *62*, 760-771.
80. Zhang, B.; Huang, Q.; Luo, F. X.; Fu, X.; Jiang, H. X.; Jane, J. L., Effects of octenylsuccinylation on the structure and properties of high-amylose maize starch. *Carbohydr Polym* **2011**, *84*, 1276-1281.
81. Ao, Z.; Simsek, S.; Zhang, G.; Venkatachalam, M.; Reuhs, B. L.; Hamaker, B. R., Starch with a slow digestion property produced by altering its chain length, branch density, and crystalline structure. *J Agric Food Chem* **2007**, *55*, 4540-4547.
82. Parchure, A. A.; Kulkarni, P. R., Effect of food processing treatments on generation of resistant starch. *Int J Food Sci Nutr* **1997**, *48*, 257-260.
83. Singh, J.; Dartois, A.; Kaur, L., Starch digestibility in food matrix: a review. *Trends Food Sci Technol* **2010**, *21*, 168-180.
84. Oates, C. G., Towards an understanding of starch granule structure and hydrolysis. *Trends Food Sci Technol* **1997**, *8*, 375-382.
85. Thompson, D. B., Strategies for the manufacture of resistant starch. *Trends Food Sci Technol* **2000**, *11*, 245-253.
86. Champ, M. M. J., Physiological aspects of resistant starch and in vivo measurements. *J Aoac Int* **2004**, *87*, 749-755.
87. Andersson, H., The ileostomy model for the study of carbohydrate digestion and carbohydrate effects on sterol excretion in man. *Eur J Clin Nutr* **1992**, *46*, S69-S76.
88. Englyst, H. N.; Cummings, J. H., Digestion of the polysaccharides of some cereal foods in the human small-intestine. *Am J Clin Nutr* **1985**, *42*, 778-787.
89. Gidley, M. J., Hydrocolloids in the digestive tract and related health implications. *Curr Opin Colloid In* **2013**, *18*, 371-378.
90. Robyt, J. F.; French, D., Multiple attack hypothesis of alpha-amylase action - Action of porcine pancreatic human salivary and Aspergillus Oryzae alpha-amylases. *Arch Biochem Biophys* **1967**, *122*, 8-&.
91. Gilles, C.; Astier, J. P.; MarchisMouren, G.; Cambillau, C.; Payan, F., Crystal structure of pig pancreatic alpha-amylase isoenzyme II, in complex with the carbohydrate inhibitor acarbose. *Eur J Biochem* **1996**, *238*, 561-569.

92. Ramasubbu, N.; Paloth, V.; Luo, Y. G.; Brayer, G. D.; Levine, M. J., Structure of human salivary alpha-amylase at 1.6 angstrom resolution: Implications for its role in the oral cavity. *Acta Crystallogr D* **1996**, *52*, 435-446.

93. Buisson, G.; Duee, E.; Haser, R.; Payan, F., Three dimensional structure of porcine pancreatic alpha-amylase at 2.9 a resolution. Role of calcium in structure and activity. *Embo J* **1987**, *6*, 3909-3916.

94. Holm, L.; Koivula, A. K.; Lehtovaara, P. M.; Hemminki, A.; Knowles, J. K. C., Random mutagenesis used to probe the structure and function of Bacillus-Stearothermophilus alpha-amylase. *Protein Eng* **1990**, *3*, 181-191.

95. Hizukuri, S., *Starch: Analytical aspects*. CRC Press: 2006; Vol. 74, p 347.

96. Robyt, J. F.; French, D., Action pattern of porcine pancreatic alpha-amylase in relationship to substrate binding site of enzyme. *J Biol Chem* **1970**, *245*, 3917-3927.

97. Kandra, L.; Gyemant, G., Examination of the active sites of human salivary alpha-amylase (HSA). *Carbohydr Res* **2000**, *329*, 579-585.

98. Robyt, J. F., Enzymes in the hydrolysis and synthesis of starch. In *Starch Chemisry and Technology (Second Edition)*, Whistler, R. L.; BeMiller, J. N.; Paschall, E. F., Eds. Academic Press, Inc: 1986; pp 87-123.

99. Abdullah, M.; French, D.; Robyt, J. F., Multiple attack by alpha-amylases. *Arch Biochem Biophys* **1966**, *114*, 595-563.

100. Weill, C. E.; Burch, R. J.; Vandyk, J. W., An alpha-amyloglucosidase that produces beta-glucose. *Cereal Chem* **1954**, *31*, 150-158.

101. Norouzian, D.; Akbarzadeh, A.; Scharer, J. M.; Young, M. M., Fungal glucoamylases. *Biotechnol Adv* **2006**, *24*, 80-85.

102. Takahashi, T.; Kato, K.; Ikegami, Y.; Irie, M., Different behavior towards raw starch of 3 forms of glucoamylase from a Rhizopus Sp. *J Biochem-Tokyo* **1985**, *98*, 663-671.

103. Morris, V. J.; Gunning, A. P.; Faulds, C. B.; Williamson, G.; Svensson, B., AFM images of complexes between amylose and Aspergillus niger glucoamylase mutants, native, and mutant starch binding domains: A model for the action of glucoamylase. *Starch-Starke* **2005**, *57*, 1-7.

104. Sorimachi, K.; LeGalCoeffet, M. F.; Williamson, G.; Archer, D. B.; Williamson, M. P., Solution structure of the granular starch binding domain of Aspergillus niger glucoamylase bound to beta-cyclodextrin. *Structure* **1997**, *5*, 647-661.

105. Swanson, S. J.; Emery, A.; Lim, H. C., Kinetics of maltose hydrolysis by glucoamylase. *Biotechnol Bioeng* **1977**, *19*, 1715-1718.

106. Hiromi, K.; Nitta, Y.; Numata, C.; Ono, S., Subsite affinities of glucoamylase: Examination of validity of subsite theory. *Biochim Biophys Acta* **1973**, *302*, 362-375.

107. Robyt, J. F., Enzymes and their action on starch. In *Starch chemistry and technology (Third edition)*, BeMiller, J. N.; Whistler, R. L., Eds. Academic press: 2009; pp 237-292.
108. Dhital, S.; Lin, A. H. M.; Hamaker, B. R.; Gidley, M. J.; Muniandy, A., Mammalian mucosal alpha-glucosidases coordinate with alpha-amylase in the initial starch hydrolysis stage to have a role in starch digestion beyond glucogenesis. *PLoS ONE* **2013**, *8*, e62546.
109. Lin, A. H. M.; Nichols, B. L.; Quezada-Calvillo, R.; Avery, S. E.; Sim, L.; Rose, D. R.; Naim, H. Y.; Hamaker, B. R., Unexpected high digestion rate of cooked starch by the Ct-maltase-glucoamylase small intestine mucosal alpha-glucosidase subunit. *PLoS ONE* **2012**, *7*.
110. Dhital, S.; Shrestha, A. K.; Gidley, M. J., Relationship between granule size and in vitro digestibility of maize and potato starches. *Carbohydr Polym* **2010**, *82*, 480-488.
111. Al-Rabadi, G. J.; Torley, P. J.; Williams, B. A.; Bryden, W. L.; Gidley, M. J., Effect of extrusion temperature and pre-extrusion particle size on starch digestion kinetics in barley and sorghum grain extrudates. *Animal Feed Science and Technology* **2011**, *168*, 267-279.
112. Englyst, H. N.; Kingman, S. M.; Hudson, G. J.; Cummings, J. H., Measurement of resistant starch in vitro and in vivo. *British Journal of Nutrition* **1996**, *75*, 749-755.
113. Menten, L.; Michaelis, M. I., Die kinetik der invertinwirkung. *Biochemistry-Us* **1913**, *49*, 333–369.
114. Butterworth, P. J.; Warren, F. J.; Ellis, P. R., Human alpha-amylase and starch digestion: An interesting marriage. *Starch/Starke* **2011**, *63*, 395-405.
115. Butterworth, P. J.; Warren, F. J.; Grassby, T.; Patel, H.; Ellis, P. R., Analysis of starch amylolysis using plots for first-order kinetics. *Carbohydr Polym* **2012**, *87*, 2189-2197.
116. Goni, I.; Garcia-Alonso, A.; Saura-Calixto, F., A starch hydrolysis procedure to estimate glycemic index. *Nutr Res* **1997**, *17*, 427-437.
117. Warren, F. J.; Zhang, B.; Waltzer, G.; Gidley, M. J.; Dhital, S., The interplay of α-amylase and amyloglucosidase activities on the digestion of starch in in vitro enzymic systems. *Carbohydr Polym* **2014**, Accepted for publication.
118. Warren, F. J.; Butterworth, P. J.; Ellis, P. R., Studies of the effect of maltose on the direct binding of porcine pancreatic alpha-amylase to maize starch. *Carbohydr Res* **2012**, *358*, 67-71.
119. Lopez-Rubio, A.; Flanagan, B. M.; Shrestha, A. K.; Gidley, M. J.; Gilbert, E. P., Molecular rearrangement of starch during in vitro digestion: Toward a better understanding of enzyme resistant starch formation in processed starches. *Biomacromolecules* **2008**, *9*, 1951-1958.
120. Cheetham, N. W. H.; Tao, L. P., Variation in crystalline type with amylose content in maize starch granules: an X-ray powder diffraction study. *Carbohydr Polym* **1998**, *36*, 277-284.

121. Ring, S. G.; Lanson, K. J.; Morris, V. J., Static and dynamic light-scattering studies of amylose aolutions. *Macromolecules* **1985**, *18*, 182-188.

122. Gidley, M. J.; Cooke, D.; Darke, A. H.; Hoffmann, R. A.; Russell, A. L.; Greenwell, P., Molecular order and structure in enzyme-resistant retrograded starch. *Carbohydr Polym* **1995**, *28*, 23-31.

123. Berry, C. S., Resistant starch - Formation and measurement of starch that survives exhaustive digestion with amylolytic enzymes during the determination of dietary fiber. *J Cereal Sci* **1986**, *4*, 301-314.

124. Eerlingen, R. C.; Delcour, J. A., Formation, analysis, structure and properties of type-III enzyme resistant starch. *J Cereal Sci* **1995**, *22*, 129-138.

125. Eerlingen, R. C.; Jacobs, H.; Delcour, J. A., Enzyme-resistant starch .5. Effect of retrogradation of waxy maize starch on enzyme susceptibility. *Cereal Chem* **1994**, *71*, 351-355.

126. Eerlingen, R. C.; Deceuninck, M.; Delcour, J. A., Enzyme-resistant starch .2. Influence of amylose chain-length on resistant starch formation. *Cereal Chem* **1993**, *70*, 345-350.

127. Leeman, A. M.; Karlsson, M. E.; Eliasson, A. C.; Bjorck, I. M. E., Resistant starch formation in temperature treated potato starches varying in amylose/amylopectin ratio. *Carbohydr Polym* **2006**, *65*, 306-313.

128. Cai, L.; Shi, Y.-C., Structure and digestibility of crystalline short-chain amylose from debranched waxy wheat, waxy maize, and waxy potato starches. *Carbohydr Polym* **2010**, *79*, 1117-1123.

129. Colonna, P.; Leloup, V.; Buleon, A., Limiting factors of starch hydrolysis. *Eur J Clin Nutr* **1992**, *46*, S17-S32.

130. Eerlingen, R. C.; Crombez, M.; Delcour, J. A., Enzyme-resistant starch .1. Quantitative and qualitative influence of incubation-time and temperature of autoclaved starch on resistant starch formation. *Cereal Chem* **1993**, *70*, 339-344.

131. Slade, L.; Levine, H., Recent advances in starch retrogradation. *Industrial polysaccharides: The impact of biotechnology and advanced methodologies* **1987**, 387-430.

132. Gidley, M. J.; Bulpin, P. V., Aggregation of amylose in aqueous systems: The effect of chain-length on phase-behavior and aggregation kinetics. *Macromolecules* **1989**, *22*, 341-346.

133. Gidley, M. J., Factors affecting the crystalline type (A-C) of native starches and model compounds - A rationalisation of observed effects in terms of polymorphic structures. *Carbohydr Res* **1987**, *161*, 301-304.

134. Montesanti, N.; Veronese, G.; Buleon, A.; Escalier, P. C.; Kitamura, S.; Putaux, J. L., A-type crystals from dilute solutions of short amylose chains. *Biomacromolecules* **2010**, *11*, 3049-3058.

135. Burchard, W., Das viskositätsverhalten von amylose in verschiedenen lösungsmitteln. *Die Makromolekulare Chemie* **1963**, *64*, 110-125.

136. Leloup, V. M.; Colonna, P.; Ring, S. G.; Roberts, K.; Wells, B., Microstructure of amylose gels. *Carbohydr Polym* **1992**, *18*, 189-197.

137. Cairns, P.; Sun, L.; Morris, V. J.; Ring, S. G., Physicochemical studies using amylose as an in vitro model for resistant starch. *J Cereal Sci* **1995**, *21*, 37-47.

138. Jane, J. L.; Robyt, J. F., Structure studies of amylose-V complexes and retrograded amylose by acation of alpha-amylases, and a new method for preparing amylodextrins. *Carbohydr Res* **1984**, *132*, 105-118.

139. Zhang, G. Y.; Ao, Z.; Hamaker, B. R., Slow digestion property of native cereal starches. *Biomacromolecules* **2006**, *7*, 3252-3258.

140. Bird, A. R.; Lopez-Rubio, A.; Shrestha, A. K.; Gidley, M. J., Resistant starch in vitro and in vivo: Factors determining yield, structure, and physiological relevance. In *Modern Biopolymer Sciences*, Kasapis, S., Norton, I. T., & Ubbink, J. B. , Ed. Academic Press: London, 2009; pp 449–510.

141. Eliasson, A. C.; Ljunger, G., Interactions between Amylopectin and Lipid Additives during Retrogradation in a Model System. *Journal of the Science of Food and Agriculture* **1988**, *44*, 353-361.

142. Tufvesson, F.; Wahlgren, M.; Eliasson, A. C., Formation of amylose-lipid complexes and effects of temperature treatment. part 2. Fatty acids. *Starch-Starke* **2003**, *55*, 138-149.

143. Tufvesson, F.; Wahlgren, M.; Eliasson, A. C., Formation of amylose-lipid complexes and effects of temperature treatment. Part 1. Monoglycerides. *Starch-Starke* **2003**, *55*, 61-71.

144. Eliasson, A.-C.; Wahlgren, M., Starch-lipid interactions and their relevance in food products. *Starch in food: structure, function, and applications. Woodhead, Cambridge* **2004**, 441-454.

145. Kowblansky, M., Calorimetric investigation of inclusion complexes of amylose with long-chain aliphatic compounds containing different functional groups. *Macromolecules* **1985**, *18*, 1776-1779.

146. Godet, M.; Bouchet, B.; Colonna, P.; Gallant, D.; Buleon, A., Crystalline amylose ‐ fatty acid complexes: Morphology and crystal thickness. *Journal of Food Science* **1996**, *61*, 1196-1201.

147. Galloway, G. I.; Biliaderis, C. G.; Stanley, D. W., Properties and structure of amylose‐glyceryl monostearate complexes formed in solution or on extrusion of wheat flour. *Journal of Food Science* **1989**, *54*, 950-957.
148. Tufvesson, F.; Skrabanja, V.; Björck, I.; Elmståhl, H. L.; Eliasson, A.-C., Digestibility of starch systems containing amylose–glycerol monopalmitin complexes. *Lwt-Food Sci Technol* **2001**, *34*, 131-139.
149. Seneviratne, H.; Biliaderis, C., Action of α-amylases on amylose-lipid complex superstructures. *J Cereal Sci* **1991**, *13*, 129-143.
150. Buleon, A.; Duprat, F.; Booy, F. P.; Chanzy, H., Single-crystals of amylose with a low degree of polymerization. *Carbohydr Polym* **1984**, *4*, 161-173.
151. Jacobs, H.; Delcour, J. A., Hydrothermal modifications of granular starch, with retention of the granular structure: A review. *J Agric Food Chem* **1998**, *46*, 2895-2905.
152. Jacobs, H.; Mischenko, N.; Koch, M. H.; Eerlingen, R. C.; Delcour, J. A.; Reynaers, H., Evaluation of the impact of annealing on gelatinisation at intermediate water content of wheat and potato starches: A differential scanning calorimetry and small angle X-ray scattering study. *Carbohydr Res* **1998**, *306*, 1-10.
153. Tester, R. F.; Debon, S. J. J., Annealing of starch: A review. *Int J Biol Macromol* **2000**, *27*, 1-12.
154. Lan, H.; Hoover, R.; Jayakody, L.; Liu, Q.; Donner, E.; Baga, M.; Asare, E.; Hucl, P.; Chibbar, R., Impact of annealing on the molecular structure and physicochemical properties of normal, waxy and high amylose bread wheat starches. *Food Chem* **2008**, *111*, 663-675.
155. Hoover, R.; Vasanthan, T., The effect of annealing on the physicochemical properties of wheat, oat, potato and lentil starches. *J Food Biochem* **1993**, *17*, 303-325.
156. Brumovsky, J. O.; Thompson, D. B., Production of boiling-stable granular resistant starch by partial acid hydrolysis and hydrothermal treatments of high-amylose maize starch. *Cereal Chem* **2001**, *78*, 680-689.
157. Lauro, M.; Suortti, T.; Autio, K.; Linko, P.; Poutanen, K., Accessibility of barley starch granules to alpha-amylase during different phases of gelatinization. *J Cereal Sci* **1993**, *17*, 125-136.
158. Gunaratne, A.; Hoover, R., Effect of heat–moisture treatment on the structure and physicochemical properties of tuber and root starches. *Carbohydr Polym* **2002**, *49*, 425-437.
159. Zavareze, E. d. R.; Dias, A. R. G., Impact of heat-moisture treatment and annealing in starches: A review. *Carbohydr Polym* **2011**, *83*, 317-328.
160. Lopez-Rubio, A.; Htoon, A.; Gilbert, E. P., Influence of extrusion and digestion on the nanostructure of high-amylose maize starch. *Biomacromolecules* **2007**, *8*, 1564-1572.

161. Hsein-Chih, H. W.; Sarko, A., The double-helical molecular structure of crystalline B-amylose. *Carbohydr Res* **1978**, *61*, 7-25.

162. Hsien-Chih, H. W.; Sarko, A., The double-helical molecular structure of crystalline A-amylose. *Carbohydr Res* **1978**, *61*, 27-40.

163. Imberty, A.; Perez, S., A revisit to the three‐dimensional structure of B‐type starch. *Biopolymers* **1988**, *27*, 1205-1221.

164. Pfannemüller, B., Influence of chain length of short monodisperse amyloses on the formation of A-and B-type X-ray diffraction patterns. *Int J Biol Macromol* **1987**, *9*, 105-108.

165. Faraj, A.; Vasanthan, T.; Hoover, R., The effect of extrusion cooking on resistant starch formation in waxy and regular barley flours. *Food Res Int* **2004**, *37*, 517-525.

166. Shrestha, A. K.; Ng, C. S.; Lopez-Rubio, A.; Blazek, J.; Gilbert, E. P.; Gidley, M. J., Enzyme resistance and structural organization in extruded high amylose maize starch. *Carbohydr Polym* **2010**, *80*, 699-710.

167. Colonna, P.; Barry, J. L.; Cloarec, D.; Bornet, F.; Gouilloud, S.; Galmiche, J. P., Enzymic susceptibility of starch from pasta. *J Cereal Sci* **1990**, *11*, 59-70.

168. Robertson, M. D.; Currie, J. M.; Morgan, L. M.; Jewell, D. P.; Frayn, K. N., Prior short-term consumption of resistant starch enhances postprandial insulin sensitivity in healthy subjects. *Diabetologia* **2003**, *46*, 659-665.

169. Morris, K. L.; Zemel, M. B., Glycemic index, cardiovascular disease, and obesity. *Nutr Rev* **1999**, *57*, 273-276.

170. Blazek, J.; Gilbert, E. P., Effect of enzymatic hydrolysis on native starch granule structure. *Biomacromolecules* **2010**, *11*, 3275-3289.

171. Hasjim, J.; Lavau, G. C.; Gidley, M. J.; Gilbert, R. G., In vivo and in vitro starch digestion: Are current in vitro techniques adequate? *Biomacromolecules* **2010**, *11*, 3600-3608.

172. Tahir, R.; Ellis, P. R.; Butterworth, P. J., The relation of physical properties of native starch granules to the kinetics of amylolysis catalysed by porcine pancreatic alpha-amylase. *Carbohydr Polym* **2010**, *81*, 57-62.

173. Bertoft, E.; Manelius, R., A method for the study of the enzymatic-hydrolysis of starch granules. *Carbohydr Res* **1992**, *227*, 269-283.

174. Dhital, S.; Shrestha, A. K.; Gidley, M. J., Effect of cryo-milling on starches: Functionality and digestibility. *Food Hydrocolloids* **2010**, *24*, 152-163.

175. Zhang, G. Y.; Venkatachalam, M.; Hamaker, B. R., Structural basis for the slow digestion property of native cereal starches. *Biomacromolecules* **2006**, *7*, 3259-3266.

176. Slaughter, S. L.; Ellis, P. R.; Butterworth, P. J., An investigation of the action of porcine pancreatic alpha-amylase on native and gelatinised starches. *Biochim Biophys Acta* **2001**, *1525*, 29-36.

177. Faulks, R. M.; Bailey, A. L., Digestion of cooked starches from different food sources by porcine alpha-amylase. *Food Chem* **1990**, *36*, 191-203.

178. Chung, H. J.; Liu, Q.; Hoover, R., Impact of annealing and heat-moisture treatment on rapidly digestible, slowly digestible and resistant starch levels in native and gelatinized corn, pea and lentil starches. *Carbohydr Polym* **2009**, *75*, 436-447.

179. Debet, M. R.; Gidley, M. J., Why do gelatinized starch granules not dissolve completely? Roles for amylose, protein, and lipid in granule "ghost" integrity. *J Agric Food Chem* **2007**, *55*, 4752-4760.

180. Poutanen, K.; Lauro, M.; Suortti, T.; Autio, K., Partial hydrolysis of gelatinized barley and waxy barley starches by alpha-amylase. *Food Hydrocolloids* **1996**, *10*, 269-275.

181. Wang, S. J.; Copeland, L., Molecular disassembly of starch granules during gelatinization and its effect on starch digestibility: a review. *Food Funct* **2013**, *4*, 1564-1580.

182. Kimura, A.; Robyt, J. F., Reaction of enzymes with starch granules - Kinetics and products of the reaction with glucoamylase. *Carbohydr Res* **1995**, *277*, 87-107.

183. Dona, A. C.; Pages, G.; Gilbert, R. G.; Kuchel, P. W., Starch granule characterization by kinetic analysis of their stages during enzymic hydrolysis: H-1 nuclear magnetic resonance studies. *Carbohydr Polym* **2011**, *83*, 1775-1786.

184. Chiba, S., Molecular mechanism in alpha-glucosidase and glucoamylase. *Biosci Biotechnol Biochem* **1997**, *61*, 1233-1239.

185. Shrestha, A. K.; Blazek, J.; Flanagan, B. M.; Dhital, S.; Larroque, O.; Morell, M.; Gilbert, E. P.; Gidley, M. J., Molecular, mesoscopic and microscopic structure evolution during amylase digestion of maize starch granules *Carbohydr Polym* **2012**, *90*, 23-33.

186. Fujii, M.; Kawamura, Y., Synergistic action of alpha-amylase and glucoamylase on hydrolysis of starch. *Biotechnol Bioeng* **1985**, *27*, 260-265.

187. Lineback, D. R., The starch granule: Organization and properties. *Bakers Dig* **1984**, *58*, 16-21.

188. Fujii, M.; Homma, T.; Taniguchi, M., Synergism of alpha-amylase and glucoamylase on hydrolysis of native starch granules. *Biotechnol Bioeng* **1988**, *32*, 910-915.

189. Brewer, L. R.; Cai, L. M.; Shi, Y. C., Mechanism and enzymatic contribution to in vitro test method of digestion for maize starches differing in amylose content. *J Agric Food Chem* **2012**, *60*, 4379-4387.

190. Fannon, J. E.; Hauber, R. J.; BeMiller, J. N., Surface pores of starch granules. *Cereal Chem* **1992**, *69*, 284-288.

191. Fannon, J. E.; Shull, J. M.; BeMiller, J. N., Interior Channels of Starch Granules. *Cereal Chem* **1993**, *70*, 611-613.

192. Helbert, W.; Schulein, M.; Henrissat, B., Electron microscopic investigation of the diffusion of Bacillus licheniformis alpha-amylase into corn starch granules. *Int J Biol Macromol* **1996**, *19*, 165-169.

193. Hiromi, K.; Ohnishi, M.; Tanaka, A., Subsite structure and ligand-binding mechanism of glucoamylase. *Mol Cell Biochem* **1983**, *51*, 79-95.

194. Atkin, N. J.; Abeysekera, R. M.; Robards, A. W., The events leading to the formation of ghost remnants from the starch granule surface and the contribution of the granule surface to the gelatinization endotherm. *Carbohydr Polym* **1998**, *36*, 193-204.

195. Cooke, D.; Gidley, M. J., Loss of crystalline and molecular order during starch gelatinization: Origin of the enthalpic transition. *Carbohydr Res* **1992**, *227*, 103-112.

196. Cameron, R. E.; Donald, A. M., A small-angle X-ray-scattering study of starch gelatinization in excess and limiting water. *J Polym Sci, Part B: Polym Phys* **1993**, *31*, 1197-1203.

197. Fannon, J. E.; BeMiller, J. N., Structure of corn starch paste and granule remnants revealed by low-temperature scanning electron-microscopy after cryopreparation. *Cereal Chem* **1992**, *69*, 456-460.

198. Zhang, B.; Dhital, S.; Gidley, M. J., Synergistic and antagonistic effects of α-amylase and amyloglucosidase on starch digestion. *Biomacromolecules* **2013**, *12*, 1945-1954.

199. Schirmer, M.; Hochstotter, A.; Jekle, M.; Arendt, E.; Becker, T., Physicochemical and morphological characterization of different starches with variable amylose/amylopectin ratio. *Food Hydrocolloids* **2013**, *32*, 52-63.

200. Nelson, N., A photometric adaptation of the Somogyi method for the determination of glucose. *J Biol Chem* **1944**, *153*, 375-380.

201. Cave, R. A.; Seabrook, S. A.; Gidley, M. J.; Gilbert, R. G., Characterization of starch by size-exclusion chromatography: The limitations imposed by shear scission. *Biomacromolecules* **2009**, *10*, 2245-2253.

202. Clay, P. A.; Gilbert, R. G., Molecular-weight distributions in free-radical polymerizations .1. Model development and implications for data interpretation. *Macromolecules* **1995**, *28*, 552-569.

203. Vilaplana, F.; Hasjim, J.; Gilbert, R. G., Amylose content in starches: Toward optimal definition and validating experimental methods. *Carbohydr Polym* **2012**, *88*, 103-111.

204. Tizzotti, M. J.; Sweedman, M. C.; Tang, D.; Schaefer, C.; Gilbert, R. G., New ^{1}H NMR procedure for the characterization of native and modified food-grade starches. *J Agric Food Chem* **2011**, *59*, 6913-6919.

205. Tan, I.; Flanagan, B. M.; Halley, P. J.; Whittaker, A. K.; Gidley, M. J., A method for estimating the nature and relative proportions of amorphous, single, and double-helical components in starch granules by C-13 CP/MAS NMR. *Biomacromolecules* **2007**, *8*, 885-891.

206. Obanni, M.; BeMiller, J. N., Ghost microstructures of starch from different botanical sources. *Cereal Chem* **1996**, *73*, 333-337.

207. Bowler, P.; Evers, A. D.; Sargent, J., Dehydration artifacts in gelatinized starches. *Starch-Starke* **1987**, *39*, 46-49.

208. Langton, M.; Hermansson, A. M., Microstructural changes in wheat-starch dispersions during heating and cooling. *Food Microstruct* **1989**, *8*, 29-39.

209. Robertson, G. H.; Wong, D. W. S.; Lee, C. C.; Wagschal, K.; Smith, M. R.; Orts, W. J., Native or raw starch digestion: A key step in energy efficient biorefining of grain. *J Agric Food Chem* **2006**, *54*, 353-365.

210. Atkin, N. J.; Abeysekera, R. M.; Cheng, S. L.; Robards, A. W., An experimentally-based predictive model for the separation of amylopectin subunits during starch gelatinization. *Carbohydr Polym* **1998**, *36*, 173-192.

211. Jane, J.-L.; Chen, Y. Y.; Lee, L. F.; McPherson, A. E.; Wong, K. S.; Radosavljevic, M.; Kasemsuwan, T., Effects of amylopectin branch chain length and amylose content on the gelatinization and pasting properties of starch. *Cereal Chem* **1999**, *76*, 629-637.

212. Vilaplana, F.; Gilbert, R. G., Two-dimensional size/branch length distributions of a branched polymer. *Macromolecules* **2010**, *43*, 7321-7329.

213. Witt, T.; Gidley, M. J.; Gilbert, R. G., Starch digestion mechanistic information from the time evolution of molecular size distributions. *J Agric Food Chem* **2010**, *58*, 8444-8452.

214. Cuevas, R. P.; Gilbert, R. G.; Fitzgerald, M. A., Structural differences between hot-water-soluble and hot-water-insoluble fractions of starch in waxy rice (Oryza sativa L.). *Carbohydr Polym* **2010**, *81*, 524-532.

215. Biliaderis, C. G.; Page, C. M.; Maurice, T. J.; Juliano, B. O., Thermal characterization of rice starches: a polymeric approach to phase-transitions of granular starch. *J Agric Food Chem* **1986**, *34*, 6-14.

216. Gidley, M. J.; Bociek, S. M., Molecular organization in starches: A 13C CP/MAS NMR study. *J Am Chem Soc* **1985**, *107*, 7040-7044.

217. Gidley, M. J.; Bociek, S. M., C-13 CP/MAS NMR studies of amylose inclusion complexes, cyclodextrins, and the amorphous phase of starch granules: Relationships between glycosidic linkage conformation and solid-state C-13 chemical-shifts. *J Am Chem Soc* **1988**, *110*, 3820-3829.

218. Veregin, R. P.; Fyfe, C. A.; Marchessault, R. H., C-13 CP/MAS NMR study of the polypivalolactone polymorphs. *Macromolecules* **1986**, *19*, 2379-2383.

219. Horii, F.; Yamamoto, H.; Hirai, A.; Kitamaru, R., Structural study of amylose polymorphs by cross-polarization magic-angle spinning, C-13-NMR spectroscopy. *Carbohydr Res* **1987**, *160*, 29-40.

220. Snape, C. E.; Morrison, W. R.; Maroto-Valer, M. M.; Karkalas, J.; Pethrick, R. A., Solid state C-13 NMR investigation of lipid ligands in V-amylose inclusion complexes. *Carbohydr Polym* **1998**, *36*, 225-237.

221. Steeneken, P. A. M., Rheological properties of aqueous suspensions of swollen starch granules. *Carbohydr Polym* **1989**, *11*, 23-42.

222. Evans, I. D.; Lips, A., Viscoelasticity of gelatinized starch dispersions. *J Texture Stud* **1992**, *23*, 69-86.

223. Lagarrigue, S.; Alvarez, G., The rheology of starch dispersions at high temperatures and high shear rates: a review. *Journal of Food Engineering* **2001**, *50*, 189-202.

224. Stokes, J. R., Rheology of industrially relevant microgels. *Microgel Suspensions: Fundamentals and Applications* **2011**, 327-353.

225. Fisher, L. R.; Carrington, S. P.; Odell, J. A., Deformation mechanics of individual swollen starch granules. In *Starch structure and functionality*, Frazier, P. J.; Donald, A. M.; Richmond, P., Eds. The Royal Society of Chemistry: Cambridge, UK, 1997; pp 105-114.

226. Han, X. Z.; Hamaker, B. R., Association of starch granule proteins with starch ghosts and remnants revealed by confocal laser scanning microscopy. *Cereal Chem* **2002**, *79*, 892-896.

227. Bagley, E. B.; Christianson, D. D., Swelling capacity of starch and its relationship to suspension viscosity - Effect of cooking time, temperature and concentration. *J Texture Stud* **1982**, *13*, 115-126.

228. Desse, M.; Fraiseau, D.; Mitchell, J.; Budtova, T., Individual swollen starch granules under mechanical stress: evidence for deformation and volume loss. *Soft Matter* **2010**, *6*, 363-369.

229. Evans, I. D.; Haisman, D. R., Rheology of gelatinized starch suspensions. *J Texture Stud* **1980**, *10*, 347-370.

230. Bongaerts, J. H. H.; Fourtouni, K.; Stokes, J. R., Soft-tribology: Lubrication in a compliant PDMS-PDMS contact. *Tribol Int* **2007**, *40*, 1531-1542.

231. Selway, N.; Stokes, J. R., Insights into the dynamics of oral lubrication and mouthfeel using soft tribology: Differentiating semi-fluid foods with similar rheology. *Food Res Int* **2013**, *54*, 423-431.

232. Hoover, R.; Ratnayake, W. S., Determination of total amylose content of starch. In R. E. Wrolstad, T. E. Acree, E. A. Decker, M. H. Penner, D. S. Reid, S. J. Schwartz, C. F. Shoemaker, D. Smith, & P. Sporns (Eds.), Current protocols in food analytical chemistry -

Water, protein, enzymes, lipids and carbohydrates. Hoboken: Wiley-Interscience. **2001**, pp. 689-691.

233. Bongaerts, J. H. H.; Rossetti, D.; Stokes, J. R., The lubricating properties of human whole saliva. *Tribol Lett* **2007**, *27*, 277-287.

234. Davies, G. A.; Stokes, J. R., On the gap error in parallel plate rheometry that arises from the presence of air when zeroing the gap. *J Rheol* **2005**, *49*, 919-922.

235. Stokes, J. R.; Boehm, M. W.; Baier, S. K., Oral processing, texture and mouthfeel: From rheology to tribology and beyond. *Curr Opin Colloid In* **2013**, *18*, 349-359.

236. Gabriele, A.; Spyropoulos, F.; Norton, I. T., A conceptual model for fluid gel lubrication. *Soft Matter* **2010**, *6*, 4205-4213.

237. Eliasson, A. C., Viscoelastic behavior during the gelatinization of starch .1. Comparison of wheat, maize, potato and waxy-barley starches. *J Texture Stud* **1986**, *17*, 253-265.

238. Stokes, J. R.; Macakova, L.; Chojnicka-Paszun, A.; de Kruif, C. G.; de Jongh, H. H. J., Lubrication, Adsorption, and Rheology of Aqueous Polysaccharide Solutions. *Langmuir* **2011**, *27*, 3474-3484.

239. Ellis, H. S.; Ring, S. G.; Whittam, M. A., A comparison of the viscous behavior of wheat and maize starch pastes. *J Cereal Sci* **1989**, *10*, 33-44.

240. Rao, M. A.; Okechukwu, P. E.; Da Silva, P. M. S.; Oliveira, J. C., Rheological behavior of heated starch dispersions in excess water: role of starch granule. *Carbohydr Polym* **1997**, *33*, 273-283.

241. Tan, I.; Torley, P. J.; Halley, P. J., Combined rheological and optical investigation of maize, barley and wheat starch gelatinisation. *Carbohydr Polym* **2008**, *72*, 272-286.

242. Farres, I. F.; Douaire, M.; Norton, I. T., Rheology and tribological properties of Ca-alginate fluid gels produced by diffusion-controlled method. *Food Hydrocolloids* **2013**, *32*, 115-122.

243. Nishida, C.; Uauy, R.; Kumanyika, S.; Shetty, P., The joint WHO/FAO expert consultation on diet, nutrition and the prevention of chronic diseases: process, product and policy implications. *Public health nutrition* **2004**, *7*, 245-250.

244. Warren, F. J.; Zhang, B.; Waltzer, G.; Gidley, M. J.; Dhital, S., The interplay of alpha-amylase and amyloglucosidase activities on thedigestion of starch in in vitro enzymic systems. *Carbohydr Polym* **2015**, *117*, 192-200.

245. Zhang, B.; Dhital, S.; Gidley, M. J., Densely packed matrices as rate determining features in starch hydrolysis. *Trends Food Sci Technol* **2014**, Submitted.

246. Lai, L. S.; Kokini, J. L., Physicochemical changes and rheological properties of starch during extrusion. *Biotechnology Progress* **1991**, *7*, 251-266.

247. Liu, W. C.; Halley, P. J.; Gilbert, R. G., Mechanism of degradation of starch, a highly branched polymer, during extrusion. *Macromolecules* **2010**, *43*, 2855-2864.

248. Moretti, R.; Thorson, J. S., A comparison of sugar indicators enables a universal high-throughput sugar-1-phosphate nucleotidyltransferase assay. *Anal Biochem* **2008**, *377*, 251-258.

249. Lopez-Rubio, A.; Flanagan, B. M.; Gilbert, E. P.; Gidley, M. J., A novel approach for calculating starch crystallinity and its correlation with double helix content: A combined XRD and NMR study. *Biopolymers* **2008**, *89*, 761-768.

250. Gilbert, R. G.; Gidley, M. J.; Hill, S.; Kilz, P.; Rolland-Sabate, A.; Stevenson, D. G.; Cave, R. A., Characterizing the size and molecular weight distribution of starch: Why it is important and why it is hard. *Cereal Food World* **2010**, *55*, 139-143.

251. Jiang, H.; Horner, H. T.; Pepper, T. M.; Blanco, M.; Campbell, M.; Jane, J.-l., Formation of elongated starch granules in high-amylose maize. *Carbohydr Polym* **2010**, *80*, 533-538.

252. Xie, F. W.; Flanagan, B. M.; Li, M.; Sangwan, P.; Truss, R. W.; Halley, P. J.; Strounina, E. V.; Whittaker, A. K.; Gidley, M. J.; Dean, K. M.; Shamshina, J. L.; Rogers, R. D.; McNally, T., Characteristics of starch-based films plasticised by glycerol and by the ionic liquid 1-ethyl-3-methylimidazolium acetate: A comparative study. *Carbohydr Polym* **2014**, *111*, 841-848.

253. Godet, M. C.; Buleon, A.; Tran, V.; Colonna, P., Structural features of fatty acid-amylose complexes. *Carbohydr Polym* **1993**, *21*, 91-95.

254. Wang, K.; Hasjim, J.; Wu, A. C.; Henry, R. J.; Gilbert, R. G., Variation in amylose fine structure of starches from different botanical sources. *J Agric Food Chem* **2014**, *62*, 4443-4453.

255. Li, M.; Hasjim, J.; Xie, F. W.; Halley, P. J.; Gilbert, R. G., Shear degradation of molecular, crystalline, and granular structures of starch during extrusion. *Starch-Starke* **2014**, *66*, 595-605.

256. Shrestha, A. K.; Blazek, J.; Flanagan, B. M.; Dhital, S.; Larroque, O.; Morell, M. K.; Gilbert, E. P.; Gidley, M. J., Molecular, mesoscrpic and microscopic tructure evolution during amylase digestion of extruded maize and high-amylose maize starches. *Carbohydr Polym* **2015**, *118*, 224-234.

257. Liao, K. S.; Chen, H. M.; Awad, S.; Yuan, J. P.; Hung, W. S.; Lee, K. R.; Lai, J. Y.; Hu, C. C.; Jean, Y. C., Determination of free-volume properties in polymers without orthopositronium components in positron annihilation lifetime spectroscopy. *Macromolecules* **2011**, *44*, 6818-6826.

258. Ranawana, V.; Clegg, M. E.; Shafat, A.; Henry, C. J., Postmastication digestion factors influence glycemic variability in humans. *Nutr Res* **2011**, *31*, 452-459.

259. Grant, L. A., Effects of starch isolation, drying, and grinding techniques on its gelatinization and retrogradation properties. *Cereal Chem* **1998**, *75*, 590-594.

260. Kayisu, K.; Hood, L. F., Effects of dehydration and storage conditions on the pancreatic alpha-amylase susceptibility of various starches. *Journal of Food Science* **1979**, *44*, 1728-1731.

261. Malumba, P.; Massaux, C.; Deroanne, C.; Masimango, T.; Bera, F., Influence of drying temperature on functional properties of wet-milled starch granules. *Carbohydr Polym* **2009**, *75*, 299-306.

262. Setiawan, S.; Widjaja, H.; Rakphongphairoj, V.; Jane, J. L., Effects of drying conditions of corn kernels and storage at an elevated humidity on starch structures and properties. *J Agric Food Chem* **2010**, *58*, 12260-12267.

263. Whistler, R. L.; Goatley, J. L.; Spencer, W. W., Effect of drying on the physical properties and chemical reactivity of corn starch granules. *Cereal Chem* **1959**, *36*, 84-90.

264. Apinan, S.; Yujiro, I.; Hidefumi, Y.; Takeshi, F.; Myllarinen, P.; Forssell, P.; Poutanen, K., Visual observation of hydrolyzed potato starch granules by alpha-amylase with confocal laser scanning microscopy. *Starch-Starke* **2007**, *59*, 543-548.

265. Whistler, R. L.; Spencer, W. W.; Goatley, J. L.; Nikuni, Z., Effect of drying on the presence of cavities in corn starch granules. *Cereal Chem* **1958**, *35*, 331-336.

266. Dhital, S.; Shelat, K. J.; Shrestha, A. K.; Gidley, M. J., Heterogeneity in maize starch granule internal architecture deduced from diffusion of fluorescent dextran probes. *Carbohydr Polym* **2013**, *93*, 365-373.

267. Dhital, S.; Shrestha, A. K.; Hasjim, J.; Gidley, M. J., Physicochemical and structural properties of maize and potato starches as a function of granule size. *J Agric Food Chem* **2011**, *59*, 10151-10161.

268. vanSoest, J. J. G.; Tournois, H.; deWit, D.; Vliegenthart, J. F. G., Short-range structure in (partially) crystalline potato starch determined with attenuated total reflectance Fourier-transform IR spectroscopy. *Carbohydr Res* **1995**, *279*, 201-214.

269. Waigh, T. A.; Perry, P.; Riekel, C.; Gidley, M. J.; Donald, A. M., Chiral side-chain liquid-crystalline polymeric properties of starch. *Macromolecules* **1998**, *31*, 7980-7984.

270. Cohen, J. S.; Yang, T. C. S., Progress in food dehydration. *Trends Food Sci Technol* **1995**, *6*, 20-25.

271. Huber, K. C.; BeMiller, J. N., Channels of maize and sorghum starch granules. *Carbohydr Polym* **2000**, *41*, 269-276.

272. Huber, K. C.; BeMiller, J. N., Visualization of channels and cavities of corn and sorghum starch granules. *Cereal Chem* **1997**, *74*, 537-541.

273. Payan, F.; Haser, R.; Pierrot, M.; Frey, M.; Astier, J. P.; Abadie, B.; Duee, E.; Buisson, G., 3-Dimensional structure of alpha-amylase from porcine pancreas at 5-A

resolution-active-site location. *Acta Crystallographica Section B: Structural Science* **1980**, *36*, 416-421.

274. Liu, H. S.; Yu, L.; Simon, G.; Dean, K.; Chen, L., Effects of annealing on gelatinization and microstructures of corn starches with different amylose/amylopectin ratios. *Carbohydr Polym* **2009**, *77*, 662-669.

275. Gidley, M. J., Quantification of the structual features of starch polysaccharides by NMR spectroscopy. *Carbohydr Res* **1985**, *139*, 85-93.

276. Ahmed, M.; Lelievre, J., Effect of various drying procedures on the crystallinity of starch isolated from wheat grains. *Starch - Stärke* **1978**, *30*, 78-79.

277. Muhr, A.; Blanshard, J.; Bates, D., The effect of lintnerisation on wheat and potato starch granules. *Carbohydrate Polymers* **1984**, *4*, 399-425.

278. Eliasson, A. C.; Larsson, K.; Miezis, Y., On the possibility of modifying the gelatinization properties of starch by lipid surface coating. *Starch - Stärke* **1981**, *33*, 231-235.

279. Zhang, Z. D.; Gao, W. Y.; Li, X.; Jiang, Q. Q.; Xia, Y. Z.; Wang, H. Y.; Huang, L. Q.; Guo, L. P., Effect of different drying methods on the physicochemical and functional properties of Dioscorea opposita Thunb. starch. *Starch-Starke* **2013**, *65*, 219-226.

280. Liu, H. H.; Chaudhary, D.; Roberts, J.; Weed, R.; Sullivan, J.; Buckman, S., The interaction in sorbitol-plasticized starch bionanocomposites via positron annihilation lifetime spectroscopy and small angle X-ray scattering. *Carbohydr Polym* **2012**, *88*, 1172-1176.

Appendix 1

Supporting information for Chapter 4

Mechanism for Starch Granule Ghost Formation Deduced from Structural and Enzyme Digestion Properties

*Bin Zhang, Sushil Dhital, Bernadine M. Flanagan, and Michael J. Gidley**

Centre for Nutrition and Food Sciences, Queensland Alliance for Agriculture and Food Innovation, The University of Queensland, St. Lucia, Brisbane, QLD 4072, Australia

* Corresponding author.

Phone: +61 7 3365 2145; Fax: +61 7 3365 1177. Email address: m.gidley@uq.edu.au (M. J. Gidley)

A1.1 Methods

A1.1.1 Protein contents and mineral compositions

Protein contents (6.25×N) were determined using a LECO CNS 2000 autoanalyzer (LECO Corp., St. Joseph, MI, USA) following the method of Jung et al.[1] Mineral contents were determined by dry ashing at 550 °C. Mineral compositions of starch samples were analyzed by inductively coupled plasma optical emission spectrometry (Vista Pro ICP-OES, Varian Pty. Ltd., Mulgrave, VIC, Australia) at spectral wavelengths of 422, 766, 279, 588, 213 and 181 nm for calcium, potassium, magnesium, sodium, phosphorus, and sulfur, respectively. Results were expressed as means with standard deviations of duplicate measurements.

A1.1.2 Differential scanning calorimetry

A differential scanning calorimeter (Q2000, TA Instruments, New Castle, USA) with an intra cooler was used to examine the thermal properties of starch samples. Starch samples (~2 mg) were mixed with 20 mg de-ionized water, and hermetically sealed in high-pressure stainless steel pans. The pans were held from 20 to 180 ˚C at a rate of 10 ˚C/min, in a

chamber constantly purged with nitrogen at a flow rate of 40 mL/min. The resultant thermograms were analyzed using TA Instruments Universal Analysis software.

A1.2 Results

Table A1-1. Mineral compositions of starches before and after SDS extraction.

sample	calcium (ppm)	potassium (ppm)	magnesium (ppm)	sodium (ppm)	phosphorus (ppm)	sulfur (ppm)
MS	55±4	46±8	36±1	51±3	155±6	158±57
MS-SDS	78±32	14±1	16±2	260±14	117±10	487±10
PS	270±11	209±19	63±1	75±3	578±3	43±2
PS-SDS	74±2	35±12	19±2	766±11	566±4	675±73

Table A1-2. Compositions and properties of starches before and after SDS extraction.

sample	starch granules		granule ghosts	
	amylose content[a] (%)	protein content (%)	yield (%)	amylose content[a] (%)
MS	23.3±1.0	0.36±0.02	67.1±4.3	8.4±0.6
MS-SDS	ND	0.28±0.02	57.7±5.8	ND
PS	18.3±0.4	0.17±0.01	46.0±1.6	6.7±0.4
PS-SDS	ND	0.11±0.01	53.3±1.9	ND

[a] calculated as the ratio of the area under the curve (AUC) of the debranched SEC distribution curves for the larger branches to the total AUC for all branches.

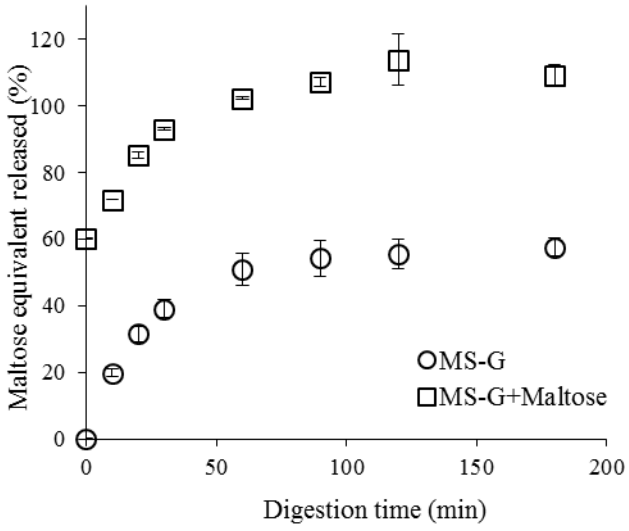

Figure A1-1. The influence of maltose on the kinetics of α-amylase digestion.

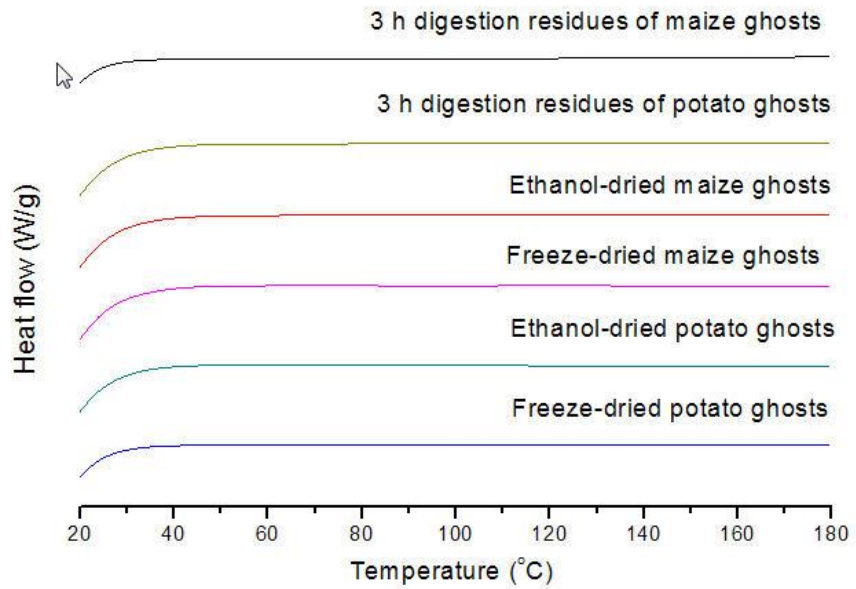

Figure A1-2. DSC thermograms for starch granule ghost in water.

Reference

1. Jung, S.; Rickert, D. A.; Deak, N. A.; Aldin, E. D.; Recknor, J.; Johnson, L. A.; Murphy, P. A., Comparison of Kjeldahl and Dumas methods for determining protein contents of soybean products. *J Am Oil Chem Soc* **2003**, *80*, 1169-1173.

Appendix 2

Supporting information for Chapter 5

Lubrication and Rheology of Swollen Starch Granule Suspensions from Maize and Potato

Bin Zhang[a, b], *Nichola Selway*[c], *Kinnari J. Shelat*[a, b, c], *Sushil Dhital*[a, b], *Jason R. Stokes*[b, c], *and Michael J. Gidley*[a, b, *]

[a] Centre for Nutrition and Food Sciences, Queensland Alliance for Agriculture and Food Innovation, The University of Queensland, St. Lucia, Brisbane, QLD 4072, Australia

[b] ARC Centre of Excellence in Plant Cell Walls, The University of Queensland, St. Lucia, Brisbane, QLD 4072, Australia

[c] School of Chemical Engineering, The University of Queensland, St. Lucia, Brisbane, QLD 4072, Australia

* Corresponding author.

Phone: +61 7 3365 2145; Fax: +61 7 3365 1177. Email address: m.gidley@uq.edu.au (M. J. Gidley)

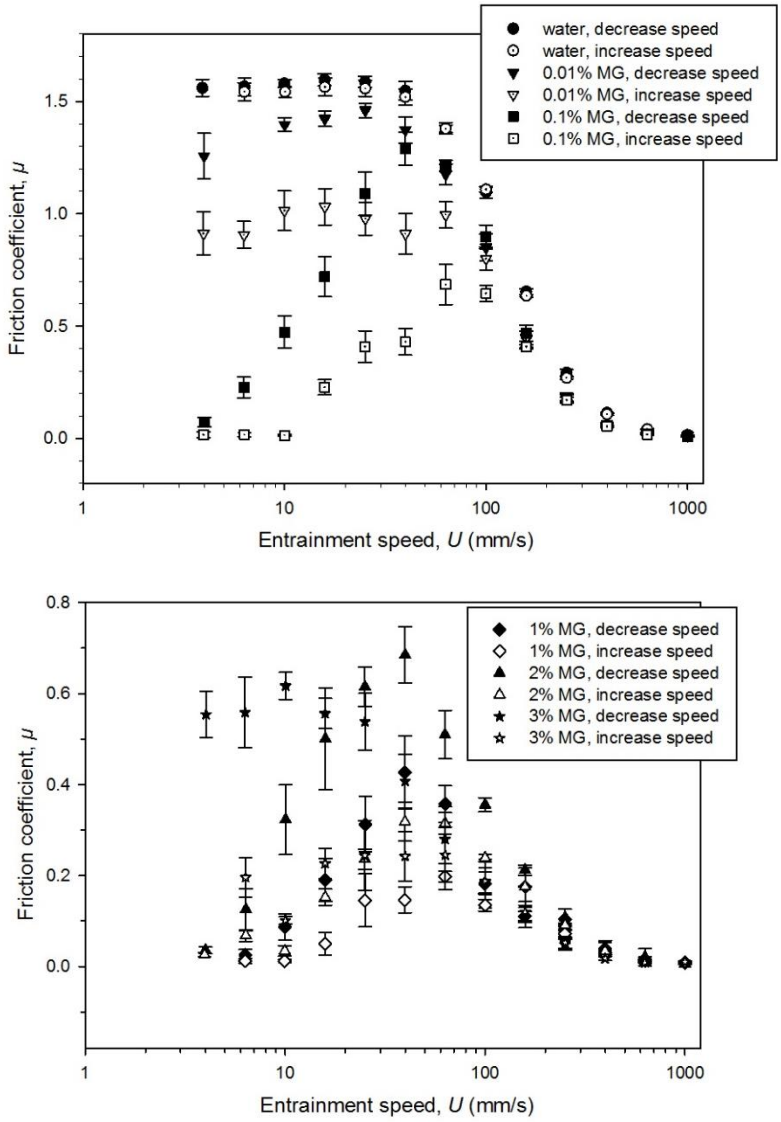

Figure A2-1. Friction coefficient as a function of entrainment speed (decreasing speed, closed symbols; increasing speed, open symbols) for maize ghost suspensions at different concentrations. (MG, maize starch ghost suspension).

Appendix 3

Supporting information for Chapter 6

Extrusion Induced Low-Order Starch Matrices: Enzymic Hydrolysis and Structure

Bin Zhang[†], *Sushil Dhital*[†], *Bernadine M. Flanagan*[†], *Paul Luckman*[‡], *Peter J. Halley*[‡], *and Michael J. Gidley*[†, *]

[†] Centre for Nutrition and Food Sciences, Queensland Alliance for Agriculture and Food Innovation, The University of Queensland, St. Lucia, Brisbane, QLD 4072, Australia

[‡] School of Chemical Engineering, and Australian Institute for Bioengineering and Nanotechnology, The University of Queensland, St. Lucia, Brisbane, QLD 4072, Australia

* Corresponding author.

Phone: +61 7 3365 2145; Fax: +61 7 3365 1177. Email address: m.gidley@uq.edu.au (M. J. Gidley)

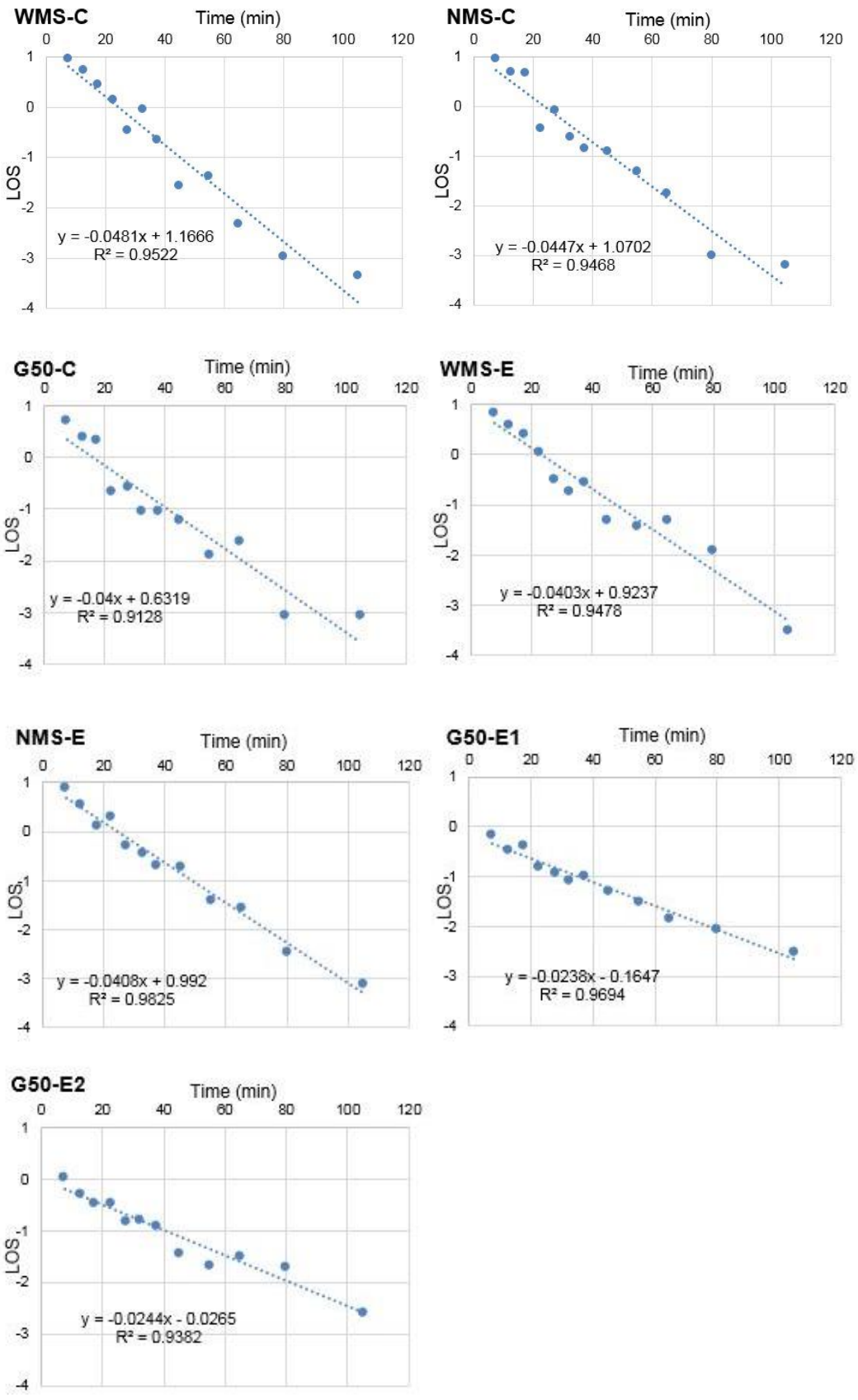

Figure A3-1. LOS plots for starches in cooked and extrudate forms. (WMS, waxy maize starch; NMS, normal maize starch; G50, high-amylose maize starch; E, extrudate; C, cooked)

Table A3-1. Relative yields of size fraction extruded normal and high-amylose maize starches. (NMS, normal maize starch; G50, high-amylose maize starch; E, extrudate)

Sieve fraction size	Relative yield (%)	
	G50-E2	NMS-E
>150 µm	8.7(1.1)	6.0(0.8)
125 – 150 µm	7.3(1.3)	3.6(0.4)
90 – 125 µm	47.3(2.6)	55.7(3.1)
75 – 90 µm	8.6(0.7)	4.6(0.5)
53 – 75 µm	9.8(1.0)	8.1(1.1)
32 – 53 µm	17.8(1.9)	19.9(1.5)
20 – 32 µm	0.5(0.2)	2.1(0.6)

Appendix 4

The Interplay of α-Amylase and Amyloglucosidase Activities on the Digestion of Starch in *In Vitro* Enzymic Systems

(This chapter has been published in Carbohydr. Polym., 2015, 117, 192-200.)

*Frederick J. Warren, Bin Zhang, Gina Waltzer, Michael J. Gidley, and Sushil Dhital**

Centre for Nutrition and Food Sciences, ARC Centre of Excellence in Plant Cell Walls, Queensland Alliance for Agriculture and Food Innovation, The University of Queensland, St Lucia, Brisbane, QLD 4072, Australia

* Corresponding author.

Phone: +61 7 3365 2145; Fax: +61 7 3365 1177. Email address:

m.gidley@uq.edu.au (M. Gidley)

A4.1 Introduction

Complex carbohydrates have been recommended to make up over 50% of the energy intake in the human diet (Nishida, Uauy, Kumanyika & Shetty, 2004). The main source of digestible carbohydrate in the human diet is starch, a complex carbohydrate comprised of two glucose polymers, amylose, an essentially linear polymer of α-(1→4) linked anhydroglucose resides, and amylopectin, a large branched molecule comprising chains of α-(1→4) linked anhydroglucose resides linked by α-(1→6) branch points (Gidley et al., 2010). Following ingestion, the α-(1→4) linkages are hydrolysed by α-amylase to produce predominantly maltose, maltotriose and branched α-limit dextrins, which are then hydrolysed to glucose by the brush border enzymes maltase-glucoamylase and sucrase-isomaltase, to be absorbed into the portal blood (Beeren, Petersen, Bøjstrup, Hindsgaul & Meier, 2013; Butterworth, Warren & Ellis, 2011; Diaz-Sotomayor et al., 2013; Nichols,

Avery, Sen, Swallow, Hahn & Sterchi, 2003; Nichols et al., 2009). Thus, ingestion of starchy foods may result in significant departures in blood glucose levels. It has been known for some time that different starchy foods elicit very different postprandial blood glucose responses (Crapo, Reaven & Olefsky, 1977; Wolever & Jenkins, 1986), and this has been attributed to differences in the rate and extent of digestion between different starch containing foods (Butterworth, Warren & Ellis, 2011; Butterworth, Warren, Grassby, Patel & Ellis, 2012; Dona, Pages, Gilbert & Kuchel, 2010; Holm, Lundquist, Björck, Eliasson & Asp, 1988).

Due to the time and expense of carrying out human feeding trials, and the difficulty of elucidating mechanistic information regarding the differences in digestion rate between different starch containing foods from human studies, a great deal of research effort has been focused on developing *in vitro* models of starch digestion. These may use either pancreatic extracts or purified enzymes to digest starch to sugars (Butterworth, Warren, Grassby, Patel & Ellis, 2012; Dona, Pages, Gilbert & Kuchel, 2010; Englyst, Kingman & Cummings, 1992; Hasjim, Lavau, Gidley & Gilbert, 2010; Slaughter, Ellis & Butterworth, 2001; Woolnough, Bird, Monro & Brennan, 2010). From such experiments the rate and extent of starch digestion may be rapidly and conveniently assessed in the laboratory, and from there it may be possible to suggest mechanisms by which some starchy foods are more slowly digested than others, potentially allowing the rational design of foods with more favourable digestion profiles (Butterworth, Warren, Grassby, Patel & Ellis, 2012; Dhital, Shrestha & Gidley, 2010; Goñi, Garcia-Alonso & Saura-Calixto, 1997; Goñi, Garcia-Diz, Mañas & Saura-Calixto, 1996; Slaughter, Ellis & Butterworth, 2001; Tahir, Ellis & Butterworth, 2010; Zhang, Dhital & Gidley, 2013).

Achieving these aims requires reliable and robust *in vitro* assay techniques, analysed in a logical manner that reflects the kinetics of the enzymes involved. Two main approaches have been taken to mimic the *in vivo* digestion process *in vitro*. The first alternative is to use purified pancreatic α-amylase in isolation at an enzyme activity representative of activities measured in the human small intestine (Slaughter, Ellis & Butterworth, 2001). This approach has not been generally adopted, however, due to the paucity of available studies on enzyme activities in the human small intestine. This makes it hard to accurately determine the activity of α-amylase in the

small intestine, and the surprisingly low α-amylase activities in the studies that do exist can pose technical problems for *in vitro* experiments due to the difficulty in measuring such low enzyme activities (Auricchio, Rubino & Mürset, 1965; Borgström, Dahlqvist, Lundh & Sjövall, 1957; Butterworth, Warren & Ellis, 2011; Layer, Jansen, Cherian, Lamers & Goebell, 1990; Slaughter, Ellis & Butterworth, 2001). A second and more widely adopted alternative, is to use a combination of α-amylase (or pancreatin containing α-amylase activity) with a fungal amyloglucosidase under conditions which are determined to give results after a fixed time of digestion that are in line with the findings from ileostomy studies (Englyst & Cummings, 1985; Englyst, Kingman & Cummings, 1992; Hasjim, Lavau, Gidley & Gilbert, 2010; Muir & O'Dea, 1993). From a practical view point, this has advantages as it provides an assay where a significant proportion of digestion will be completed in an experimentally accessible timeframe, and amyloglucosidase will convert all the products from α-amylase to glucose, so that the glucose oxidase-peroxidase (GOPOD) assay can be used to quantify the products of digestion. The most popular implementation of this approach has been the Englyst assay, in which starch is digested by a combination of α-amylase and amyloglucosidase, and glucose release is determined after 20 min (termed rapidly digestible starch, or RDS), 120 min (termed slowly digestible starch, or SDS) and the remaining undigested starch (termed resistant starch, or RS). Although used extensively, the Englyst assay is a limited approach as it fails to take into account that starch digestion is a 1st order kinetic process, and may be analysed more succinctly with a 1st order kinetic model, as has been discussed elsewhere ((Butterworth, Warren, Grassby, Patel & Ellis, 2012; Dhital, Warren, Butterworth, Ellis & Gidley, 2014; Goñi, Garcia-Alonso & Saura-Calixto, 1997). As the conditions for the Englyst and related assays are calibrated against the results of ileostomy studies, it has been suggested by a number of workers that the results of *in vitro* experiments may be directly extrapolated to the *in vivo* situation (Englyst, Veenstra & Hudson, 1996; Englyst, Englyst, Hudson, Cole & Cummings, 1999; Englyst, Vinoy, Englyst & Lang, 2003; Zhang & Hamaker, 2009). While it appears logical that the faster a starch is digested *in vitro*, the faster it is likely to be digested *in vivo*, great care should be taken when extrapolating from *in vitro* experiments, as the enzyme activities and conditions used are markedly different from those present in the human intestine (Ells, Seal, Kettlitz, Bal & Mathers, 2005; Hasjim, Lavau, Gidley & Gilbert, 2010; Seal et al., 2003).

Amyloglucosidase has been assumed to act predominantly on the products of α-amylase digestion, rapidly converting them to glucose, which has the advantage of removing the inhibitory effects of maltose on amylase activity during long digests (although it should be remembered that maltose is not a very potent inhibitor of α-amylase)(Alkazaz, Desseaux, Marchis-Mouren, Payan, Forest & Santimone, 1996; Seigner, Prodanov & Marchis-Mouren, 1985; Warren, Butterworth & Ellis, 2012). Amyloglucosidase is also capable of hydrolysing α-(1→6) linkages, which α-amylase is unable to attack, removing limit dextrins, and allowing starch digestion to go to completion, as is the case *in vivo* where brush border enzymes undertake the same function (Diaz-Sotomayor et al., 2013; Nichols, Avery, Sen, Swallow, Hahn & Sterchi, 2003; Nichols et al., 2009).

Recently, a number of workers have noted that there is an apparent synergism in the action of α-amylase and amyloglucosidase, particularly when attacking granular starches, as amyloglucosidase is capable of directly attacking starch granules, as well as hydrolysing α-amylase digestion products (Brewer, Cai & Shi, 2012; Kimura & Robyt, 1995; Miao, Zhang, Mu & Jiang, 2011; Ueda, 1981; Zhang, Dhital & Gidley, 2013). This has important consequences for interpreting the results of *in vitro* digestion studies, as varying the concentration of one, or both, enzymes may have unpredictable consequences on the rate and extent of starch digestion. In the present paper, we undertake a systematic study of the effects of varying concentrations of α-amylase and amyloglucosidase over a wide range on the rate and extent of the digestion of granular maize and potato starch. The products of digestion are measured using the GOPOD assay (specific to glucose) and the 4-hydroxybenzoic acid hydrazide (PAHBAH) reducing sugar assay, which is sensitive to not only glucose, but also maltose and maltotriose products of amylolysis (as well as, to a lesser extent, other products e.g. α-limit dextrins). The resultant digestion time courses are analysed by 1st order kinetics and log of slope (LOS) plots (Butterworth, Warren, Grassby, Patel & Ellis, 2012; Edwards, Warren, Milligan, Butterworth & Ellis, 2014) to determine the rate and extent of digestion, and using initial rates, to allow comparison between experiments when the enzyme activity is too low to significantly deplete the substrate, and thus allow determination of a 1st order rate constant. The results obtained will allow targeted design of future starch

digestion experiments through a thorough understanding of the contributions of α-amylase and amyloglucosidase to overall digestion rates.

A4.2 Materials and methods

A4.2.1 Materials

Potato starch (S-4251) (PS) was purchased from Sigma–Aldrich Pty Ltd., Sydney, Australia and regular maize starch (MS) was purchased from Penford Australia Ltd., Sydney, Australia. The average apparent amylose contents of PS and MS, determined by an iodine colorimetric method(Hoover & Ratnayake, 2001), were 36.8% and 27.1% respectively.

Porcine pancreatic α-amylase was obtained from Sigma-Aldrich® (Cat. no. A6255), and had an activity of 49700 U/mL as defined by the manufacturer (confirmed by assay against soluble starch). One unit was defined by the manufacturer as the amount of enzyme required to liberate 1.0 mg of maltose from starch in 3 minutes at pH 6.9 at 20ºC. Fungal amyloglucoside (*A. Niger*) was obtained from Megazyme® (Megazyme E-AMGDF), and had an activity of 3,260 U/mL as defined by the manufacturer (confirmed by assay against soluble starch). One unit was defined by the manufacturer as the amount of enzyme required to release one micromole of glucose from soluble starch per minute (10mg/ml starch; pH 4.5; 40ºC). All other chemicals were obtained from Sigma-Aldrich® and were of the highest quality available.

A4.2.2 Starch digestion

Starch (100 mg) was accurately weighed and added to a 15 mL polypropylene tube. To this was added 9.9 mL of acetate buffer (0.2 M, pH 6, containing 200 mM $CaCl_2$ and 0.5 mM $MgCl_2$). The pH value chosen is a compromise between the pH optima of the two enzymes, and would be expected to result in adequate activity from both enzymes. This was incubated in a water bath at 37 ˚C and 100 µL of a mixture of α-amylase and amyloglucosidase, diluted with buffer, was added to give the appropriate enzyme activities for each assay. Aliquots (200 µL) were taken at time intervals between 20 min and 4 h and immediately placed in boiling water for 5 minutes to inactivate the enzymes (Slaughter, Ellis, & Butterworth, 2001). These

were then centrifuged (2000g, 5 min) to remove any unreacted starch residue and the supernatant analysed for glucose (GOPOD) and reducing sugar (PAHBAH). The GOPOD assay (Thermo Electron Noble Pk, Victoria, Australia. Cat # TR 15104)) was carried out as per the manufactures instructions. The glucose value was multiplied by a factor of 0.9 to convert glucose concentration into starch with results presented as gram per 100 g dry starch. All the measurements were carried out in duplicate and results are expressed as means ± standard deviation of replicates. The PAHBAH reducing assay was carried out as described by Morretti and Thorson (Moretti & Thorson, 2008), using maltose standards. The reducing sugar values were also converted to starch equivalents and the results presented as gram per 100 g dry starch.

A4.2.3 Data analysis

Enzymic starch digestion is a pseudo-first order kinetic process, producing a digestion curve that is initially linear with a constant rate at early time points as the substrate is not significantly depleted (Slaughter, Ellis & Butterworth, 2001). As the reaction proceeds and the substrate is depleted the reaction rate shows an exponential decay that may be fitted using the familiar 1st order equation:

$$C = C_{inf}(1 - e^{-kt})$$

Where C is the amount of starch digested at time t, C_{inf} is the amount of starch digested at the reaction end point, and k is the pseudo-first order rate constant (Butterworth, Warren, Grassby, Patel & Ellis, 2012; Edwards, Warren, Milligan, Butterworth & Ellis, 2014). For the purposes of the present study, the data were analysed in two ways from both the reducing sugar and glucose analyses. Initial rates were obtained from the slope of the initial linear region of digestion curves. This allowed rates to be obtained for all enzyme concentrations, including when there was not enough enzyme activity to significantly deplete the substrate concentration during the time course of the reaction, and thus accurately determine a 1st order rate constant. First order rate constants were obtained using the log of slope (LOS) plot method (Butterworth, Warren, Grassby, Patel & Ellis, 2012), where the data permitted.

A4.3 Results

Digestion rates for potato starch and maize starch were measured at a wide range of α-amylase and amyloglucosidase concentrations. Both starches showed systematic variation in the rate and extent of digestion at different enzyme concentrations. Both α-amylase and amyloglucosidase activities appear to independently enhance the rate of digestion of native starch when used alone or in combination. A simple visual inspection of the digestion curves for both maize and potato starch (Figures A4-1 and A4-2) at a range of α-amylase and amyloglucosidase activities shows that there is an increase in both the rate and extent of starch digestion, when measured both through reducing sugar and glucose assay, with both increasing α-amylase activity at a fixed amyloglucosidase activity, and increasing amyloglucosidase activity at a fixed α-amylase activity. As would be expected, in the absence of amyloglucosidase, α-amylase releases very little glucose from potato or maize starch, the primary products of α-amylase being maltose and maltotriose (Prodanov, Seigner & Marchis-Mouren, 1984; Seigner, Prodanov & Marchis-Mouren, 1987). Thus, the GOPOD assay detects only a very small amount of product, while reductometry indicates significant breakdown of starch when α-amylase alone is present. The addition of even small amounts of amyloglucosidase activity leads to a dramatic increase in glucose release, as would be expected (McCleary, Gibson & Mugford, 1997; Pazur & Ando, 1959; Tester, Qi & Karkalas, 2006). It should be noted that in no case does the starch digestion rate in the absence of amyloglucosidase (measured by reductometry) equal the rate following the addition of amyloglucosidase, and increasing amyloglucosidase activity at a fixed α-amylase activity will always lead to an increasing rate of digestion- clearly indicating that the role for amyloglucosidase during *in vitro* digestion procedures is not simply to convert products of α-amylase digestion to glucose. As indicated in Figure A4-1b and A4-2b, even in the absence of α-amylase, amyloglucosidase will directly attack starch granules to liberate glucose (Kimura & Robyt, 1995; Ueda, 1981). It should be noted in Figures A4-1b and A4-2b that, because maltose was used as a standard for the reducing sugar assay, when a large amount of amyloglucosidase was present, and hence a significant amount of product was released in the form of glucose, the reducing sugar assay apparently over estimates the amount of starch digested, resulting in some values above 100%.

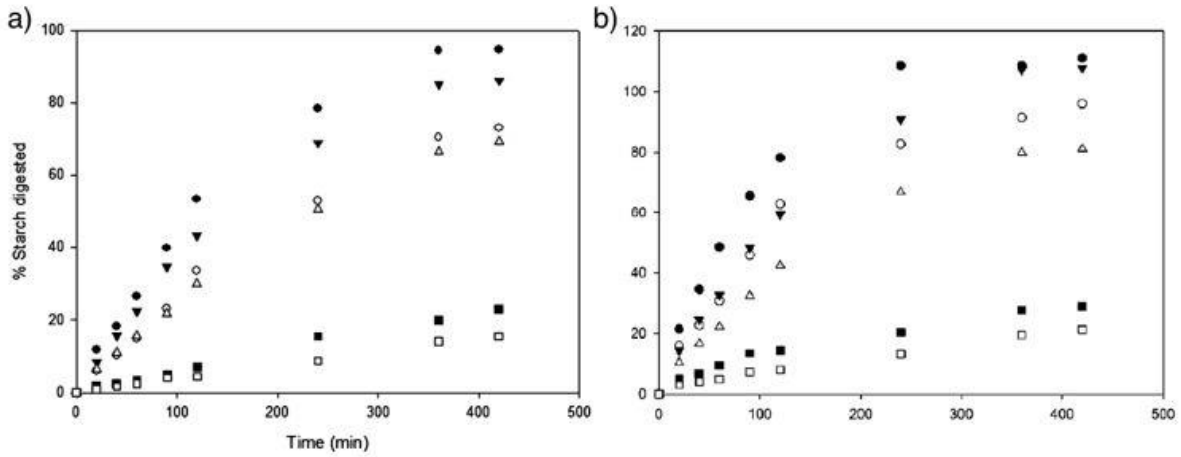

Figure A4-1. Exemplar raw data for maize starch digestion at various enzyme activities. A. Measured by glucose assay. B. Measured by reducing sugar assay. Closed circles, 2 U α-amylase and 1.12 U amyloglucosidase per mL; Open circles, 2 U α-amylase and 0.28 U amyloglucosidase per mL; Closed triangles, 1 U α-amylase and 0.56 U amyloglucosidase per mL; Open triangles, 0.5 U α-amylase and 0.56 U amyloglucosidase per mL; Closed squares, 0 U α-amylase and 1.12 U amyloglucosidase per mL; Open squares, 0 U α-amylase and 0.14 U amyloglucosidase per mL.

At low total enzyme activities, the observed digestion curves are not of a logarithmic form, for example the closed squares and open squares in Figure A4-2 a and A4-2b, i.e. insufficient substrate is converted to product during the time course of the reaction to result in a significant decay in the overall rate of reaction. Under such conditions, the digestion progress curves are essentially linear, and therefore unsuitable for first-order kinetic analysis, severely limiting the amount of information that may be obtained about the progress of the reaction. While a simple reaction velocity may be calculated, as has been done in the present study for comparative purposes, a rate coefficient and reaction end point may not be determined. The quantity of enzyme required to achieve a reaction rate adequate to consume a significant amount of substrate, and subsequently produce a logarithmic digestion curve, was dependant on the substrate used. Maize, a more rapidly digested starch granule, displayed a logarithmic digestion curve at far lower total enzyme concentrations than potato starch granules, a more slowly digested starch, showing a logarithmic curve in all the examples shown in Figure A4-1, whereas in Figure A4-2

the lower enzyme concentrations (closed squares and open squares), are essentially linear.

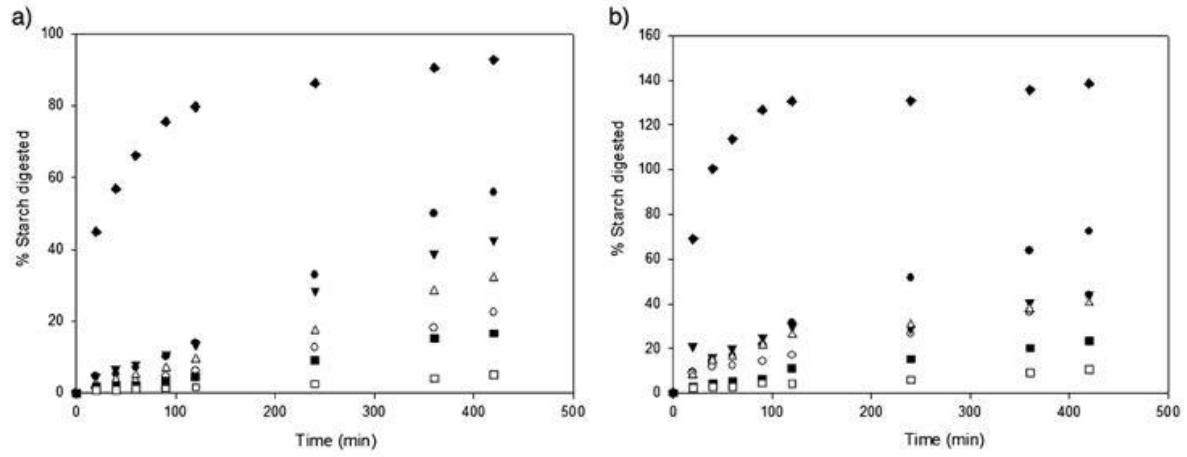

Figure A4-2. Exemplar raw data for potato starch digestion at various enzyme activities. A. Measured by glucose assay. B. Measured by reducing sugar assay. Closed diamonds, 24 U α-amylase, 18 U amyloglucosidase; Closed circles, 2 U α-amylase and 1.12 U amyloglucosidase per mL; Closed triangles, 2 U α-amylase and 0.28 U amyloglucosidase per mL; Open circles, 1 U α-amylase and 0.56 U amyloglucosidase per mL; Open triangles, 0.5 U α-amylase and 0.56 U amyloglucosidase per mL; Closed squares, 0 U α-amylase and 1.12 U amyloglucosidase per mL; Open squares, 0 U α-amylase and 0.14 U amyloglucosidase per mL.

As the enzyme activity is increased, both the rate and extent of digestion is increased. A useful way to visualise this is through the use of surface plots, allowing the effects of both α-amylase and amyloglucosidase on the rate of starch digestion to be viewed simultaneously. Looking first at the data for maize starch (Figure A4-3a and A4-3b), the initial rate (*v*) of digestion in the absence of amyloglucosidase is close to zero when sugar production is measured by glucose assay, as would be expected. Measured by reductometry, the initial rate is low at low α-amylase concentration, but then increases linearly with increasing α-amylase concentration. The initial rate for amyloglucosidase in the absence of α-amylase is uniformly low, measured by either method, indicating the importance of the combined action of α-amylase and amyloglucosidase on starch. There are some minor irregularities

observed in the surface plots, but these are likely to be the result of errors in the data being amplified through the interpolation procedure used to generate the plots.

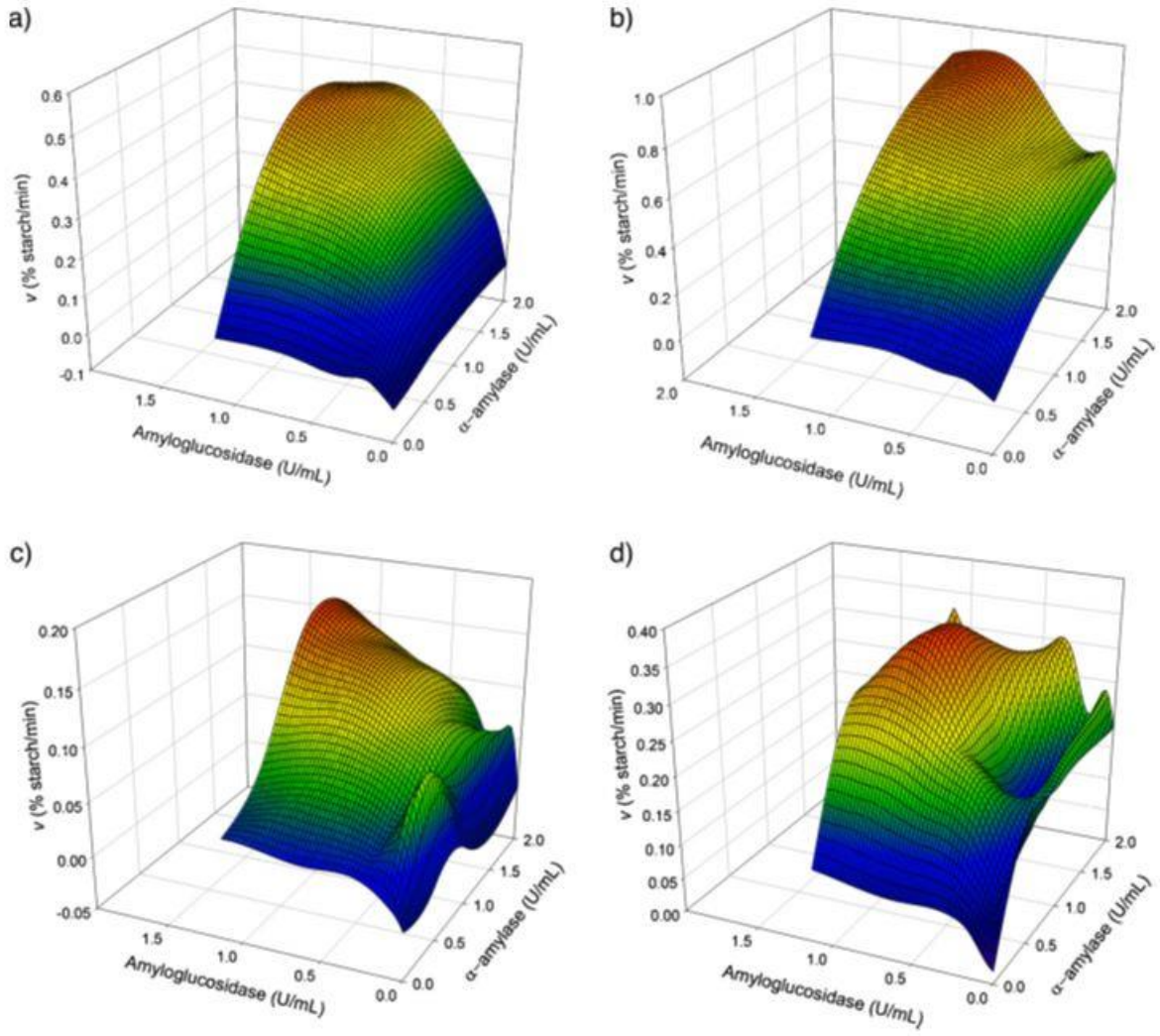

Figure A4-3. Initial rates of starch digestion at various α-amylase and amyloglucosidase activities for starch shown as interpolated surface plots. A. Maize starch measured by glucose assay; B. Maize starch measured by reducing sugar assay; C. Potato starch measured by glucose assay. D. Potato starch measured by reducing sugar assay.

The method used to measure the action of the two enzymes has some influence on the results. Measurement by reductometry results in rates that are dependent equally on the activity of both enzymes. Indeed a plot of *v* against the cumulative activity of both enzymes results in a linear plot (R^2 = 0.79) (Figure A4-4a), indicating that both enzymes have nearly equal roles in the production of reducing sugar, a

surprising result given the differences in enzyme activities between the two enzymes. A similar plot produced for *v* measured by glucose assay (Figure A4-4b) reveals a far more complex relationship. Glucose release is dependent on the action of amyloglucosidase, and amyloglucosidase activity is much faster on the products of α-amylase than acting directly on starch, but this is contingent on having an adequate amyloglucosidase activity (relative to α-amylase) to generate significant amounts of glucose. Thus, a complex relationship results in which at each α-amylase concentration, there is a dramatic increase in rates with increasing amyloglucosidase activity, which saturates at high amyloglucosidase activities. It should be noted that during initial stages of the reaction, from which initial rates were obtained, maltose levels in the absence of amyloglucosidase were not sufficient to have a significant inhibitory action on α-amylase, so increases in initial rate on addition of amyloglucosidase cannot be ascribed to the removal of product inhibition by conversion of maltose to glucose (Warren, Butterworth & Ellis, 2012).

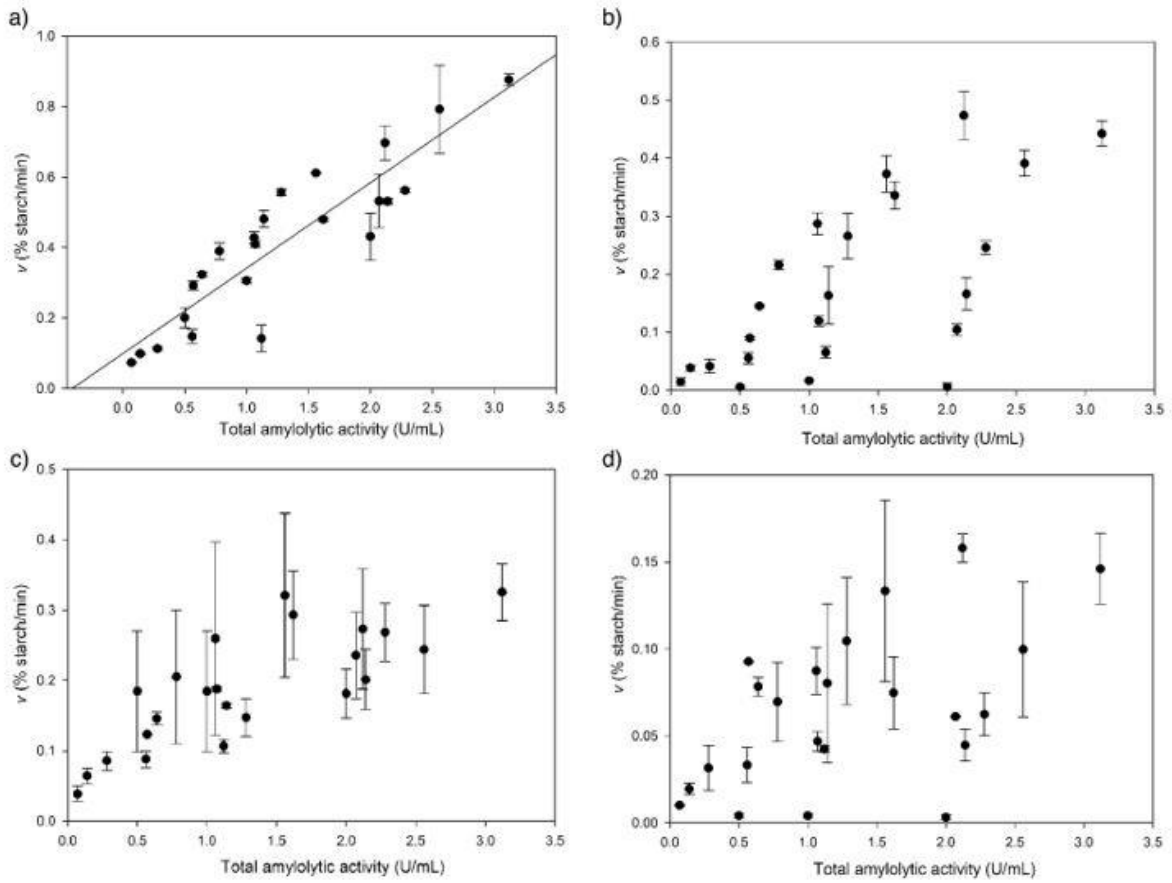

Figure A4-4. Plots of total amylolytic activity (the sum of α-amylase and amyloglucosidase activity) against *v*. Values are shown ±S.D. A. Maize starch measured by reducing sugar assay; B. Maize starch measured by glucose assay; C.

Potato starch measured by reducing sugar assay; D. Potato starch measured by glucose assay.

First order rate constants (*k*) were also obtained from LOS plot analysis of the reaction progress curve (Butterworth, Warren, Grassby, Patel & Ellis, 2012). In this case a single rate constant was used to describe the total reaction curve. It should be noted that a faster rate may have been present, as observed by Butterworth *et al.* (Butterworth, Warren, Grassby, Patel & Ellis, 2012), but for comparative purposes it was found that a single rate constant could adequately describe the reaction curves observed in the present study. For maize starch the reaction rate constants (*k*) were found to follow a very similar pattern, with relation to enzyme activity, as the initial rates (Figure A4-5a and A4-5c). The values for the terminal extent of digestion (C_∞) also vary dependent on enzyme activity. Measured by both GOPOD assay and reductometry, complete digestion of the starch is dependent on adequate levels of activity of both enzymes (Figure A4-5b and A4-5d). Potato starch is significantly more resistant to enzyme hydrolysis than maize starch, as has been well established in the literature (Dhital, Shrestha & Gidley, 2010; Tahir, Ellis & Butterworth, 2010), but what is less well appreciated is how this impacts upon the design of experiments to monitor the digestion of these slow to digest substrates. In the present study it was found that rate constant values could not be determined when the total enzyme activity (α-amylase and amyloglucosidase combined) was below 3 U per mg of starch (when product was measured by GOPOD assay), as there was insufficient enzyme activity present to adequately deplete the starch during the time course of the reaction, resulting in an essentially linear reaction curve (Figure A4-2a and A3-2b). As a consequence, there was not enough data available to interpolate surface plots, similar to those produced for maize starch; complete data for all the values of *k* and C_{inf} that could be obtained are presented in Table A4-S2.

Reaction curves approaching a logarithmic form can be obtained at lower enzyme concentrations when product is measured by reducing sugar assay (e.g. comparing the open squares and closed squares in Figure A4-1a and A4-1b), presumably as with low amyloglucosidase activity significant proportions of the product released is in the form of maltose or longer oligosaccharides, and has not been converted to glucose. While at the same enzyme activity, the rate of hydrolysis of potato starch

was always found to be slower than maize starch (Figures A4-3 and A4-4), it was found that at high enzyme activities, potato starch could be completely hydrolysed, at a rate comparable to that which can be achieved for maize starch (Figure A4-2a and A4-2b, and Table A4-S2). Thus, there is no fraction of potato starch which is intrinsically resistant to hydrolysis, rather it has a structure which at comparable enzyme activities is more slowly digested than maize starch, but the rate and extent of digestion is simply a function of time and enzyme activity.

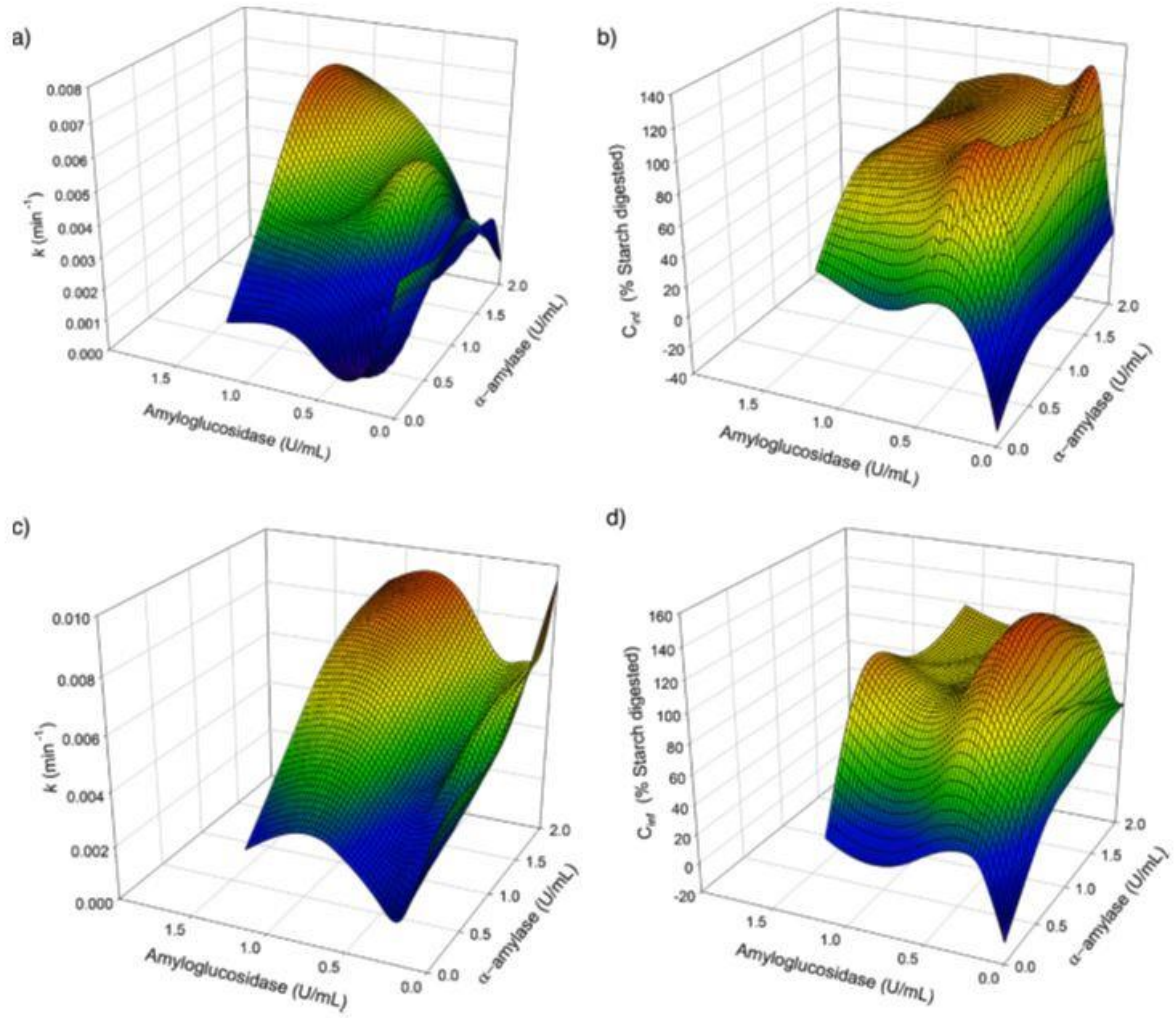

Figure A4-5. LOS plot parameters for maize starch digestion at various α-amylase and amyloglucosidase activities shown as interpolated surface plots. A. *k* measured by glucose assay. B. C_{inf} measured by glucose assay. C. *k* measured by reducing assay. D. C_{inf} measured by reducing assay.

A4.4 Discussion

The data presented in the current work represent a detailed exploration of the effect of varying activities of α-amylase and amyloglucosidase on the hydrolysis rates of two common granular starches, maize and potato. This work builds upon previous literature suggesting that unexpected effects occur when α-amylase and amyloglucosidase are used together, which cannot be explained through the actions of the individual enzymes (Zhang, Dhital & Gidley, 2013). Two methods of determining starch breakdown were used, glucose assay and reducing sugar assay, allowing the simultaneous determination of the total amount of sugar released through starch hydrolysis, and the amount of sugar converted all the way to glucose. Thus, in this study we were able to compare the overall rate of starch breakdown, with the rate of conversion of the starch fully to glucose.

An immediate observation is that the reaction rate (*k* or *v*) is far more dependent on the combined activity of both enzymes when that activity is measured by glucose release (Figure A4-3a and A4-3c). Clearly, as amyloglucosidase is responsible for the production of the majority of glucose, in the absence of amyloglucosidase the reaction rate falls to nearly zero when the glucose assay is used, while the starch is being digested at a significant rate, as measured by reducing sugar assay. The addition of small amounts of amyloglucosidase does not immediately result in the hydrolysis rate measured by both methods becoming equal when the rates are measured by glucose assay, indicating that when the α-amylase activity is greatly in excess of the amyloglucosidase activity, the rate of product produced by α-amylase exceeds the rate at which amyloglucosidase can convert this product and granular starch to glucose (see reaction scheme in Figure A4-6), especially considering that amyloglucosidase is relatively inefficient at converting shorter α-amylase products (maltose and maltotriose) to glucose (Sierks & Svensson, 2000; Zhang, Dhital & Gidley, 2013). The rates (*k*) of hydrolysis only approach similar values for the two measurement methods when the amount of α-amylase and amyloglucosidase were similar, i.e. adequate amyloglucosidase was present to convert all the α-amylase products to glucose (Tables A4-S1 and A4-S2). The initial rates (*v*) were always faster when measured by reducing sugar assay (Figure A4-4), but this can be accounted for as the reducing sugar assay used maltose as a standard, and would therefore overestimate the amount of product produced if some of the product was in the form of glucose.

The amount of starch hydrolysed at the endpoint of the reaction, termed C_∞, also showed dependence on enzyme activity. For neither of the starches was a fraction observed which was fully resistant to enzyme digestion, as has often been suggested to exist, in particular for native potato starch (Åkerberg, Liljeberg, Granfeldt, Drews & Björck, 1998; Planchot, Colonna, Gallant & Bouchet, 1995; Tester, Qi & Karkalas, 2006). Figures A4-5b and A4-5d clearly illustrate that once an adequate activity of both enzymes is used, the amount of maize starch digested at the reaction completion point plateaus at 100% starch digestion, while the digestion rate (Figure A4-5a and A4-5c) continues to increase. A similar pattern was observed for potato starch (Table A4-S2), although significantly more enzyme was required to achieve 100% digestion. It should be noted that when measured by reducing sugar assay the value of C_{inf} is overestimated somewhat as at high amyloglucosidase activities the majority of the maltose is converted to glucose, which was not taken into account in the present calculations for simplicity. These observations have important implications for the concept of resistant starch as measured *in vitro* and *in vivo*. Resistant starch may be most succinctly defined through a physiological description as “starch which avoids digestion in the small intestine, and may be fermented in the large intestine” (Åkerberg, Liljeberg, Granfeldt, Drews & Björck, 1998; Dhital, Warren, Butterworth, Ellis & Gidley, 2014; Zhang & Hamaker, 2009), but resistant starch often has a secondary *in vitro* definition as “starch which is not digested after a given time during *in vitro* digestion” (Englyst, Kingman & Cummings, 1992). The results presented here suggest that this simple *in vitro* definition is inadequate, as native potato granule resistant starch (often termed RS2 (Englyst, Kingman & Cummings, 1992; Sajilata, Singhal & Kulkarni, 2006)) is not completely enzyme resistant, nor is any fraction of it completely enzyme resistant. The fraction of the starch that is resistant to digestion is simply a function of the amount of enzyme used and the digestion time. With analogy to the *in vivo* situation, the resistance of the starch (i.e. the proportion that reaches the large intestine), will be a function of the amylolytic enzyme activity which is present in the small intestine and the time exposed to that enzyme (i.e. small intestinal transit time). Thus, the key determinant from an *in vitro* assay of whether a proportion of a starch will be resistant to digestion *in vivo* is the rate at which the starch is digested under defined conditions of enzyme activity, rather than any reaction endpoint. The more slowly

digested a starch is *in vitro*, the higher the likelihood there is of a fraction of that starch reaching the large intestine *in vivo*, subject to individual variations in intestinal enzyme activities and transit rates. Consequently, the inter- and intra-individual variations in enzyme secretion levels and transit times means that the amount of any given starch that reaches the large intestine will vary for both an individual and populations i.e. physiologically resistant starch levels are intrinsically variable.

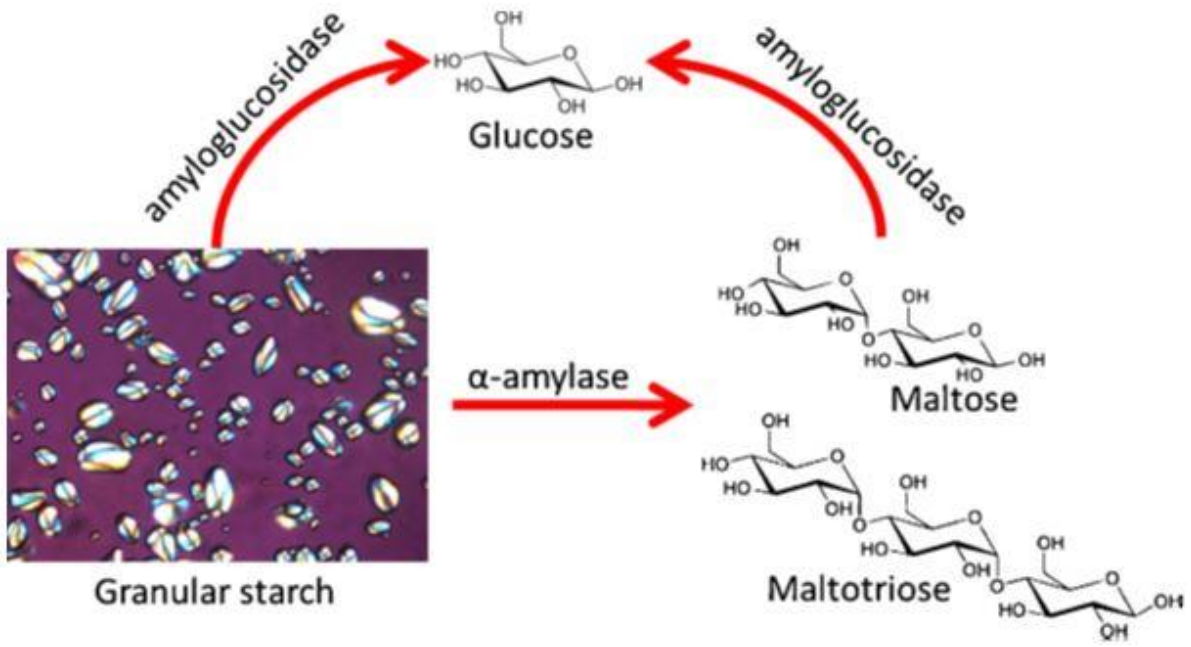

Figure A4-6. Schematic showing a reaction scheme whereby α-amylase acts directly on starch, releasing mainly maltose and maltotriose, while amyloglucosidase acts both releases glucose directly from action on starch, and from action on the products of amylolysis.

A4.5 Conclusions

In the present work, the digestion rate and extent of two starches was measured for a wide range of enzyme activities. There was a large and systematic variation in digestion rate and extent, depending on both the relative activities of the enzymes and the measurement methods used. The data presented is expected to be of use in future studies of *in vitro* starch digestion, through informing the design of experiments to achieve adequate reaction rates necessary to allow first order reaction kinetic analysis. In the present study it was found that a minimum of 2 U/mL of α-amylase and 1.12 U/mL of amyloglucosidase was required to produce curves

that were rapid enough to be analysed by 1st order kinetic methods, using both glucose and reducing sugar assay, and which resulted in a C_{inf} value of 100% of starch being digested.

Furthermore, the results show that native potato starch granules (an archetypal 'resistant' starch), although digested slowly, do not have a fraction which is completely resistant to digestion *in vitro*. Therefore, the endpoint of an *in vitro* enzymic digestion should not be used in isolation to predict an absolute value for resistant starch. The finding that potato starch granules can be completely digested *in vitro* given enough enzyme and time illustrates the likely dependence of *in vivo* resistant starch levels on endogenous enzyme activity and small intestinal passage rate, either or both of which may vary between meals and/or between individuals. *In vitro* assays can be a useful indicator but should not be expected to provide accurate quantitative prediction of *in vivo* resistance levels.

References

Åkerberg, A. K., Liljeberg, H. G., Granfeldt, Y. E., Drews, A. W., & Björck, I. M. (1998). An *in vitro* method, based on chewing, to predict resistant starch content in foods allows parallel determination of potentially available starch and dietary fiber. *The Journal of Nutrition, 128*(3), 651-660.

Alkazaz, M., Desseaux, V., Marchis-Mouren, G., Payan, F., Forest, E., & Santimone, M. (1996). The mechanism of porcine pancreatic α-amylase. Kinetic evidence for two additional carbohydrate-binding sites. *European Journal of Biochemistry/FEBS, 241*(3), 787-796.

Auricchio, S., Rubino, A., & Mürset, G. (1965). Intestinal glycosidase activities in the human embryo, fetus, and newborn. *Pediatrics, 35*(6), 944-954.

Beeren, S. R., Petersen, B. O., Bøjstrup, M., Hindsgaul, O., & Meier, S. (2013). Time-resolved in-situ observation of starch polysaccharide degradation pathways. *ChemBioChem*., 14(18), 2506–2511.

Borgström, B., Dahlqvist, A., Lundh, G., & Sjövall, J. (1957). Studies of intestinal digestion and absorption in the human. *Journal of Clinical Investigation, 36*(10), 1521.

Brewer, L. R., Cai, L., & Shi, Y.-C. (2012). Mechanism and enzymatic contribution to in vitro test method of digestion for maize starches differing in amylose content. *Journal of Agricultural and Food Chemistry, 60*(17), 4379-4387.

Butterworth, P. J., Warren, F. J., & Ellis, P. R. (2011). Human α-amylase and starch digestion: An interesting marriage. *Starch-Stärke, 63*(7), 395-405.

Butterworth, P. J., Warren, F. J., Grassby, T., Patel, H., & Ellis, P. R. (2012). Analysis of starch amylolysis using plots for first-order kinetics. *Carbohydrate Polymers, 87*(3), 2189-2197.

Crapo, P. A., Reaven, G., & Olefsky, J. (1977). Postprandial plasma-glucose and -insulin responses to different complex carbohydrates. *Diabetes, 26*(12), 1178-1183.

Dhital, S., Shrestha, A. K., & Gidley, M. J. (2010). Relationship between granule size and *in vitro* digestibility of maize and potato starches. *Carbohydrate Polymers, 82*(2), 480-488.

Dhital, S., Warren, F. J., Butterworth, P. J., Ellis, P. R., & Gidley, M. J. (2014). Mechanisms of starch digestion by α-amylase–structural basis for kinetic properties. *Critical Reviews in Food Science and Nutrition*. http://dx.doi.org/10.1080/10408398.2014.922043.

Diaz-Sotomayor, M., Quezada-Calvillo, R., Avery, S. E., Chacko, S. K., Yan, L., Lin, A., Ao, Z., Hamaker, B. R., & Nichols, B. L. (2013). Maltase-glucoamylase modulates gluconeogenesis: Sucrase-isomaltase dominates starch digestion glucogenesis. *Journal of Pediatric Gastroenterology and Nutrition, 57*(6), 704–712.

Dona, A. C., Pages, G., Gilbert, R. G., & Kuchel, P. W. (2010). Digestion of starch: *In vivo* and *in vitro* kinetic models used to characterise oligosaccharide or glucose release. *Carbohydrate Polymers, 80*(3), 599-617.

Edwards, C. H., Warren, F., Milligan, P. J., Butterworth, P., & Ellis, P. (2014). A novel method for classifying starch digestion by modelling the amylolysis of plant foods using first-order enzyme kinetic principles. *Food & Function*. http://dx.doi.org/10.1039/C4FO00115J

Ells, L. J., Seal, C. J., Kettlitz, B., Bal, W., & Mathers, J. C. (2005). Postprandial glycaemic, lipaemic and haemostatic responses to ingestion of rapidly and slowly digested starches in healthy young women. *British Journal of Nutrition, 94*(6), 948-955.

Englyst, H. N., & Cummings, J. H. (1985). Digestion of the polysaccharides of some cereal foods in the human small intestine. *The American Journal of Clinical Nutrition, 42*(5), 778-787.

Englyst, H. N., Kingman, S., & Cummings, J. (1992). Classification and measurement of nutritionally important starch fractions. *European Journal of Clinical Nutrition, 46*, S33-50.

Englyst, H. N., Veenstra, J., & Hudson, G. J. (1996). Measurement of rapidly available glucose (RAG) in plant foods: A potential in vitro predictor of the glycaemic response. *British Journal of Nutrition, 75*(3), 327-338.

Englyst, K. N., Englyst, H. N., Hudson, G. J., Cole, T. J., & Cummings, J. H. (1999). Rapidly available glucose in foods: An *in vitro* measurement that reflects the glycemic response. *The American Journal of Clinical Nutrition, 69*(3), 448-454.

Englyst, K. N., Vinoy, S., Englyst, H. N., & Lang, V. (2003). Glycaemic index of cereal products explained by their content of rapidly and slowly available glucose. *British Journal of Nutrition, 89*(3), 329-340.

Gidley, M. J., Hanashiro, I., Hani, N. M., Hill, S. E., Huber, A., Jane, J.-L.,et al. (2010). Reliable measurements of the size distributions of starch molecules in solution: Current dilemmas and recommendations. *Carbohydrate Polymers, 79*(2), 255-261.

Goñi, I., Garcia-Alonso, A., & Saura-Calixto, F. (1997). A starch hydrolysis procedure to estimate glycemic index. *Nutrition Research, 17*(3), 427-437.

Goñi, I., Garcia-Diz, L., Mañas, E., & Saura-Calixto, F. (1996). Analysis of resistant starch: A method for foods and food products. *Food Chemistry, 56*(4), 445-449.

Hasjim, J., Lavau, G. C., Gidley, M. J., & Gilbert, R. G. (2010). *In vivo* and *in vitro* starch digestion: Are current in vitro techniques adequate? *Biomacromolecules, 11*(12), 3600-3608.

Holm, J., Lundquist, I., Björck, I., Eliasson, A., & Asp, N. (1988). Degree of starch gelatinization, digestion rate of starch in vitro, and metabolic response in rats. *The American Journal of Clinical Nutrition, 47*(6), 1010-1016.

Hoover, R., & Ratnayake, W. (2001). Current Protocols in Food Analytical Chemistry. In *Determination of total amylose content of starch*. John Wiley & Sons

Kimura, A., & Robyt, J. F. (1995). Reaction of enzymes with starch granules: Kinetics and products of the reaction with glucoamylase. *Carbohydrate Research, 277*(1), 87-107.

Layer, P., Jansen, J., Cherian, L., Lamers, C., & Goebell, H. (1990). Feedback regulation of human pancreatic secretion. Effects of protease inhibition on duodenal delivery and small intestinal transit of pancreatic enzymes. *Gastroenterology, 98*(5 Pt 1), 1311.

McCleary, B. V., Gibson, T. S., & Mugford, D. C. (1997). Measurement of total starch in cereal products by amyloglucosidase-α-amylase method: Collaborative study. *Journal of AOAC International, 80*(3), 571-579.

Miao, M., Zhang, T., Mu, W., & Jiang, B. (2011). Structural characterizations of waxy maize starch residue following *in vitro* pancreatin and amyloglucosidase synergistic hydrolysis. *Food Hydrocolloids, 25*(2), 214-220.

Moretti, R., & Thorson, J. S. (2008). A comparison of sugar indicators enables a universal high-throughput sugar-1-phosphate nucleotidyltransferase assay. *Analytical Biochemistry, 377*(2), 251-258.

Muir, J. G., & O'Dea, K. (1993). Validation of an in vitro assay for predicting the amount of starch that escapes digestion in the small intestine of humans. *The American Journal of Clinical Nutrition, 57*(4), 540-546.

Nichols, B. L., Avery, S., Sen, P., Swallow, D. M., Hahn, D., & Sterchi, E. (2003). The maltase-glucoamylase gene: Common ancestry to sucrase-isomaltase with complementary starch digestion activities. *Proceedings of the National Academy of Sciences, 100*(3), 1432-1437.

Nichols, B. L., Quezada-Calvillo, R., Robayo-Torres, C. C., Ao, Z., Hamaker, B. R., Butte, N. F., Marini, J., Jahoor, F., & Sterchi, E. E. (2009). Mucosal maltase-glucoamylase plays a crucial role in starch digestion and prandial glucose homeostasis of mice. *The Journal of Nutrition, 139*(4), 684-690.

Nishida, C., Uauy, R., Kumanyika, S., & Shetty, P. (2004). The joint WHO/FAO expert consultation on diet, nutrition and the prevention of chronic diseases: Process, product and policy implications. *Public Health Nutrition, 7*(1A; SPI), 245-250.

Pazur, J. H., & Ando, T. (1959). The action of an amyloglucosidase of *Aspergillus niger* on starch and malto-oligosaccharides. *Journal of Biological Chemistry, 234*(8), 1966-1970.

Planchot, V., Colonna, P., Gallant, D., & Bouchet, B. (1995). Extensive degradation of native starch granules by α-amylase from *aspergillus fumigatus*. *Journal of Cereal Science, 21*(2), 163-171.

Prodanov, E., Seigner, C., & Marchis-Mouren, G. (1984). Subsite profile of the active center of porcine pancreatic α-amylase. Kinetic studies using maltooligosaccharides as substrates. *Biochemical and Biophysical Research Communications, 122*(1), 75-81.

Sajilata, M., Singhal, R. S., & Kulkarni, P. R. (2006). Resistant starch: A review. *Comprehensive Reviews in Food Science and Food Safety, 5*(1), 1-17.

Seal, C. J., Daly, M. E., Thomas, L. C., Bal, W., Birkett, A. M., Jeffcoat, R., & Mathers, J. C. (2003). Postprandial carbohydrate metabolism in healthy subjects and those with type 2 diabetes fed starches with slow and rapid hydrolysis rates determined *in vitro*. *British Journal of Nutrition, 90*(05), 853-864.

Seigner, C., Prodanov, E., & Marchis-Mouren, G. (1987). The determination of subsite binding energies of porcine pancreatic α-amylase by comparing hydrolytic activity towards substrates. *Biochimica et Biophysica Acta (BBA)-Protein Structure and Molecular Enzymology, 913*(2), 200-209.

Seigner, C., Prodanov, E., & Marchis-Mouren, G. (1985). On porcine pancreatic α-amylase action: Kinetic evidence for the binding of two maltooligosaccharide molecules (maltose, maltotriose and *o*-nitrophenylmaltoside) by inhibition studies. *European Journal of Biochemistry, 148*(1), 161-168.

Sierks, M. R., & Svensson, B. (2000). Energetic and mechanistic studies of glucoamylase using molecular recognition of maltose OH groups coupled with site-directed mutagenesis. *Biochemistry, 39*(29), 8585-8592.

Slaughter, S. L., Ellis, P. R., & Butterworth, P. J. (2001). An investigation of the action of porcine pancreatic α-amylase on native and gelatinised starches. *Biochimica et Biophysica Acta (BBA)-General Subjects, 1525*(1), 29-36.

Tahir, R., Ellis, P. R., & Butterworth, P. J. (2010). The relation of physical properties of native starch granules to the kinetics of amylolysis catalysed by porcine pancreatic α-amylase. *Carbohydrate Polymers, 81*(1), 57-62.

Tester, R., Qi, X., & Karkalas, J. (2006). Hydrolysis of native starches with amylases. *Animal Feed Science and Technology, 130*(1), 39-54.

Ueda, S. (1981). Fungal glucoamylases and raw starch digestion. *Trends in Biochemical Sciences, 6*, 89-90.

Warren, F. J., Butterworth, P. J., & Ellis, P. R. (2012). Studies of the effect of maltose on the direct binding of porcine pancreatic α-amylase to maize starch. *Carbohydrate Research*, 358, 67–71.

Wolever, T., & Jenkins, D. (1986). The use of the glycemic index in predicting the blood glucose response to mixed meals. *The American Journal of Clinical Nutrition, 43*(1), 167-172.

Woolnough, J., Bird, A., Monro, J., & Brennan, C. (2010). The effect of a brief salivary α-amylase exposure during chewing on subsequent *in vitro* starch digestion curve profiles. *International Journal of Molecular Sciences, 11*(8), 2780-2790.

Zhang, B., Dhital, S., & Gidley, M. J. (2013). Synergistic and antagonistic effects of α-amylase and amyloglucosidase on starch digestion. *Biomacromolecules*, 14(6), 1945–1954.

Zhang, G., & Hamaker, B. R. (2009). Slowly digestible starch: Concept, mechanism, and proposed extended glycemic index. *Critical Reviews in Food Science and Nutrition, 49*(10), 852-867

Supplementary information for:

The Interplay of α-Amylase and Amyloglucosidase Activities on the Digestion of Starch in *In Vitro* Enzymic Systems

Table A4-S1. Full kinetic parameters and S.D. (standard deviation of duplicates) for maize starch digestion at various activities of α-amylase and amyloglucosidase. N.D. (not determined due to reaction rate being inadequate to produce a logarithmic reaction progress curve).

α-amylase (U/mL)	Amyloglucosidase (U/mL)	Total amylolytic activity (U/mL)	*v* (% Starch digested/min) (Glucose assay)	S.D.	*v* (% Starch digested/min) (Reducing assay)	S.D.	*k* x 10^{-3} (min^{-1}) (Glucose assay)	S.D.	C_{inf} (% starch digested) (Glucose assay)	S.D.	*k* x 10^{-3} (min^{-1}) (Reducing assay)	S.D.	C_{inf} (% starch digested) (Reducing assay)	S.D.
0	0.07	0.07	0.01	0.01	0.07	0.00	N.D.	N.D.	N.D.	N.D.	3.15	1.20	16.23	7.33
0	0.14	0.14	0.04	0.01	0.10	0.00	N.D.	N.D.	N.D.	N.D.	1.9	0.14	35.20	2.23
0	0.28	0.28	0.04	0.01	0.11	0.00	N.D.	N.D.	N.D.	N.D.	2	0.14	46.21	4.47
0	0.56	0.56	0.06	0.01	0.15	0.02	1.55	0.21	35.94	1.83	3.6	1.13	34.24	5.10
0	1.12	1.12	0.07	0.01	0.14	0.04	1.8	0.85	48.14	15.85	2.95	1.48	36.61	5.15
0.5	0	0.5	0.01	0.00	0.20	0.03	3.65	0.49	1.61	0.72	5.05	0.78	36.76	0.82
0.5	0.07	0.57	0.09	0.00	0.29	0.01	1.95	0.49	47.84	11.07	3.5	0.99	76.32	10.68
0.5	0.14	0.64	0.14	0.00	0.32	0.01	2.1	0.57	72.48	17.86	3.45	0.49	85.81	7.51
0.5	0.28	0.78	0.22	0.01	0.39	0.02	2	0.28	111.98	24.74	3.25	0.21	110.65	12.75
0.5	0.56	1.06	0.29	0.02	0.43	0.02	3.1	0.85	104.21	11.95	4.65	0.21	101.99	5.48
0.5	1.12	1.62	0.34	0.02	0.48	0.01	4.1	0.00	90.39	0.08	5.05	0.07	121.77	24.55
1	0	1	0.02	0.00	0.31	0.01	3.8	1.13	2.75	1.75	5.15	0.64	53.48	1.42
1	0.07	1.07	0.12	0.01	0.41	0.01	2.9	1.70	50.71	24.93	4.45	0.78	89.56	12.39
1	0.14	1.14	0.16	0.05	0.48	0.02	2	0.28	98.47	17.60	5.1	0.85	94.38	11.60
1	0.28	1.28	0.27	0.04	0.56	0.01	3.9	0.85	91.84	16.54	4.35	1.34	133.28	22.89
1	0.56	1.56	0.37	0.03	0.61	0.00	4.35	0.78	100.89	13.68	5.8	0.85	118.36	9.88
1	1.12	2.12	0.47	0.04	0.70	0.05	6.5	0.99	92.14	15.45	7.1	0.28	114.98	6.67
2	0	2	0.01	0.01	0.43	0.07	N.D.	N.D.	N.D.	N.D.	9.45	2.05	66.12	6.69
2	0.07	2.07	0.10	0.01	0.53	0.08	2.2	0.71	49.88	7.02	6.85	1.63	70.12	12.32

2	0.14	2.14	0.17	0.03	0.53	0.01	1.85	0.78	101.94	25.46	6.4	1.98	91.66	13.61
2	0.28	2.28	0.25	0.01	0.56	0.01	2.5	0.28	117.21	2.10	6.25	1.48	113.58	23.23
2	0.56	2.56	0.39	0.02	0.79	0.12	4.6	1.41	109.93	19.30	8.15	0.78	110.20	6.55
2	1.12	3.12	0.44	0.02	0.88	0.02	6.4	2.55	100.19	25.91	8.65	0.78	117.83	5.13

Table A4-S2. Full kinetic parameters and S.D. (standard deviation of duplicates) for potato starch digestion at various activities of α-amylase and amyloglucosidase. N.D. (not determined due to reaction rate being inadequate to produce a logarithmic reaction progress curve).

α-amylase (U/mL)	Amyloglucosidase (U/mL)	Total amylolytic activity (U/mL)	*v* (% Starch digested/min) (Glucose assay)	S.D.	*v* (% Starch digested/min) (Reducing assay)	S.D.	*k* x 10^{-3} (min^{-1}) (Glucose assay)	S.D.	C_{inf} (% starch digested) (Glucose assay)	S.D.	*k* x 10^{-3} (min^{-1}) (Reducing assay)	S.D.	C_{inf} (% starch digested) (Reducing assay)	S.D.
0	1.12	1.12	0.04	0.00	0.11	0.01	N.D.	N.D.	N.D.	N.D.	4.75	0.78	32.45	1.40
0	0.56	0.56	0.03	0.01	0.09	0.01	N.D.	N.D.	N.D.	N.D.	5.4	1.70	22.33	0.12
0	0.28	0.28	0.03	0.01	0.09	0.01	N.D.	N.D.	N.D.	N.D.	5.6	1.41	22.47	0.39
0	0.14	0.14	0.02	0.00	0.06	0.01	N.D.	N.D.	N.D.	N.D.	7	3.54	9.26	7.67
0	0.07	0.07	0.01	0.00	0.04	0.01	N.D.	N.D.	N.D.	N.D.	6.45	1.48	3.47	2.72
0.5	1.12	1.62	0.07	0.02	0.29	0.06	N.D.	N.D.	N.D.	N.D.	3.7	0.00	63.98	23.10
0.5	0.56	1.06	0.09	0.01	0.26	0.14	N.D.	N.D.	N.D.	N.D.	4.55	2.33	64.09	11.70
0.5	0.28	0.78	0.07	0.02	0.21	0.09	N.D.	N.D.	N.D.	N.D.	3.8	0.00	60.88	10.66
0.5	0.14	0.64	0.08	0.01	0.15	0.01	N.D.	N.D.	N.D.	N.D.	5.65	2.33	32.35	10.33
0.5	0.07	0.57	0.09	0.00	0.12	0.00	N.D.	N.D.	N.D.	N.D.	6.75	0.35	34.20	2.59
0.5	0	0.5	0.00	0.00	0.18	0.09	N.D.	N.D.	N.D.	N.D.	3.95	1.06	34.08	1.44
1	1.12	2.12	0.16	0.01	0.27	0.09	3.1	0.57	73.97	15.82	2.9	0.28	74.07	6.84
1	0.56	1.56	0.13	0.05	0.32	0.12	1.65	0.21	75.55	6.62	4	1.56	73.11	4.27
1	0.28	1.28	0.10	0.04	0.15	0.03	1.55	0.21	68.18	15.68	2.6	1.70	76.19	40.00
1	0.14	1.14	0.08	0.05	0.16	0.00	N.D.	N.D.	N.D.	N.D.	1.85	0.49	74.49	15.81
1	0.07	1.07	0.05	0.01	0.19	0.00	N.D.	N.D.	N.D.	N.D.	3.95	1.20	43.56	3.98
1	0	1	0.00	0.00	0.18	0.09	N.D.	N.D.	N.D.	N.D.	3.15	1.06	37.21	0.13
2	1.12	3.12	0.15	0.02	0.33	0.04	1.65	0.07	110.03	13.06	2.85	0.92	101.64	23.92
2	0.56	2.56	0.10	0.04	0.24	0.06	1.5	0.42	66.81	20.65	3.15	1.06	85.87	39.50

2	0.28	2.28	0.06	0.01	0.27	0.04	2.2	1.70	41.38	28.38	3.55	0.49	47.19	0.83
2	0.14	2.14	0.04	0.01	0.20	0.04	N.D.	N.D.	N.D.	N.D.	3.2	0.14	35.52	3.73
2	0.07	2.07	0.06	0.00	0.24	0.06	2.35	0.07	20.14	4.43	5.35	0.35	33.84	7.59
2	0	2	0.00	0.00	0.18	0.04	0.45	0.21	14.30	5.35	4.45	0.92	19.03	6.81
4	2.24	6.24	0.30	0.02	0.75	0.12	5.15	1.63	69.66	13.55	6.6	0.71	109.79	26.32
8	4.48	12.48	0.45	0.08	0.88	0.10	6.7	0.57	68.40	3.15	6.85	0.21	96.21	6.73
16	8.96	24.96	0.50	0.09	1.87	0.12	N.D.	N.D.	75.93	15.30	7.85	1.48	70.21	4.12
16	13.5	29.5	1.05	0.04	1.94	0.10	8.35	0.21	76.14	2.07	6.85	2.90	90.00	48.43
24	13.5	37.5	1.15	0.00	2.22	0.01	16.35	3.32	75.53	2.66	9.95	0.21	79.41	23.02
24	18	42	1.40	0.03	2.48	0.04	21.05	1.63	75.78	0.08	26.05	10.39	120.24	15.88

References

Slaughter, S. L., Ellis, P. R., & Butterworth, P. J. (2001). An investigation of the action of porcine pancreatic α-amylase on native and gelatinised starches. *Biochimica et Biophysica Acta (BBA)-General Subjects, 1525*(1), 29-36.

Appendix 5

Amylase Binding to Starch Granules under Hydrolysing and Non-Hydrolysing Conditions

(This chapter has been published in Carbohydr. Polym., 2014, 113, 97-107.)

*Sushil Dhital, Frederick J. Warren, Bin Zhang, and Michael J. Gidley**

Centre for Nutrition and Food Sciences, ARC Centre of Excellence in Plant Cell Walls, Queensland Alliance for Agriculture and Food Innovation, The University of Queensland, St Lucia, Brisbane, QLD 4072, Australia

* Corresponding author.

Phone: +61 7 3365 2145; Fax: +61 7 3365 1177. Email address: m.gidley@uq.edu.au (M. Gidley)

A5.1 Introduction

Starch is a major component in the human diet, as well as a feedstock for a range of industrial processes. The enzymic hydrolysis of starches to smaller oligomers either in living organisms or industrial processes involves the action of α-amylase (AA), an endo-acting enzyme that hydrolyses α-1,4 glycosidic bonds of amylose or amylopectin molecules. The amylolysis rate, extent and pattern of starch granules vary depending upon the barriers the enzyme encounters to access and then bind to the starch granules; or upon structural features of starch granules that prevent catalysis after initial binding. These mechanisms have been recently reviewed (Dhital, Warren, Butterworth, Ellis & Gidley, 2013).

Studies of starch hydrolysis either *in vivo* or *in vitro* inevitably provide an average value from a population of starch granules. Recent evidence, however, indicates that there is a great deal of heterogeneity in the internal architecture (Dhital, Shelat, Shrestha & Gidley, 2013) and physical and chemical structures (Liu et al., 2013) within individual granules. This could in principle affect enzyme binding and ultimately the catalytic process.

Studies of amylase binding to starch granules by solution depletion assay at 0 ^{o}C, found a dependence of enzyme affinity for starch on the surface area, and therefore particle size of starch granules (Schwimmer & Balls, 1949; Walker & Hope, 1963; Warren, Royall, Gaisford, Butterworth & Ellis, 2011). Due to the lack of visualisation of enzyme bound to the granules, it could not be determined from these studies whether the enzyme was uniformly bound to all granules or preferentially bound to individual granules with special granular structures.

The morphological changes of starch granules during α-amylolysis have been investigated by analysis of remnant undigested granules by using various microscopic techniques such as light (bright or polarised field) (Leach & Schoch, 1961), scanning electron (Planchot, Colonna, Gallant & Bouchet, 1995), transmission electron (Gallant, Bouchet & Baldwin, 1997), atomic force (Sujka & Jamroz, 2009) and confocal laser scanning (Apinan et al., 2007; Lynn & Cochrane, 1997) microscopy. The α-amylolysis patterns of starches from different botanical origins have been described, for example, cereal starches are hydrolysed from the inside of granules towards the periphery (endo-corrosion, inside-out or centrifugal hydrolysis pattern); whereas high-amylose and tuber starches are hydrolysed from the surface towards the interior of granules (exo-corrosion, outside-in, or centripetal hydrolysis pattern). These differences in digestion pattern have been inferred to be related to the surface features of granular starch, possibly reflecting the presence of pores and channels within cereal starches that allow amylase to penetrate towards the less organised granule interior compared to the rigid and smooth surface and interior of tuber starches (Huber & BeMiller, 1997; Jane & Shen, 1993; Pan & Jane, 2000). Although these techniques provide general information regarding the hydrolysis pattern, they do not allow the visualisation of enzyme at the sites of hydrolysis.

Previous authors have attempted to visualise the location of enzyme molecules hydrolysing inside granules. Thomson *et al.* (1994) carried out real-time atomic force microscopic (AFM) imaging of wheat starch degradation by α-amylase. The AFM method is, however, limited to observations of the granule surface, and could not directly visualise the location of enzyme molecules. Similarly, Helbert *et al.* (1996) studied the degradation of starch granules with direct localisation of the amylase by immunogold-labelling. The method, however, was unable to quantify the gold labelling efficiency of enzymes. Furthermore, the cross-sectioning of granules for electron microscopic observation may

induce artefacts, for example cracks resembling the channels. Most recently, Tawil *et al*. (2010) used synchrotron ultraviolet fluorescence microscopy to visualize the adsorption and diffusion of amylase during starch degradation. The technique directly visualised the location of protein by imaging the auto-fluorescence from tryptophan present in AA. This method, while a powerful technique, can only visualise one granule at a time, rather than whole populations of granules. Furthermore, fluorescence from AA cannot be discriminated from other granule associated protein components.

Thus different aspects of the mechanism of amylase reaction with starch granules have been proposed as the outcome of observation using different techniques. However, there are a number of questions which remain unresolved:

1. Do enzymes bind uniformly to the granule surface?
2. Do the surface structure and botanical origin of starch granules affect amylase binding?
3. Why is there heterogeneity in starch granule digestion?
4. Is the heterogeneity of starch granules digestion related to enzyme binding?
5. Do surface features such as pores and channels enhance the diffusion of amylase inside the granules?

The present paper aims to address these questions based on the outcomes of direct localisation of fluorescein isothiocyanate (FITC) and tetramethylrhodamine isothiocyanate (TRITC) labelled AA during binding (under both non-hydrolysing (0 ˚C) and hydrolysing (37 ˚C) conditions) of starch granules from different botanical origins using confocal microscopy. The role of surface pores and channels towards amylase action was further studied through visualization of the diffusion of fluorescent dextran probes followed by diffusion of labelled AA into starch granules.

A5.2 Materials and methods

A5.2.1 Materials

Potato starch (PS, Sigma S4251) was purchased from Sigma-Aldrich, Australia. Three types of maize starches: high amylose maize starch (Gelose 80) (HAMS, G80), regular maize starch (MS) and waxy maize starch (WMS) were purchased from Penford Australia Ltd., (Lane Cove, Sydney, Australia).

A5.2.2 α-Amylase labelling with FITC and TRITC

α-Amylase from porcine pancreas (**A6255, Sigma)** was labelled with FITC (F7250, Sigma) and TRITC (87918, Sigma) at 10× molar excess in carbonate buffer (0.1M, pH 9) following the method of The & Feltkamp (1970). The unbound FITC from the conjugate was separated using a desalting column (Sephadex, PD-10) with phosphate buffered saline buffer (PBS, P4417, Sigma, pH 7.2). Following labelling, the enzyme solution was immediately aliquoted and frozen for storage. The enzyme was defrosted immediately prior to use. Freezing did not affect the enzyme activity. The dye: protein (F/P) molar ratio is defined as the ratio of moles of fluorescent moiety to moles of protein in the conjugate (The & Feltkamp, 1970), and was 2.36 and 4.67 for the FITC- and TRITC-AA conjugates respectively. A unit of activity was defined as the enzyme required to liberate 1.0 mg of maltose from starch in 3 minutes at pH 6.9 and 37 ^{o}C, and activity was found to be 1078 and 1713 unit/mg of protein for FITC and TRITC conjugates respectively, compared to 2485 unit/mg of protein for the unlabelled enzyme. The protein concentration of FITC, TRITC and unlabelled enzyme stock solutions was 1.39, 2.56 and 29 mg/mL, respectively.

Michaelis-Menten kinetic parameters for unlabelled and FITC labelled AA were determined using MS as a substrate, using a modification of the method of Tahir *et al.* (2010). Briefly, 4 mL of various concentrations of starch (2.5-25 mg/mL) in PBS buffer were incubated at 37 ˚C in a water bath. At time 0, enzyme was added to a concentration of 1.5 nM. At 0, 4, 8 and 12 min, 300 µL of starch suspension was removed and immediately added to 300 µL of 0.3 M Na_2CO_3 in a microcentrifuge tube to stop the reaction. These samples were then centrifuged at 16,000 g for 5 min to remove unreacted starch, and 300 µL of supernatant removed to a fresh microfuge tube. The reducing sugar content was measured by the *para*-hydroxybenzoic acid hydrazide (PAHBAH) assay (**H9882, Sigma**) as described by Moretti & Thorson (2008) and expressed as maltose reducing sugar equivalents. Kinetic parameters were obtained from non-linear regression analysis using Sigmaplot® 12.5. All kinetic analysis was carried out in triplicate.

A5.2.3 Confocal laser scanning microscopy

Unless otherwise stated, labelled α-amylase (FITC-AA and TRITC-AA) was observed using a confocal microscope (LSM 700, Carls Zeiss, Germany) with a Plan-Apochromat 20× lens (with digital zoom of 2× for maize, waxy maize), with and without differential interference contrast (DIC) using Zen Black 2011 software (Carl Zeiss Version 7.1). Starch images were taken using a frame size of 1024 × 1024 at a scan speed of 8 bit and a pixel

dwell time of 1.58 µs, from an optical slice of 2 µm thickness. All imaging was performed with a 10 mW argon ion laser at 2% power with excitation of 488 nm and 555 nm for FITC and TRITC respectively, either singly or in combination.

A5.2.4 Enzyme binding to starch granules at 0 ˚C

The binding of FITC- and TRITC-AA conjugates to MS and PS granules was monitored at 0 ˚C. A 10 mg/mL starch granule dispersion (2 mL) in sodium acetate buffer (0.2 M, pH 6.0) in 10 mL flat bottom tubes (97×16 mm) was immersed fully in an ice water bath placed above a stirrer plate. The dispersion was equilibrated for 10 min with continuous stirring at 200 rpm to ensure that the starch suspension obtained a temperature of 0 ^{o}C. The binding experiment was carried out in three different combinations. In the first set, 0.8 unit of FITC-AA conjugate per mg of starch was added and 100 µL aliquots were transferred to 1.5mL microfuge tubes after 5, 10 and 20 min of incubation. Subsequently, 0.8 units TRITC-AA conjugate per mg of starch was added to the same incubation tube and aliquots were taken 5, 10 and 20 min after addition of the second enzyme. In a second set, TRITC-AA conjugate was added first followed by FITC-AA conjugate as described for the first set. In a third set, both FITC and TRITC-AA conjugates were added simultaneously. Aliquots were immediately centrifuged at 2000 g for 30 s, supernatants discarded, and the starch pellet observed using the confocal microscope as described in section 2.3.

A5.2.5 Enzyme binding to porous starch

In order to evaluate the roles of surface pores and channels in enzyme binding, porous starch granules were obtained by hydrolysing 3 mL of 1% maize starch suspension with 0.8 units per mg of AA (un-labelled) for 20 min at 37 ˚C. The reaction was halted by the addition of 10 mL of absolute ethanol. The tube was centrifuged at 2000 g for 5 min. The pellet was washed 3 times with deionised water and the volume adjusted to 3 mL with acetate buffer (0.2M, pH 6.0). The tube was then incubated at 0 ˚C for 10 min under the same mixing condition (200 rpm), and the binding experiment was carried out as described in section 2.4.

A5.2.6 Evaluation of the role of pores and channels during initial amylolysis

To evaluate the role of pores (and channels) in the initial stages of amylolysis, 250 µL (2 mg/mL in distilled water) of average molecular weight >65000 Da TRITC dextran (Sigma, T1162) was mixed with 5 mL of 10 mg/mL MS in acetate buffer (0.2 M, pH 6.0) with 0.02% (w/v) sodium azide overnight at 37 ˚C under stirring (200 rpm). The FITC-AA conjugate

(0.8 unit/mg of starch) was added to the solution and incubated for 1 h under the same condition. Aliquots (50 µL) were taken after 5, 30 and 60 min. The diffusion of dextran probes inside maize starch granules and the status of diffused probes following further amylolysis were assessed by observing the granules after centrifugation as described in sections 2.3 and 2.4.

A5.2.7 Enzymic digestion of granular starches

Enzymic digestion was carried out using 0.1, 0.4 and 0.8 unit of FITC-AA conjugate per mg of starch (WMS, MS, PS or HAMS). Starch suspension (5 mL, 10 mg/mL) in acetate buffer (0.2M, pH 6, containing 0.02% (w/v) sodium azide) was incubated with FITC-AA conjugate and mixed at 37 ˚C. At set times between 5 and 1440 min of incubation, aliquots (100 µL) were transferred into 1.5 mL microcentrifuge tubes and immediately centrifuged at 2000 *g* for 30 s. The supernatant was used to determine the reducing sugar content using the PAHBAH assay as described by Moretti & Thorson (2008), and starch pellets from 0.1 and 0.8 unit of FITC-AA conjugate were used for confocal microscopic observation. Pellets from 0.8 unit of FITC-AA conjugate were also oven dried at 40 ˚C overnight for electron microscopic observation.

A5.2.8 Scanning electron microscopy

The oven-dried samples were thinly spread onto circular metal stubs covered with double-sided adhesive carbon tape, and then platinum coated in a Sputter coater (Eiko IB3, Mito, Japan). Images of the granules were acquired with a JEOL 6300 scanning electron microscope (JEOL Ltd., Tokyo, Japan) under an accelerating voltage of 5 kV. Multiple micrographs of each sample were examined at multiple magnifications and typical representative images selected.

A5.3 Results

A5.3.1 Kinetic analysis of FITC labelled and unlabelled α-amylase

Michaelis-Menten kinetic parameters were obtained for both the FITC labelled and unlabelled enzymes. The V_{max} value was found to drop from 30.50 (± 3.10) to 15.27 (±1.65) μM/min following labelling of the enzyme, indicating that the addition of the FITC significantly reduced the catalytic activity of the enzyme. The K_m value, however, was relatively unchanged following labelling, with a value of 12.94 (±2.67) and 17.30 (±3.52) mg/mL for the unlabelled and labelled enzyme respectively. Thus, while the labelling had a large effect on the enzyme's catalytic rate, substrate binding was far less affected. This

indicated that the labelled enzyme was still able to bind to starch with an affinity similar to the unlabelled form.

A5.3.2 α-Amylase binding to native starch granules

Representative confocal microscopic images of FITC and TRITC-AA conjugates bound to MS after 5 and 20 min of incubation under non-hydrolysing condition (0 ˚C) are shown in **Figure A5-1A**, and clearly reflect the heterogeneity of AA (both FITC and TRITC) binding to MS granules.

Double labelling of maize starch, using FITC-AA conjugate followed by TRITC-AA conjugate, is shown in **Figure A5-1B**. It can be observed that the TRITC-AA conjugate added after 20 min of incubation at 0 ˚C, binds to exactly the same granules at the same locations, as the FITC-AA conjugate was bound previously. In some granules (as marked), FITC-AA conjugate was observed in the core of granules as well as the surface, while TRITC-AA, which has had less incubation time, is only bound at the granule surface.

Double labelling of TRITC-AA followed by FITC-AA, as presented in supplementary information **Figure A5-S1**, followed a similar pattern as shown in **Figure A5-1B**. Labelling of FITC-AA simultaneously with TRITC-AA on maize starch granules is presented in supplementary information **Figure A5-S2**. Similar to sequential labelling, one subsequent to the other, when used together the two conjugates also show the heterogeneous, but preferential binding towards specific maize granules.

Similar to MS, **Figure A5-1C** shows the heterogeneity of FITC- and TRITC-AA conjugates binding to the surface of PS granules. The binding is more heterogeneous in PS compared to MS, with apparently a smaller fraction of the granules showing fluorescence after both 5 and 20 min incubation time. In contrast to MS, binding was mostly limited to the outer circumference of PS granules. Binding was not observed to be dependent on granule size.

Double labelling of PS, FITC-AA conjugate followed by TRITC-AA conjugate, is shown in **Figure A5-1D**. Specificity of binding location to PS was also observed similar to that of MS. TRITC-AA conjugate added after 20 min of incubation at 0 ˚C, bound to the same granules/location where FITC-AA conjugate was bound previously. The double labelling of TRITC-AA followed by FITC-AA, as presented in supplementary information **Figure A5-S3**, also followed a similar pattern to that of individual labelling as shown in **Figure A5-1C**.

Similarly, double labelling of FITC-AA and TRITC-AA together on PS granules is presented in supplementary information **Figure A5-S4**. In parallel to double labelling, one followed by the other, the two conjugates added simultaneously also showed heterogeneous, but preferential, binding to specific PS granules.

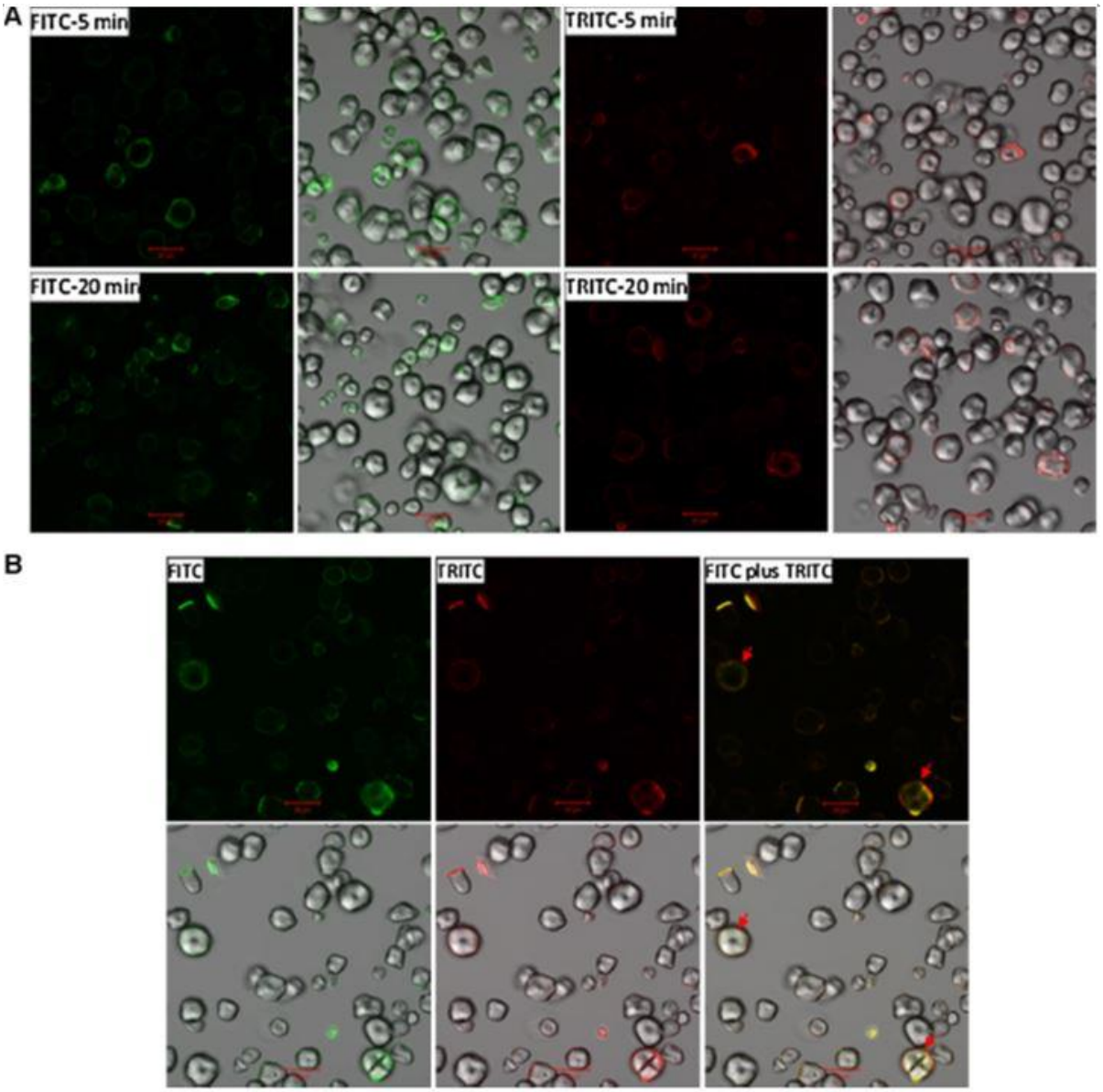

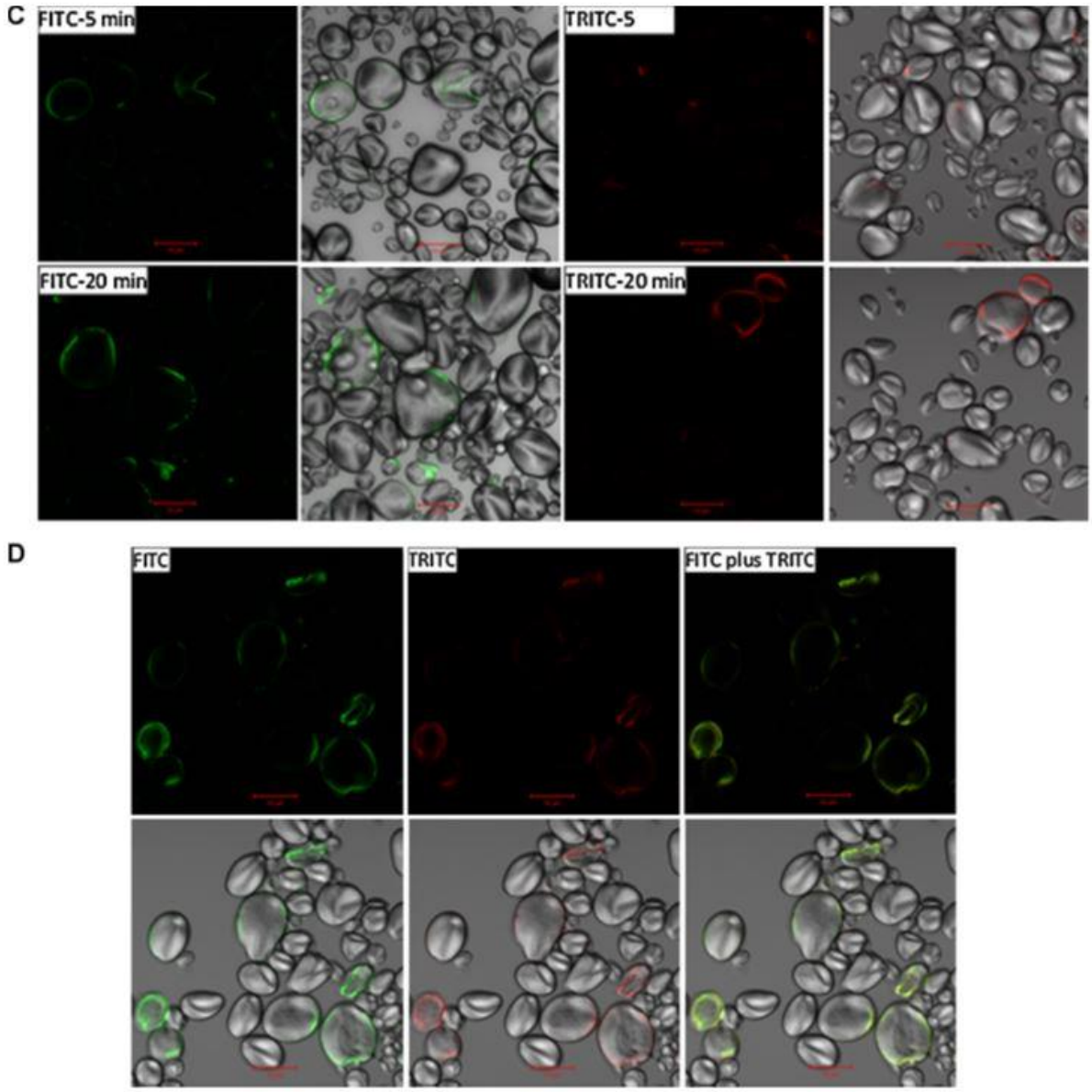

Figure A5-1. (A) Confocal (first and third column) and differential interference contrast (second and fourth column) images of bound FITC- and TRITC-AA conjugate on maize starch granules incubated for 5 and 20 minutes at 0 ˚C. (B) Confocal (top panel) and differential interference contrast (bottom panel) images of bound FITC- and TRITC-AA conjugate on maize starch granules incubated for 25 min at 0 ˚C. TRITC-AA conjugate, 8 units per mg of starch, was added after 20 min incubation of FITC-AA conjugate. (C) Confocal (first and third column)) and differential interference contrast (second and fourth column)) images of bound FITC- and TRITC-AA conjugate on potato starch granules incubated for 5 and 20 min at 0 ˚C. (D) Confocal (top panel)) and differential interference contrast (bottom panel) images bound FITC- and TRITC-AA conjugate on potato granules incubated for 25 min at 0 ˚C. TRITC-AA conjugate, 8 unit pre mg of starch, was added after 20 min incubation of FITC-AA conjugate.

A5.3.3 Amylase binding to enzyme treated (porous) starch granules

In order to study the effect of starch porosity on amylase binding, porous MS was obtained by partial hydrolysis with 0.8 unit of unlabelled amylase per mg of starch for 20 min as described in section 5.2.4. Numerous pores on the surface of maize starch granules were observed after 20 min of hydrolysis as seen in **Figure A5-2A**. Though limited by magnification and resolution, channels extending towards the granule interior can be seen in the confocal microscopic picture (**Figure A5-2B**). The confocal and differential interference contrast images after 5 min incubation of porous starch with the FITC-AA conjugate are shown in **Figure A5-2C**. Compared to non-porous granules (**Figure A5-1A**), amylase can freely diffuse inside the porous granules as observed by the higher intensity of the FITC-AA conjugate in the granule interior (marked by the solid arrow in **Figure A5-2D**). For non-porous or less porous granules, enzyme was concentrated in the outer surfaces, as marked by the dotted arrow in **Figure A5-2D**, similar to what was observed for untreated MS in **Figure A5-1A**.

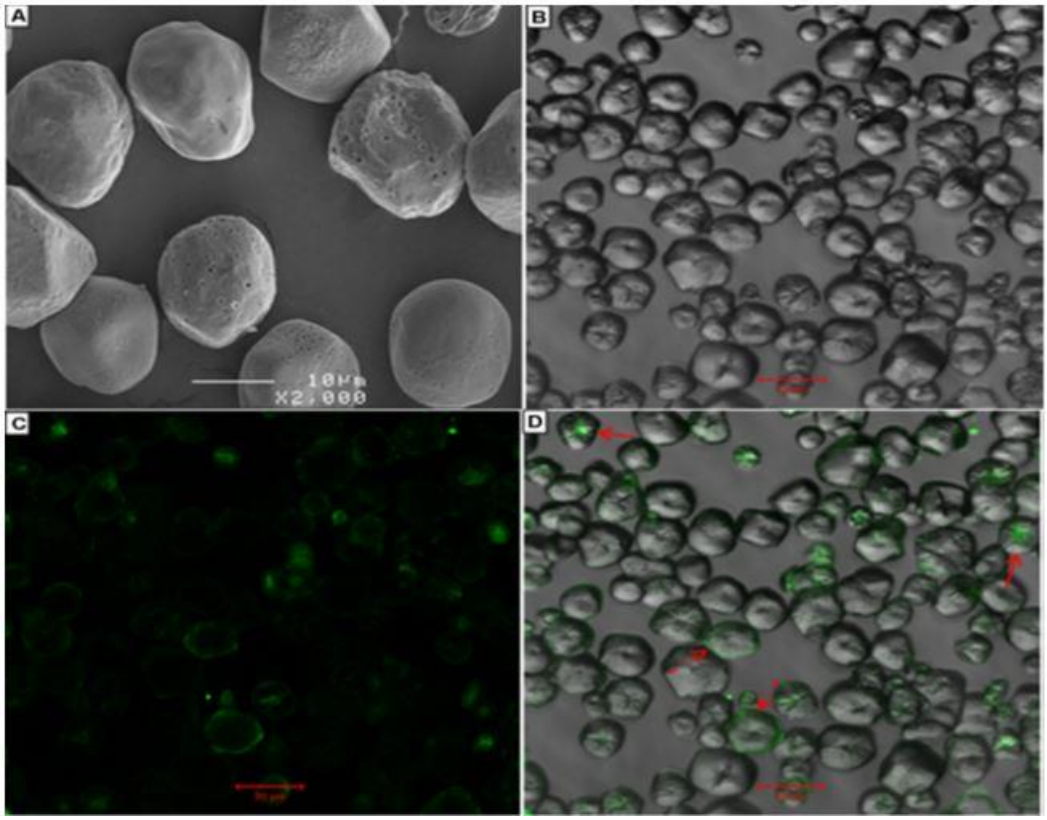

Figure A5-2. Electron, confocal and differential interference contrast images of porous granules. A: Electron microscopic picture of maize starch granules incubated with non-labelled AA for 20 min at 37 ˚C. B, C, and D: Confocal microscopic and differential

interference contrast images of porous granules bound with FITC-AA conjugate for 5 min at 0 ˚C.

A5.3.4 Diffusion of dextran probes and initial amylolysis of starch granules

As shown in **Figure A5-3B** and **C**, following an overnight incubation with TRITC labelled dextran, a small number of granules have (red) dextran probes inside them (shown by arrows in **Figure A5-3B** and **C**). After 5 min amylolysis, granules are observed with varying degrees of hydrolysis (damage) with the green fluorescence (FITC-AA conjugate) bound either to the interior or the peripheral regions of the granules (**Figure A5-3 D, E** and **F**). TRITC dextran was still observed in some granules, but there was not an obvious co-localization between TRITC dextran and FITC-AA (shown by arrows in **Figure A5-3E** and **F**). After incubation for 30 and 60 min, however, the TRITC dextran was not observed, suggesting that starch hydrolysis by the amylase had resulted in release of the labelled dextran.

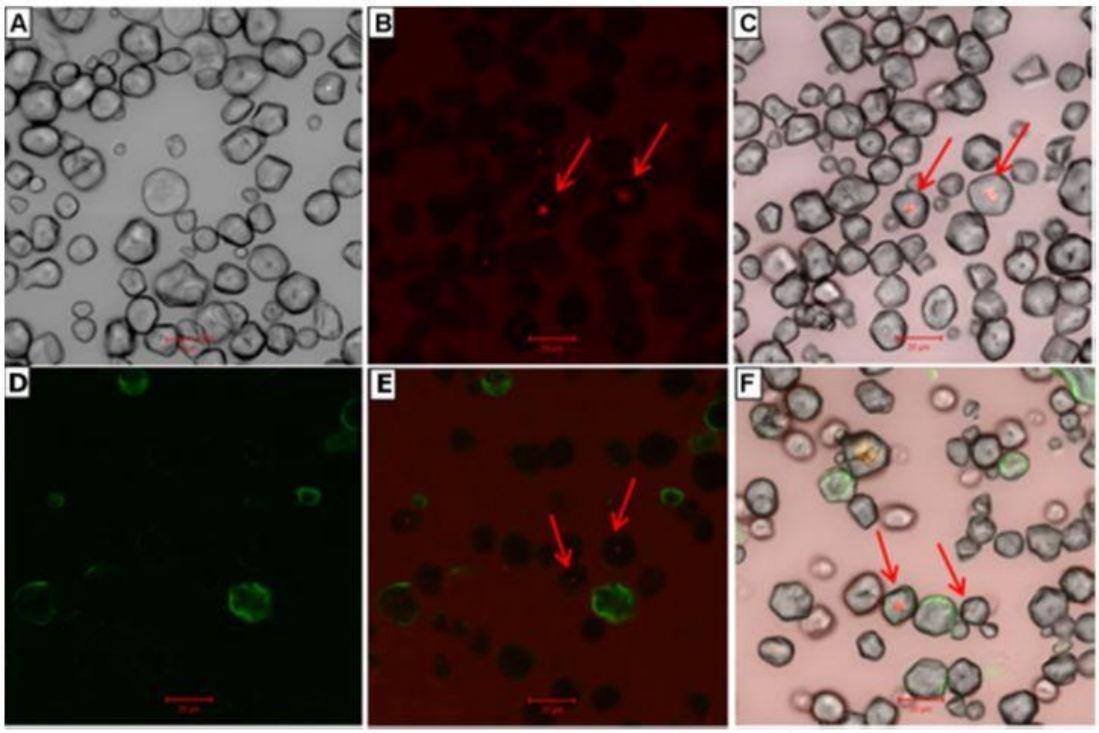

Figure A5-3. Confocal and differential interference contrast images of diffused dextran probes and initial amylolysis of maize starch granules with diffused dextran probes. A: Maize starch granules (differential interference contrast image), B and C: confocal and differential interference contrast images of diffused dextran probes inside the maize starch granules after overnight incubation. D, E: confocal image after 5 min of amylolysis by FITC-AA conjugate. F: Differential interference contrast image after 5 min of amylolysis by FITC-AA conjugate.

A5.3.5 Amylolysis of granular starches

The digestion progress curves of MS and PS with 0.1, 0.4, and 0.8 unit of FITC-AA conjugate are shown in **Figure A5-4**. As expected, the extent of hydrolysis is dependent upon the concentration of enzyme applied, as the substrate concentration is constant in all cases. The hydrolysis extent of starches followed the order of WMS>MS>PS>HAMS at all the enzyme concentrations used in the experiment.

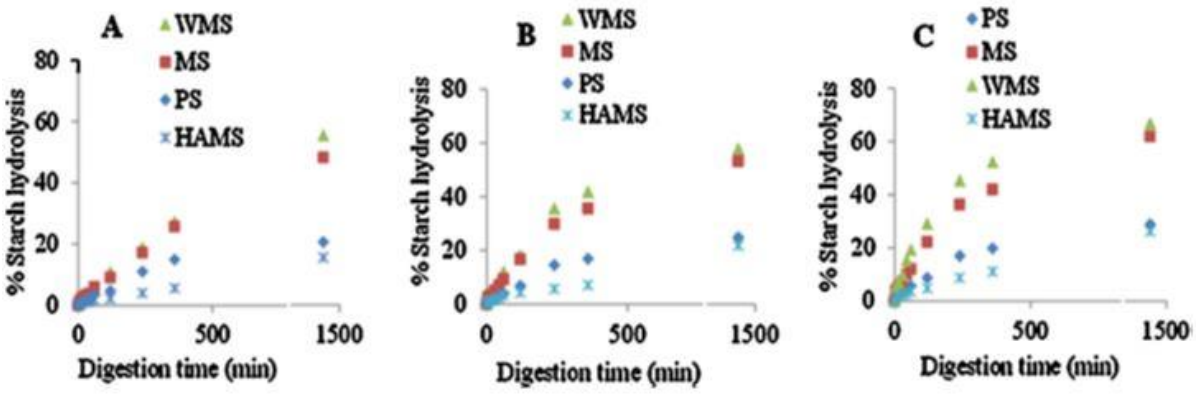

Figure A5-4. FITC-AA conjugate catalysed hydrolysis rate of starches; waxy maize (WMS), maize (MS), potato (PS), high amylose maize- Gelose 80 (HAMS). A, B, and C represents the digestogram at 0.1, 0.4 and 0.8 unit of FITC-AA conjugate per mg of starch.

The hydrolysis pattern observed by electron microscopy is shown in **Figures A5-5** and **A5-6**, and supplementary information **Figures A5-S5, A5-S6** for MS, PS, WMS and HAMS (Gelose 80) respectively. A-type polymorphic starches (WMS and MS) were hydrolysed by formation and enlargement of pores during the digestion time course, whereas B-polymorphic starches, PS and HAMS, were hydrolysed from the surface of the granules towards the interior.

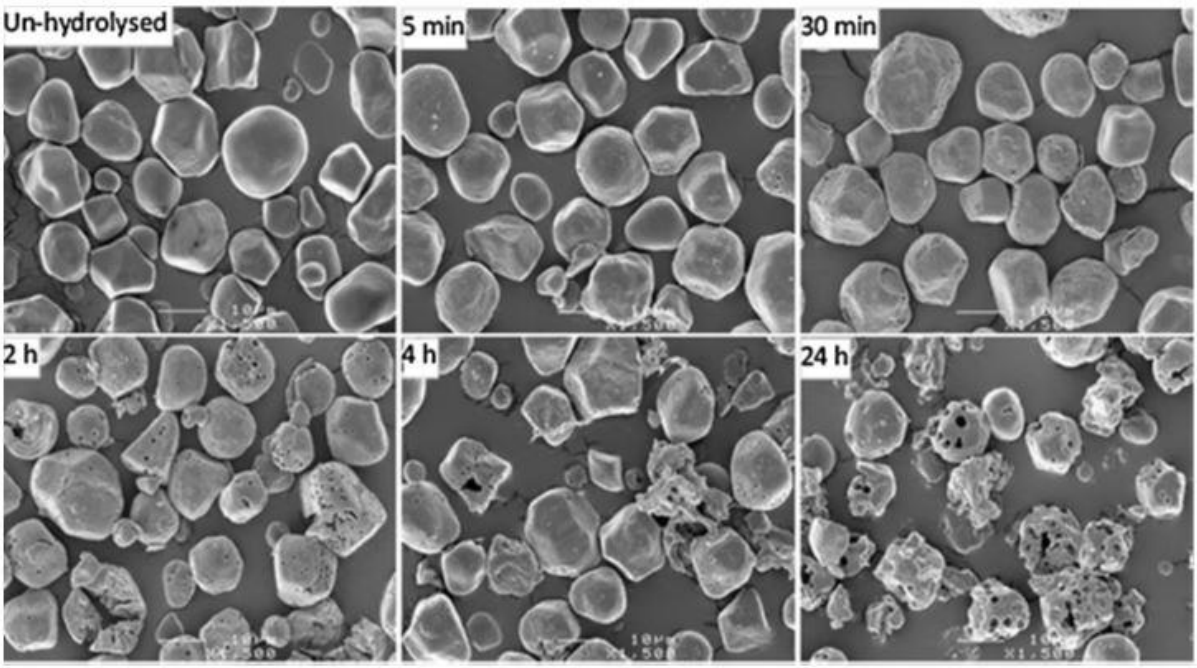

Figure A5-5. Electron microscopic images of un-hydrolysed maize starch granules and granule remnant after hydrolysis for 5 min, 30 min, 2 h, 4 h and 24 h with 0.8 unit FITC-AA conjugate per mg of starch.

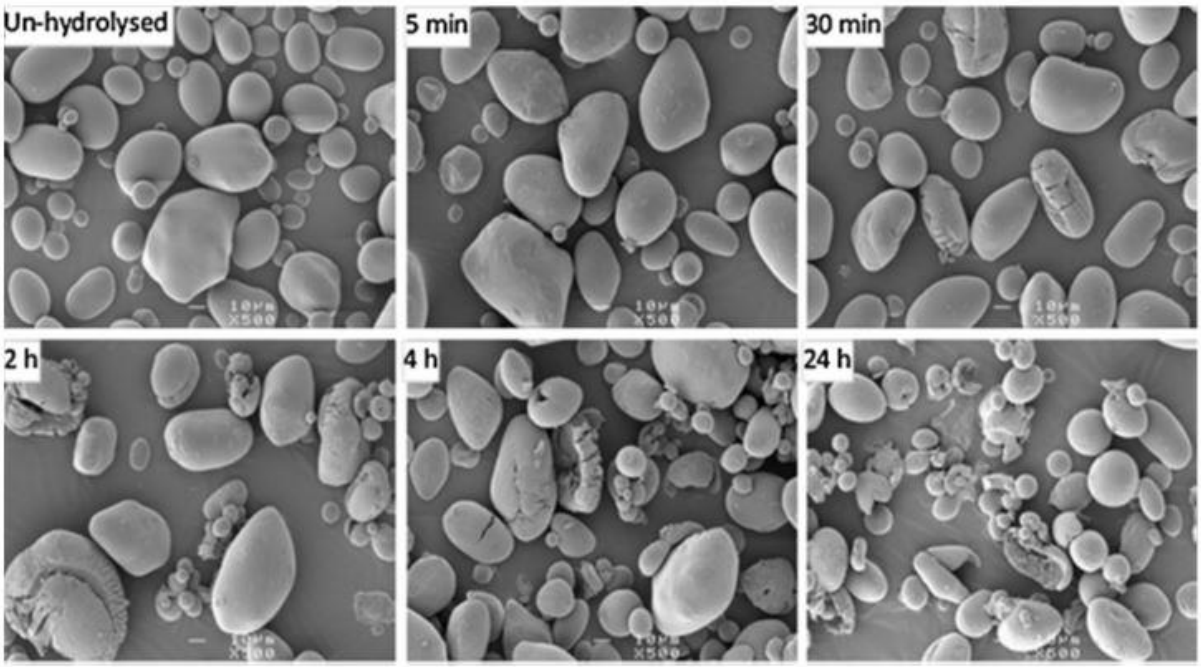

Figure A5-6. Electron microscopic images of un-hydrolysed potato starch granules and granule remnant after hydrolysis for 5 min, 30 min, 2 h, 4 h and 24 h with 0.8 unit FITC-AA conjugate per mg of starch.

Confocal and differential interference contrast images of hydrolysed MS and PS (0.8 units FITC-AA conjugate per mg of starch) are presented in **Figure A5-7**. Similarly, confocal and differential interference contrast images of MS and PS incubated with 0.1 units FITC-AA conjugate per mg of starch, and WMS and HAMS at both enzyme concentrations are presented in supplementary information **Figures A5-S7, S8** and **S9** respectively. The digestion pattern of MS with labelled enzymes was observed to be heterogeneous. In the initial 5 min of incubation, separate populations of high and low enzyme labelled granules were observed. On further incubation to 2 h, in contrast to the initial heterogeneous binding, almost all of the granules (**Figure A5-7**) showed bound FITC-AA conjugate, with only a few exceptions. Electron microscopy also showed that almost all the MS granules after 2 h incubation were similarly porous. In contrast to MS, more selective enzyme binding of FITC-AA conjugate to digested residues of PS was observed (**Figure A5-7).** This is in accordance with SEM observations, where only a few PS granules were eroded during the digestion time course. Enzyme binding was found to be concentration dependent; at higher enzyme concentrations (0.8 units per mg of starch) comparatively more granules were observed with bound enzyme compared to a lower enzyme concentration (0.1 units per mg of starch). Binding was still observed to be preferential (heterogeneous) even at higher enzyme concentrations.

For MS and WMS, the enzyme which initially bound to the outer surface, subsequently diffused towards the granule interior with longer incubation times (**Figures A5-7,** supplementary information **Figure A5-S7, A5-S8**). For example, the intensity and number of granules with internal fluorescence after 2 h of incubation time was comparatively higher than that at 30 min incubation. In contrast, the diffusion of enzyme inside PS and HAMS granules was not observed. They were digested from the outer surface towards the interior. Even after 24 h incubation time, a few granules were highly eroded with enzyme bound at the erosion surfaces whereas the rest were intact without any substantial enzyme binding (**Figure A5-7**).

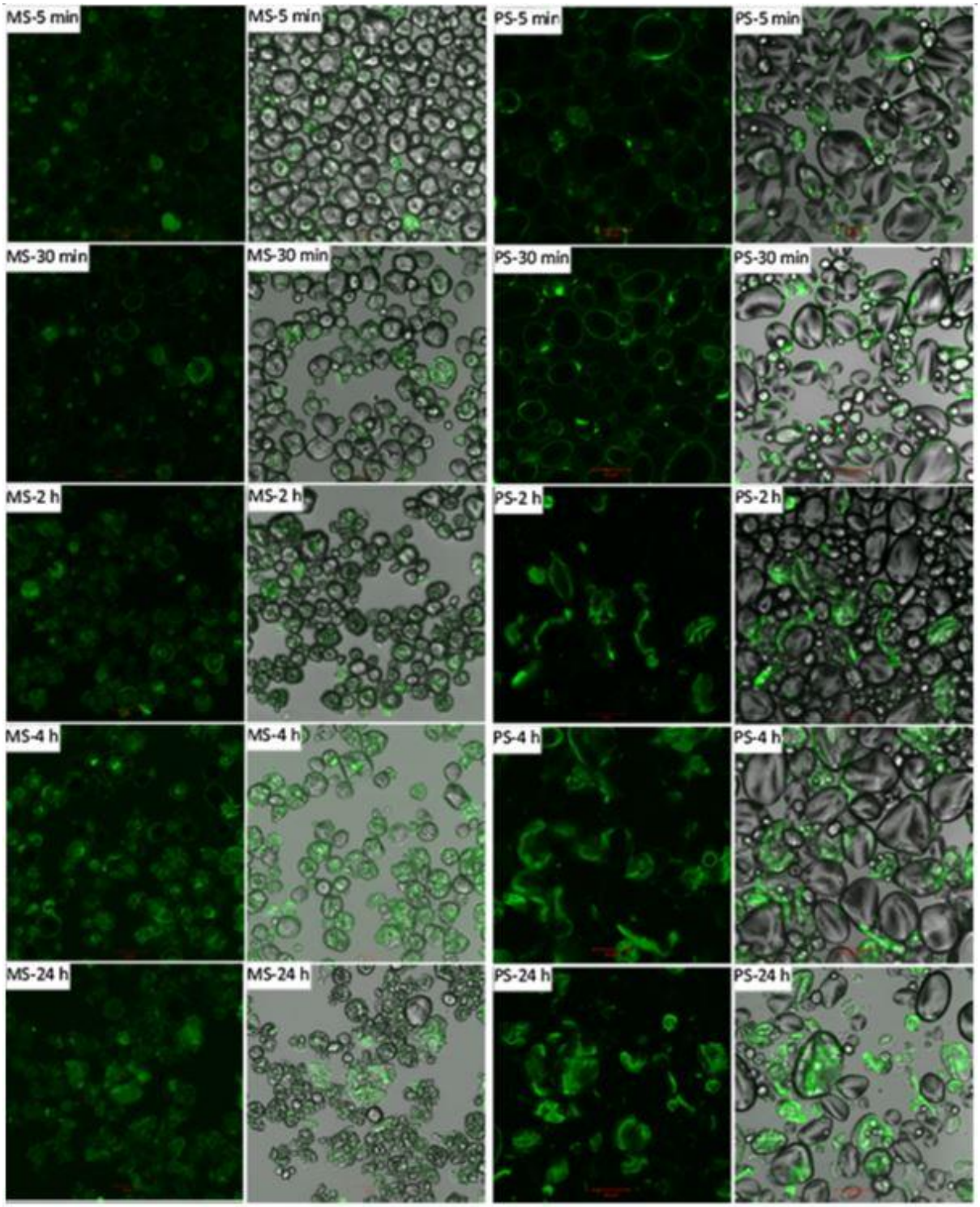

Figure A5-7. Confocal (first and third column) and differential interference contrast (second and third column) images of maize (MS) and potato (PS) starch granule remnants after hydrolysis for 5 min, 30 min, 2 h, 4 h and 24 h with 0.8 unit FITC-AA conjugate per mg of starch.

A5.4 Discussion

For the first time, we have been able to identify the location of bound amylase to starch granules under both non-hydrolysing and hydrolysing conditions. The results obtained lead us to propose that the heterogeneity of amylase action on starch granules during hydrolysis is due to preferential or selective binding of amylase to the granule surface. The possible reasons for the preferential binding are discussed below.

A5.4.1 Binding of amylase to starch granules under non-hydrolysing conditions

Interactions between amylase and starch granules require transportation of the amylase by diffusion to the solid starch granules. The initial interaction (binding) of enzyme to starch surfaces may involve (1) non-catalytic binding i.e. adherence of enzyme to the granule surface by non-specific hydrogen bonding between OH groups of the starch moieties and enzyme (protein) molecule or by Van der Waals interactions; or (2) catalytic binding i.e. binding with at least 5 contiguous glucose residues in the active site of the enzyme (Prodanov, Seigner & Marchis-Mouren, 1984; Seigner, Prodanov & Marchis-Mouren, 1987).

Initial binding can affect the subsequent catalytic events. If the binding occurs at the active site, catalysis can proceed. Alternatively, if the binding is non-catalytic in nature, the overall rate of enzyme action is decreased as enzyme molecules have to dissociate from the nonspecific sites and return to solution before they can rebind to the starch substrate (Henis, Yaron, Lamed, Rishpon, Sahar & Katchalski-Katzir, 1988). Measuring the concentration of enzyme that is not bound to starch granules during the experiment conducted under non-hydrolysing condition (usually 0 ˚C) has been used to determine the binding rates of amylase to starch granules (Walker & Hope, 1963; Warren, Royall, Gaisford, Butterworth & Ellis, 2011). These experiments, however, represent an average of both catalytic and non-catalytic binding over a population of granules.

The efficiency of enzyme adsorption has been previously reported to be inversely proportional to the granule size, or, more precisely, to the surface area of the granules (Schwimmer & Balls, 1949; Walker & Hope, 1963; Warren, Royall, Gaisford, Butterworth & Ellis, 2011). The higher relative binding efficiency of smaller granules may be a factor contributing to higher digestion rate of smaller starch granules naturally occurring in bulk samples or obtained from fractionation of starches compared to larger granules (Dhital, Shrestha & Gidley, 2010b; Tahir, Ellis & Butterworth, 2010).

Roughness and porosity at the surface of MS granules (Dhital, Shrestha & Gidley, 2010a), in addition to increasing the available surface area, can also elevate the probability of catalytic binding due to the presence of more accessible (available) starch molecules on exposed, damaged, rough, and/or porous structures. The less organised regions are more accessible for initial enzyme binding compared to regions with greater molecular order (Warren, Royall, Gaisford, Butterworth & Ellis, 2011).

The enzyme preference towards some specific granules in both MS and PS is not apparently related to granule size or surface area, and is therefore more likely to be governed by the 'available substrate' (starch chains that are sufficiently accessible as single chains to potentially lead to catalytic binding) than the 'available surface area'. Based on the data reported here, we propose that there can be localised variation in the amount of 'available substrate' within or at the granule surface due to local polymer organisation factors, and that enzyme binds preferentially to these specific regions of the granule. This is also evident in **Figure A5-2**, where the preferential binding of enzyme to porous regions was observed. In contrast, for granules without pores, enzyme was concentrated at the outer periphery similar to non-treated starch (**Figure A5-1A**). The hilum (**Figure A5-2**, bold arrow) appeared to be the least organised part of the granules since a relatively high proportion of enzyme was bound in the hilum area within 5 min of incubation under non-hydrolysing condition.

The role of local surface structures in controlling the specificity of enzyme binding was evident during double (consecutive) labelling experiments as shown in **Figure A5-1B** and supplementary information **Figure A5-S1** for MS, and **Figure A5-1D** and supplementary information **Figure A5-S3** for PS. The fresh enzyme bound at exactly the same granule sites that had previously bound enzyme. The structural features associated with granules which bind amylase compared to those which do not is the subject of current investigations.

A5.4.2 Amylolysis of starches

The FITC-AA conjugate at 0.1, 0.4 and 0.8 units per mg of starch granules was used to study the hydrolysis of starches with both A- (WMS, MS) and B- (PS, HAMS) type polymorphism. The rate and extent of starch digestion were proportional to the concentration of enzyme (**Figure A5-4)**. As expected, the hydrolysis extent, at all enzyme concentrations, was highest in WMS, followed by MS, PS and HAMS. The role of molecular, supra-molecular and granular structures that affect the hydrolysis rate and

extent of starch granules after initial binding has been recently reviewed (Dhital, Warren, Butterworth, Ellis & Gidley, 2014). The electron microscopic images of granule remnants after amylolysis with 0.8 unit FITC-AA conjugate per mg of starch (**Figures A5-5, A5-6,** supplementary information **Figures A5-S5** and **A5-S6**) were in agreement with several previous reports (Dhital, Shrestha & Gidley, 2010a, b; Planchot, Colonna, Gallant & Bouchet, 1995; Zhang, Dhital & Gidley, 2013).

A5.4.3 Binding of amylase to starch granules at hydrolysing conditions

For the first time, we have been able to localise amylase on starch granules during binding and hydrolysis. Recently, Tawil *et al.* (2010) studied the location of bacterial amylase in maize and waxy maize starches using light and synchrotron UV fluorescence microscopy (measuring the auto-fluorescence of tryptophan in the enzyme). Starch samples were incubated with enzyme under a microscope, and the changes in the granule morphology were observed at different times. The experimental methodology employed by Tawil *et al.* (2010) while highly innovative, was in some ways limited, as the authors were only able to visualise one granule at a time, and the enzyme-starch interaction was observed under a microscope coverslip, meaning that no mixing or temperature control could be employed. The present study builds upon the findings of Tawil *et al.* (2010) by extending the study of the localisation of enzyme during binding and hydrolysis of starch to starch samples from multiple botanical origins, under a range of conditions, and with whole populations of granules.

The adsorption of enzyme to starch granules during hydrolysis was found to be a highly selective process. This selectivity is reflected in confocal microscopic images taken at different digestion times (**Figure A5-7** and supplementary information **Figures A5-S7, A5-S8** and **A5-S9)**. Similar to enzyme binding under non-hydrolysing conditions, after 5 min incubation under hydrolysing conditions, the binding of FITC-AA conjugate to MS is more homogenous compared to that of PS (**Figure A5-7** and supplementary information **Figure A5-S7**). Confocal microscopy observations of amylase binding to MS and WMS at different incubation times (**Figure A5-7,** supplementary information **Figure A5-S7, A5-S8**) appear to confirm the usually accepted ‘inside-out’ digestion pattern for A-polymorphic starches ascribed to the presence of pores and channels that allow the easy diffusion of enzymes inside the granule to access the less organised interior. However, the mere presence of surface pores and channels does not necessarily mean that enzymes diffuse through them to the granule interior. In the present study, it was observed that very few of the maize

starch granules for which labelled dextran was able to diffuse to their hilum, also showed diffusion of labelled enzyme to their hilum (**Figure A5-3**).

In contrast to A-polymorphic WMS and MS (**Figure A5-7,** supplementary information **Figure A5-S7, A5-S8**), the enzyme was bound only to selective granules in B-polymorphic starches (PS and HAMS, **Figure A5-7** and supplementary information **Figure A5-S7, A5-S9**) during incubation under hydrolysing conditions. This selectivity between granules and within granules would suggest that the enzyme binding is restricted to sites on the starch granule surface that are suitable for enzyme catalytic actions, as it is these regions that are subsequently degraded by enzyme, while granules without enzyme bound are left untouched. Thus, the comparatively homogenous binding of amylase under both non-hydrolysing and hydrolysing conditions in MS suggests that the surface of maize starch contains more readily available substrates possibly at the periphery of the pores. The enzyme initially catalytically binds at these substrates and keeps hydrolysing with enlargement of pores (channels) until the enzyme can access the less organised hilum region. After that, the enzyme starts hydrolysing from the hilum towards the granule surface. In contrast, due to the absence of pores and channels in PS and HAMS, amylase catalytically binds the granules that have a damaged surface or exposed substrate and keep hydrolysing externally, so called ‘exo-corrosion’ (Dhital, Shrestha & Gidley, 2010b). The inaccessibility of enzyme to the granule interior further suggests that the surface structure of PS and HAMS is rate limiting to the hydrolysis of these starches.

A5.5 Conclusions

This study shows that amylase binds to starch granules in selected local regions under both hydrolysing and non-hydrolysing conditions. It is proposed that binding occurs to those regions which have less local molecular order and therefore contain abundant potential binding sites for α-amylase. Once bound, subsequent catalytic action exposes more potential binding sites, thus granule digestion becomes comparatively easier during digestion, resulting in extensive digestion of some granules in the presence of limited if any digestion of other granules. The different behaviour of α-amylase to dextran probes of similar size suggests that physical accessibility is not the determinant for enzyme localisation, and that therefore binding interactions are more likely to be the most important factor in determining the specificity of enzyme location.

References

Apinan, S., Yujiro, I., Hidefumi, Y., Takeshi, F., Myllärinen, P., Forssell, P., & Poutanen, K. (2007). Visual observation of hydrolyzed potato starch granules by α-amylase with Confocal Laser Scanning Microscopy. *Starch/Stärke*, 59(11), 543-548.

Dhital, S., Shelat, K., Shrestha, A. K., & Gidley, M. J. (2013). Heterogeneity in maize starch granule internal architecture deduced from diffusion of fluorescent dextran probes. *Carbohydrate Polymers*, 93, 365– 373.

Dhital, S., Shrestha, A. K., & Gidley, M. J. (2010a). Effect of cryo-milling on starches: Functionality and digestibility. *Food Hydrocolloids*, 24(2), 152-163.

Dhital, S., Shrestha, A. K., & Gidley, M. J. (2010b). Relationship between granule size and *in vitro* digestibility of maize and potato starches. *Carbohydrate Polymers*, 82(2), 480-488.

Dhital, S., Warren, F. J., Butterworth, P. J., Ellis, P. R., & Gidley, M. J. (2014). Mechanisms of starch digestion by α-amylase – structural basis for kinetic properties. *Critical Reviews in Food Science and Nutrition*, accepted for publication.

Gallant, D. J., Bouchet, B., & Baldwin, P. M. (1997). Microscopy of starch: Evidence of a new level of granule organization. *Carbohydrate Polymers*, 32(3), 177-191.

Helbert, W., Schülein, M., & Henrissat, B. (1996). Electron microscopic investigation of the diffusion of Bacillus licheniformis α-amylase into corn starch granules. *International journal of Biological Macromolecules*, 19(3), 165-169.

Henis, Y. I., Yaron, T., Lamed, R., Rishpon, J., Sahar, E., & Katchalski-Katzir, E. (1988). Mobility of enzymes on insoluble substrates: The β-amylase-starch gel system. *Biopolymers*, 27(1), 123-138

Huber, K. C., & BeMiller, J. N. (1997). Visualization of channels and cavities of corn and sorghum starch granules. *Cereal Chemistry*, 74(5), 537-541.

Jane, J. L., & Shen, J. J. (1993). Internal structure of the potato starch granule revealed by chemical gelatinization. *Carbohydrate Research*, 247, 279-290.

Liu, D., Parker, M. L., Wellner, N., Kirby, A. R., Cross, K., Morris, V. J., & Cheng, F. (2013). Structural variability between starch granules in wild type and in *ae* high-amylose mutant maize kernels. *Carbohydrate Polymers*, 97(2), 458-468.

Leach, H. W., & Schoch, T. J. (1961). Structure of the starch granule. II. Action of various amylases on granular starches. *Cereal Chemistry*, 38(1), 34-36.

Lynn, A., & Cochrane, M. P. (1997). An evaluation of confocal microscopy for the study of starch granule enzymic digestion. *Starch/Stärke*, 49(3), 106-110.

Moretti, R., & Thorson, J. S. (2008). A comparison of sugar indicators enables a universal high-throughput sugar-1-phosphate nucleotidyltransferase assay. *Analytical Biochemistry*, 377(2), 251-258.

Pan, D. D., & Jane, J. L. (2000). Internal structure of normal maize starch granules revealed by chemical surface gelatinization. *Biomacromolecules*, 1(1), 126-132.

Planchot, V., Colonna, P., Gallant, D. J., & Bouchet, B. (1995). Extensive degradation of native starch granules by α-amylase from *Aspergillus fumigatus*. *Journal of Cereal Science*, 21(2), 163-171.

Prodanov, E., Seigner, C., & Marchis-Mouren, G. (1984). Subsite profile of the active center of porcine pancreatic α-amylase. Kinetic studies using maltooligosaccharides as substrates. *Biochemical and Biophysical Research Communications*, 122(1), 75-81.

Schwimmer, S., & Balls, A. (1949). Starches and their derivatives as adsorbents for malt α-amylase. *Journal of Biological Chemistry*, 180(2), 883-894.

Seigner, C., Prodanov, E., & Marchis-Mouren, G. (1987). The determination of subsite binding energies of porcine pancreatic α-amylase by comparing hydrolytic activity towards substrates. *Biochimica et Biophysica Acta (BBA)-Protein Structure and Molecular Enzymology*, 913(2), 200-209.

Sujka, M., & Jamroz, J. (2009). α-Amylolysis of native potato and corn starches–SEM, AFM, nitrogen and iodine sorption investigations. *LWT-Food Science and Technology*, 42(7), 1219-1224.

Tahir, R., Ellis, P. R., & Butterworth, P. J. (2010). The relation of physical properties of native starch granules to the kinetics of amylolysis catalysed by porcine pancreatic α-amylase. *Carbohydrate Polymers*, 81(1), 57-62.

Tawil, G., Jamme, F., Réfrégiers, M., Viksø-Nielsen, A., Colonna, P., & Buléon, A. (2010). *In situ* tracking of enzymatic breakdown of starch granules by synchrotron UV fluorescence microscopy. *Analytical Chemistry*, 83(3), 989-993.

The, T. H., & Feltkamp, T. E. W. (1970). Conjugation of fluorescein isothiocyanate to antibodies: I. Experiments on the conditions of conjugation. *Immunology*, 18(6), 865 - 873.

Thomson, N., Miles, M., Ring, S., Shewry, P., & Tatham, A. (1994). Real-time imaging of enzymatic degradation of starch granules by atomic force microscopy. *Journal of Vacuum Science & Technology B*: *Microelectronics and Nanometer Structures*, 12(3), 1565-1568.

Walker, G. J., & Hope, P. M. (1963). The action of some α-amylases on starch granules. *Biochemical Journal*, 86(3), 452- 462

Warren, F. J., Royall, P. G., Gaisford, S., Butterworth, P. J., & Ellis, P. R. (2011). Binding interactions of α-amylase with starch granules: The influence of supramolecular structure and surface area. *Carbohydrate Polymers*, 86(2), 1038-1047.

Zhang, B., Dhital, S., & Gidley, M. J. (2013). Synergistic and antagonistic effects of α-amylase and amyloglucosidase on starch digestion. *Biomacromolecules*, 14 (6), 1945–1954.

Supporting information for

Amylase binding to starch granules under hydrolysing and non-hydrolysing conditions

*Sushil Dhital, Frederick J. Warren, Bin Zhang, and Michael J. Gidley**

Centre for Nutrition and Food Sciences, ARC Centre of Excellence in Plant Cell Walls, Queensland Alliance for Agriculture and Food Innovation, The University of Queensland, St Lucia, Brisbane, QLD 4072, Australia

* Corresponding author.

Phone: +61 7 3365 2145; Fax: +61 7 3365 1177. Email address: m.gidley@uq.edu.au (M. Gidley)

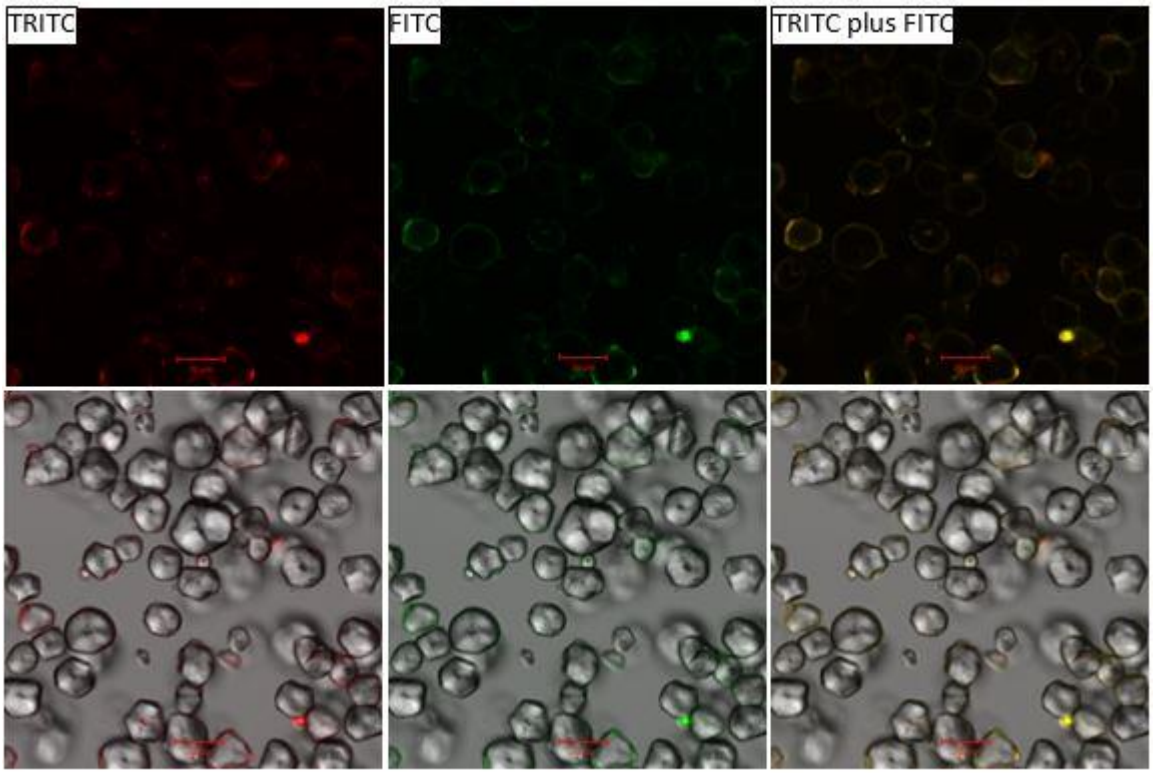

Figure A5-S1. Confocal (top panel) and differential interference contrast (bottom panel) images of bound TRITC- and FITC-AA on maize starch granules incubated for 25 min at 0 ˚C. FITC-AA conjugate, 8 units per mg of starch, was added after 20 min incubation of TRITC-AA conjugate.

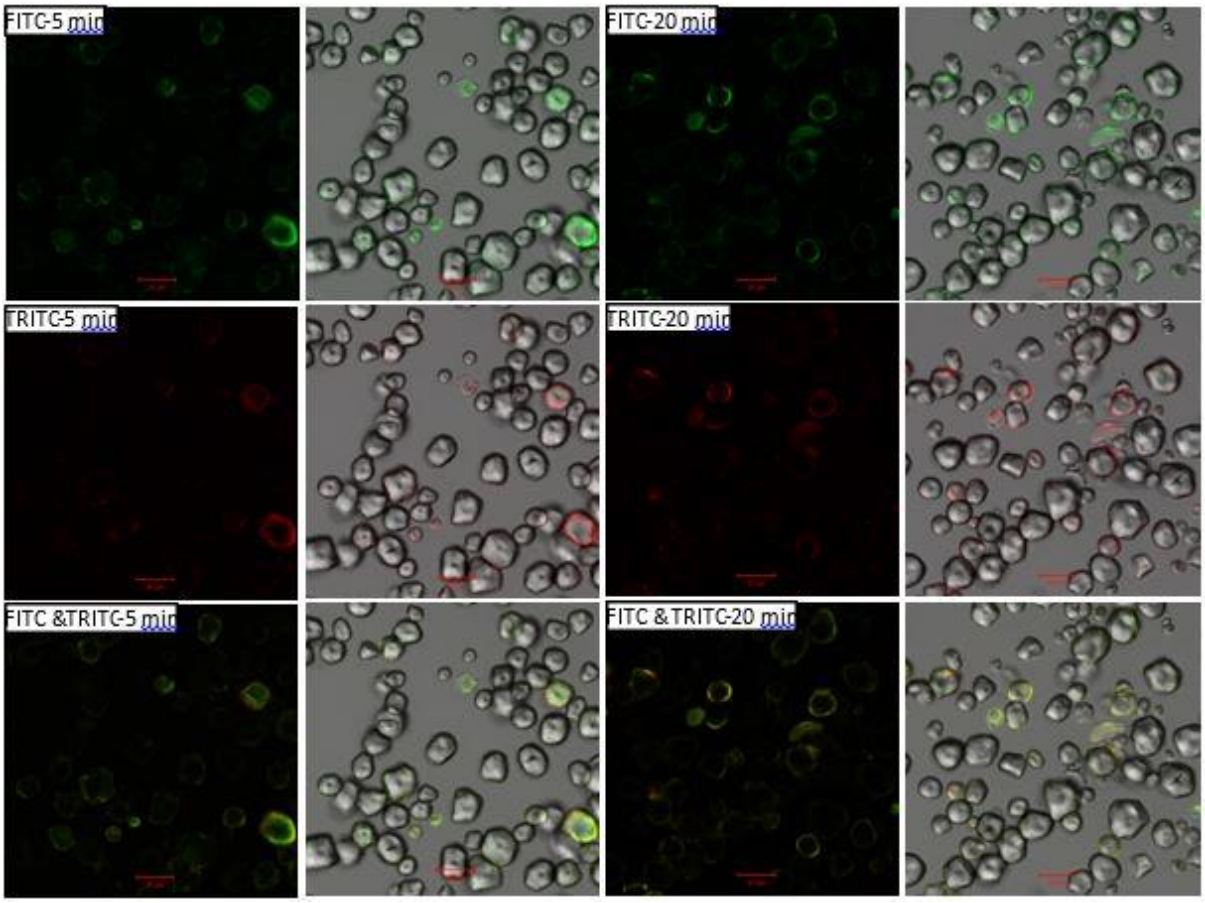

Figure A5-S2. Double labelling of FITC- and TRITC-AA conjugates in maize starch granules. Confocal (first and third column) and differential interference contrast (second and fourth column) images after 5 min and 20 min of incubation at 0 ˚C.

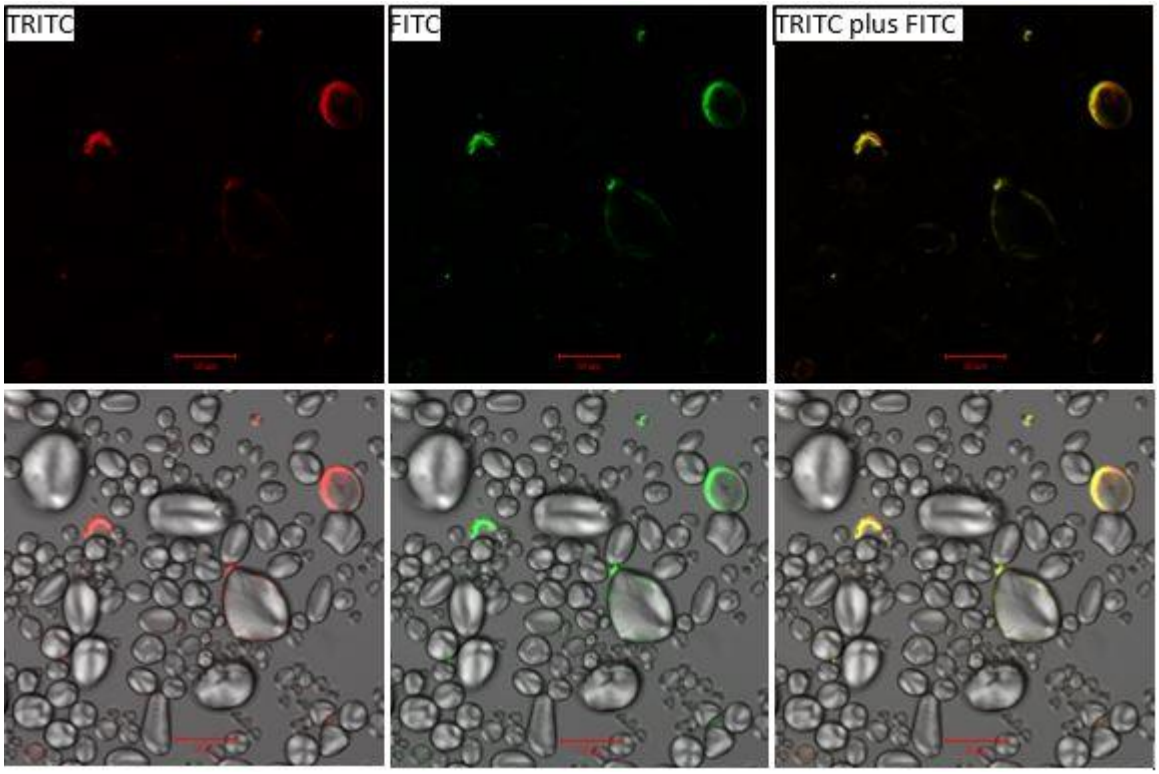

Figure A5-S3. Confocal (top panel) and differential interference contrast (bottom panel) images of bound TRITC- and FITC-AA on potato starch granules incubated for 25 min at 0 ˚C. FITC-AA conjugate, 8 units per mg of starch, was added after 20 min incubation of TRITC-AA conjugate.

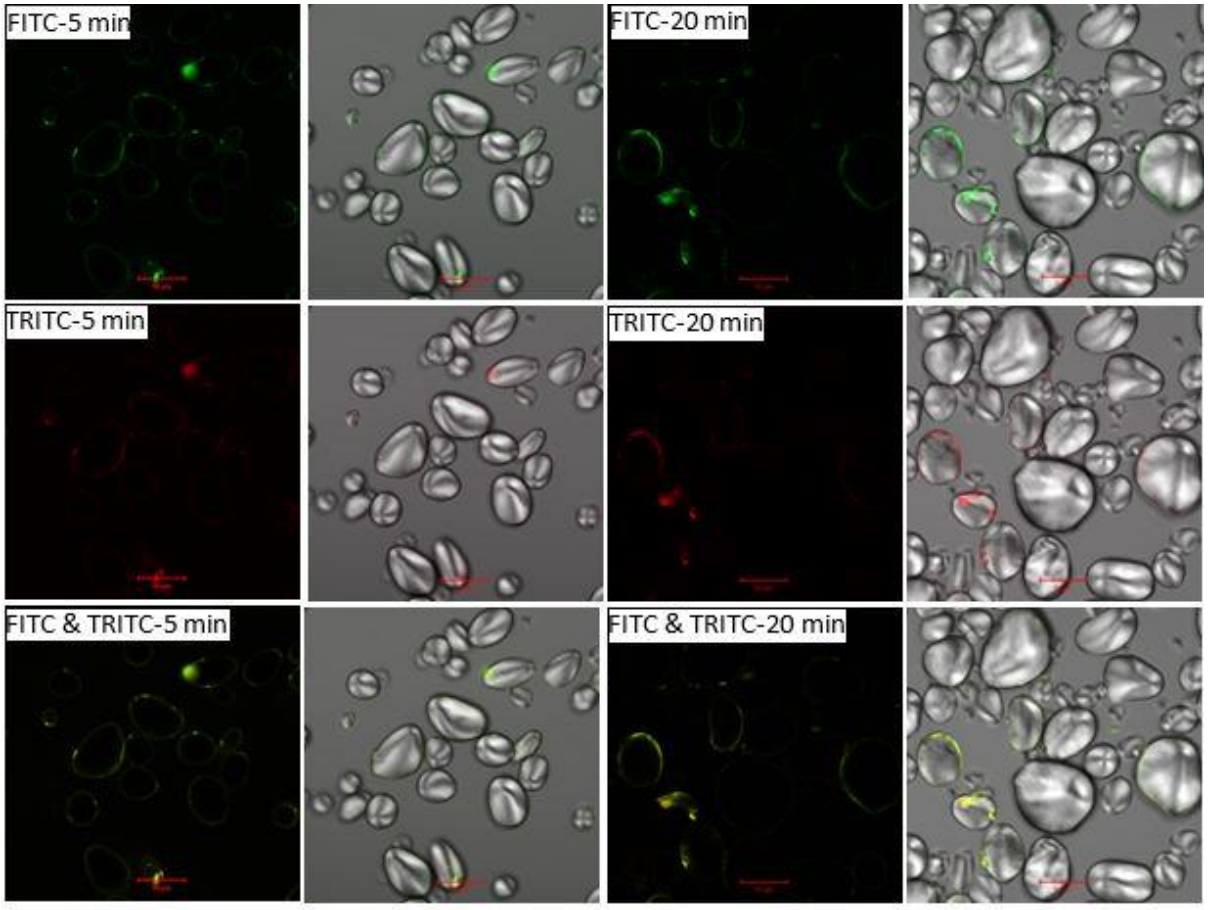

Figure A5-S4: Double labelling of FITC- and TRITC-AA conjugates in potato starch granules. Confocal (first and third column) and differential interference contrast (second and fourth column) images after 5 min and 20 min of incubation at 0 ˚C.

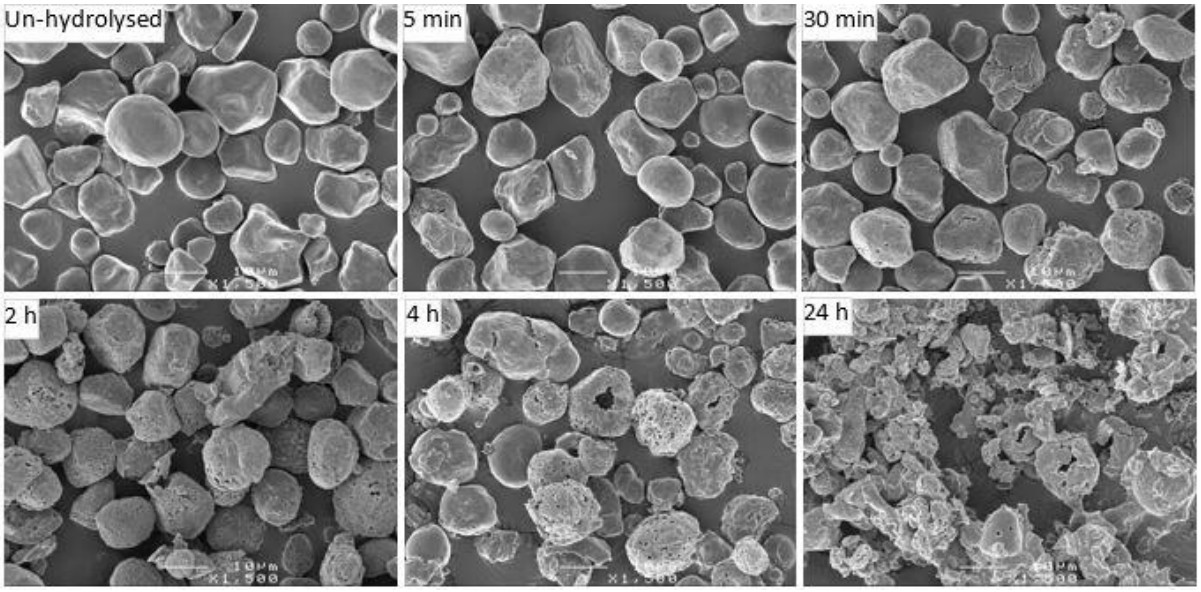

Figure A5-S5. Electron microscopic images of un-hydrolysed waxy maize starch granules and granule remnant after hydrolysis for 5 min, 30 min, 2 h, 4 h and 24 h with 0.8 unit FITC-AA conjugate per mg of starch.

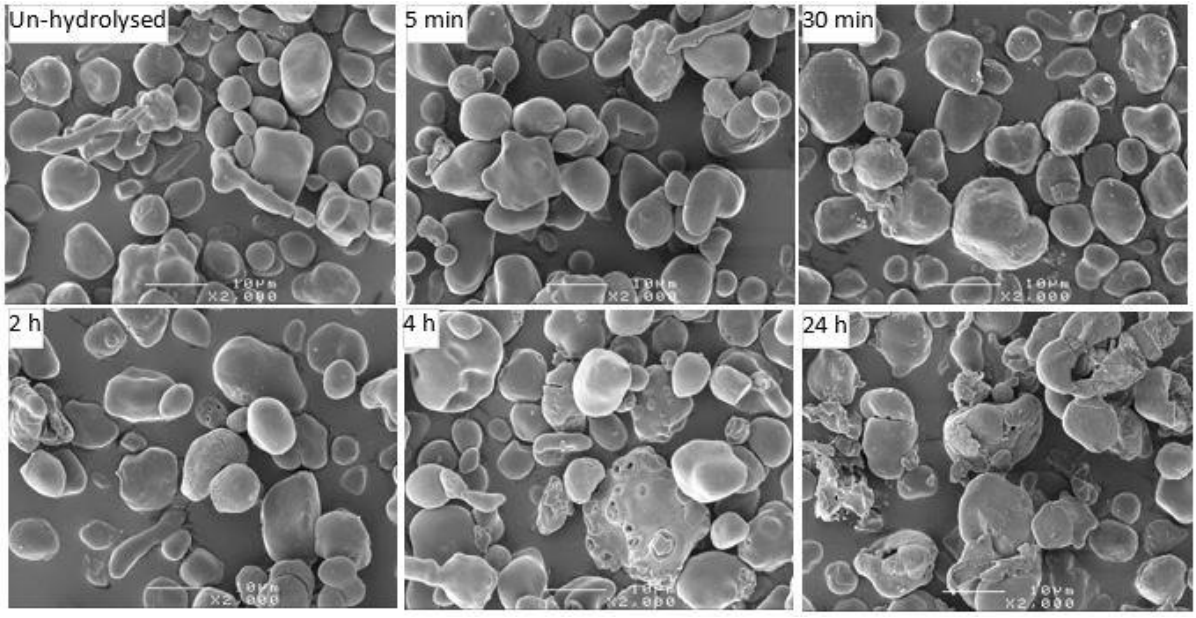

Figure A5-S6. Electron microscopic images of un-hydrolysed high amylose maize starch (Gelose 80) granules and granule remnant after hydrolysis for 5 min, 30 min, 2 h, 4 h and 24 h with 0.8 unit FITC-AA conjugate per mg of starch.

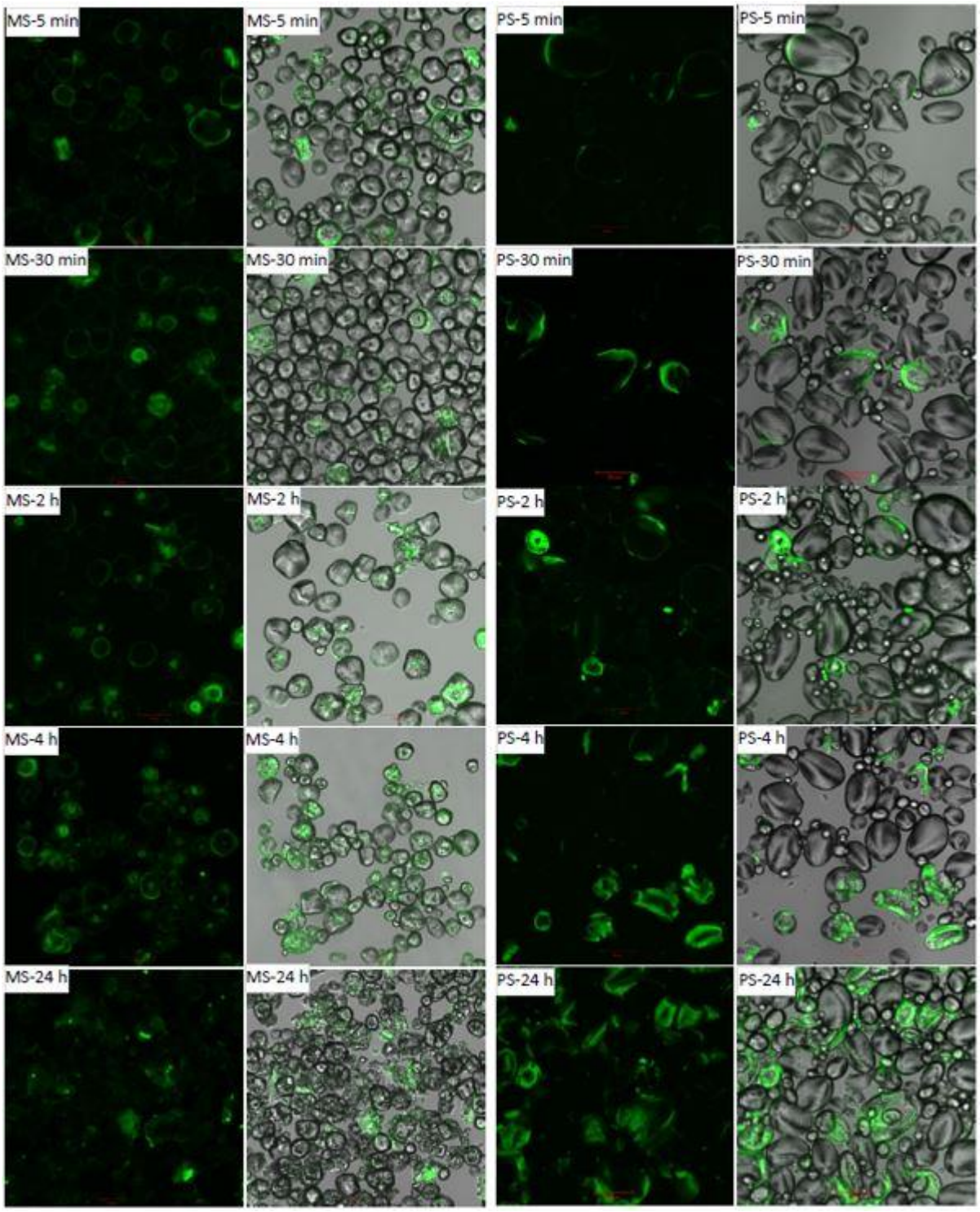

Figure A5-S7. Confocal (first and third column) and differential interference contrast (second and fourth column) images of maize (MS) and potato (PS) starch granule remnants after hydrolysis for 5 min, 30 min, 2 h, 4 h and 24 h with 0.1 unit FITC-AA conjugate per mg of starch.

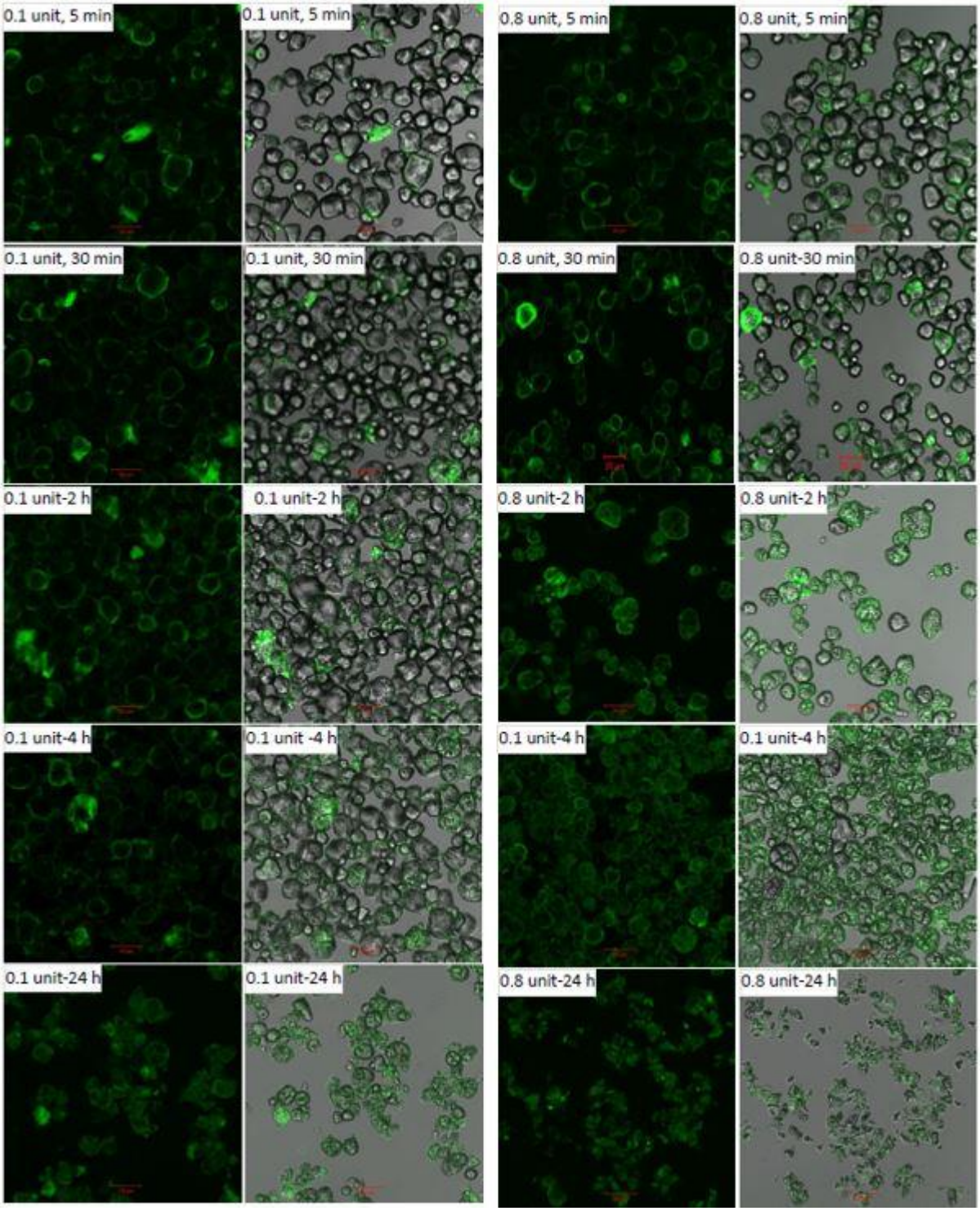

Figure A5-S8. Confocal (first and third column) and differential interference contrast (second and fourth column) images of waxy maize starch granule remnants after hydrolysis for 5 min, 30 min, 2 h, 4 h and 24 h with 0.1 and 0.8 unit FITC-AA conjugate per mg of starch.

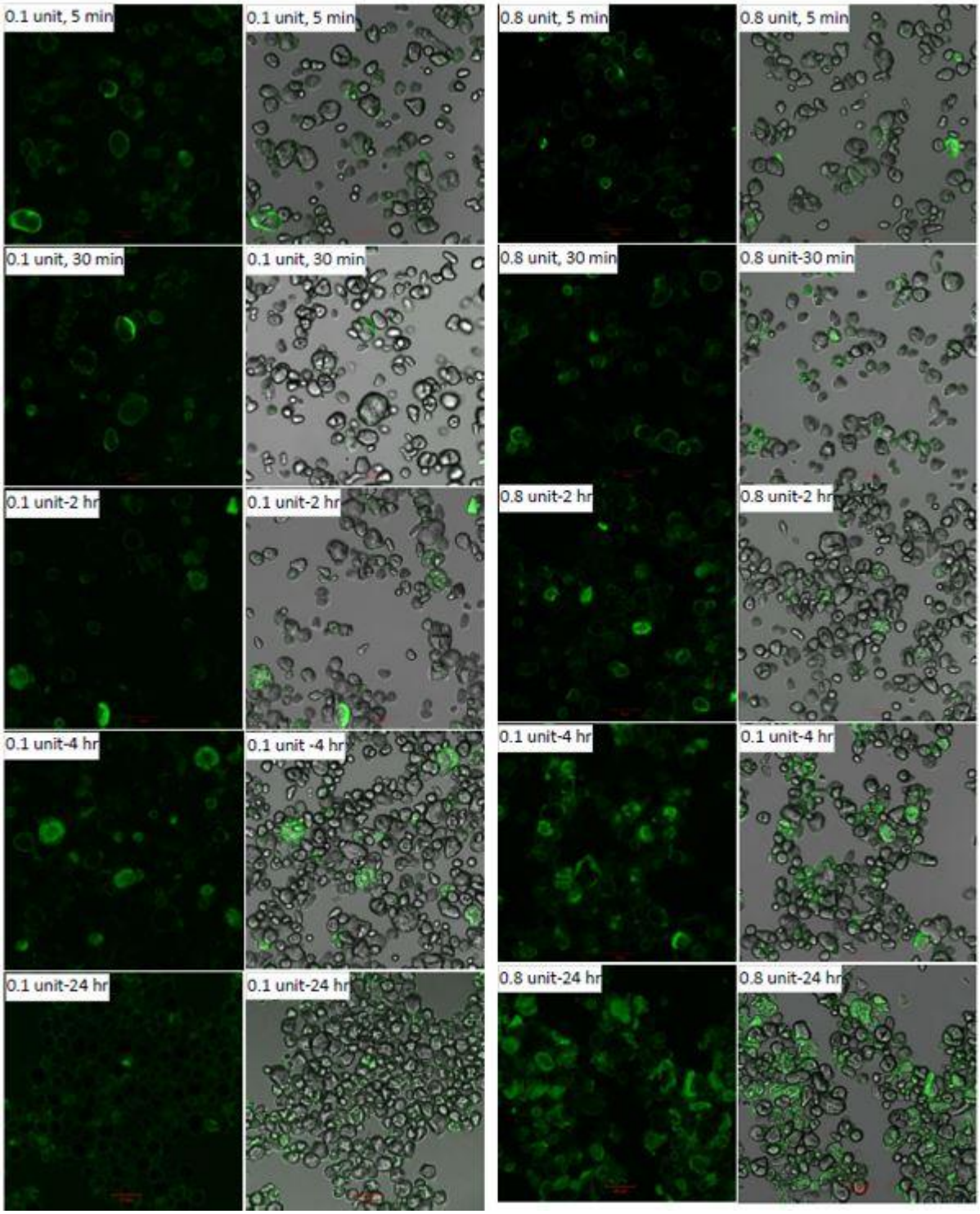

Figure A5-S9. Confocal (first and third column) and differential interference contrast (second and fourth column) images of high amylose maize starch (Gelsoe 80) granule remnants after hydrolysis for 5 min, 30 min, 2 h, 4 h and 24 h with 0.1 and 0.8 unit FITC-AA conjugate per mg of starch.